Terms and Conditions of Use of Digitised Theses from Trinity College Library Dublin

Copyright statement

All material supplied by Trinity College Library is protected by copyright (under the Copyright and Related Rights Act, 2000 as amended) and other relevant Intellectual Property Rights. By accessing and using a Digitised Thesis from Trinity College Library you acknowledge that all Intellectual Property Rights in any Works supplied are the sole and exclusive property of the copyright and/or other IPR holder. Specific copyright holders may not be explicitly identified. Use of materials from other sources within a thesis should not be construed as a claim over them.

A non-exclusive, non-transferable licence is hereby granted to those using or reproducing, in whole or in part, the material for valid purposes, providing the copyright owners are acknowledged using the normal conventions. Where specific permission to use material is required, this is identified and such permission must be sought from the copyright holder or agency cited.

Liability statement

By using a Digitised Thesis, I accept that Trinity College Dublin bears no legal responsibility for the accuracy, legality or comprehensiveness of materials contained within the thesis, and that Trinity College Dublin accepts no liability for indirect, consequential, or incidental, damages or losses arising from use of the thesis for whatever reason. Information located in a thesis may be subject to specific use constraints, details of which may not be explicitly described. It is the responsibility of potential and actual users to be aware of such constraints and to abide by them. By making use of material from a digitised thesis, you accept these copyright and disclaimer provisions. Where it is brought to the attention of Trinity College Library that there may be a breach of copyright or other restraint, it is the policy to withdraw or take down access to a thesis while the issue is being resolved.

Access Agreement

By using a Digitised Thesis from Trinity College Library you are bound by the following Terms & Conditions. Please read them carefully.

I have read and I understand the following statement: All material supplied via a Digitised Thesis from Trinity College Library is protected by copyright and other intellectual property rights, and duplication or sale of all or part of any of a thesis is not permitted, except that material may be duplicated by you for your research use or for educational purposes in electronic or print form providing the copyright owners are acknowledged using the normal conventions. You must obtain permission for any other use. Electronic or print copies may not be offered, whether for sale or otherwise to anyone. This copy has been supplied on the understanding that it is copyright material and that no quotation from the thesis may be published without proper acknowledgement.

PhD in Pharmacy

The Design, Synthesis and Biological Evaluation of

Novel Multiple Targeting Anti-Cancer Agents

By

Brian William Moran ((B.A.) Mod.))

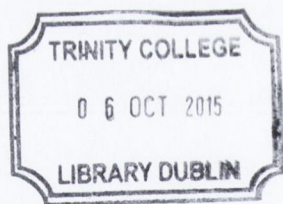A thesis presented to the University of Dublin for the degree of Doctor of Philosophy.

Based on research carried out under the supervision of

Dr. John J. Walsh

School of Pharmacy and Pharmaceutical Sciences

Trinity College Dublin

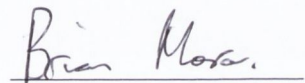## August 2015

Declaration

The work described in this thesis has not been submitted as an exercise for a degree at any other university. The work described herein is entirely my own, except where duly acknowledged. I agree that the library of the University of Dublin, Trinity College Dublin may lend or copy this thesis on request.

Brian William Moran

Abstract

The purpose of the work undertaken within this project was to design and synthesis novel anti-cancer targeting compounds building upon previous work undertaken under the supervision of Dr. John J. Walsh in the School of Pharmacy and Pharmaceutical Sciences.

The thesis is introduced with a brief overview of the hallmark traits associated with carcinogenesis developing a particular emphasis on those relating to the tumour's vasculature. A discussion of the various anti-angiogenic treatments in the clinic are discussed with those targeting the vacscular endothelial growth factor (VEGF) pathway given a particular emphasis, before discussing the matrix metalloproteinases (MMPs) and Aminopeptidase N (APN), enzymes involved in the degradation of the extracellular matrix (ECM) which facilitate the transformation of tumour growth to malignancy and their endogenous and synthetic inhibitors. Following this, the discussion of vasculature targeting agents in the treatment of cancer will place emphasis on those targeting the colchicine binding site of tubulin, the dimeric protein which assembles to form the microtubular network important in the cell cycle. Finally, the introductory chapter is concluded with a statement of the overarching aims of the work described herein involving the conjugation of anti-angiogenic compounds to a pre-existing anti-vascular targeting scaffold in the evolution of novel multiple targeting anti-cancer chemotherapeutics.

Chapter 2 focuses on the synthesis of novel merged designed multiple ligands (DMLs) expanding upon the pharmacophore developed during previous work outlined within the group leading to the design of novel compounds that target multiple pathways implicated in the pathogenesis of cancer. This is achieved by fixing the hydroxamic acid moiety shown in Chapter 1 to inhibit APN and MMPs to the pre-existing anti-proliferative and anti-tubulin

polymerisation agent scaffold. The evaluation of the biological activity of these compounds is also described.

The work in Chapter 3 was directed towards the expansion of the pre-existing pharmacophore by the migration of an important ketone to an adjacent carbon in attempts to lead to the development of a novel family of tubulin-targeting compounds while circumventing certain issues involved in the synthesis of the already established compounds. The synthetic methods employed are described in addition to analysis of the problematic synthetic steps faced.

In Chapter 4, it is aimed to combine the anti-tumour effect of curcumin with that of the established pharmacophore employing a fused DML mode to attach the 1,3-diketone functionality exhibited in curcumin. The successful synthetic approach to hybrid compound *(4.18)* in addition to its evaluated biological activity is described.

In Chapter 5, the phenolic position and the B-ring alcoholic position is manipulated to provide an attachment point for a succinate linker to synthesis three novel hybrids with dihydroartemisin, a compound shown to induce anti-tumour effects including anti-migratory and anti-angiogenic effects. A detailed discussion of the NMR spectra of the first hybrid synthesised using the methods described in this chapter is included alongside biological evaluation in PC-3 cell based assays.

Chapter 6 describes the synthetic protocols employed towards completion of the synthesis of compounds described in Chapters 2-5. This is accompanied by spectral determination of each of these compounds.

Chapter 7 describes the biological protocols employed to evaluated the effect of the compounds synthesised on APN activity, cell proliferation and cell migration.

Table of Contents

Table of Figures

Table of Schemes

Table of Tables

Table of Graphs

List of Abbreviations

%	Per cent
^{13}C NMR	Carbon Nuclear Magnetic Resonance
^{1}H NMR	Hydrogen Nuclear Magnetic Resonance
5-FU	5-fluorouracil
AHPA	(2S,3R) 3-amino-2-hydroxy-4-phenylbutanoic acid
ALL	Acute lymphoblastic lymphoma
APB	Aminopeptidase B
APN	Aminopeptidase N
Asp	Aspartic acid
BAEC	Bovine endothelial aortic cells
bFGF	Basic Fibroblast growth factor
Boc	*tert*-butyl carbamate
BuLi	n-butyllithium
CA-1-P	Combretastatin A-1 phosphate
CA-4	Combretastatin A-4
CA-4-P	Combretastatin A-4 phosphate
CD13	Cluster differential 13
CO_2	Carbon dioxide
CTCL	Cutaneous T cell lymphoma
DCC	*N,N'*-Dicyclohexylcarbodiimide
DCM	Dichloromethane
DHA	Dihydroartemisinin
DIBAL	Diisobutylaluminium hydride
DMAP	*N, N*-dimethylaminopyridine

DMF	*N, N*-dimethylformamide
DML	Designed multiple ligand
DMP	Dess-Martin periodinane
DMSO	Dimethylsulfoxide
DMXAA	(5,6-Dimethyl-9-oxo-9*H*-xanthen-4-yl)-acetic acid
DNA	Deoxyribonucleic acid
DR5	Death receptor 5
EC	Endothelial cell
EDCI	1-ethyl-3-(3-dimethylaminopropyl)carbodiimide
EtOAc	Ethyl acetate
EtOH	Ethanol
FDA	Food and Drug Administration
Fmoc	Fluorenylmethyloxycarbonyl
g	Gram
GTP	Guanosine tri-phosphate
h	Hours
H_2O_2	Hydrogen peroxide
HDAC	Histone deacetylase
HIF 1α	Hypoxia inducible factor
HPV	Human papillomavirus
HRMS	High resolution mass spectrometry
HUVEC	Human umbilical vein endothelial cell
IC_{50}	Half maximal inhibitory concentration
IR	Infra-red
kDa	Kilodalton
LDA	Lithium diisopropylamide
Leu	Leucine

LiAlH$_4$	Lithium aluminium hydride
LTA$_4$H	Leukotriene A-4 hydrolase
M	Moles/Litre
m/z	Mass per charge ratio
MAPK	Mitogen activated protein kinase
MCPBA	*meta*-chloroperoxybenzoic acid
MDR1	Poly-glycoprotein
MeOH	Methanol
Mg	Magnesium
mg	Milligram
MHC	Major histocompatibility complex
min	Minutes
mL	Millilitre
MMP	Matrix metalloproteinases
MMPs	Matrix metalloproteases
MT	Microtubule
MTD	Maximum tolerated dose
MT-MMP	Membrane-type matrix metalloproteinase
MTT	3-(4,5-dimethylthiazol-2-yl)-2,5-diphenyltetrazolium bromide
NaBH$_4$	Sodium borohydride
NaCN	Sodium cyanide
NaHCO$_3$	Sodium bicarbonate
NaHMDS	Sodium bis(trimethylsilyl) amide
NaOH	Sodium hydroxide
NBS	*N*-bromosuccinimide
NF-κβ	Nuclear factor κβ

NGR	Asparagine-Glycine-Arginine
NP	Nanoparticle
NSCLC	Non-small cell lung cancer
°C	Degrees celcius
PBr_3	Phosphorous tribromide
PC-3	Prostate cancer-3
PDC	Pyridinium dichromate
PDGF	Platelet derived growth factor
PFP	Pentafluorophenol
Phe	Phenylalanine
PLGA	Polylactic-glycolic acid
PPA	Poly-phosphoric acid
Pro	Proline
PyBrop	Bromo-tris(pyrrolidino)-phosphonium hexafluorophosphate
R_f	Retardation factor
RGD	Arginine-Glycine-Aspartic acid
RTK	Receptor Tyrosine Kinase
SAPK	Stress activated protein kinase
SAR	Structure-activity relationship
SARS	Severe acute respiratory syndrome
SEM	Standard error from the mean
SN_2	Bimolecular substitution
$SnCl_4$	Tin (IV) tetrachloride
TBAF	Tetrabutyl ammonium fluoride
TBDMS	*tert*-butyldimethylsilyl
TBDMSCl	*tert*-butyldimethylsilyl chloride

TBDPS	*tert*-butyldiphenylsilyl
TBDPSCl	*tert*-butyldiphenylsilyl chloride
TBDPSOH	*tert*-butyl diphenylsilanol
TC	Tip cell
TFA	Tri-fluoroacetate
TGEV	Transmissible gastroenteritis virus
TGFβ1	Transforming growth factor beta 1
TIMP	Tissue inhibitors of metalloproteinases
TLC	Thin layer chromatography
TNF-α	Tumour necrosis factor α
uPA	Urokinase plasminogen activator
UV	Ultra-violet
Val	Valine
VEGF	Vascular endothelial growth factor
VEGFR	Vascular endothelial growth factor
VTA	Vasculature targeting agent
WHO	World Health Organisation
ZBG	Zinc binding group
μm	Micrometre

Acknowledgements

I would firstly like to thank Dr John Walsh, without whom there would never have been a project in the first place. I'd like to thank him mainly for always being there when needed and providing supervision and guidance throughout the past few years. It will always be appreciated.

I'd also like to thank the technical staff who helped out throughout the project. Dr. John O'Brien and Manuel Ruether for using their expertise in NMR, without which I would never have managed to complete this project. Similarly I extend great thanks towards Brian Talbot for running the HRMS samples. Also I am extremely grateful to the School of Pharmacy as a whole for always being reliable to lend help when required, in particular to the technician Joe Reilly.

Without the other members of the group who have shared their time with me, the last four and a half years would have been a whole lot more difficult. Thank you to Katerina, Adrian, Gary and Elaine in particular for always understanding any crazy moods over the time and as well to the people who have already left the group Orla, Tao, Deirdre and Paul for providing all kinds of guidance and support. I have been lucky to be in a Department populated with many great people and the team of postgraduates who have shared the lunch room and coffee times with me. I've had many good times with you all and hope to keep in touch with you.

I am extremely grateful for the people who have helped me out through the past few months with any proof reading that has been asked of you.

Thanks to all my friends who have kept me sane or at least tried their very best! I look forward to being reintegrated into the group again.

My family, in particular my mother Maire have always been there for me and helped me out in so many different ways. The constant support I received from herself, my father Paul, my sisters Claire and Niamh and my brother Ciaran were always needed. Without it, I'd have never have made it here. Thank you so much.

Finally, I'm sure there's somebody out there who's been forgotten about, so thank you and please forgive my forgetfulness!

Chapter 1: Introduction

1.1   An overview of cancer.

Worldwide, second only to heart disease as the leading cause of death is a collection of over 200 diseases affecting a large amount of different tissues known as cancer, or malignant neoplasia, accounting for approximately 7.6 million deaths per year (or approximately 23% of all deaths) according to recent statistics.[1] With incidence rates expected to increase by the year 2020 to approximately 15 million new cancer diagnoses and 12 million cancer deaths annually,[2] strong efforts are being made to bring new means of therapy to fight this cancer epidemic. In an Irish context, this equates to a current average of 8,000 deaths and 30,000 new diagnoses per year,[3] expected to rise to over 40,000 per year by the year 2020.[4]

All cancers exhibit one similar disease trait in particular, namely a fundamental abnormality resulting in the unregulated, rapid division and proliferation of cells in a localised area of tissue leading to the formation of a mass known as a tumour. These tumour cells possess the ability to invade local parts of the body and also to further advance to more distant organs through a process of metastasis forming secondary or tertiary tumours in these distal locations. A tumour growth in itself is not necessarily diagnostic of cancer. Unlike cancerous malignant tumours, benign tumours are those that do not possess the ability to metastasise, thus not leading to progression towards the malignant disease state.[5]

Initially tumour cell growth is localised to the affected part of the body, the most common organs affected being the lung, prostate, colon, stomach and liver in men and breast, colon, cervix, lung and stomach in women.[1] As expected by such diverse locations of disease discovery, a broad array of signs and symptoms of cancer manifest themselves, dependant upon the locality of the cancer growth and metastatic state. For example, in cancer of the colon,

changes in bowel functions are often noticed, while in the case of breast cancer a lump on the breast is commonly observed.[6] The symptoms arise from the tumour growing to such a size that it will begin to encroach on nearby organs, blood vessels, and nerves. The resultant pressure on the local environment results in these cancer symptoms. Depending on the disease's location, symptoms will be noticed earlier in the carcinogenesis allowing a better clinical outcome. Pancreatic cancers unfortunately tend to grow to too large a size before exhibition of stomach or back pain upon interaction with nearby nerves. However, development of such symptoms tends to occur subsequent to metastasis, complicating treatment and leading to a relatively high rate of mortality.[7] In contrast, more visible tumours such as testicular cancers tend to lead to higher survival rates due to the symptomatic lump being visible at an earlier stage. Figure 1.1 illustrates occurrence of the multitude of cancers and their respective contribution towards total cancer deaths in men and women.

Estimated New Cases*

			Males	Females			
Prostate	217,730	28%		Breast	207,090	28%
Lung & bronchus	116,750	15%		Lung & bronchus	105,770	14%
Colon & rectum	72,090	9%		Colon & rectum	70,480	10%
Urinary bladder	52,760	7%		Uterine corpus	43,470	6%
Melanoma of the skin	38,870	5%		Thyroid	33,930	5%
Non-Hodgkin lymphoma	35,380	4%		Non-Hodgkin lymphoma	30,160	4%
Kidney & renal pelvis	35,370	4%		Melanoma of the skin	29,260	4%
Oral cavity & pharynx	25,420	3%		Kidney & renal pelvis	22,870	3%
Leukemia	24,690	3%		Ovary	21,880	3%
Pancreas	21,370	3%		Pancreas	21,770	3%
All Sites	789,620	100%		All Sites	739,940	100%

Estimated Deaths

			Males	Females			
Lung & bronchus	86,220	29%		Lung & bronchus	71,080	26%
Prostate	32,050	11%		Breast	39,840	15%
Colon & rectum	26,580	9%		Colon & rectum	24,790	9%
Pancreas	18,770	6%		Pancreas	18,030	7%
Liver & intrahepatic bile duct	12,720	4%		Ovary	13,850	5%
Leukemia	12,660	4%		Non-Hodgkin lymphoma	9,500	4%
Esophagus	11,650	4%		Leukemia	9,180	3%
Non-Hodgkin lymphoma	10,710	4%		Uterine Corpus	7,950	3%
Urinary bladder	10,410	3%		Liver & intrahepatic bile duct	6,190	2%
Kidney & renal pelvis	8,210	3%		Brain & other nervous system	5,720	2%
All Sites	299,200	100%		All Sites	270,290	100%

Figure 1.1: The areas of the body most susceptible to cancer cases and deaths.[8]

The initiation of tumourigenesis is caused by a series of dynamic changes in the genome, either as a result of hereditary or environmental stimuli. It must be noted that ideal control of environmental and lifestyle factors can actually play a very important role in cancer prevention. A recent report states that approximately 90-95% of all cancer cases are derived from easily variable lifestyle and environmental factors whereas just 5-10% of cases are resulting from genetic predisposition to the contraction of cancer.[9] This point is exemplified by studies of the relative incidences of breast cancer in identical twins where in only 20% of cases did both twins develop cancerous growths.[10] Prominent examples of the lifestyle and environmental factors inducing cancer development are tobacco use (responsible for 25-30% of total cancer deaths and 87 % of lung cancer deaths),[11] alcohol abuse,[12] diet,[13] obesity [14], oncoviruses such as hepatitis B[15] and Human papillomavirus (HPV),[16] as well as exposure to radiation such as UV light.[17] Taken into consideration with the presence of a variety of naturally occurring cancer preventative compounds in many fruits, vegetables and spices such as reservatrol,[18] lycopene,[19] curcumin [20] and capsaicin,[20b] it is shown that the promotion of simple improvements in lifestyle could pre-empt new cancer cases serving to reduce the increasing burden of cancer on society.

However such improvements alone would not lead directly to the complete removal of cancer as a threat to human life, necessitating the development of improved therapeutic methods. Recent developments in the understanding of cancer have led to increasing optimism regarding the development of new treatments for cancer counteracting the drawbacks associated with current clinical practises.

1.1.1 Treatment of cancer.

As cancer is not just one disease, but a large family of many diseases exhibiting similar properties of uncontrolled cell growth, there is a necessity for a number of different therapeutic regimes, depending upon the type of cancer and on the extent of tumour progression. The methods for the treatment of cancer often involve surgery, chemotherapy and radiation therapy used either in isolation or in a certain combination. Historically the primary method has been

surgery,[21] still finding clinical use today, especially for the removal of solid, isolated, pre-metastatic tumours and common cancers such as breast and testicular cancer. Adjuvant chemotherapy can be used either before or after surgery to reduce the tumour size simplifying surgery, or to aid the prevention of a cancer relapse post-surgery. Provided that there has been no spread to other parts of the body, this course can lead to complete tumour removal.

Radiation therapy is the use of targeted ionising radiation to damage the DNA and subsequently kill malignant cells. It mainly finds use in the treatment of localised cancers, as post-operative prevention of tumour relapse or in conjunction with cancer chemotherapy.[22] The suitability of this treatment is limited to localised tumours, as radiation is best contained to as few parts of the body as possible as the radiation can kill healthy cell along with cancer cells. This method finds best use in non-melanoma skin cancer, breast cancer, non-small cell lung cancer, cervical cancer and prostate cancer. Although leukaemias are known to be highly sensitive to radiation, this type of treatment is not usually used due to the large spread of these cancers throughout the body. On a side note, the use of radiation can be useful in the facilitation of tumour visualisation,[23] the targeting of drugs to tumours[24] and in a non-clinical setting to study drug and protein interactions.[25]

From a medicinal chemistry standpoint, the most interesting form of cancer therapy is chemotherapy. Initial chemotherapy regimens relied on direct interactions with DNA including its alkylation by cis-platin *(1.01)* and the nitrogen mustards including mustine *(1.02)* or intercalation between strands by anthracyclines such as doxorubicin *(1.03)*.[26] The interruption of the cell division cycle by targeting rapidly proliferating cells is another paradigm in cancer treatment as shown by the anti-cancer effects of the antimitotic tubulin targeting agents such as paclitaxel *(1.04)*[27] and the cytostatic family of drugs known as the anti-metabolites[28] including 5-fluorouracil (5-FU) *(1.05)*.

Figure 1.2: Cancer chemotherapeutic agents *(1.01) - (1.05)*.

Although these traditional approaches prove to be successful in elimination of cancer cells, their inherent non-selectivity also target normal cells with rapid cell division physiology including those in the bone marrow, gastrointestinal tract and hair follicles manifesting itself in the debilitating side effects associated with these treatments including depression of the immune system,[29] nausea,[30] alopecia, infertility[31] and neurotoxicity[32] limiting the therapeutic potential of these chemotherapeutics. Other disadvantages to certain chemotherapies is the increased resistance due to the emergence of efflux pumps such as the P-glycoprotein (MDR1) reducing the intracellular drug concentration serving to diminish its therapeutic effect.[33] Additionally it is possible for the cancer cell to develop mutations resisting the chemotherapeutic effect.[34] Resulting from these inherent disadvantages associated with traditional anti-cancer medications research such, as that described in this thesis, into nullifying negative therapeutic outcomes associated with cancer is necessary. This can be achieved through the development of novel chemotherapeutics exploiting specifically pathological differences between healthy quiescent cells and the rapidly proliferating tumour cells, a more achievable task due to much research into the mechanisms underlying carcinogenesis.

5

1.2 The cellular hallmarks of cancer.

In order facilitate more selective forms of chemotherapy, it is essential to have a firm understanding of the mechanisms with which the disease progresses. Cancer is a disease state ultimately initiated by a series of mutations of the genome, as previously noted due to extrinsic or intrinsic factors. The development of cancer is a multistage process reflecting these gene's alterations, leading to the transformation of normal cells into highly malignant derivatives.[35]

There are three major families of genes implicated in tumorigenesis.[35] These are termed oncogenes, tumour suppressing genes and stability genes. Mutations of oncogenes such as SRC,[36] RAS[37] and MYC[38] lead to deregulated activation of the genes and therefore increased expression of proteins implicated in cancer development. Conversely tumour suppressor genes, including TP53[39] and RB1,[40] upon alteration lead to the downregulation of the proteins they control which tend to protect the progress of cancer. Stability genes, for example BCRA1[41], are those involved in maintaining the integrity of DNA and in its replication during mitosis. When these regulatory genes are inactivated, a rapid increase in mutations of other genes is observed potentially leading to changes in oncogenes and tumour suppressor genes. In undergoing these changes, the physiology of the cells are altered and begin to exhibit what have classically been known as the hallmarks of cancer.[5b, 42]

It has been accepted that cancer is the manifestation of at least six alterations of normal body function, working in tandem towards malignancy. These hallmarks are identified as the ability of the tumour to deregulate normal growth signals thus developing (1) self-sufficiency in growth signals and (2) becoming insensitive to the host body's own anti-growth signals, (3) the ability to evade apoptosis, (4) the ability of cells to become immortal and replicate without limits, (5) the sustained development of new blood vessels servicing the tumour, a process

known as angiogenesis and (6) the invasion of cells into nearby tissues and subsequent metastasis.

This loss of normal cell cycle regulation in the manifestation of each of these hallmarks is achieved through an increased expression of proteins associated with cancer in addition to the downregulation of those preventing cancer. These upregulated proteins afford molecular targets which can be selectively targeted to exert an anti-cancer effect. In a disease state as complex as cancer, the targeting of pathways mediated by one such protein can be compensated for by the activation of other pathways as is exemplified by the observed compensatory upregulation of basic Fibroblast Growth Factor (bFGF) in response to vascular endothelial growth factor (VEGF) inhibition in anti-angiogenic treatment.[43] The targeting of cancer is made a more difficult task as a result. Accordingly, a single drug entity with the ability to target multiple pathways would be more beneficial in cancer treatment than one obeying the often repeated "one compound, one target" mantra.[44]

The aim of the work described in this thesis is therefore to design compounds exerting effects on multiple molecular targets implicated in tumourigenesis with a particular focus addressing the reorganisation of the existing tumour vasculature in addition to the modulation of the hallmark of angiogenesis.

1.3 Angiogenesis

An adequate blood supply is vital to the development of an emerging tumour mass. In order to acquire the required O_2 and nutrients for continued proliferation, in addition for adequate removal of cellular debris, each cell in the developing tumour mass should ideally be within 100-200 μm of the nearest capillary vessel.[45] Accordingly, the reorganisation of the solid

tumour's vasculature is necessary to afford such rapid continued growth upon reaching a critical mass of 2 mm^3.[46] The physiological process of angiogenesis serves to address this issue.

Angiogenesis is the development of new blood vessels from pre-existing vasculature, playing an essential role during growth and development, wound healing and menstruation.[47] In these cases, it is a tightly regulated process kept firmly in balance by the equilibrium between pro-angiogenic and anti-angiogenic factors outlined in Figure 1.3. In the adult human, the majority of cells in the vasculature reside in their quiescent state with 0.01% of these endothelial cells in the cell cycle. In the "angiogenic switch", the activators of angiogenesis including vascular endothelial growth factor (VEGF), platelet derived growth factor (PDGF) and the matrix metalloproteinases (MMPs) are upregulated, activating the resting endothelial cells to grow new capillaries facilitating neovascularisation.[48] This pathogenic angiogenesis is observed in diseases including artherosclerosis,[49] age related macular degeneration,[50] psoriasis[51] and cancer.[52] While physiological angiogenesis is typically a short term process, pathological angiogenesis lasts longer, potentially occurring for several years resulting in increasingly disordered vascular structures.[53] Since the discovery of the importance of angiogenesis in metastasis by Folkman in 1971,[54] it has served as an well researched topic for therapy with the aim of cutting off the blood supply to tumours in a non-toxic manner through the exploitation of the alterations between the neovasculature and the typical quiescent vasculature associated with normal functioning tissues. While a number of anti-angiogenic agents have reached the clinic including bevacizumab, it has not proven to be the envisaged "silver bullet" cancer cure, finding greater use as adjuvant agents in combination with other chemotherapeutic agents.[55] In Figure 1.3, the endogenous factors involved in maintaining the angiogenic balance are listed with a schematic illustrating the difference between an angiogenic effect and an anti-angiogenic effect.
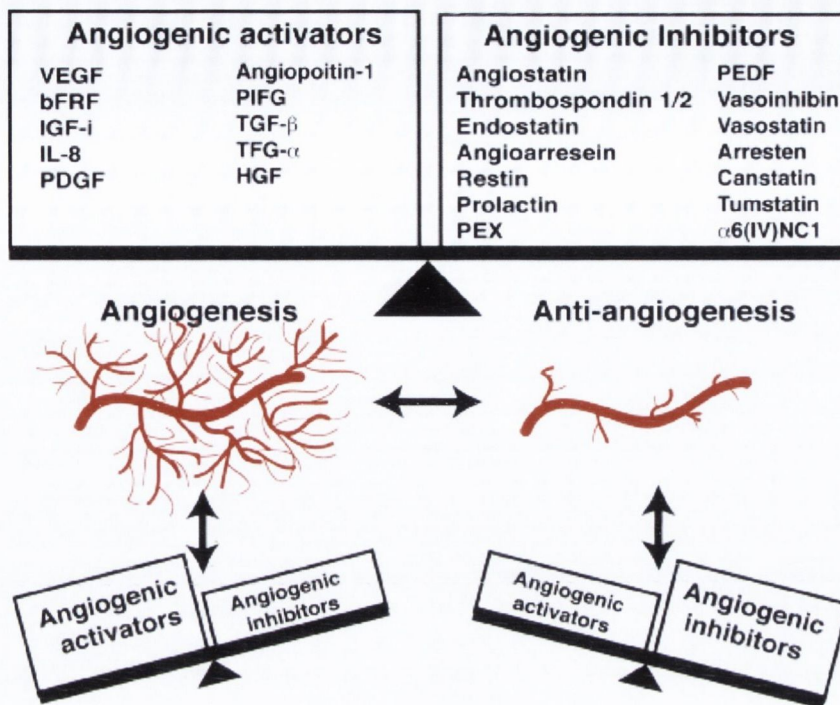
Figure 1.3: Endogenous factors involved in the angiogenic switch.[56]

1.3.1 The angiogenic process

The "angiogenic switch" is the response to certain stimuli shifting the tightly regulated balance between pro-and anti-angiogenic factors towards those promoting the process.[57] In the context of the tumour microenvironment, this is mainly the metabolic stress induced by the increased acidic and hypoxic conditions leads to the increased stability of the α subunit of hypoxia inducible factor 1 (HIF-1α),[58] consequently upregulating the growth factors involved in angiogenic process, VEGF, bFGF and PDGF. In "sprouting angiogenesis", these growth signals activate the nearby endothelial cells to enter the cell cycle and proliferate while extracellular proteinases are activated degrading the extra-cellular matrix (ECM) promoting the migration of endothelial cells (ECs) to vascularise the nearby tumour mass. These activated ECs cells, known as tip cells (TCs) develop protrusions guided into the tumour microenvironment towards other TCs.[59] The developing protrusion is supplemented by the slower movement of other endothelial cells known as stalk cells acting to support the developing neovascular structure forming a new

embryonic lumen, becoming fully formed upon linking of two branches of TCs as illustrated in Figure 1.4.
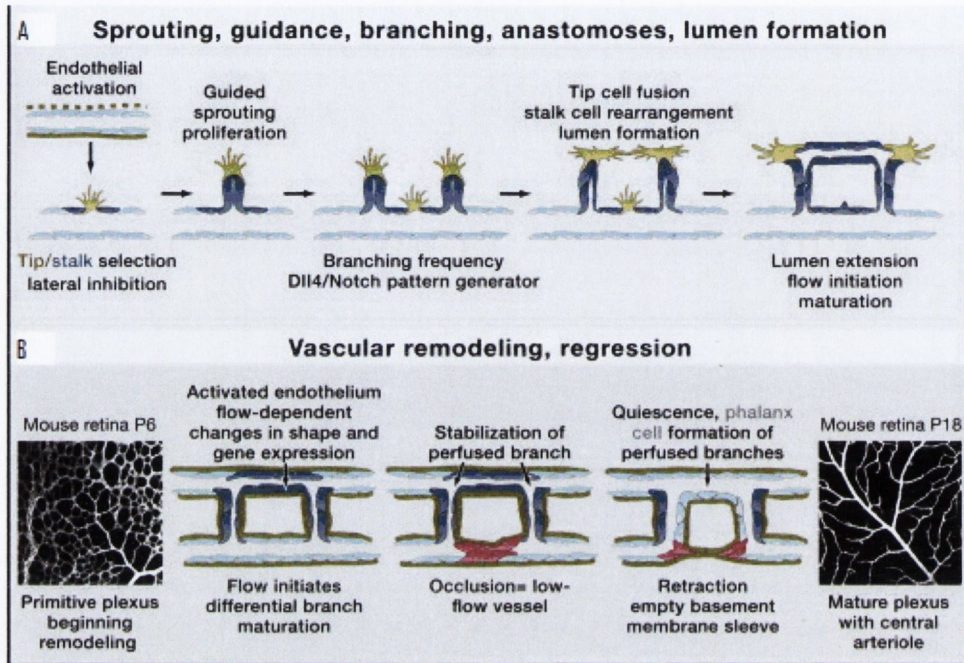
Figure 1.4: The normal physiological angiogenic process.[60]

Whereas in physiological angiogenesis, the attachment of tip cells, a process known as anastomoses leads ultimately to swift reestablishment of EC quiescence, the angiogenic effect is more prolonged in cancer. The effect of prolonged angiogenesis in the disease state compared to physiological angiogenesis is to prevent the completely adequate reformation of the ECM or the pericyte support network associating fully to the neovasculature.[61] The vascular network of the tumour mass is therefore not able to reach the same maturity as those in normal cells generally observed as being leakier and of irregular size with significant observed variance in their blood flow throughout the tumour.[62] These differences are significant enough to theoretically provide suitable methods for selective drug targeting. Figure 1.5 illustrates the difference between the disordered tumour vasculature and the more hierarchial ordered normal vasculature.
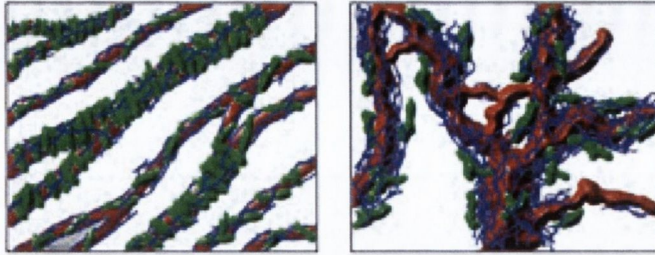
Figure 1.5: Visualisation of the more ordered vascular network in normal functioning cells (left) by comparison to the tumour's disordered network (right).[62]

The most common targets for anti-angiogenic treatment are the growth factor pathways, with that of VEGF being the most studied, and the peptidases involved in the breakdown of the ECM componnts including the matrix metalloproteinases (MMPs) and urokinase plasminogen activator (uPA).

Additionally, the clinical use of endogenous inhibitors of angiogenesis including endostatin[63] and thrombospondin-1 to re-establish the angiogenic equilibrium has been investigated in the treatment of lung cancer and metastatic melanoma respectively.[64] Treatment using these agents has not shown the anticipated results as of yet, with more work required to generate a greater effect.[65]

1.3.2 Vascular endothelial growth factor.

The most important signalling pathways in angiogenesis induction are mediated through VEGF. Members in VEGF family of growth factors (GF) include VEGF A, B, C, D and placental growth factor (PGF), which interact with their tyrosine kinase receptors VEGFR 1, 2 and 3, mainly showing an angiogenic effect through VEGFA.[66] Although VEGFR-1 is shown to have a 10-fold greater binding affinity to VEGFA, the major signalling effect in this pathway for initiation of sprouting angiogenesis occurs through the VEGFR-2 receptor. It is thought the added affinity towards the relatively inactive VEGFR-1 sequesters VEGFA from circulation,

controlling the pathway.[67] VEGFC is implicated in lymphangiogenesis through binding to VEGFR-3, a similar process to angiogenesis developing new lymphatic vessels from the pre-existing lymphatic vessels.[68]

The VEGF action is generally mediated through a paracrine pathway-the tumour cells do not express large levels of receptors, and the increased secretion of the growth factors into the extracellular space interact with the receptors on local ECs, which in contrast produce very little VEGF.[69] However VEGF can be introduced from normal blood circulation under increased recruitment of platelets whose alpha granules contain concentrated levels of VEGF, bFGF and anti-mitogenic agents including endostatin.[70] Upon binding to receptors, VEGFA catalyses the dimerisation of the receptor tyrosine kinase, exerting an effect through a number of pathways resulting in increased vascular permeability, migration and expression of MMPs among other events in the development toward malignancy.

1.3.2.1 Anti-VEGF treatment

Inactivation of VEGF signalling pathways has been shown to have clinical benefit, with the FDA approved treatments targeting this pathway including the monoclonal antibody bevazicumab (Avastin) approved in 2004 for the treatment of colorectal cancers and in 2006 lung cancer,[71] and the multi-targeting receptor tyrosine kinase (RTK) inhibitors including sunitinib *(1.06)* and sorafenib *(1.07)*, both used for the treatment of kidney cancer,[67] vandetinib *(1.08)* for metastatic thyroid cancer[72] and pazopanib *(1.09)* for treatment of soft tissue sarcoma in relapsing cancer patients.[73] However the use of these agents has found limitations compared to the significance applied upon their discovery. A recent setback for this family of drugs has been the recently revoked FDA approval for Avastin's treatment for breast cancer in 2011 due to safety concerns and its ineffectiveness in delaying the growth of tumours being cited as justification for this decision.[74]
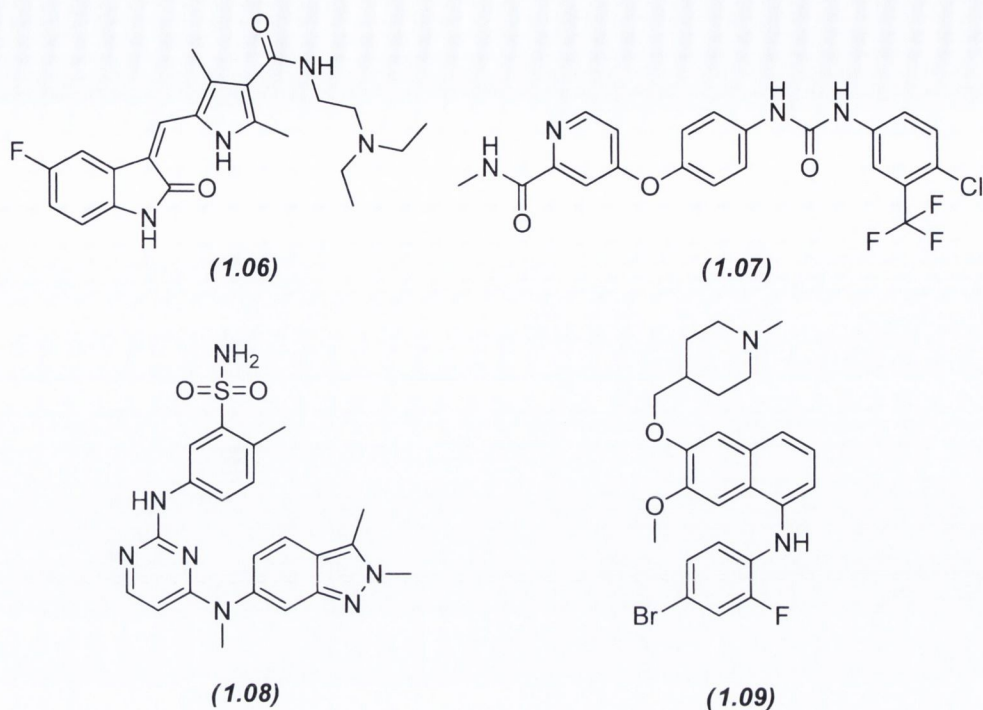
Figure 1.6: Small molecule RTK inhibitors (1.06) - (1.09).

Avastin is a monoclonal antibody which derives its activity upon binding to the circulating VEGF preventing its interaction with the VEGFRs, acting in a sense as an anti-growth factor. Its clinical use has mainly been found as a first line treatment, for example in the treatment of colorectal cancer in combination with 5-FU *(1.05)*, with oxaliplatin in the treatment of lung cancers and paclitaxel in the treatment of advanced nonsquamous non-small cell lung cancer (NSCLC).[75] The benefits associated with Avastin treatment are not as measurable as was once expected upon discovery, with survival rates measured in the months as opposed to years. Though highly specific for targeting VEGFA, in the tumour mass, upregulation of other growth factors including bFGF has been observed allowing compensation for the diminished VEGF signalling effect and the subsequent resistance to this form of treatment rendering it useless in the case of relapse.[43] Additionally it has been shown unsuitable for use in the adjuvant setting in colon cancer cases,[76] while safety concerns over the increased incidences of embolism in patients have been raised.[77]

Other monoclonal antibodies (mAbs) operating in a similar mode include cetuximab, commonly used in monotherapy for treatment of metastatic colorectal cancer and panitumumab for the same disease. These show similar drawbacks with resistance development as Avastin.[78]

Although the specificity of these mAbs for their target proteins is quite a scientific achievement, their lack of promiscuity can be seen as inhibitory to their ultimate use, owing to the swift development of resistance to their treatment. Consequently, therapeutic use has been found for the compounds in Figure 1.6, which are all small molecule inhibitors of the VEGF receptors.[79] While not specific targets for one enzyme, the inherent promiscuity associated with small molecules allows for the theoretical shutdown of multiple pathways preventing compensatory mechanisms taking effect. These compounds all target multiple RTKs, also proving beneficial owing to their relative ease of administration and lowered cost compared to mAb treatment.

The VEGF pathway induces expression of MMPs, which degrade the collagen supported ECM. While anti-VEGF treatments should prevent the expression of these proteinases, much research is underway towards the development of their inhibitors diminishing their role in angiogenesis and the subsequent development of metastatic disease.

1.3.3 Matrix metalloproteinases (MMPs)

The MMPs are a large family containing at least 23 Ca^{2+} dependent peptidases possessing an active site containing a Zn^{2+} metal centre.[80] Upon activation by VEGF, their principal role is to degrade and remodel the ECM, a matrix containing a complex array of collagens, elastins, fibronectin and proteoglycans to provide a support structure to the EC structure maintaining the integrity of connective tissues. Several crystal structures of MMPs have been published,[81] with Figure 1.7 showing the activated form of MMP-1.
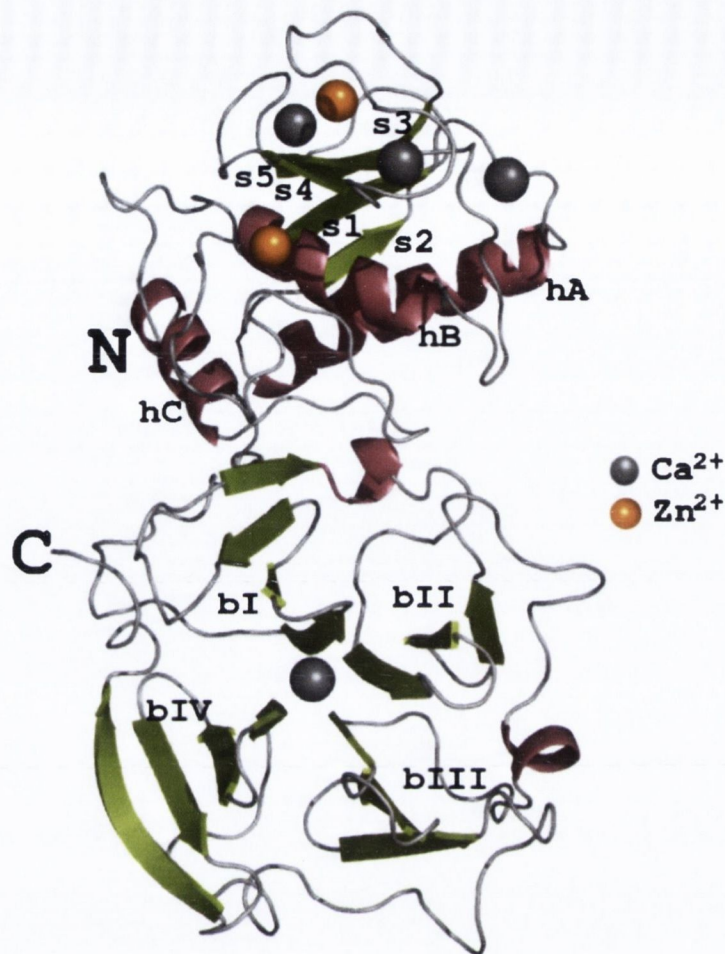
Figure 1.7: Crystal structure of activated MMP-1.[82]

Accordingly, each MMP is classified into groups including the gelatinases, collagenases stromelysins, membrane type MMPs (MT-MMPs) and matrilysins dependent upon the matrix component type. High expression of MMPs has been associated with a wide range of inflammatory pathologies including multiple sclerosis,[83] osteoarthritis,[84] Crohn's disease[85] and cancer.[86] The significant members of this type of family in a cancer context are MMP-2 and MMP-9, both gelatinases which degrade gelatin and collagen type IV,[80] in addition to MMP-1, MMP-3, MMP-7 and MMP-13.[86a]

The significant importance of levels of MMPs in cancer metastasis has long been known. Cancers with high expression of MMPs for example have shown greater invasion potential

resulting in higher rates of metastasis. For example, in one study of 83 surgically resected human colorectal cancers were examined for the presence of MMP-7. Those patients containing heightened levels of MMP-7 were shown to have greater invasion potential.[87] Activation of MMP-2 and MMP-9 have similar effects in inducing cell migration and invasion in liver cancers.[88] In MMP-9 positive tumours, a higher recurrence rate and shorter survival time was evidenced in a study of 202 patients with stage II colorectal carcinoma.[89] Similarly heightened MMP expression has been evidenced as an increased factor in liver metastases in pancreatic and colon carcinomas,[90] with MMP-2 expression leading to poor prognosis in colorectal cancer patients.[91] The presence of MMP-2 and MMP-9 has shown poor prognoses in breast cancer cases.[92] Recent studies have conversely shown that lack of expression of MMP-9 is associated with poor prognoses for Duke's B colorectal cancer with the authors postulating the MMP-9 negative cancer patients to be suitable candidates for adjuvant therapy.[93] However in general, the importance of MMP in the metastatic spread of cancer has long been firmly established.[94]

The MMPs possess a conserved active site with a tetrahedrally co-ordinated Zn^{2+} metal centre interacting with three residues and a water molecule, with flexible neighbouring hydrophobic cavities allowing interactions with larger bulky carbon substituents. Cleavage of peptides involves association of the amide carbonyl group to the zinc ion where the side chain associates with the hydrophobic pockets priming itself for nucleophilic attack by water to cleave the peptide bond as in Scheme 1.1. Inhibition of the enzyme often involves interactions with the Zn^{2+} metal centre via chelation to block up this catalytic site.[95]

Scheme 1.1: Mode of MMP mediated cleavage of enzymes.[95]

Of note is the secretion of MMPs into the ECM in zymogenic form, where cleavage by other enzymes including serine proteases, furin and plasmin functions to generate their active forms.[96] This serves to modulate their activity in addition to the control afforded at the transcription level, inducible by enhanced VEGF expression and the inhabitation of their catalytic site by a series of four endogenous cartilage derived tissue inhibitors of metalloproteinases (TIMPs) named TIMP-1, TIMP-2, TIMP-3 and TIMP-4, where overexpression of these results in a corresponding reduction in metastatic disease.[97]

The inhibitory effects of TIMPs showed great promise in mouse and rat models[98] and while interest has been shown in their adoption to treatment of human cancers,[99] these promising results have not been replicated owing to technical difficulties in bringing them to the clinic in adequate amounts.[100] Much research into the potential effect of synthetic MMP inhibitors has also been performed with the majority of them belonging of the hydroxamic acid family as described in Section 1.3.4.2. Although they have found limited use in the clinic thus far, the majority of those studied were non-selective broad spectrum MMP inhibitors exerting influence on physiological functions of MMPs.[100] More recent work is underway towards the development of more selective MMP inhibitors.[96]

17

1.3.4 Aminopeptidase N

Aminopeptidase N (APN), also known as cluster differentiation 13 (CD13),[101] is a Zn^{2+} centred type II metallopeptidase enzyme belonging to the M1 family, shown to play a role in angiogenesis and hence the development of metastatic malignancy.[102] In contrast with the soluble extracellular MMPs, it is normally bound to the cellular membrane. The catalytic site of APN is situated extracellularly with a single transmembrane region and a short intracellular chain seen at its N-terminus. A soluble form of APN in the plasma does exist,[103] however the mechanism of its dissociation from the membrane is as yet unknown. The crystal structure has recently been published in two reports showing binding to a variety of substrates inhibitors and ligands including corona viruses (Figure 1.8),[104] taking shape as a dimeric protein, with each subunit containing a 967 amino acid chain organised into four distinct domains with the catalytic site situated in domain II.[104b]
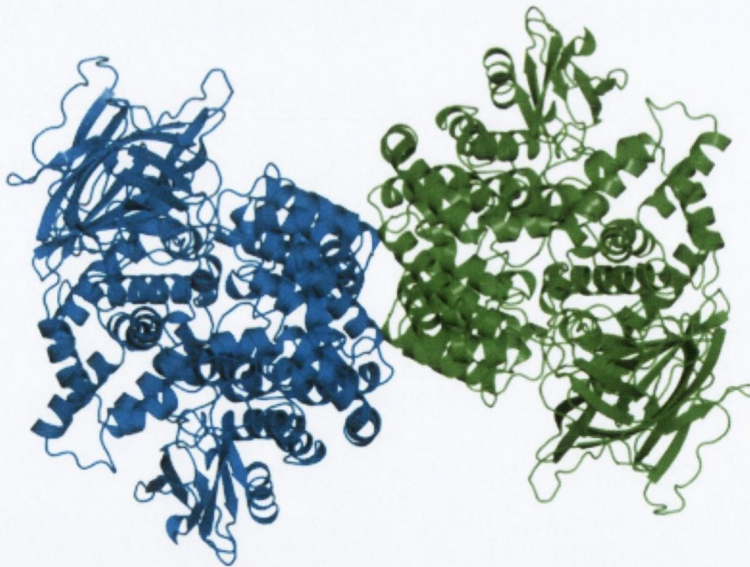
Figure 1.8: Crystal structure of the homodimeric form of aminopeptidase N.[104b]

The functions for such a relatively small protein are many. As a peptidase, it functions by catalysing the cleavage of small neutral peptide chains at the NH_2 terminus with particular affinity shown towards leucine and alanine substrates and resistance towards cleavage of proline amino acids.[105] APN plays a role in a diverse range of physiological processes including the processing of hormones.[106] In the immune system they are involved in the preparation of antigens for their presentation to major histocompatibility complexes (MHC) class II,[107] in addition to the recycling of proteins for further development,[108] and the regulation of cyclins in the cell cycle.[108] The most well described action of APN is in the renin-angiotensin system, where it cleaves angiotensin III's terminal arginine residue generating angiotensin IV to cause vasodilatory effects.[109] Additionally, APN is shown to act as a neuropeptidase for neuropeptides involved in pain pathways.[104b] Endogenous neuropeptides substance P and bradykinin are both natural inhibitors of APN.[110] As a binding receptor, affinity is shown towards coronaviruses including transmissible gastroenteritis virus (TGEV)[104a] and SARS,[111] as a means for viral cell entry via endocytosis. In its function as a signalling receptor, the phosphorylation of mitogen activated protein kinases (MAPKs) is facilitated by APN release of Ca^{2+} in monocytes.[112]

APN has been shown to play an active role in the degradation of the extracellular matrix and capillary tube formation in promotion of angiogenesis and metastasis.[102a, 113] The expression of APN is ubiquitous throughout the body, however it is dramatically upregulated in tumour cells undergoing angiogenesis, showing heightened levels in a variety of cancers, including melanoma, colon, prostate, thyroid, pancreas and lung cancers,[114] associated with the hypoxia induced upregulation of VEGF and bFGF,[102a] correlating with their increased malignancies. Heightened expression of APN is often associated with highly invasive forms of cancer and poor prognoses for patients showing large levels of the protein in plasma, with survival rates halved for patients expressing APN positive tumours.[114b, 115] The observed increase in invasive cancers when APN is expressed suggests that the inhibition of this enzyme would exert anti-migratory effects.

The low expression of APN in normal cells makes it a useful therapeutic target and additionally a marker for targeted therapy of the neoplasm. For example, the physiological development of APN-null mice has shown to proceed unimpaired, with a marked observed reduction in pathological angiogenesis.[116]

1.3.4.1 APN inhibition

Accordingly, research into the development of APN inhibitors has been undertaken with a number of different classes of inhibitors. In addition to the inhibition by bradykinin and substance P,[110] other endogenous inhibitors include elevated concentrations of leucine, proline, L-arginine and a variety of divalent cations including Ca^{2+}, Mn^{2+}, Co^{2+} and Zn^{2+}.[114c]

Similar to the binding site of the MMPs, the catalytic site in domain II of APN contains a Zn^{2+} metal centre. Much of the research into synthetic inhibitors focusses upon their chelation to this zinc. The most commonly studied APN inhibitors include peptide chains containing the unnatural amino acid (2R, 3S) 3-amino-2-hydroxy-4-phenylbutanoic acid (AHPA) *(1.10)*. While AHPA itself does not show great inhibitory activity, its peptides show strong binding due to added interactions with hydrophobic pockets neighbouring the metal centre.

These compounds include peptide chains isolated from the culture broth of *Streptomyces olivoreticuli* including the leucine conjugate of *(1.10)*, bestatin *(1.11)* in addition to its related family of derivatives of including tripeptide phebestin *(1.12)*, tetrapeptides probestin *(1.13)*[117] and amastatin *(1.14)*, which are among the most commonly studied. They all inhibit the enzyme in similar slow-binding competitive inhibitory modes,[118] with their unnatural (2R, 3S) stereochemistry seen as vital for their activity enabling their bidentate coordination to zinc.[119] Bestatin has been described as transition state analogues of the dipeptide substrate Phe-Leu.[120]

The added hydrophobic interactions with the S1' pocket is seen in bestatin, but not AHPA. In the extended peptides, for example probestin, these interactions can further be extended towards the S2' pocket, strengthening their interactions.[121] Figure 1.9 shows the binding mode of bestatin within the catalytic site.
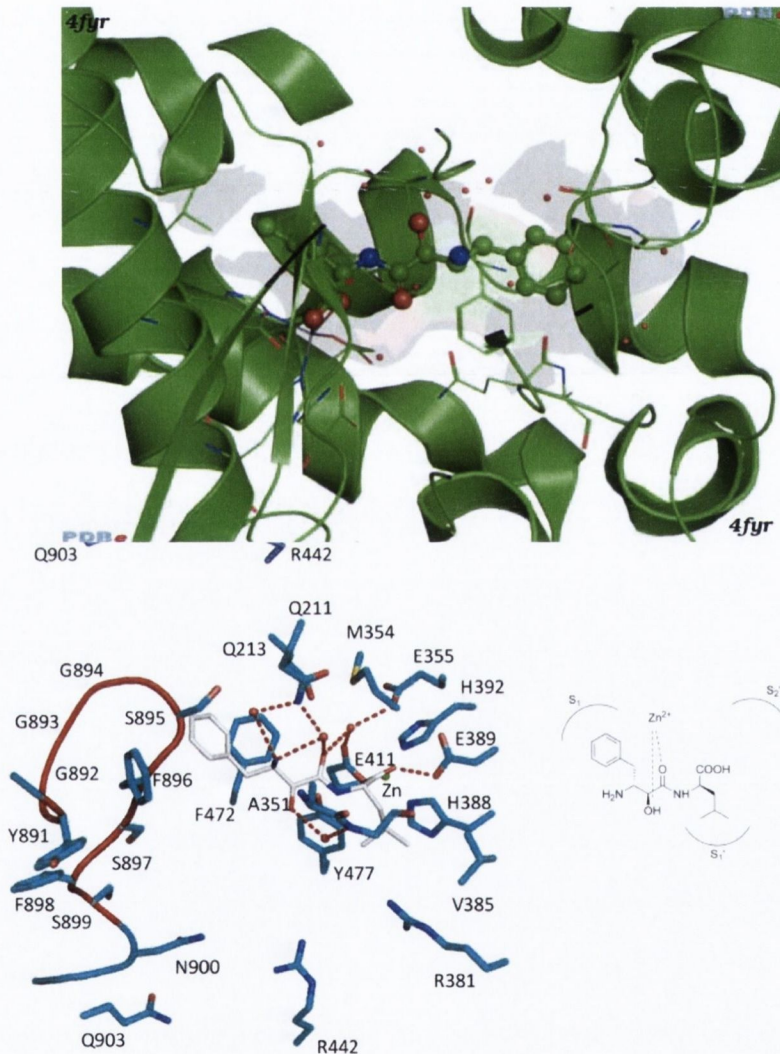
Figure 1.9: Crystal structure of APN showing its binding to bestatin, with molecular interactions shown (bottom). The Zn^{2+} metal centre is shown in green, hydrogen bonds between APN and bestatin are shown in red and APN residues are shown in blue.[104b] Schematic of bestatin binding to APN catalytic site is shown illustrating interactions with the hydrophobic pockets.[121]

Figure 1.10: Structures of AHPA derived unnatural peptides *(1.10)-(1.14)*.

Bestatin is not just an APN specific inhibitor. It also interacts with a host of similar protease enzymes including MMPs and leukotriene A_4 hydrolase (LTA_4H) resulting in degradation of collagen in the ECM. This leads to the consequential inhibition of tumour invasion[122] and the depletion of intracellular amino acids.[123] It has also proven to have an anti-angiogenic effect[124] and to inhibit the formation of active MMP-2[125] and induces apoptosis in NSCLC cell lines.[126] It exerts antiproliferative activity against a range of human leukemic cell lines.[127] In animal studies, it has proven an active anti-angiogenic therapy preventing tube-like formation of endothelial cells in murine B16-B76 melanoma tumours.[128] In clinical use, bestatin has been approved for remission maintenance therapy for acute non-lymphocytic leukaemia[129] and adjuvant therapy for resected stage I squamous-cell lung carcinoma demonstrating significantly prolonged survival.[130] The low toxicity associated with bestatin is advantageous, with just 1.6% of subjects in a test population of 2,225 having shown adverse effects to bestatin treatment. Finally, bestatin has been used in conjugation with radiotherapy in the cervical cancer Hela cell line directing tumour growth inhibition and activating apoptotic pathways.[131] This study followed the discovery that APN activity in this cell line was increased under radiation conditions.

Further isolation of compounds from culture are developing further bestatin analogues, with AHPA-Val *(1.15)* showing a four-fold increase in APN inhibition relative to bestatin's IC_{50} of 20.2 μM,[132] while probestin and phebestin both exhibit more potent IC_{50} values of 50 nM and 400 nM respectively.[114c] Synthesis of bestatin derivatives is still ongoing, uncovering its dimethylaminoethyl ester LYP *(1.16)* which inhibits the angiogenesis of cancer in human ovarian carcinoma ES-2 xenografts in mice.[133] Additionally simplified bestatin analogues *(1.17)-(1.19)* have shown similar activity against APN (K_i=3-10 μM) compared to bestatin (K_i=3.5 μM). Moreover, these compounds show an increased selectivity for APN over its soluble isoforms and APB, an aminopeptidase for which bestatin is also a substrate. Compounds *(1.18)* and *(1.19)* were also tested in their racemic form owing to their epimerisation at the testing pH of 7-8.

(1.15)　　　　　　(1.16)

R=H, *(1.17)*
R=CH$_2$Ph *(1.18)*
R= CH$_2$CH(CH$_3$)$_2$ *(1.19)*
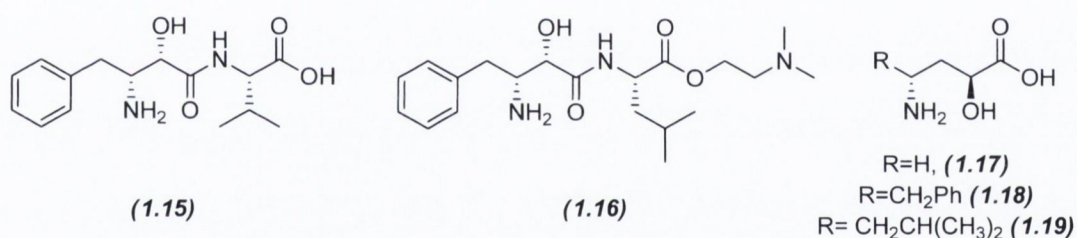
Figure 1.11: Natural, semisynthetic and synthetic derivatives of bestatin showing anti-angiogenic activity *(1.15) – (1.19)*.

Many other compounds are known to inhibit APN activity, including actinonin,[134] homothalamide, betulinic acid and curcumin to be discussed in more detail in Chapter 4.[135] Amino-tetralones such as *(1.20)* have also shown a specific anti-APN effect (IC_{50} 0.5 μM), however its physiological instability plagues the potential for their adaptation to the clinic.[136] Variations in the structure show the importance of retention of the carbonyl group and primary amine to activity, as both reduced hydroxyl and protected amino forms of this compound both show no activity. However modification of the carbonyl group to yield oxime ether *(1.21)* presents a compound with inhibitory activity against APN (IC_{50} 55 μM) and LTA$_4$H (8 μM),

although diminished relative to *(1.20)*. One interesting compound in this report was hydroxamic acid *(1.22)*, showing inhibition of APN almost on par with *(1.20)* (IC$_{50}$ 4 µM), while showing no activity against LTA$_4$H suggesting specificity towards APN in the M1 family. This hydroxamic acid moiety boasts greater chelation to APN than is observable in the parent amino-tetralone compound. Much research into the development of novel inhibitors bearing this functional group is focussed on the chelation of the Zn^{2+} in the catalytic site as detailed in the following section.
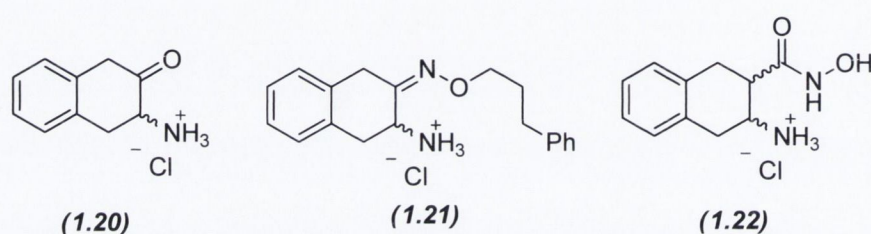
Figure 1.12: APN inhibitors based on the 3-amino-2-tetralone scaffold.

1.3.4.2 Hydroxamic acids and zinc chelation

As seen in Figure 1.9, bestatin co-ordinates to zinc, interacting with the amide carbonyl and the hydroxyl group of the AHPA subunit. This 4-membered chelating ring is the strongest interaction inside the receptor-ligand complex and can be replicated with similar peptides possessing a terminal functional group capable of chelating to zinc, for example carboxylic acids, thiocarboxylic acids and hydroxamates. Of these functionalities known as zinc binding groups (ZBGs), the hydroxamates have been the most widely studied, with capability of forming a five membered chelation allowing the two involved ligand atoms (the hydroxamic carbonyl and its hydroxyl) to approach more closely (1.9 Å - 3.3 Å) to the metal centre.[96] Additional hydrogen bonding is possible, permitting up to four interactions with the enzyme from the hydroxamate functional group as shown in Figure 1.13.

24
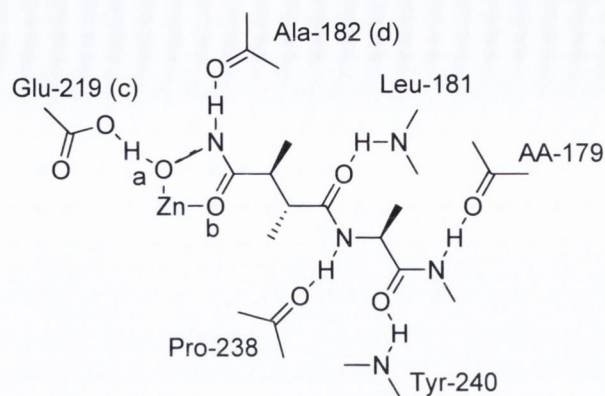
Figure 1.13: Complexation of hydroxamic acids to an MMP showing the bidentate coordination to zinc (a, b) and with Glu (c) and Ala (d) residues. (Adapted from Babine & Bender).[137]

The hydroxamates have long been researched towards the development of MMP and APN inhibitors owing to the catalytic site similarities between the two peptidases. The major drawback with the development of these compounds has been their broad specificity towards different classes of these enzymes interfering with vital physiological pathways.[138] As a result, two of the more promising hydroxamic acids for the potential treatment of cancer, batimastat *(1.23)* and marimastat *(1.24)* have been discontinued as drug candidates following clinical trials. Often musculoskeletal pain was described by the patient,[139] which could be averted using 50% of the original dosing schedule, while the clinical benefit of these compounds used in monotherapy or in combination were not advanced as first anticipated.[140] Additionally, batimastat was shown to increase metastasis to the liver when used to treat human breast carcinomas in nude mice while upregulating MMPs 2 and 9, pro-angiogenic factors and caspase 1 even in disease free animals studied.[141] Other promising compounds deemed to have failed at the clinical trial stage are prinomastat *(1.25)* whose therapeutic benefit in the treatment of NSCLC was negligible.[142] Although widely studied, it required nearly three decades of research before the first hydroxamic acid drug was granted FDA approval, with vorinostat *(1.26)* finding use for the treatment of cutaneous T cell lymphoma (CTCL) and Sezary syndrome.[143] Subsequently, the outlook for hydroxamates in the clinic has improved with positive clinical

results associated with both belinostat *(1.27)* for treatment of hepatocellular carcinoma[144] and panobinostat *(1.28)* for CTCL.[145]
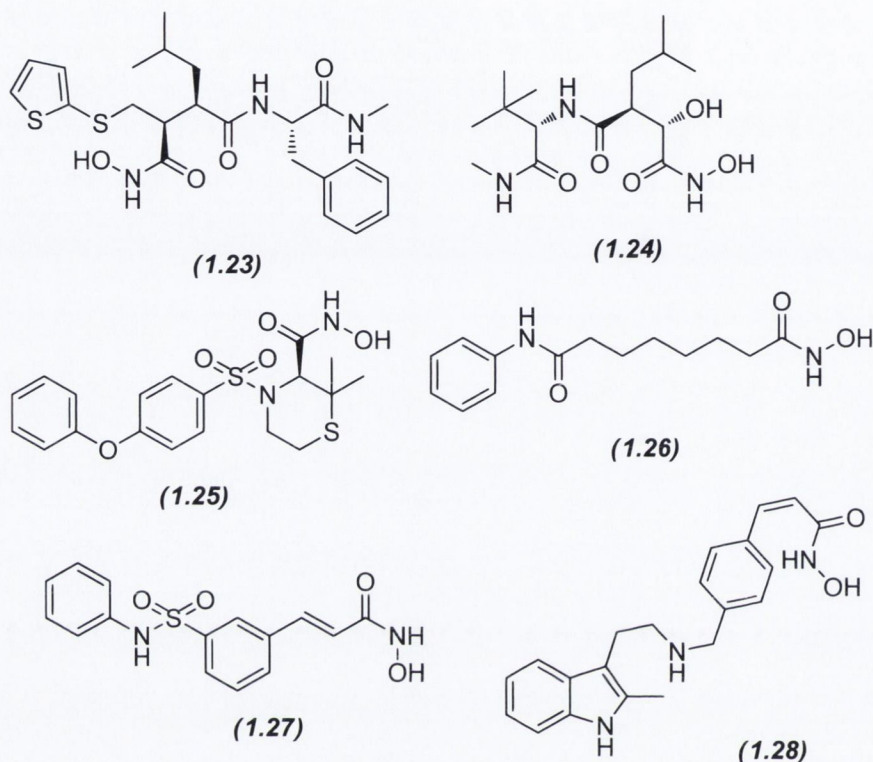
Figure 1.14: Hydroxamic acids at various stages of clinical evaluation *(1.23) - (1.28)*

Problems associated with this family of compounds can be witnessed by their metabolic instability. In addition to undergoing rapid billiary excretion,[146] they also undergo hydrolysis to return to their less active carboxylic acid form while releasing toxic NH_2OH into the system.[147] Additionally many of the compounds advanced toward the clinic were broad spectrum peptidase inhibitors interfering with normal physiological functions of these enzymes which can explain the negative results in marimastat trials.

Accordingly several groups have synthesised novel hydroxamic acids in a bid to overcome these deficiencies by varying the groups near the hydroxamate moiety to improve its metabolic stability providing a more stable longer lasting effect. For example, Hajduk used pilot NMR

studies to ensure their stability, prior to the synthesis of hydroxamic acid substrates for MMP-3 showing significant inhibitory effects with an improvement in their stability. Compounds *(1.29)* and *(1.30)* show IC_{50} values of 0.40 μM and 0.34 μM against this enzyme respectively.[148] Isomers of hydroxamic acids, called retrohydroxamates have also been synthesised to circumvent the associated metabolic liability with these compounds. In this group, the hydroxamic acid is not terminal but more integrated within the carbon chain as the hydroxamate nitrogen is alkylated. Although these compounds often exhibit lower in vitro activity, they are resistant to hydrolysis at the same rate as conventional hydroxamic acids and this added bioavailability is expected to exert a greater effect *in vivo*. Michaelides has synthesised a family of retrohydroxamic acids showing up to 100 fold improved selectivity for MMPs 2 and 3 over MMP 1, with a half life of 7 h in the plasma and a bioavailability of 95 %. Compounds *(1.31)* (MMP2, IC_{50} 58 nM. MMP3 IC_{50} 9.1 nM) and *(1.32)* (MMP2, IC_{50} 12 nM. MMP3 IC_{50} 27 nM) are both highly active against these two enzymes and while they are metabolised quickly it is not at the hydroxamic position but at the alkylated nitrogen in the hydantoin ring to compound *(1.33)* which shows heightened activity against the MMPs studied (MMP2, IC_{50} 7.8 nM. MMP3 IC_{50} 24 nM).[149]
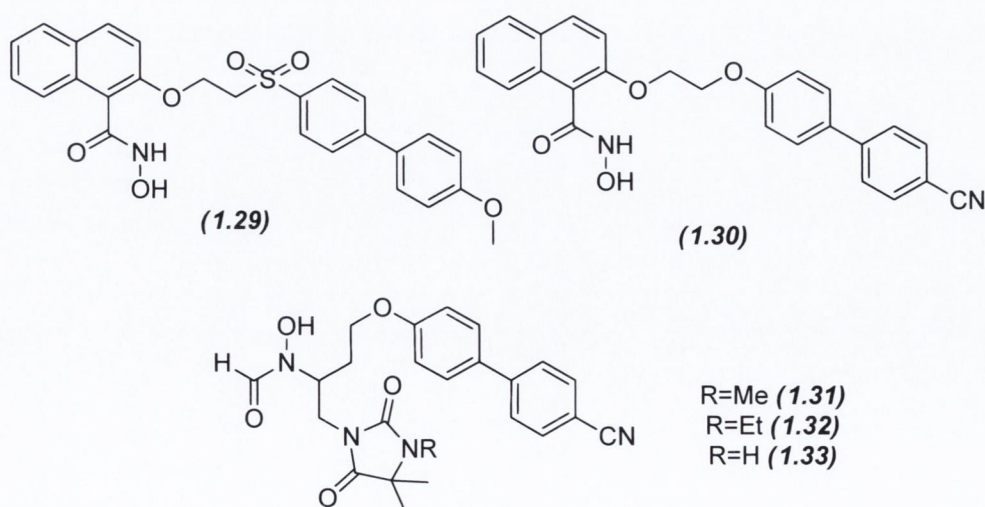
Figure 1.15: Hydroxamates and retrohydroxamates exhibiting greater stability profiles.

Inhibition of APN using this family of compounds has also been investigated using a malonic acid based scaffold to introduce hydrophobic groups near the hydroxamate group in order to probe activity. In one report, a large family of these compounds was synthesised with the leading performing compound *(1.34)* showing an IC_{50} towards APN of 82 nM, a 33 fold increase in activity relative to bestatin.[150] Other hydroxamic acid APN inhibitors include the napthylthioacetic acid derivative *(1.35)*. This compound shows isotype specificity for APN with no observable inhibition of a range of MMPs at up to 50 μM concentration. Its APN inhibition is similar to that of bestatin and it has shown an antioangiogenic effect on BAEC cells without effecting the viability of these cells.[120]
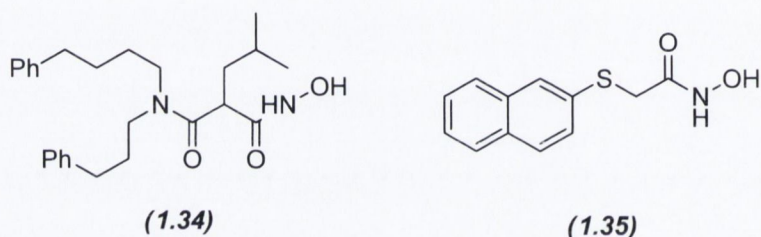
Figure 1.16: Hydroxamic acids showing APN inhibitory effects *in vitro*.

Ureido *(1.36)* and carbamate derivatives *(1.37)* of the hydroxamic acid family have also been recently synthesised showing inhibition of APN *in vitro* with IC_{50} values of 1.1 μM and 9.1 μM respectively, while *(1.36)* showed an anti-proliferative and anti-invasive effect on ES-2 ovarian cancer cells albeit showing no effect on the migration of these cells.[151] The work suggests that the isobutyl group is ideal for settling into the S1 binding pocket benzyl and phenethyl groups suggested to show binding to the more distance S2 pocket.[151]

(1.34) *(1.35)*
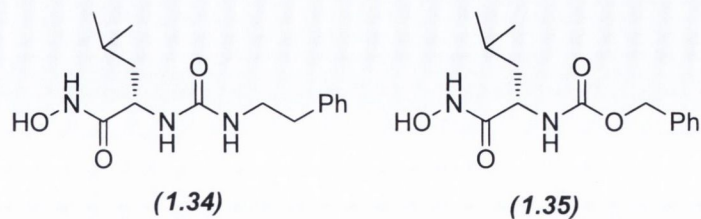
Figure 1.17: Novel ureido and carbamate hydroxamic acid derivatives.

A series of cyclic imide peptidomimetics have been synthesised by rigidification of a previous series of compounds which weren't specific for either MMPs or APN. Upon cyclisation more rigid analogues were formed, with certain compounds such as the tyrosine derived methyl ester *(1.36)* showing 150 times the affinity towards binding with MMP than APN. Conversely hydroxamic acid *(1.37)* inhibits APN with an IC_{50} of 3.1 μM with no interaction with the MMPs studied.[152] Several compounds from this study were also tested to determine anti-proliferative effects against leukemic HL-60, ovarian cancer ES-2 and adenocarcinoma A549 cells with *(1.38)* showing excellent activity against all three lines with 0.96 nM IC_{50} against the leukaemia line observed.[153]

(1.36) *(1.37)* *(1.38)*
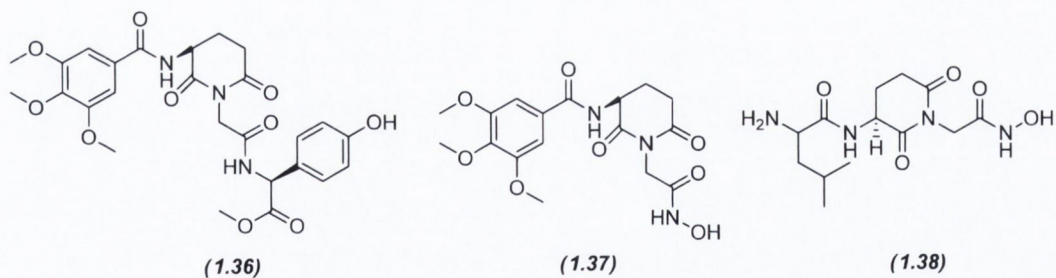
Figure 1.18: Hydroxamic acid *(1.37)* shows higher affinity to APN than MMPs. *(1.36)* is MMP specific. *(1.38)* shows greatest activity against three cell lines investigated.

Although these compounds show the way in which the hydroxamic acid moiety could be adapted to better improve their activity, these compounds have not yet had follow up studies in the clinic. It would be interesting to see how they fare in more regulated trials. However the successful methodologies employed in making the hydroxamic acid based inhibitors more

selective towards specific targets and more bioavailable suggest that finally the long promised era of hydroxamic acids in the clinic based on their regulation of peptidases is nearing.

Related to the hydroxamic acids are compounds containing phosphorous analogues of ketones known as phosphinic acids. A number of reports have shown the great inhibitory effect that these compounds exert on APN.[154] The activity attributable to these compounds results from their ability to chelate to zinc, via the two oxygen atoms attached to the central phosporous, while also binding to hydrophobic pockets either side of the metal centre, while these reports suggest that the presence of butyl or phenethyl groups is ideal for binding to the neighbouring hydrophobic pockets. A number of members of this family have been evaluated showing submicromolar activity in the APN inhibition assay, with the IC_{50} of α_1-(aminoalkyl)-α_2-(hydroxyalkyl)phosphinic acid *(1.39)* measured at 60 nM, among the most active APN inhibitors discovered. Additionally, other members of the family, *(1.40)* and *(1.41)* exhibit IC_{50} values of 0.47 µM and 0.24 µM respectively. These early results for this family of compounds are quite encouraging and it is possible that the anti-APN effect that they show could be adapted to the clinic.

(1.39)   *(1.40)*   *(1.41)*
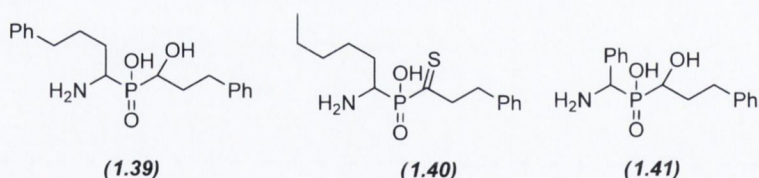
Figure 1.19: Phosphinic acid APN inhibitors.

1.3.4.3 APN and tumour homing peptides

In the previous sections there was significant discussion on inhibitors of the APN enzyme, however, its greatest clinical potential could conceivably come from its ability to recognise certain amino acid chains. While the hydroxamic acids do show potential for their development

into widespread clinical use, with a few exceptions at the moment they do not show perfect selectivity for APN only, being promiscuous binders to other receptors with their potential for side effects associated with their clinical use. It has been shown that certain peptides containing the CNGRC sequence are capable of homing to the tumour site. Pasqualini *et al* have shown that it is aminopeptidase N that is the receptor site to where this peptide binds.[155]

This has implications for the selective delivery of drugs to the tumour site, as it opens up the possibility to conjugate non-selective chemotherapies to this peptide, thus enabling selective delivery of agents to the tumour site. A number of approaches have been attempted towards this end including the fusion of tumour necrosis factor alpha (TNF-α), doxorubicin, cis-platin and endostatin with CNGRC.[156] The conjugate with TNF-α is currently undergoing clinical trials where it has displayed no dose limiting toxicity and disease stabilisation over the course of 6 months.[157] Another clinical trial where the conjugate is administered with doxorubicin has also shown a similar effect in the treatment of ovarian cancers with 10 out of 15 patients showing stable disease lasting 5.6 months without dose limiting toxicity.[158]

This treatment is not only an anti-angiogenic therapy, but also acts as a vasculature targeting agent,[159] one which attacks the pre-existing tumour vasculature in order to disrupt blood flow to the tumours swiftly. This is another emerging paradigm in anti-neoplastic treatment with there being two main investigative branches of anti-vasculature therapy at the moment, namely the ligand directed vascular targeting agents (VTAs) which use antibodies, peptides and growth factors to deliver cytotoxic agents to the tumour, and the small molecule VTAs exploiting pathophysiological differences between tumour endothelial cells and those expressed in normal function bodies.[160] CNGRC complexes belong to the ligand directed family of VTAs, while the more commonly encountered VTAs include the small molecule VTAs in particular those interacting with the microtubulular framework. This series of potential anti-cancer agents are discussed in the next section.

1.4 Vascular Targeting Agents

Angiogenesis is a process required in the development of tumours past the tumour volume of 2 mm^3. It also provides the growing tumour mass with the means to invade nearby tissue and frees tumour cells to perfuse into existing blood vessels facilitating metastasis. One problem with anti-angiogenic therapy is that by the time treatment begins, the tumour may have already progressed to a size where it is already well vascularised lessening the potential therapeutic effect. However, there is an emerging theory that anti-angiogenic therapy can trim the newer developing blood vessels in the mass in order to facilitate a more "normalised" vascular structure with a more even blood flow throughout allowing drugs to enter into the tumour mass in a more homogeneous manner. This process is called normalisation of the tumour.[161] By contrast the vascular targeting agents have been shown to exert a rapid necrotic effect on tumours by shutting down their vascular frameworks within minutes as only the select few endothelial cells at important vascular junctions need be killed or even morphologically disrupted.[162] However a viable rim of ECs remains allowing swift recuperation of the tumour vasculature.[163] It is here that angiogenic treatment can show showing potential possible synergistic effects if used as a combination therapy with VTAs. The approaches toward achieving vascular shutdown are outlined in this section beginning with the ligand based VTAs.

1.4.1 Ligand targeted VTAs

The studies regarding the ligand targeted VTAs has been dominated by the aforementioned NGR containing tumour homing peptides which bind to APN, typically containing two distinct parts, being the locater of the tumour site and the effector, which upon release inside the tumour mass shows an effect.

VEGF has been linked to the toxin gelonin, and using the expression of its receptors in the endothelium in the tumour microenvironment has allowed the release of gelonin in a controlled

manner in PC-3 xenografts in BALB/c nude mice. The effect of this treatment was seen as the tumour mass was reduced to 16% of that of untreated controls.[164]

In addition to growth factors and peptides, the ligands can also be of the mAb type. An example of an mAb undergoing recent clinical evaluation is bavituximab,[165] showing potential use as a monotherapeutic agent or in combination with conventional chemotherapy. By selectively binding to phosphatidylserine, upregulated in EC cells and apoptotic cancer cells, it can exert its VTA effect. Other mAbs used to target tumour cells by delivering anti-microtubule agents directly have previously been extensively reviewed.[166]

Integrins are attachment proteins playing a key role in angiogenesis, being upregulated upon hypoxia induced transcription of VEGF, to facilitate migration of the cells. The $a_v\beta_3$ integrin is upregulated in activated endothelial cells undergoing angiogenesis, hence being a tumour marker.[167] The attachment of proteins containing the RGD sequence to $a_v\beta_3$ provides a means to target the vasculature in a similar fashion to NGR peptide mediated tumour homing. For example doxorubicin has been conjugated to an RGD containing peptide, enhancing the efficacy it possesses against breast cancer cell lines in mice with an associated reduction in toxicity.[168] Through platinum coordination, both the anti-angiogenic agent valatinib and the RGD containing peptide were integrated together using individual attachments to the protein albumin developing a novel means towards the selectiving targeting of the endothelium.[169] Fumagillin is also an anti-angiogenic agent which has been shown to inhibit the integrin $a_v\beta_3$, when administered in nanoparticulate form to patients for the treatment of artherosclerosis. Accordingly, there is the possibility to adapt this method towards targeting cancers.[170]

1.4.2 Small molecule based VTAs

The small molecule based VTAs are dominated by those shown to be microtubule targeting agents, however other small molecule VTAs have been identified and these include the

flavonoid compound, (5,6-dimethyl-9-oxo-9H-xanthen-4-yl)-acetic acid (DMXAA) *(1.42)*. Its mechanism of action is poorly understood, however recent reports suggest that it is a multiple kinase inhibitor interacting with VEGF receptors.[171] Several derivatives of DMXAA have been synthesised, with similar activity, where alkyl substituents have been positioned at various points throughout the parent structure.

(1.42)
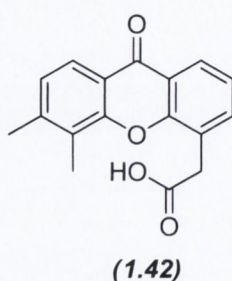
Figure 1.20: The flavonoid VTA DMXAA *(1.42)*.

Animal studies have shown this compound to induce a long term response to treatment over 60 days in mice bearing CT-26 colon adenocarcinomas.[172] Clinical trials have advanced to stage III in combination with paclitaxel and carboplatin in treatment of squamous and non-squamous NSCLC following early stage clinical trials suggesting a 5 month median survival advantage in treated patients.[173] However in two stage III clinical trials, patients treated with *(1.42)* showed no extended survival time relative to the placebo group.[174]

1.4.2.1 Tubulin binding agents

The major family of small molecule VTAs interact with the dynamic polymerisation of tubulin as it begins to form the microtubules. Tubulin is a small protein with a molecular weight of approximately 55 kDa existing mainly as α- and β-tubulin heterodimer although other forms do exist in addition to several isoforms of both.[175] When these heterodimers of α- and β-tubulin associate together head-to-tail they begin to form the protofilaments, which merges laterally as a band of thirteen such protofilaments to form long hollow cylinders known as microtubules (MTs). These are important components of the cytoskeleton involved in various cellular

functions, most pertinently in the regulation of cell division, segregation of chromosomes and intracellular transport.[176]

The dynamic polymerisation maintains a state of flux in which the size of the MT remains the same until it is signalled to rapidly polymerise or depolymerise, for example at various occasions throughout the cell cycle. Tubulin is polar, with the GTP bound α,β-heterodimeric subunit being added to the polymerising "plus end" only, while depolymerisation is observed only at the "minus end". This allows three modes of MT flux; polymerisation, depolymerisation and treadmilling, where polymerisation and depolymerisation occur at similar rates, ultimately maintaining constant MT length. This polymerisation finds significant importance during mitosis, forming the mitotic spindle, the support structure that segregates chromosomes during the process.[177] Affecting this dynamic polymerisation during mitosis, arrests the cell cycle, providing a target commonly exploited by conventional chemotherapy including paclitaxel.[178] The dynamic polymerisation of the MTs is illustrated in Figure 1.21.
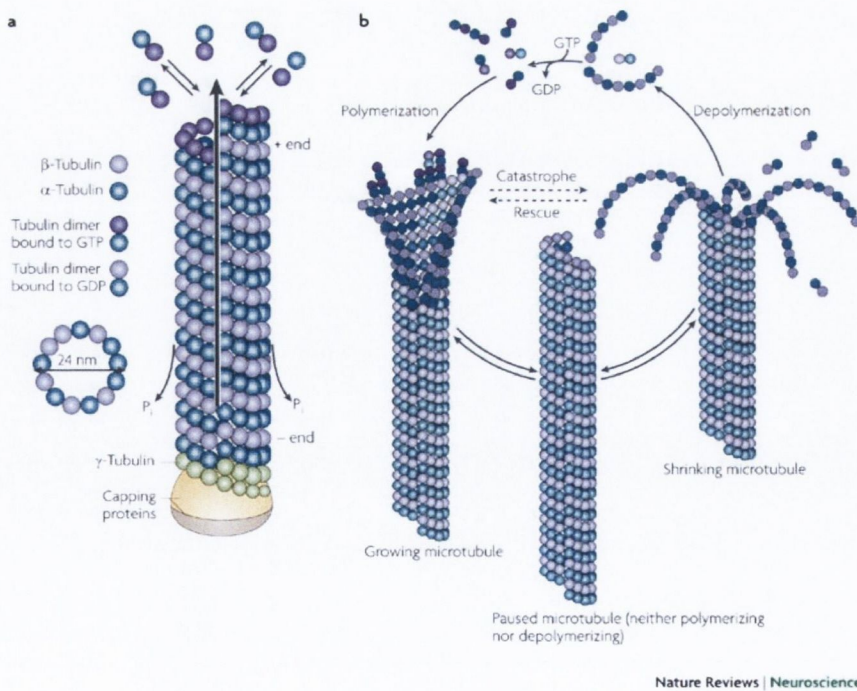
Figure 1.21: Microtubule dynamics.[179]

The tubulin protein has long proven to be a hot-bed of research into cancer chemotherapy. A wide range of compounds have exerted an influence on tubulin polymerisation, classified as being microtubule stabilising or microtubule destabilising in their effect. There have been several identified binding domains relating to different classes of compounds. The first compounds showing MT activity were the vinca alkaloids, vinblastine (*1.43*) and vincristine (*1.44*). These compounds bind to the tubulin heterodimer with a high affinity in stoichiometric equivalents at a distinct site in the β-subunit of tubulin, preventing their polymerisation. They have found use in treatment regimens for non-Hodgkin's lymphoma and acute lymphoblastic leukaemia (ALL).[180] Their side effects include hair loss and peripheral neuropathy.[177]

R=CH₃ *(1.43)*
R=CHO *(1.44)*
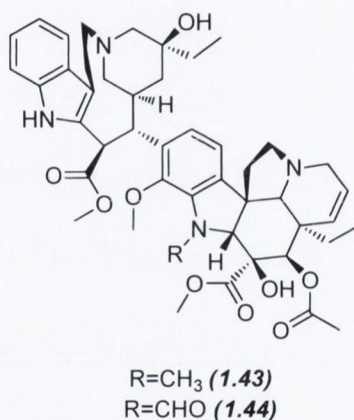
Figure 1.22: Vincristine and vinblastine which interact at the vinca alkaloid site.

Other major binding sites in the tubulin structure include the taxane binding site, the colchicine binding site and the more recently discovered laulimalide binding site.[181] The taxane binding site in the subunit is where paclitaxel (*1.04*) and docetaxel (*1.45*) exert their effect, stabilising the MTs, preventing their disassembly during the final stages of mitosis. They have found broad spectrum usage being approved for treatment of ovarian, breast and lung cancers.[177] Other agents like epothilone A *(1.46)* and discodermolide *(1.47)* interact with this site, showing more potent stabilisation of the MTs,[182] with discodermolide also showing synergistic suppression with paclitaxel in the treatment of NSCLCs.[183]

R1 = OAc, R2 = Ph *(1.04)*
R1 = H, R2 = tBu *(1.45)*

(1.46)

(1.47)
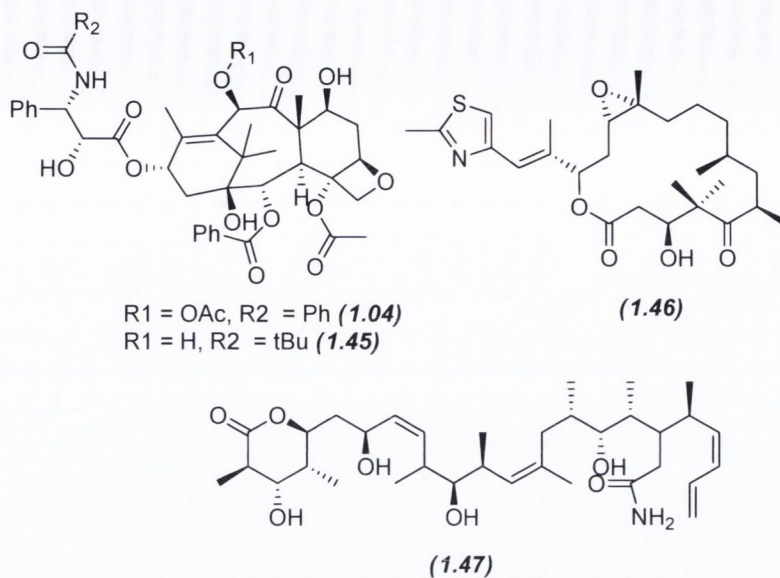
Figure 1.23: Tubulin binding agents acting at the taxane site.

Of most interest from a VTA perspective is the colchicine binding site, located in the β-subunit. As suggested, colchicine *(1.48)* binds at this site in addition to the lignan podophyllotoxin *(1.49)* and combretastatin A-4 (CA-4) *(1.50)*. The slow binding of colchicine to the heterodimer results in conformational changes of the dimer's secondary structure, preventing its subsequent association with other such species. Additionally, colchicine is not able to bind to already polymerised tubulin,[184] binding irreversibly however to the unpolymerised heterodimer.[185]

In addition to their anti-tubulin polymerisation effect, these compounds all show a disrupting effect on the vasculature with the same holding for the vinca alkaloids.[186] However, the majority of these effects in the majority of compounds are evidenced only at concentrations near the maximum tolerated dose (MTD). The exception is CA-4, where this effect is seen at one tenth of its maximum tolerated dose, offering a wide therapeutic window. Consequently, this simple stilbene has served as a lead compound for the synthesis of a wide variety of families of VTAs capable of acting at the colchicine binding site.[187] Its relative non-toxicity compared to colchicine, is likely to arise from its reversible binding kinetics, and faster metabolic turnover thus shortening its exposure time to the tissue.[188]
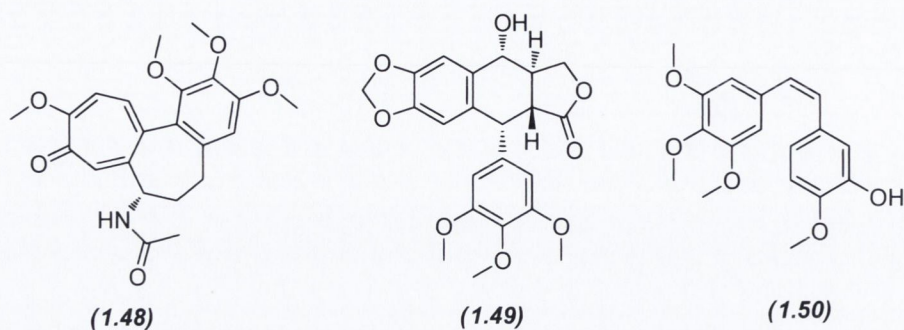
Figure 1.24: Compounds acting at the colchicine binding site.

The vascular effect of CA-4 has been postulated to result from its role in the disruption of a number of complex signalling pathways, including the RHO/RHO-kinase pathway and the myosin light chain pathway.[189] Upon binding to tubulin, the disruption of MTs in the interphase stage of mitosis, commences rapid signalling between the MT and the globular multifunctional protein actin. The effect of these is to lead to the increased polymerisation of actin, forming stress fibres increasing the distance between cells, disrupting their junctions allowing EC detachment from the vascular wall, thus increasing the vascular permeability. This increased permeability contributes to increased leakiness of the vasculature, with the consequential leakage of macromolecules leading to a greater interstitial pressure on the vasculature. This increased stress leads to further blebbing of the endothelial cells,[190] mediated by the stress activated protein kinase 2 (SAPK2), further disrupting the integrity of the blood vessels. The increased pressure on the tumour vasculature results in the stacking of red cells as illustrated in Figure 1.25. Finally, the endothelial cells detach completely, the vascular wall collapses and tumour cell death occurs en masse due to the major obstructions in blood flow and ischaemic necrosis of tumour tissue.[189, 191] Contrary to this accepted view of the vascular disruption caused by CA-4, a recent report suggests that another mechanism must be involved in the anti-vascular effect afforded by CA-4-P. This theory followed the observation that there was in fact no that elevation of interstitial pressure upon its administration.[192]
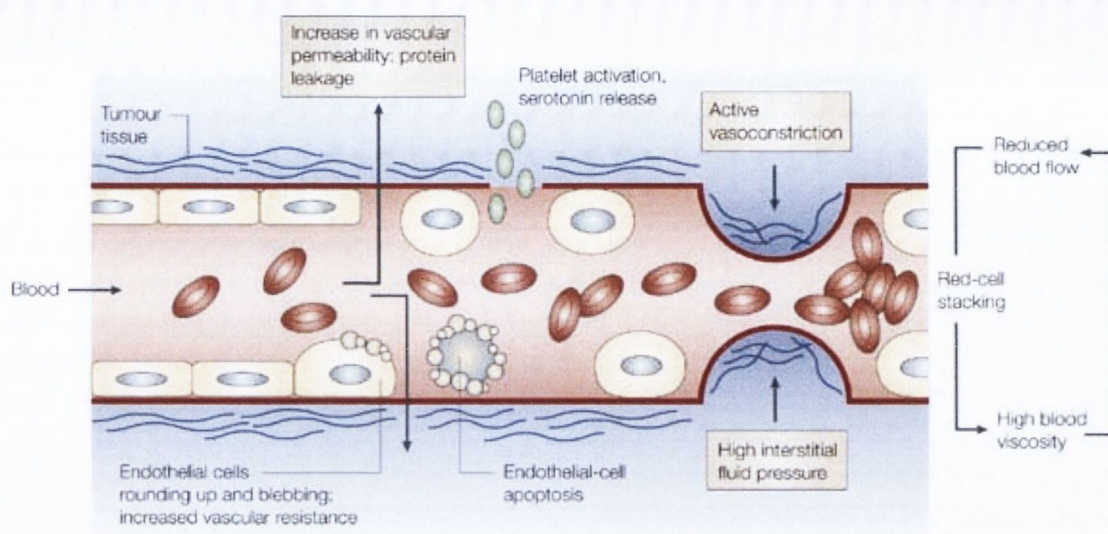
Figure 1.25: Schematic showing the vascular disruption upon CA-4 treatment.[188b]

1.4.2.2 Analogues of Combretastatin

A number of natural and synthetic analogues of CA-4 have been described including the disodium phenolic phosphate ester prodrug, CA-4 phosphate (CA-4-P) *(1.51)* and its isomer CA-1 *(1.52)*, whose phosphate ester prodrug *(1.53)* has shown improved potency relative to CA-4-P with doses of 50 mg/kg sufficient to delay the growth of colon tumour MAC29 in mice, relative to 150 mg/kg required for CA-4-P to exert an effect.[193] The phosphate prodrug serves to increase the solubility of combretastatin and is quickly cleaved by endogenous non-specific phosphatases *in vivo*.[194] In trials, the benefits relating to its safety profile are profound. In blood flow studies in P22 carcinosarcomas, the drug decreased perfusion in tumours 100 fold, whereas this effect was not replicated anywhere else. The nearest similar effect in normal tissue was the transient 7-fold reduction in blood flow in the spleen, showing the high selectivity that CA-4 possesses towards the targeting of cancer.[195] CA-4-P and CA-1-P have both advanced towards clinical trials with very few toxic effects noticed with the exception of tumour pain at moderate doses and reversible ataxia at doses exceeding the therapeutic dose required for reduction in tumour blood flow.[196] Phase 1b trials showed tolerance to CA4P in treatment with carboplatin and paclitaxel.[197] Phase II trials using the same combination in recurrent platinum resistant

ovarian cancer showed a response in 5 out of 18 patients studied, with side effects including hypertension easily treatable by glyceryl trinitrate.[198] Despite the activity of CA-4 and its low toxicity, neither itself nor any of the multitude of analogues synthesised have as of yet been approved for clinical use by the FDA. The prodrug AVE 8062 *(1.54)* does however exhibit a better solubility profile than any other combretastatin[199] and is currently undergoing phase III clinical trials in patients with advanced-stage soft tissue sarcoma.[200]

(1.51)

R=H *(1.52)*
R=PO₃Na₂*(1.53)*

(1.54)
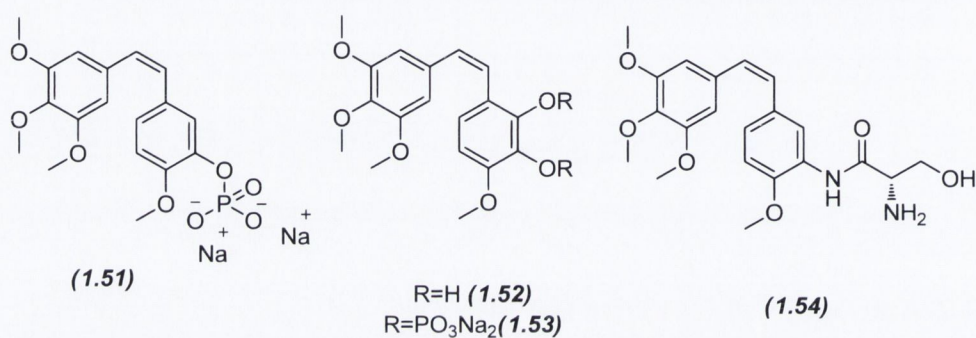
Figure 1.26: Natural combretastatin analogues and their prodrugs

The inherent instability of CA-4 as it isomerises to its significantly less biologically active trans isomer *(1.55)* spontaneously and in vivo necessitates the abundance of research into the synthesis of its derivatives. Iso CA-4 *(1.56)*[187b] and phenstatin *(1.57)*[201] both retain activity, suggesting the importance of maintaining the proximity between the two aryl rings. Accordingly, the majority of synthetic work has focussed on the maintenance of the important stereochemistry around the alkene, with incorporation of rings of varying sizes and use of different bioisosteres usually used to achieve this objective.[202] While many different compounds have been synthesised; for example with varying ring sizes *(1.58)*,[203] use of heterocyclic rings including indoles *(1.59)*[204] and imidazoles *(1.60)*,[205] and isosteric changes such as sulfonamides *(1.61)* which maintain the required orientation between the aryl rings, we are still awaiting a suitable clinical candidate that demonstrate improvement on the activity of prodrug forms of CA-4.
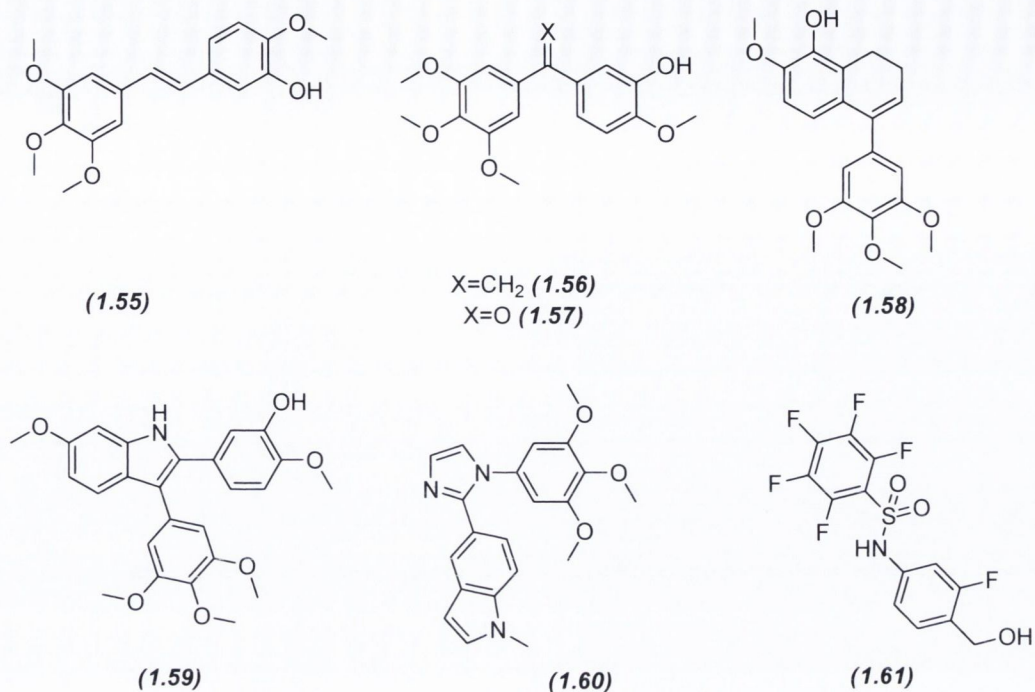
Figure 1.27: A brief account of structural modifications made to the combretastatin scaffold.

1.5 Aims of project

To date, study data generated by former PhD students from the Walsh group has resulted in the generation of several series of potent inhibitors of tubulin polymerisation as well as dual acting hybrids targeting tubulin dynamics and APN. While compounds within this work show undoubted promise, the idea of creating designed multiple ligands or indeed appending on other molecular targets has to date not been explored, other than those targeting APN to our most studied tubulin inhibitor RS180. The aims of the project are therefore to;

1) Design, synthesise and evaluate a novel series of designed multiple ligands (DMLs); by exploiting the carbonyl functionality on our lead tubulin inhibitors RS180 and GS117 to attach the zinc chelating hydroxamic acid functionality for recognition by APN.

2) Design and synthesise an isomeric form of RS180.

3) Design, synthesise and evaluate a novel DML, targeting tubulin polymerisation and APN, that incorporates the 1,3-diketone functionality of curcumin into RS180. Curcumin is one of the active constituents found in the rhizome of the natural spice *Curcuma longa* that is a known inhibitor of APN and is being widely investigated for its potential role in the treatment of different cancer forms.

4) Design synthesise and evaluate hybrids that merge tubulin inhibitors discovered by the Walsh group with artesunate, a classical anti-malarial but also an inhibitor of tumour angiogenesis.

Chapter 2

2.1 Introduction

As referenced in the introductory chapter, compounds bearing hydroxamate functional groups have shown strong inhibitory activity against the zinc centred metalloprotease enzymes implicated in functions such as tumour growth, invasion and metastasis. Hydroxamic acids have shown to be up to 1000 fold more active than their carboxylic acid counterparts at binding with aminopeptidase N (APN), histone deacetylase (HDAC) and matrix metalloproteinases (MMPs).[96, 206] This results from the closer bidentate coordination of the hydroxamate group to the Zn^{2+} metal centre located within their binding sites.[207,208] A number of hydroxamic acid based drug candidates have been identified exhibiting prominent anti-tumour activity targeting these enzymes including vorinostat used clinically for the treatment of cutaneous T cell lymphoma (CTCL) and Sezary syndrome,[143] proving the potential clinical application of compounds bearing this functional group. In principle, it was felt that our tubulin-targeting architectural design was suitably functionalised, especially with the carbonyl moiety, to allow for the incorporation of a hydroxamic acid moiety to ultimately provide us with dual-targeting inhibitors of tubulin polymerisation and APN (Figure 2.1).

The work described in this chapter is focused on the synthesis and evaluation of a novel class of DMLs where the hydroxamic acid moiety is conjugated to the tubulin binding agents previously synthesised within the group.[209] With both targeting groups incorporated it is expected that these compounds will exert anti-proliferative, anti-metastatic, anti-angiogenic and anti-vasculature effects.

The previous work undertaken within the group has focussed on the development of compounds shown to exert an anti-tubulin effect sharing structural properties with those of CA-4 *(1.50)* and colchicine *(1.48)*. A series of optimisation steps resulted in the development of a pharmacophore containing features including a trimethoxyaryl ring (A-Ring) which is bound to another aromatic ring containing a phenolic oxygen (C-ring), through either a 6 or 7-membered aliphatic ring (B-ring), ideally containing a carbonyl functionality at C-7. Tubulin inhibition studies have been shown the potency of[209] these compounds based on the method of Shelanski et al.[210] Following these results, a structure-activity relationship (SAR) has been devised for this family of compounds showing the important aspects of the molecule required for activity as microtubule targeting agents theoretically binding to the colchicine binding site[211] as outlined in Figure 2.1.
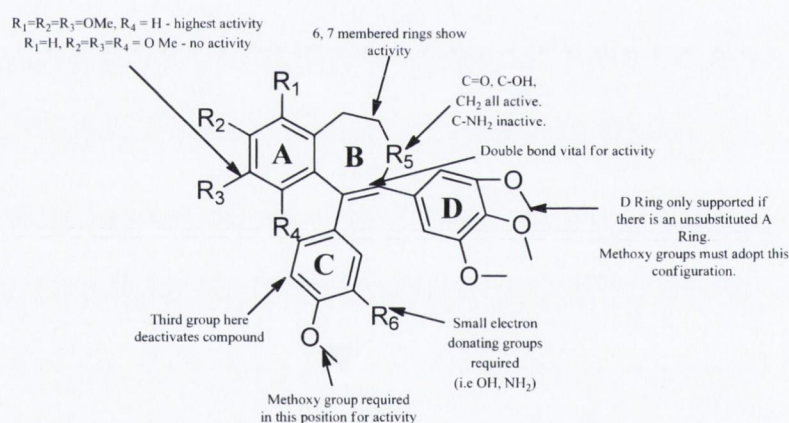
Figure 2.1: Pharmacophore map of compounds previously synthesised within the research group.

The two archetypal compounds originating from these studies are RS180 *(2.01)* and GS117 *(2.02)*. The work described in this chapter describes the modification of these compounds to create a family of novel DMLs that have exploited the carbonyl moiety to introduce the hydroxamic acid functionality *via* an oxime ether linker unit (Figure 2.2).
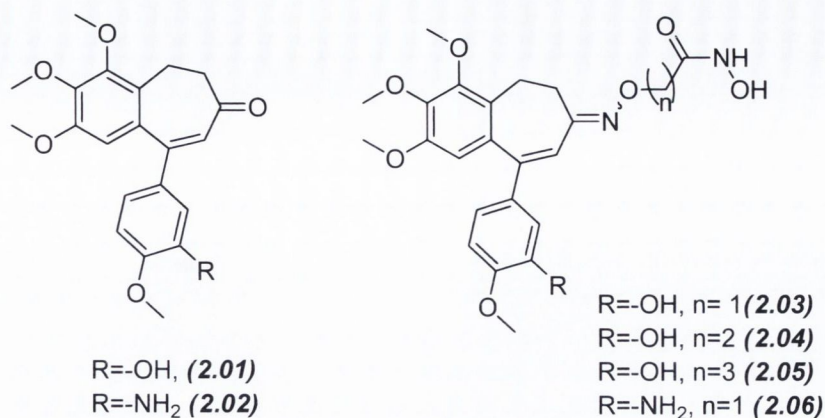
Figure 2.2: Lead compounds *(2.01)* and *(2.02)* and the planned hydroxamic acid designed multiple ligands *(2.03-2.06)*.

At the conclusion of their respective synthetic procedures, each of these compound's biological activity was measured for activity against APN,[135b] cellular proliferation[212] and migration[213] potential of PC-3 cells.

2.2 Overview of Synthetic Strategy

As exemplified in Scheme 2.1 with one example, our target compounds would first require the synthesis of the C-ring protected derivative *(2.07)*, the preparation of which has already been optimised by other members of the group.[209b, 214] Following its synthesis, the condensation reaction at the C-7 carbonyl position with (O-carboxymethyl) hydroxylamine was expected to afford *(2.09)*, the oxime ether with a terminal carboxylic acid group. While this intermediate upon tetrabutylammonium fluoride (TBAF) deprotection was not anticipated to inhibit APN, it nevertheless was expected to serve as an important control later when determining the contribution of the hydroxamic acid moiety to overall APN inhibition. Following formation of the activated pentafluorophenol (PFP) ester *(2.10)*, reaction with $NH_2OH \cdot HCl$ should yield the hydroxamic acid *(2.11)*, the TBAF mediated deprotection of which should afford the target hydroxamic acid *(2.03)*. With the use of O-alkylhydroxylamines bearing increased chain lengths it should be possible to ultimately yield hydroxamic acids *(2.04)* and *(2.05)*. In the synthesis of

47

(2.06), the same strategy as that used for *(2.03)* should be possible, albeit with an aniline substituted C-ring in place of the phenol.
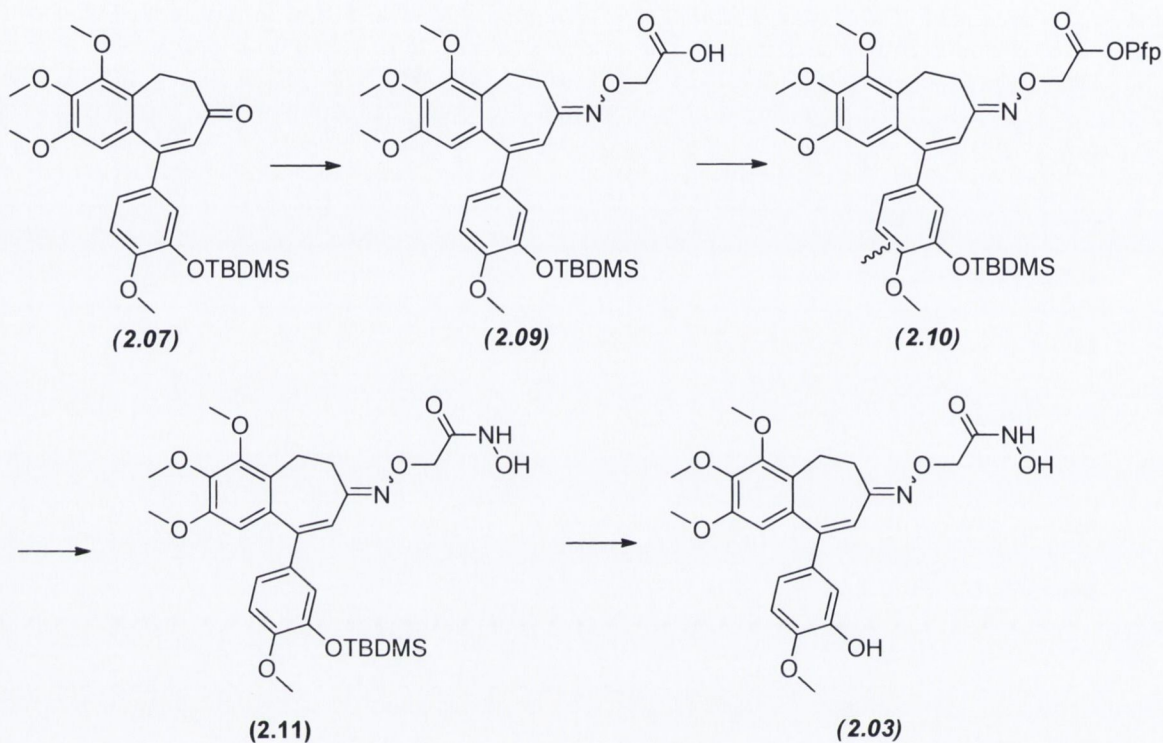
Scheme 2.1: Pathway toward the hydroxamic acid family of DMLs

2.3 Synthesis of *(2.07)*.

In brief, the approach toward the synthesis of *(2.07)*, involves the preparation of both the fused AB ring system *(2.12)* and the TBDMS protected bromophenol *(2.13)*. Organolithium coupling of these compounds yields the tricyclic ring structure *(2.14)* which can be oxidised to furnish *(2.07)*.
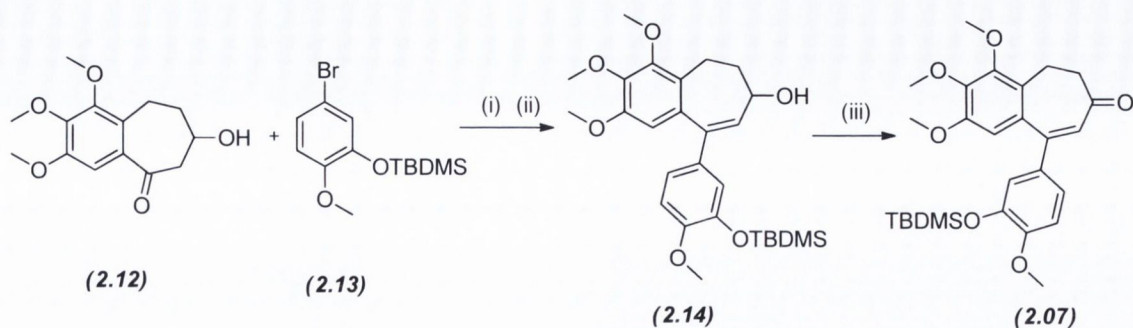
(i) BuLi, *(2.13)*, THF, N$_2$,12 h, 59% (ii) *(2.12)* (iii) Dess-Martin Periodinane, DCM, 5 min, 87%

Scheme 2.2: Coupling reaction of *(2.12)* and *(2.13)* to form the tricyclic ring structure.

The following section describes the synthetic pathways undertaken towards the synthesis of these intermediates and their subsequent coupling reaction allowing completion of the synthesis *(2.07)*.

2.3.1 Preparation of the fused AB ring system.

The important intermediate *(2.07)* has previously been synthesised using the multi-step procedure described by Hudson during the course of her Ph.D research.[209b] The first step in the synthesis of the AB bicyclic structure involved coupling of 2,3,4-trimethoxybenzaldehyde *(2.15)* to malonic acid by reflux in pyridine/piperidine (44:1 v/v ratio). This afforded (Z)-3-(2,3,4-trimethoxyphenyl)acrylic acid *(2.16)* in a high yield of 95%, while introducing the eventual carbonyl functionality at C-7 of *(2.01)*. Of particular note in this and in subsequent steps in the synthesis is the scale up of the process relative to Hudson's report. Previously, 10 g (51.00 mmol) of *(2.15)* was the largest amount of starting material that could be used. However, it was realised this could be scaled up five fold permitting amounts of starting material as high as 50 g (255.00 mmol), useful for generating larger amounts of *(2.07)* in similar timeframes. Following successful synthesis of *(2.16)*, the benzylic alkene was reduced under an atmosphere of H$_2$ using 10% Pd/C as catalyst in a 1:1 mixture of ethanol (EtOH) and ethyl acetate (EtOAc) to yield 3-(2,3,4-trimethoxyphenyl)propanoic acid *(2.17)* in quantitative yield. Generation of its acyl chloride *(2.18)* using oxalyl chloride in dry dichloromethane (DCM) with a catalytic

amount of *N, N*-dimethylformamide (DMF) under N_2, facilitated its *N, N*-dimethylaminopyridine (DMAP) catalysed coupling to Meldrum's acid to yield the adduct *(2.19)* as outlined in Scheme 2.3.
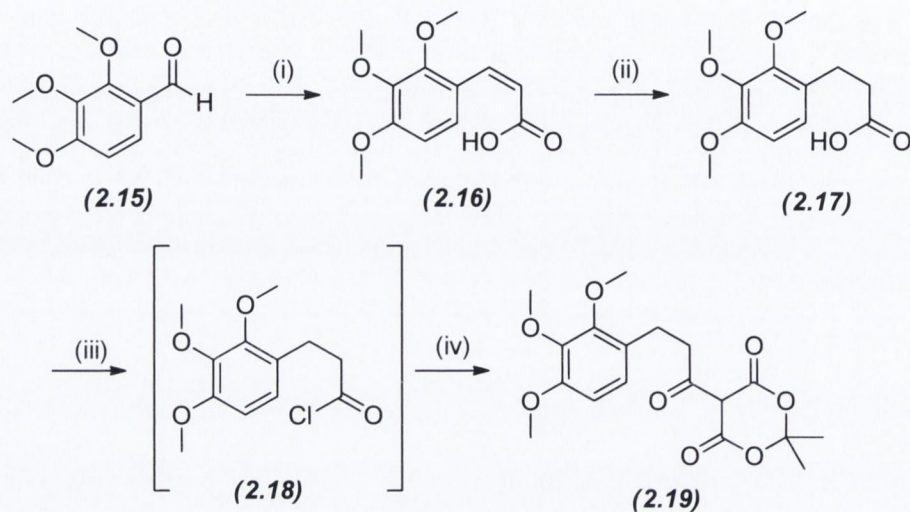
(i) Malonic acid, pyridine, piperidine, 100 °C, 5 h, 95% (ii) H_2, Pd/C, EtOH/EtOAc, 48 h, 100%
(iii) Oxalyl chloride, DMF, DCM, N_2, 2 h (iv) Meldrum's acid, DMAP, DCM, 1 h,

Scheme 2.3: Synthesis of Meldrum's acid adduct *(2.19)*.

Subsequently, *(2.19)* underwent methanolysis in a 4:1 mixture of toluene and methanol, furnishing the β-ketoester *(2.20)* in a yield of 82.5% over the two steps from compound *(2.17)*. Reduction of *(2.20)* to alcohol *(2.21)* was swiftly facilitated by treatment with sodium borohydride ($NaBH_4$) at 0 °C for 3 h in 83% yield (Scheme 2.4).
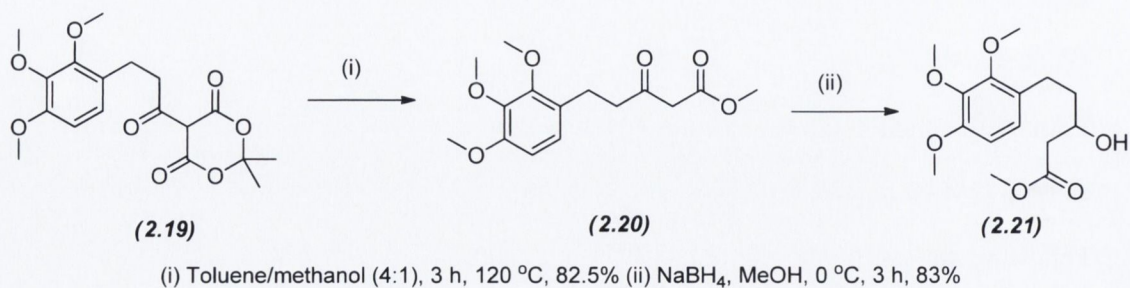
(i) Toluene/methanol (4:1), 3 h, 120 °C, 82.5% (ii) $NaBH_4$, MeOH, 0 °C, 3 h, 83%

Scheme 2.4: Synthesis of methyl ester *(2.21)*.

The *tert*-butyldiphenylsilyl (TBDPS) protected alcohol *(2.22)* was afforded in 86% yield by imidazole catalysed reaction with *tert*-butyldiphenylsilyl chloride (TBDPSCl) in DMF following overnight reaction at room temperature. Hydrolysis of *(2.22)* using 2.5 M aq. NaOH in MeOH and THF at 0 °C over 12 h afforded the acid *(2.23)* in high yield.
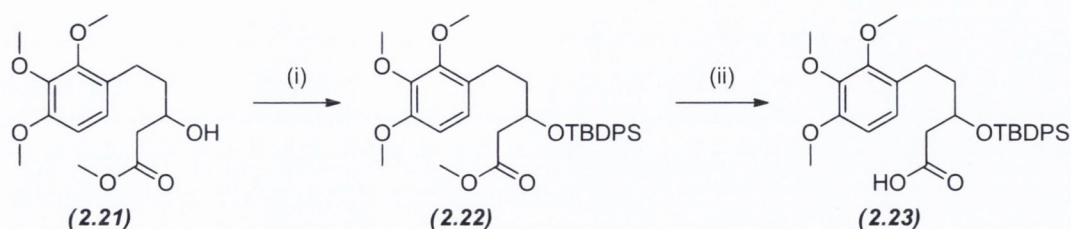
(i) TBDPSCl, Imidazole, DMF, 12 h, 75% (ii) 2.5 M NaOH, THF/MeOH, 12 h, 86%

Scheme 2.5: Synthetic pathway toward *(2.23)*.

The synthesis of the fused AB ring *(2.25)* was accomplished using the intramolecular SnCl$_4$ catalysed Friedel-Crafts acylation reaction at 0 °C over 1 h between the aromatic ring and the carboxylate group of *(2.23)*,[215] subsequent to its conversion to acyl halide *(2.23)* using oxalyl chloride in the same manner as that used in the synthesis of the Meldrum's acid coupled product *(2.19)*.
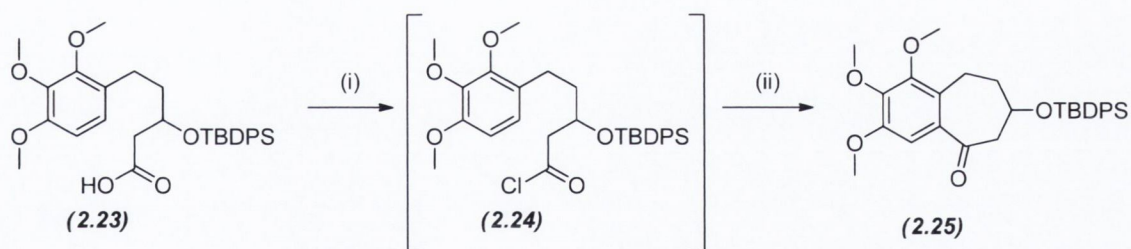
(i) Oxalyl chloride, DMF, DCM, N$_2$, 0 °C, 2 h, (ii) SnCl$_4$, DCM, N$_2$, -10 °C, 1 h, 55%

Scheme 2.6: Synthesis of bicyclic AB ring structure *(2.25)*.

Removal of the TBDPS protecting group using a 1 M solution of TBAF in THF over 6 h afforded the alcohol *(2.12)*, required for the coupling reaction detailed in Scheme 2.2, in a yield of 76%. Care was needed during the work-up procedure as the product appeared to degrade when the solvent was removed after placement in a water bath at elevated temperature. The

solvent was removed using a stream of N_2 gas before purification by flash column chromatography.

(2.25)   *(2.12)*
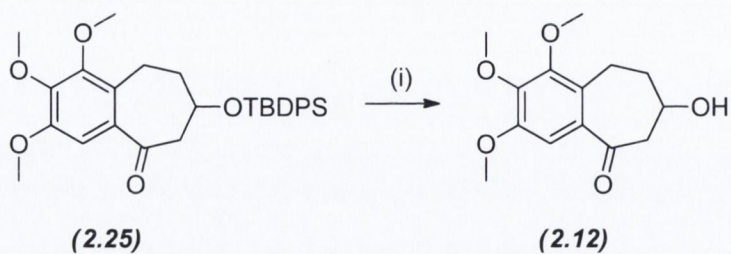
(i) 1 M TBAF in THF, THF, 0 °C, 15 min, 76%

Scheme 2.7: TBAF deprotection of *(2.25)*.

2.3.2   Preparation of the C-ring.

An efficient three step procedure beginning with the Dakin oxidation of *(2.26)* using *meta*-chloroperoxybenzoic acid (MCPBA) in DCM at 0 °C facilitated the synthesis of *(2.13)*. This afforded the formate ester *(2.27)*, isolated in crude form before its hydrolysis in 2.5 M aq. NaOH to yield the phenol *(2.28)*. Subsequent *tert*-butyldimethylsilyl (TBDMS) protection using *tert*-butyldimethylsilyl chloride (TBDMSCl) in a similar fashion to the TBDPS protection detailed in the previous section afforded the desired C-ring compound *(2.13)*.

(2.26)   *(2.27)*   *(2.28)*   *(2.13)*
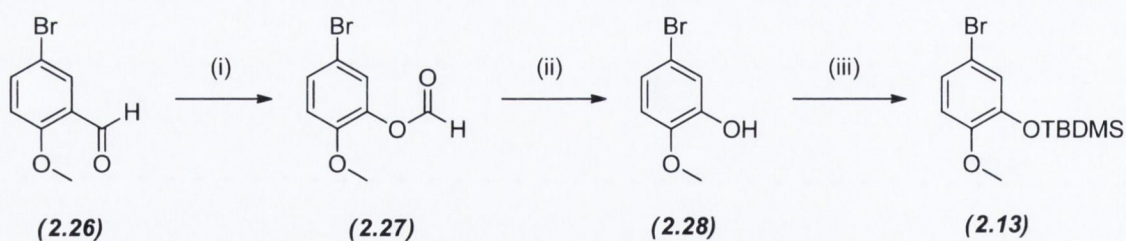
(i) MCPBA, DCM, 0 °C, 24 h (ii) 2.5 M NaOH, MeOH, 80% (iii) TBDMSCl, Imidazole, DMF, 89%

Scheme 2.8: Synthesis of the C-Ring *(2.13)*.

2.3.3 Completed synthesis of compound *(2.07)*.

The completion of the synthesis of *(2.07)* was accomplished using the pathway as outlined in Scheme 2.2. Lithium-halogen exchange is a common mechanism of forming aryl carbanions under relatively mild conditions. In this case bromobenzaldehyde *(2.13)* was treated with an excess of n-butyllithium (BuLi)[216] in THF at -78 °C, forming the reactive organolithium species *(2.29)* within 20 min. Upon addition of *(2.12)* to this intermediate, nucleophilic attack on its free carbonyl led to the formation of the tertiary alcohol *(2.30)* which eliminated upon acidic work up to furnish *(2.14)*. The mild oxidation of the allylic alcohol of *(2.14)* using Dess-Martin periodinane (DMP)[217] functioned as expected to complete the synthesis of *(2.07)*.
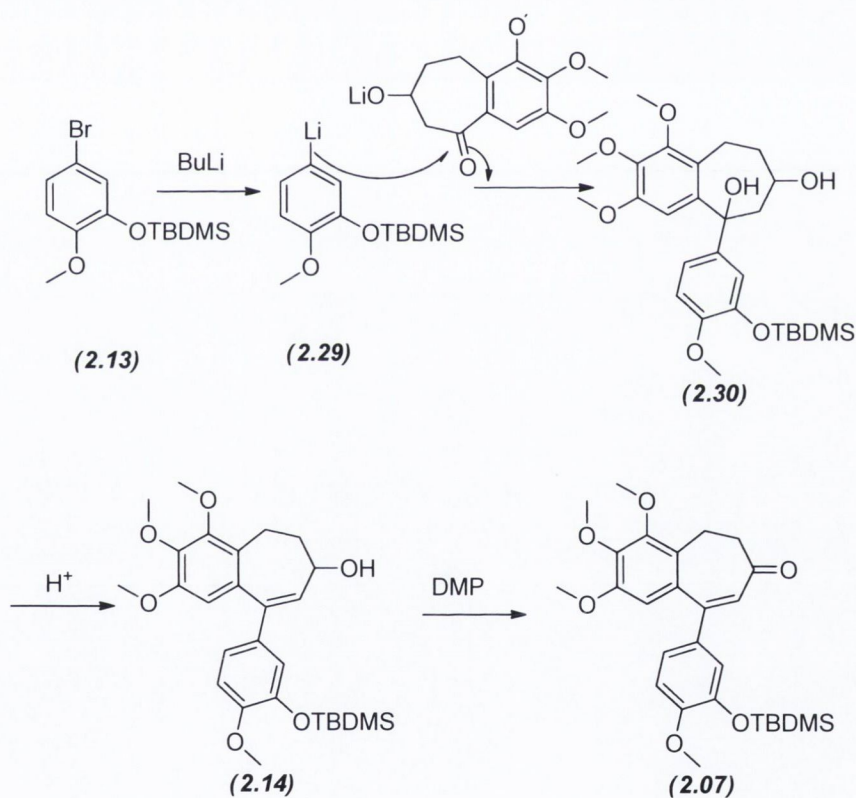
Scheme 2.9: Halogen-lithium exchange mediated formation of *(2.14)*.

2.4 Synthesis of the hydroxamic acid family of compounds.

Having successfully completed the synthesis of *(2.07)*, it was now possible to manipulate this compound in new ways. As the major objective of this work was to synthesise a series of compounds possessing hydroxamic acids linked to the RS180 *(2.01)* scaffold by means of an oxime ether functionality at the C-7 position, the reactivity of this carbonyl to nucleophilic substitution relative to the Michael accepting centre was first investigated. This was in order to ensure these undesired side reactions were avoided. If the incoming nucleophilic amine were to attack the B-ring's alkene centre, the loss of unsaturation in the B-ring would be severely detrimental to the activity of this series of compounds, as evidenced by earlier data on the dihydro derivative of *(2.01)*. As a test case and following a procedure used by O'Byrne,[218] NH$_2$OH.HCl was added to *(2.07)* in H$_2$O/EtOH (4:1) forming the oxime *(2.31)* within 2 h in high yield to give a 1:1 mixture of syn and anti-isomers. Although it was possible to separate these isomers from each other, their spontaneous interconversion was observed over time rendering their separation futile. For this reason, all oxime intermediates within this series remained as a mixture of isomers.

The obvious potential for the phenol deprotected derivative of this intermediate to also inhibit tubulin polymerisation *(2.01)* and as a control for the APN assay, dictated that an appropriate amount of it be subjected to the conditions required for the liberation of the phenol moiety. Thus the TBDMS group was removed using 1 M TBAF in THF over 10 min to afford *(2.32)*.
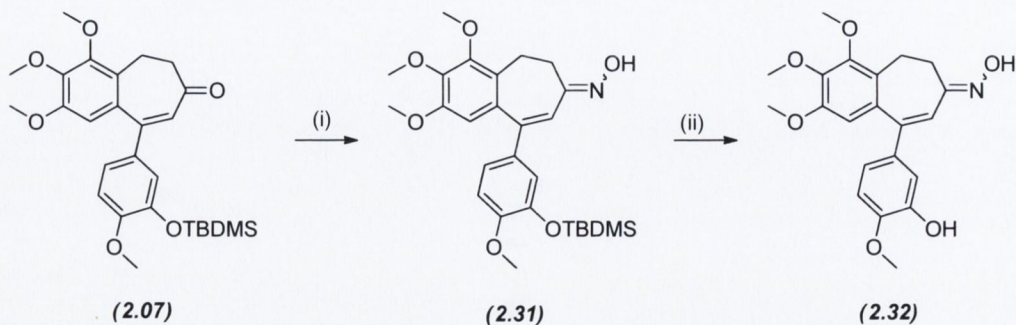
(i) NH$_2$OH.HCl, NaOAc, H$_2$0/EtOH (1:4), 1 h, 76% (ii) 1 M TBAF in THF, THF, 15 min, 97%

Scheme 2.10: Synthesis of oxime *(2.32)*.

Upon completion of the successful synthesis of *(2.32)*, an analogous oximination reaction step using (O-carboxymethyl) hydroxylamine hemihydrochloride was used to introduce an oxime ether spacer group at the C-7 position of *(2.07)* to give the carboxylic acid *(2.09)*. Following the synthesis of the activated PFP ester *(2.10)* using standard *N,N'*-dicyclohexylcarbodiimide (DCC) coupling methods, the hydroxamate functionality was afforded following the hour long reaction with NH$_2$OH.HCl in H$_2$O and EtOH. This reaction was also attempted using DMF as a solvent with DIPEA functioning as the tertiary base. While the reaction proceeded swiftly to completion, it was noted that the DMF was difficult to remove from the product, resulting in reduced product purity. The product of this reaction *(2.11)* was deprotected using 1 M TBAF in THF as previous to yield the hydroxamic acid *(2.03)*, in 86.4% yield.
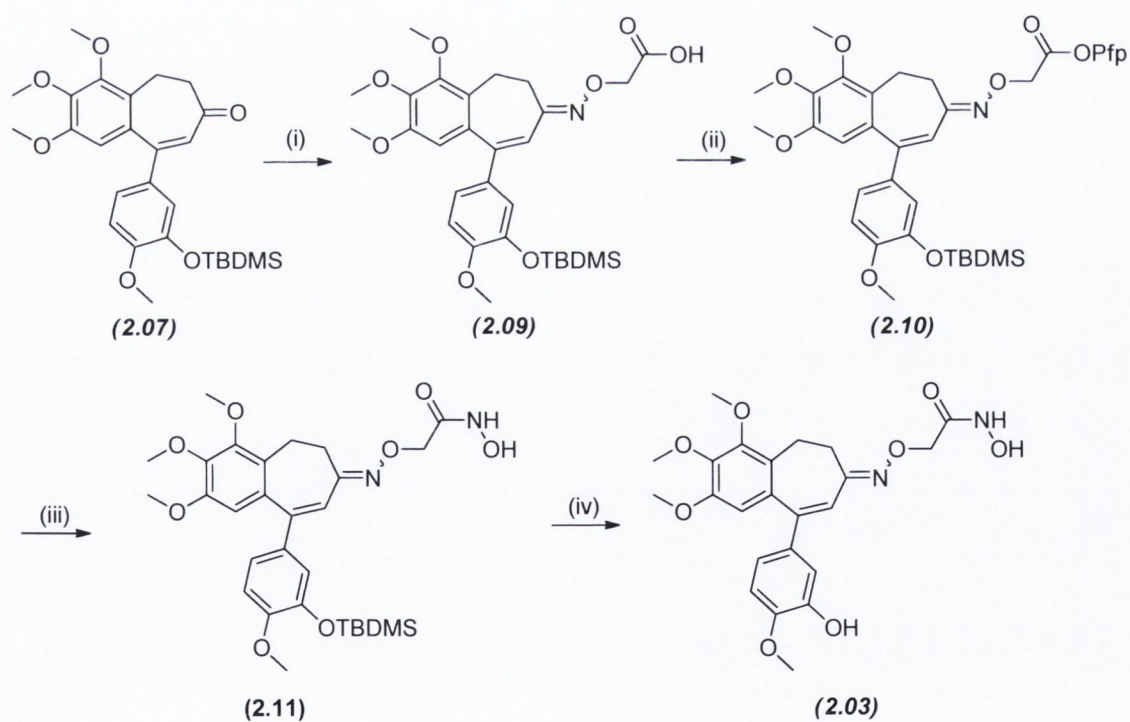
(i) (O-carboxymethyl)hydroxylamine hemihydrochloride, NaOAc, EtOH/H$_2$O, 4 h, 76% (ii) PFPOH, DCC, DCM, 1 h, 89% (iii) NH$_2$OH.HCl, NaOAc, EtOH/H$_2$O, 30 min 54% (iv) TBAF, THF, 15 min, 86%

Scheme 2.11: Synthesis of *(2.03)*.

2.4.1   Spectral interpretation of *(2.03)*

High resolution mass spectrometry (HRMS) analysis of the compound gave an m/z of 459.1778 corresponding to the mass of the protonated form of *(2.03)*. The infra-red (IR) spectrum shows peaks at 3425 cm^{-1}, 3135 cm^{-1} and 1674cm^{-1} corresponding to O-H, N-H and C=O stretches respectively. As in the case of the oxime *(2.33)*, the hydroxamic acid *(2.03)* and its intermediates through the synthetic pathway existed both in syn and anti- forms at the oxime ether position, exhibiting the same or very similar R$_f$s to each other making their separation very difficult. Taking into consideration the spontaneous interconversion between the isomers of *(2.33)*, it was decided to not make any further attempt to isolate *(2.03)* in both its syn and anti forms after initial purification using preparative thin layer chromatography (TLC). As a result the spectra obtained on *(2.03)*, showed a significant doubling of some peaks indicative of an approximate 2:1 ratio between the major and minor isomers.

Signals corrsesponding to each isomer is most evident in the region between 4.5 to 5.0 ppm, where two peaks are witnessed. These integrate together for two protons and can be assigned as two singlets corresponding to the protons of the oxime ether linkage, shifted far downfield resulting from significant deshielding as they neighbour both an oxygen atom and a hydroxamic acid. The four methoxy groups in this compound show significant doubling of peaks in the region between 3.64 ppm and 3.95 ppm, as do the two CH$_2$ units within the B-ring seen as multiplets between 2.76 ppm and 3.03 ppm. The aromatic and double bond region shows five protons with similar degree of signal overlap between isomers. Two broad singlets complete the spectrum; at 5.78 ppm the phenolic hydroxyl group can be observed, whereas the broad singlet seen at 8.34 is attributable to the proton attached to the nitrogen of the hydroxamate moiety.

The doubling of signals is more pronounced in the ^{13}C NMR spectrum with the appearance of 42 signals in total in a compound that only contains 23 carbons in total Figure 2.4. Inspection of the spectra show that the majority of these peaks however are paired, with each pair of peaks

visible in an approximate 2:1 ratio suggesting this is the ratio of the presence of the major

isomer relative to the minor isomer. Considering the pairing of the peaks, there are three pairs of

CH_2 peaks visible; two in the aliphatic region corresponding to the ring CH_2 peaks, while

another pairing appears in the region of 70 ppm corresponding to the CH_2 unit in the oxime

ether component of the molecule. The methoxy carbons do not show any pairing suggesting

there is no difference in resonance at these positions and accounting for there not being an exact

doubling in the amount of peaks seen in the spectrum. There are ten CH signals in the aromatic

region corresponding to the 5 CH carbons that are expected in the structure. It is also possible to

observe a doubling of the ester carbonyl peak at 167.6 ppm. The hydroxamate C=N peak can be

attributed to that resonating slightly upfield of the ester at 162.7 ppm. Sixteen quaternary peaks

in the region from 128.2 ppm to 159.3 ppm show the presence of the expected 9 quaternary

carbons.
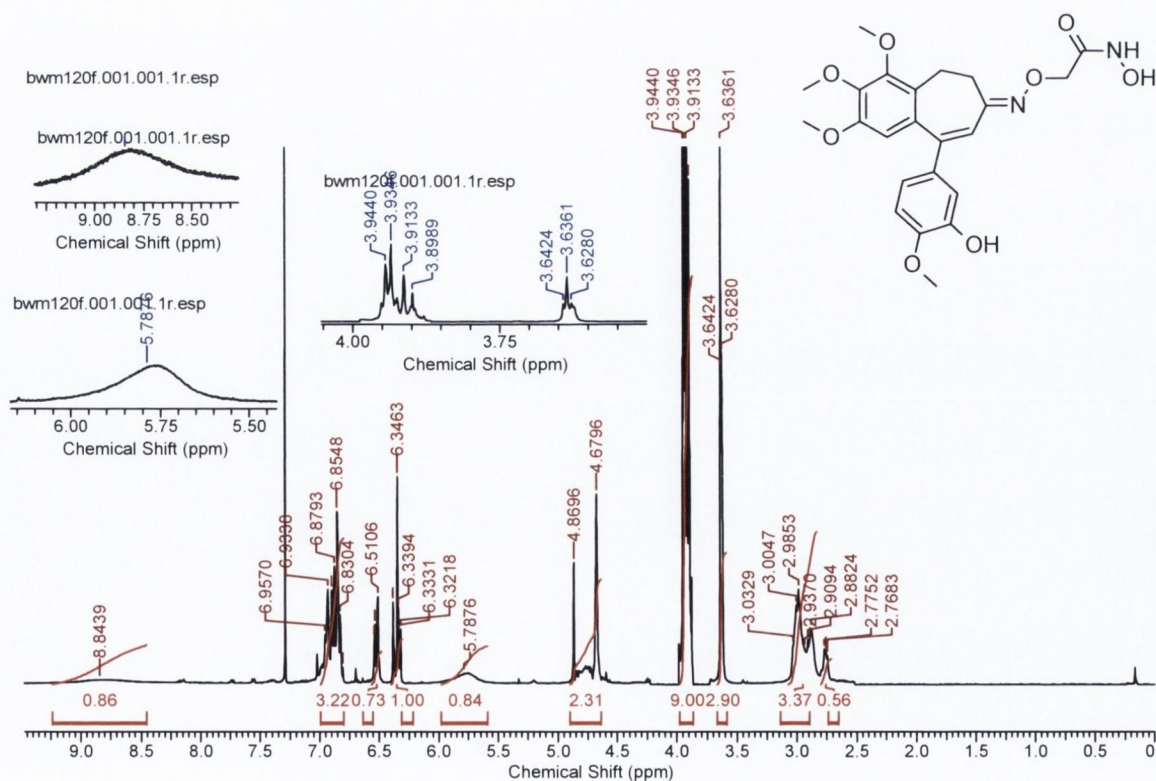
Figure 2.3: ^{1}H NMR spectrum of *(2.03)*.

57
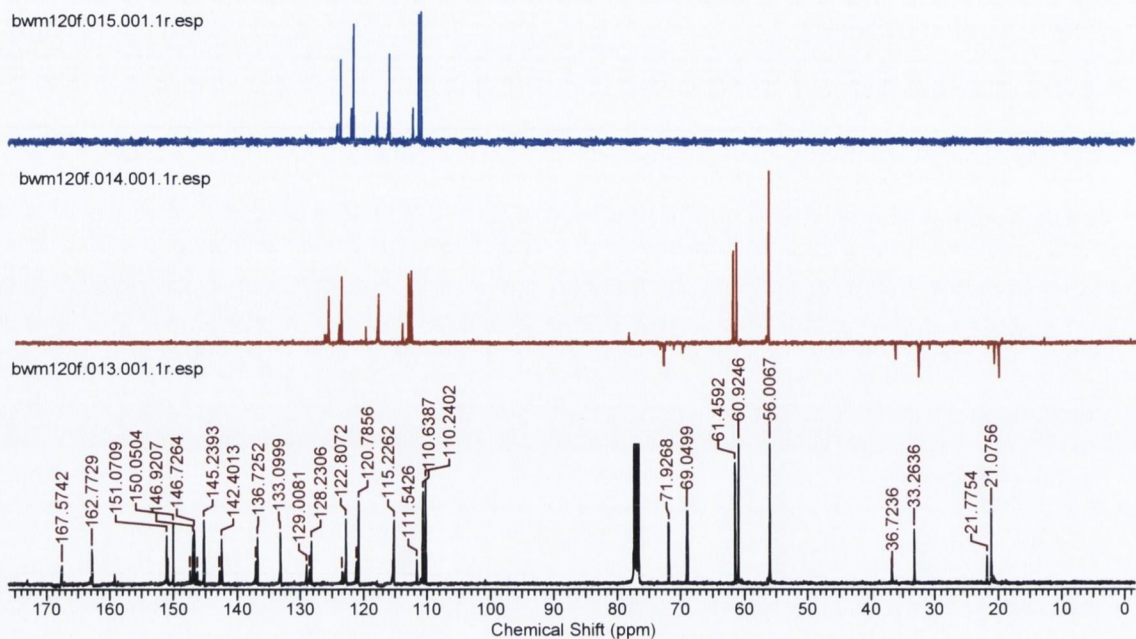
Figure 2.4: ¹³C NMR spectra of *(2.03)*.

2.4.2 Expansion of the linker between the RS180 and hydroxamate groups.

Following the successful completion of the synthesis of *(2.03)*, it was decided to investigate if chain length between the oxime moiety and the hydroxamic acid group affected activity. This objective should be attainable using 3-(aminooxy)propanoic acid *(2.33)* and 4-(aminooxy)butanoic acid *(2.34)* as the hydroxylamines in the oxime formation reaction with *(2.07)*.
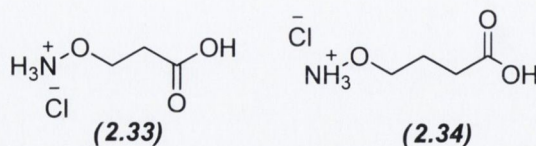
Figure 2.5: Hydroxylamine salts required for the synthesis of *(2.04)* and *(2.05)*.

As these compounds are not commercially available, their synthesis was required before further advancement. It has been shown that treatment of the benzophenone oxime with bases including Na metal and NaH produce the benzophenone oxime *(2.35)* anion which can participate in the bimolecular substitution (SN$_2$) reaction to O-alkylate the oxime.[219] Utilising the alkylation properties of the anion would theoretically lead to the synthesis of a benzophenone oxime ether which upon hydrolysis in aq. HCl[220] would result in an efficient pathway toward the required functionalised hydroxylamines.

Benzophenone oxime *(2.35)* is easily synthesised by reflux of benzophenone with NH$_2$OH.HCl in H$_2$O/EtOH over 10 h in near quantitative yield.[221] Initial attempts toward the alkylation of *(2.35)* with the readily available 3-bromopropanoic acid *(2.36)* and 4-chlorobutanoic acids *(2.37)* to yield benzophenone oxime ethers *(2.38)* and *(2.39)* proved unsuccessful (Scheme 2.12). The generation of the benzophenone oxime was afforded through use of 2 equivalents of either NaOMe, sodium metal or NaH. Following a reaction period of 30 min, the cessation of H$_2$ gas evolution was noted with the observation of a discernible yellow colour of the oxime anion at its most intense with the use of NaH as base. Upon addition of the alkyl halides, either 3-bromopropanoic acid or 4-chlorobutyric acid, the quenching of the yellow colour suggested consumption of the oxime anion. Unfortunately, this was due to the acid base reaction between the anion and the carboxylic acid group of the alkyl halide. Further attempts to pre-form the carboxylate salts using DIPEA to circumvent the acid-base reaction with the oxime anion evidenced no improvements on reaction progress.
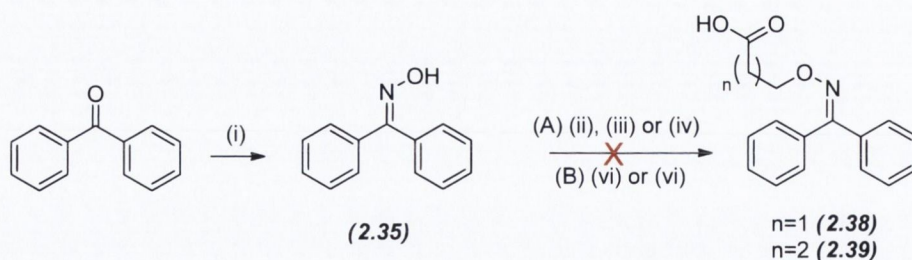
(i) $NH_2OH.HCl$, $EtOH/H_2O$ (1:3), 10 h, 98% (ii) 2 Eq Na^o, 30 min, N_2, DMF (iii) NaH (60 %), N_2, DMF, 20 min (iv) NaOMe, DMF, N_2, 30 min, (v) 3-bromopropanoic acid, DMF, 10 min (vi) 4-chlorobutanoic acid, DMF, 10 min

Scheme 2.12: Initial attempts towards benzophenone oxime ethers *(2.38)* **and** *(2.39)*.

As illustrated in Scheme 2.13, it was ultimately decided to mask the acidic nature of the starting materials by effecting their esterification directing the oxime anion towards attack at their alkyl halide centre. The sweet smelling esters *(2.40)* and *(2.41)* were obtained by reaction of a 4 M 1,4-dioxane solution of HCl in EtOH over 12 h in moderate respective yields of 48% and 37%, however these yields could easily be improved upon after taking particular care with the work up procedure. These products are volatile and prone to evaporation with the reaction solvent during the rotary evaporation step. These esters successfully alkylated the benzophenone oxime generated using NaH in DMF under an N_2 atmosphere as desired furnishing *(2.42)* and *(2.43)* in respective yields of 50% and 43%. Finally, *(2.33)* and *(2.34)* were obtained as their HCl salts upon their overnight hydrolysis of both the oxime and ester groups using concentrated HCl in DCM at room temperature. These products were obtained as white powders following repeated washing with hexane to remove the benzophenone side product.

X=Br, n=1 *(2.36)*   X=Br, n=1 *(2.40)*, 48%   a) X=Br, n=1 *(2.42)*, 50%   n=1 *(2.33)*, 70%
X=Cl, n=2 *(2.37)*   X=Cl, n=2 *(2.41)*, 37%   b) X=Br, n=2 *(2.43)*, 43%   n=2 *(2.34)*, 73%

(i) 4 M HCl/1,4 dioxane, EtOH, 12 h (ii) *(2.35)*, 60% NaH, N_2, 30 min
(iii) a) *(2.40)* or b) *(2.41)*, 10 h (iv) Conc. HCl, DCM, 12 h
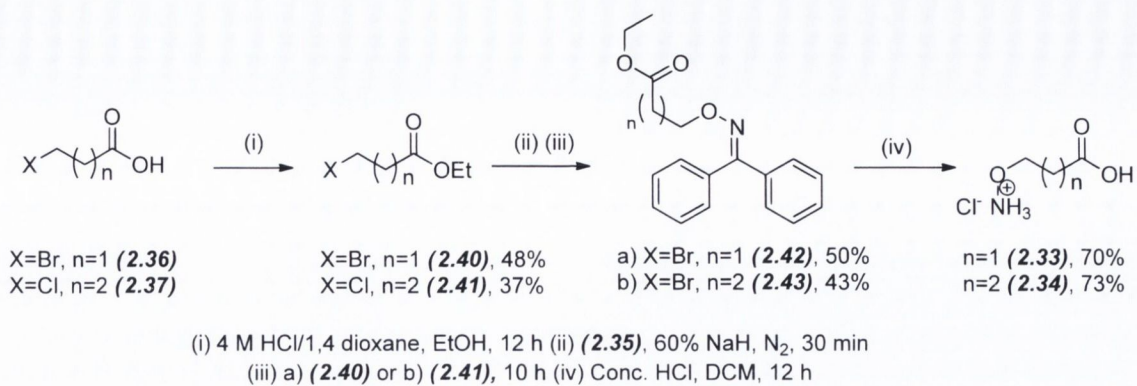
Scheme 2.13: Synthesis of *(2.33)* and *(2.34)*.

Having successfully synthesised *(2.33)* and *(2.34)*, the path to the synthesis of compounds *(2.04)* and *(2.05)* was now clear. The procedure adopted was identical to that used to secure *(2.03)* (Scheme 2.14). The synthesis of these compounds was achieved with *(2.07)* being converted to *(2.04)* and *(2.05)* with total percentage yields of 17% and 52% respectively, comparing to 31.5% for the synthesis of *(2.03)*. The only change in reaction conditions needed was observed in the oximination reaction, where increased reaction times of 24 h and 16 h were required for the synthesis of *(2.44)* and *(2.45)* respectively relative to the 4 h reaction time required for synthesis of *(2.09)*. In conclusion, the successful replication of this synthesis should have further applications for future expansion of the series of compounds being prepared in the group, as it suggests that this is a robust pathway towards the synthesis of hydroxamic acid based DMLs. By utilisation of a wider variety of linker groups for example, a large family of these compounds could be synthesised based on this work. In fact, Coogan[222] and Stack[214] have already applied this methodology to their work achieving the synthesis of their own DMLs containing the hydroxamic acid functional group.
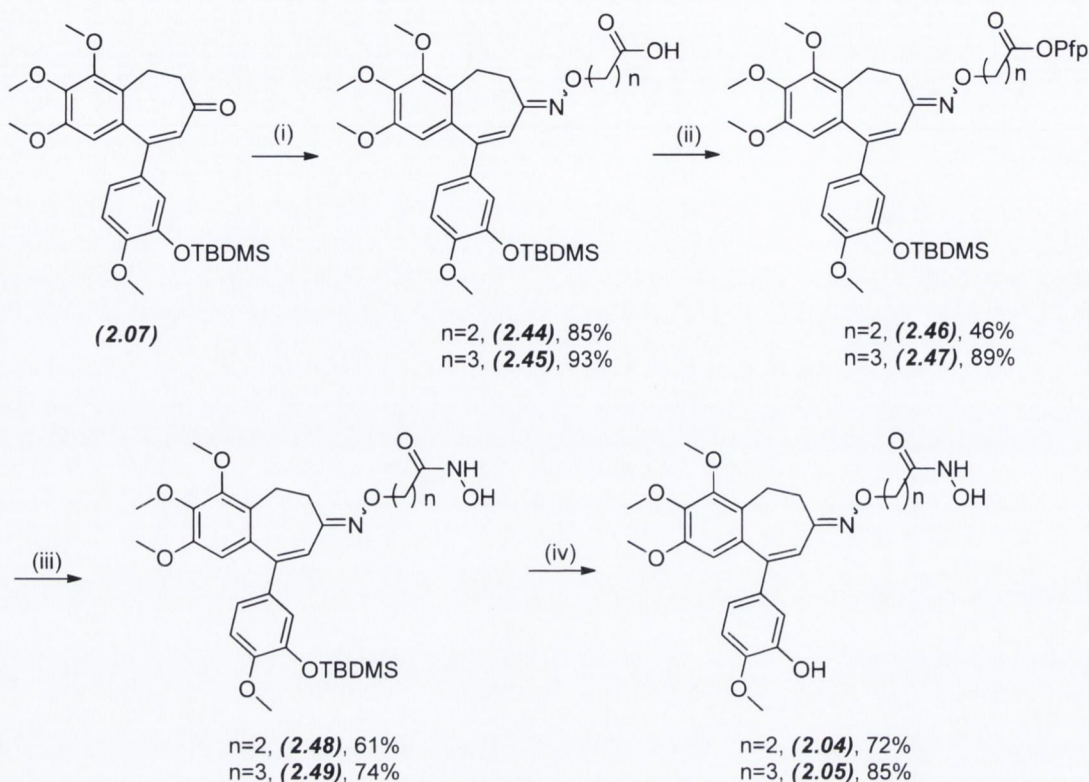
(i) a) *(2.33)*, NaOAc, EtOH/H$_2$O, 24 h or b) *(2.34)*, NaOAc, EtOH/H$_2$O, 16 h (ii) PFPOH, DCC, DCM, 1 h (iii) NH$_2$OH.HCl, NaOAc, EtOH/H$_2$O, 30 min (iv) TBAF, THF, 15 min.

Scheme 2.14: Final synthesis of compounds *(2.04)* and *(2.05)*.

2.4.3   Spectra of *(2.04)* and *(2.05)*.

In the ^{1}H NMR spectrum of *(2.04)*, the multiplet seen at 2.54 ppm corresponds to the methylene bridge adjacent to the carbonyl. Whereas this signal would be expected to resonate as a triplet similar to those seen in its precursor compounds including *(2.40)* and *(2.42)*, the appearance of less defined multiplet structures is attributable to the compound's dual isomers. The multiplet at 3 ppm integrating to 4 H shows no deviation from those expected from the B-ring CH$_2$ protons. The multiplet at 3.72 ppm integrating to 2 H is consistent with that expected for a CH$_2$ unit neighbouring an oxygen atom. Four signals integrate to a combined total of 12 methoxy protons between 3.55 ppm and 3.95 ppm. Similar to *(2.03)* the splitting of their signals is due to the appearance of a major isomer and a minor isomer of the compound. The peaks in this region are consistent with those expected to arise from the 4 methoxy peaks in the system. A broad signal

at 5.8 ppm indicates the presence of phenolic proton, a suggestion supported by the expected

disappearance of the TBDMS groups in the furthest upfield region. Between 6.5 ppm and 7.00

ppm there are a series of multiplets integrating to 5 protons, consistent with the 1 alkene proton

and 4 aromatic protons in the compound's structure.
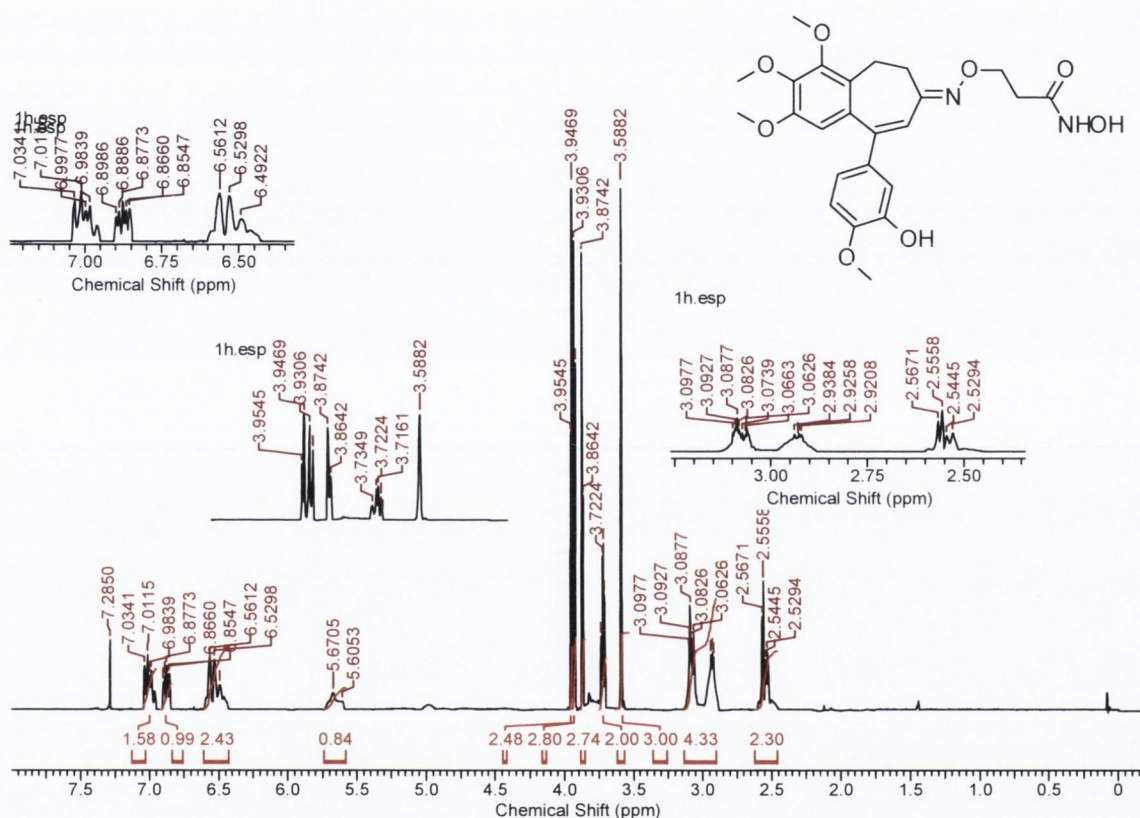
Figure 2.6: ^{1}H NMR spectrum of (2.04).

The ^{13}C NMR spectrum also suggests the presence of the compound as a mixture of its isomers.

In the region between 20 ppm and 70 ppm, there are 8 CH$_2$ signals, representing 4 pairs of

signals for the four CH$_2$ carbons. There are 4 signals between 55 pm and 60 ppm, again

consistent with those expected from the methoxy substituted carbons. Ten signals appear

between 100 and 130 ppm on the DEPT 90 consistent with 5 pairs of CH signals. Finally the

peak at 169.2 ppm suggests that of the carbonyl group of the hydroxamic acid functionality. The

peak at 164.3 is consistent with that of the oxime quaternary carbon. Finally, the mass spectrum

shows an m/z ratio of 493.1816 consistent with 493.1825, the calculated m/z of the sodium adduct of *(2.04)*.
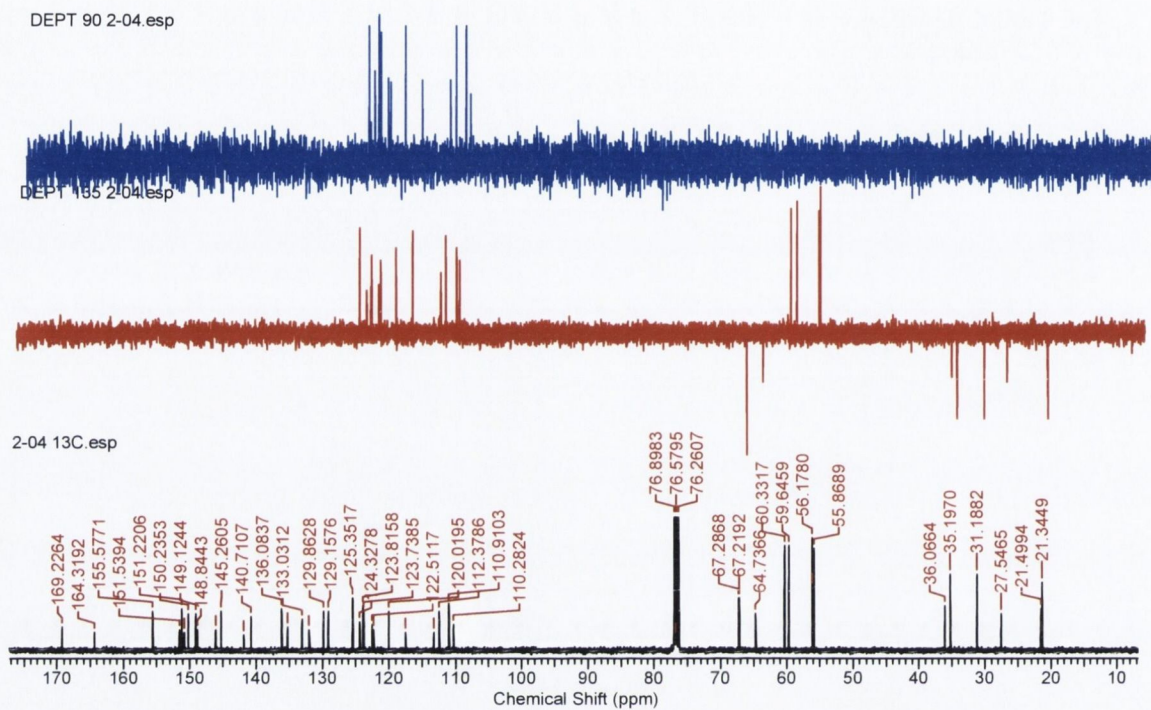
Figure 2.7: ^{13}C NMR spectra of *(2.04)*.

The ^{1}H NMR spectrum of *(2.05)* is similar to that of *(2.04)* showing multiplets integrating to two protons each at 1.4 ppm, 2.4 ppm and 3.7 ppm, consistent with the expected resonances of the 6 protons in the oxime ether side chain. The methoxy groups show similar splitting of their signals as do the aromatic signals. There is abroad singlet peak at 8.18 ppm corresponding to the proton bound to the hydroxamic acid functional group's nitrogen, while at 5.7 ppm, the broad peak of the phenolic proton is evident.

The ^{13}C NMR spectrum displays a similar pattern to that seen in *(2.04)*, with an extra pair of CH$_2$ signals seen in the furthest upfield region, showing the extra carbon in the side chain. The quaternary peaks at 170.1 ppm and 165.4 ppm are consistent with the hydroxamate carbonyl

carbon and the oxime carbon respectively. The m/z of 487.2084 is consistent with that of the (M+H)$^+$ ion of 487.2075.
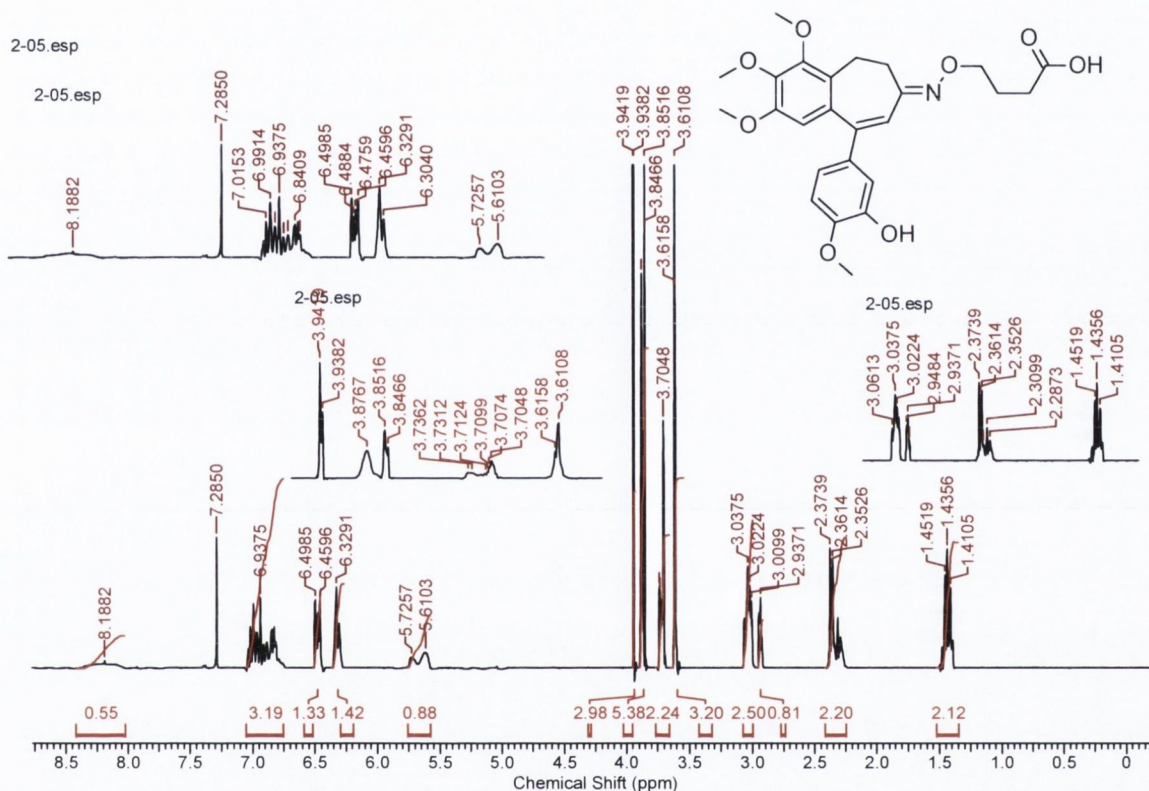
Figure 2.8: ^{1}H NMR spectrum of (2.05).
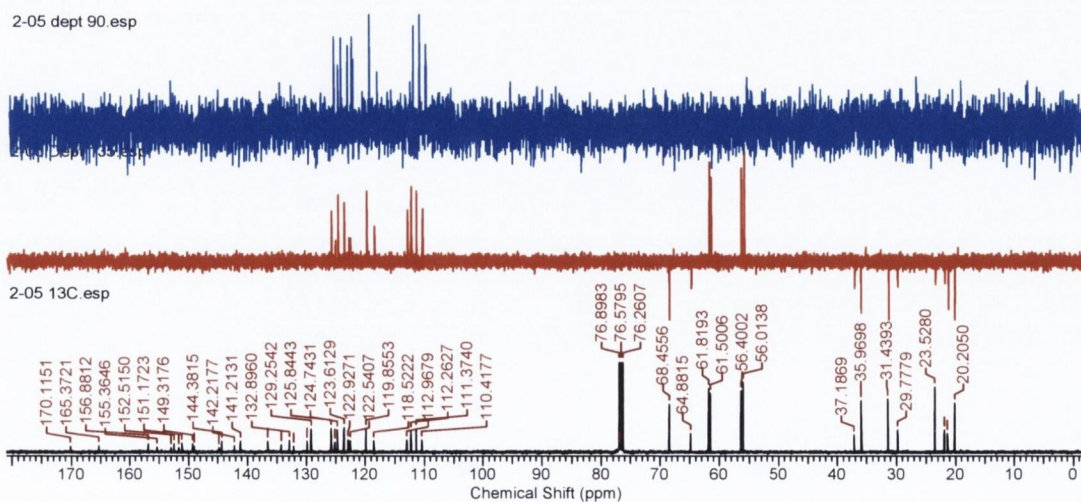
Figure 2.9: ^{13}C NMR spectra of *(2.05)*.

2.4.4 Synthesis of compounds *(2.50) – (2.52)*.

In order to quantify the expected importance of the hydroxamate functional group on biological activity, the carboxylic acid analogues *(2.50)-(2.52)* of these compounds were synthesised following the TBAF mediated deprotection of the carboxylic acid intermediates *(2.09)*, *(2.44)* and *(2.45)*. This step was performed with the high efficiency, affording each carboxylic acid in high yields of 79% to 85% after 15 min reaction time.

n=1, *(2.09)*
n=2, *(2.44)*
n=3, *(2.45)*

n=1, *(2.50)*, 79%
n=2, *(2.51)*, 82%
n=3, *(2.52)*, 85%
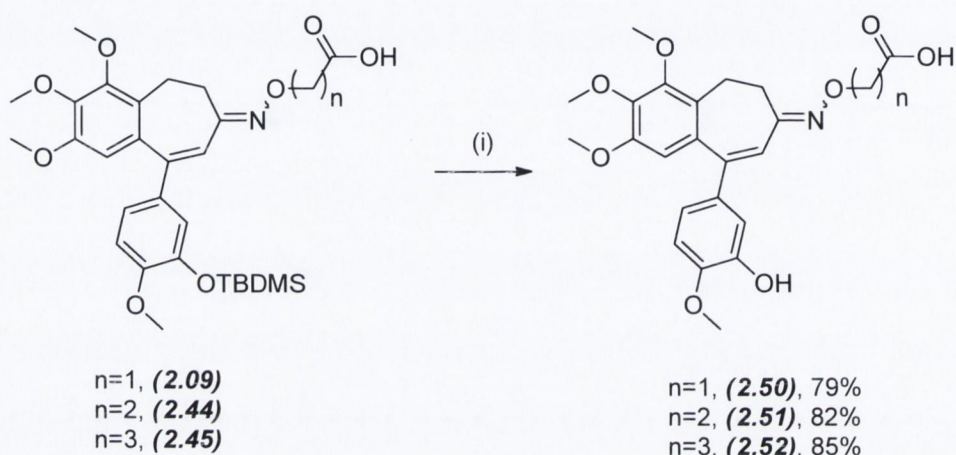
(i) 1M TBAF in THF, THF, 0 °C, 15 min

Scheme 2.15: Synthesis of the carboxylic acids *(2.50)-(2.52)*.

2.5 Synthesis of aniline analogues of *(2.03)*.

Further expansion of the series of hydroxamic acid based DMLs was accomplished, replacing the C-ring phenol with an aniline group, while still bearing the *ortho* methoxy group as before. The synthesis of aniline compound *(2.02)* has previously been accomplished by our group showing excellent anti-proliferative activity similar to that of RS180. It is anticipated that this C-ring modification would have similar improvements on the effects of *(2.03)*, while also providing an attachment point for small, neutral amino acids that are known substrates for APN. As previously mentioned, APN expression is known to be high in various tumours including those of the thyroid, colon, and prostate.[114b, 114d,114a] Accordingly, the attachment of amino acids cleaved by this enzyme, for example leucine, could lead to a more selective targeting of these

types of cancers, releasing compound *(2.06)* in a more controlled manner at the tumour site similar to the colon cancer targeting amino acid prodrugs of 5-aminosalicylic acid.[223] Furthermore, the introduction of an amino acid could potentially enhance the water solubility of these compounds.[224] In order to study the effects of this modification, the synthesis of compound *(2.06)* and its aniline leucine conjugate, *(2.53),* was accomplished as detailed in the following sections following the application of the palladium catalysed Suzuki-Miyaura reaction[225] to form the tricyclic ring structure.

(2.06)   *(2.53)*
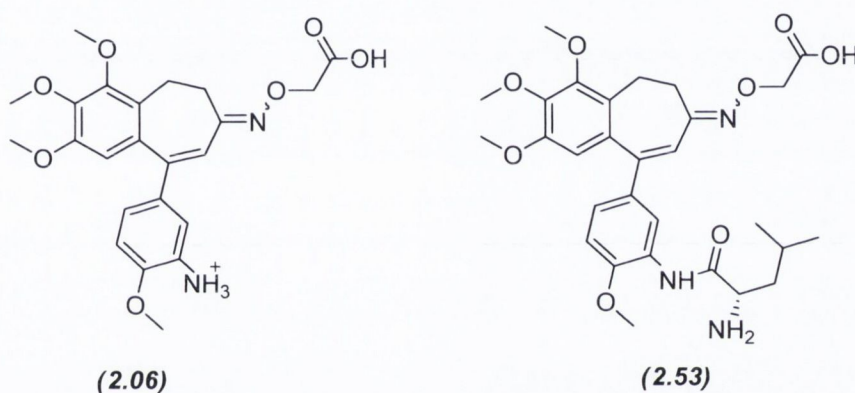
Figure 2.10: Synthetic targets *(2.06)* and *(2.53)*.

2.5.1   The Suzuki Reaction

The versatility of the Suzuki reaction makes it a very useful tool in synthetic organic chemistry, originally facilitating the coupling between aryl organoboronic acids and aryl or vinyl halides using a palladium based catalyst.[226] The scope of the reaction has however been expanded since its initial report to include unconjugated compounds including alkyl halides as substrates[227] following development of a range of novel catalysts[228] to improve the activation of this reaction. Further expansion has allowed the use of "pseudohalides" such as triflates and tosylates as reaction substrates.[229] Suzuki reactions have been used during important stages in the total syntheses of many natural products including the marine sponge derived MT stabilising agents discodermolide[230] and epothilone A.[231] The coupling of 7-membered rings containing vinyl

triflates to a range of organoboronic acids and esters has previously been reported,[232] suggesting the possibility for adoption of this synthetic methodology into the synthesis of our compounds. This is advantageous, as the Suzuki protocol enables the employment of milder reaction conditions, with the use of water as a co-solvent simplifying the handling of the reaction relative to the organolithium coupling detailed toward the synthesis of *(2.01)*. In the synthesis of the aniline compounds, the vinyl triflate *(2.54)* and aryl boronic ester *(2.55)* are first prepared, prior to coupling using a Suzuki procedure (Scheme 2.16).
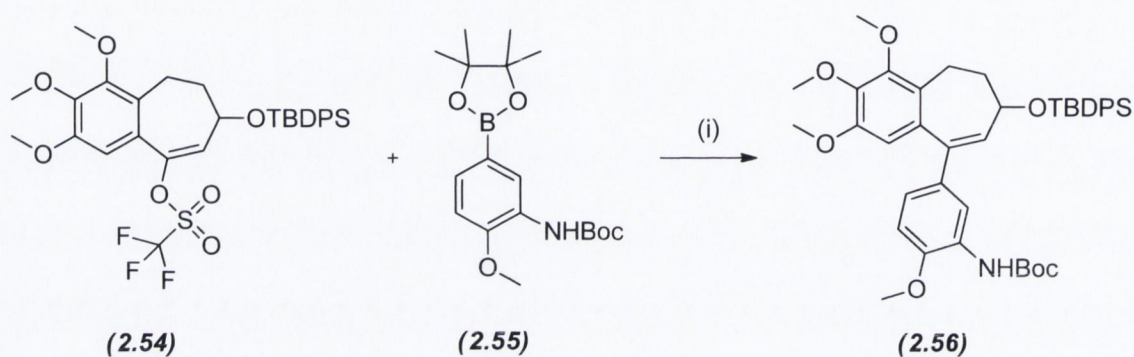
(i) K_2CO_3, Pd(PPh$_3$)$_4$, Toluene/H$_2$O/EtOH (6:1:1), 60 °C, 50 min, 83%

Scheme 2.16: Suzuki coupling of vinyl triflate *(2.54)* and aryl boronic ester *(2.55)*.

2.5.2 Preparation of the AB Ring system for Suzuki reaction.

The protocol developed within the group,[214] involves the modification of the TBDPS protected fused bicyclic ketone *(2.25)* to form the vinyl triflate *(2.54)*. This transformation is effected in a single synthetic step in high yield of 90% using the triflating reagent 2-[*N,N*-bis(trifluoromethylsulfonyl)amino]-5-chloropyridine to react with the oxygen centre of the enolate anion of *(2.25)* generated upon its treatment with lithium diisopropylamide (LDA) over 2 hours at -78 °C in THF.
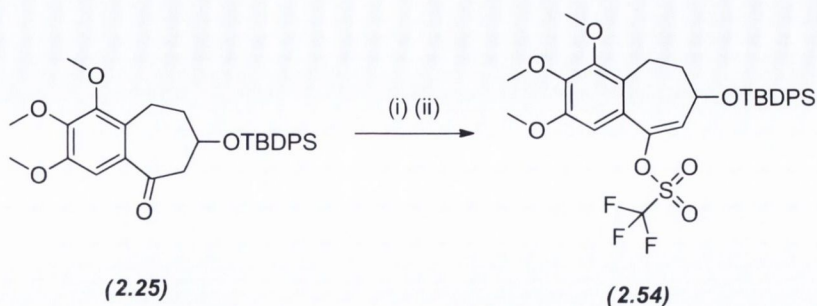
(i) LDA, THF, -70 °C, 2 h (ii) 2-[N,N- Bis(trifluoromethylsulfonyl)amino]-5-chloropyridine, THF,-78 °C, 3 h, 91%

Scheme 2.17: Single step transformation of *(2.25)* to *(2.54)*.

2.5.3 Preparation of Aryl Boronic Ester C-ring.

5-Bromo-2-methoxyaniline, an intermediate synthesised and kindly donated by Coogan,[222] was converted to the required boronate ester in two steps beginning with the *tert*-butyl carbamate (Boc) protection of the aniline following a 12 h reflux with di-tert-butyl dicarbonate at 90 °C in THF to afford *(2.57)*. Another palladium catalysed cross coupling reaction conducted, in a similar vain to the Suzuki coupling, namely the Miyaura borylation[233] of *(2.07)* afforded the desired C-ring *(2.55)*. In this example, the bromine was replaced with the boronate functionality following reflux with bis-pinacolatodiboron in DMSO for 90 min at 80 °C using KOAc as the base and 0. 3 molar equivalents of the widely used ferrocene derived catalyst PdCl₂(dppf).[234]

5-Bromo-2-methoxyaniline   *(2.57)*   *(2.55)*
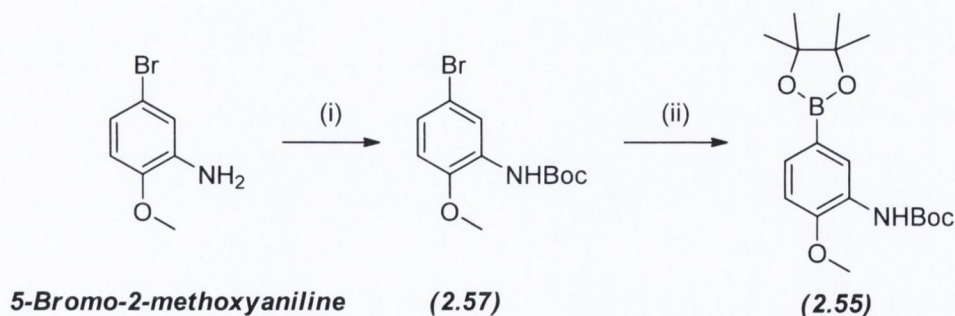
(i) Boc₂O,THF, 90 °C, 12 h, 89% (ii) bis dipinacolatodiboron,
KOAc, PdCl₂(dppf) DMSO, 80 °C, 90 min, 98%

Scheme 2.18: Synthesis of *(2.55)*

2.5.4 Suzuki coupling of *(2.54)* and *(2.55)*.

The Suzuki coupling reaction to form *(2.56)* was mediated using the palladium catalyst Pd(PPh$_3$)$_4$ as outlined in Scheme 2.16. The reaction conditions were carefully monitored as elevated temperatures were seen to lead to degradation of the products resulting in drastically lowered yields. Maintaining the temperature at 60 °C and no higher than 80 °C was an important requirement to effect this transformation, with the optimal reaction time observed to be 50 min. These conditions permitted the transformation to occur smoothly in conversion rates of up to 83%.

2.5.5 Synthesis of compounds *(2.06)* and *(2.53)*.

TBDPS deprotection of *(2.56)* using a 3 h reaction time with TBAF in THF at 0 °C afforded the alcohol *(2.58)* in 81% yield. Following the oxidation of this alcohol with DMP at 0 °C over 10 min, the ketone *(2.59)* was isolated in 82% yield. This intermediate was retained as it was necessary for the completion of the synthetic pathway toward *(2.06)*. The fluorenylmethyloxycarbonyl (Fmoc) protected alcohol *(2.60)* was kindly donated by Breen[235] and similarly oxidised using DMP in 96% yield to yield ketone *(2.61)*.
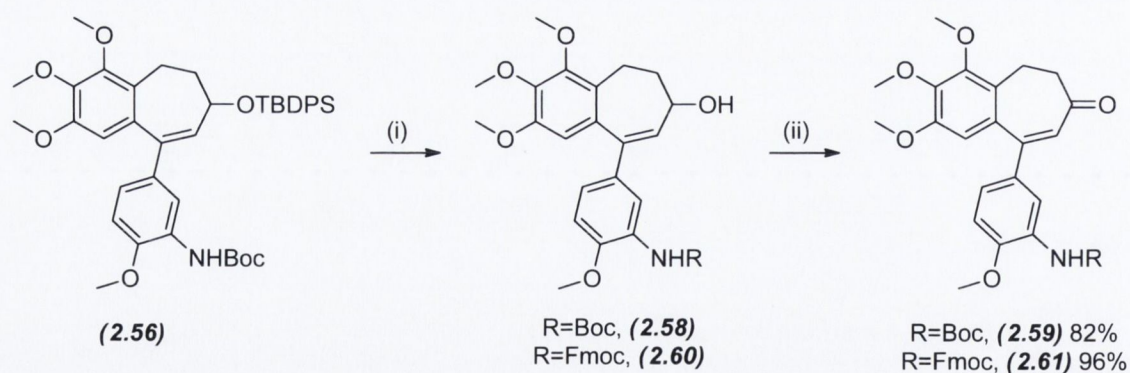
(i)1M TBAF in THF, THF, 0 °C, 3 h, 81% (ii) DMP, DCM, 0 °C, 10 min

Scheme 2.19: Synthesis of ketones *(2.59)* and *(2.61)*.

Whereas *(2.59)* was retained as seen in Scheme 2.19, the Fmoc group of *(2.61)* was removed using TBAF deprotection at 0 °C within 30 mins to yield the free aniline *(2.02)* (Scheme 2.20).

This allowed conjugation of the aniline to Fmoc protected leucine. The reaction was activated using the peptide coupling reagent bromo-tris(pyrrolidino)-phosphonium hexafluorophosphate (PyBrop)[236] to prevent racemisation of the leucine group. The successful coupling was observed after a reaction time of 6 h to afford the leucine conjugate *(2.62)* in 86% yield.
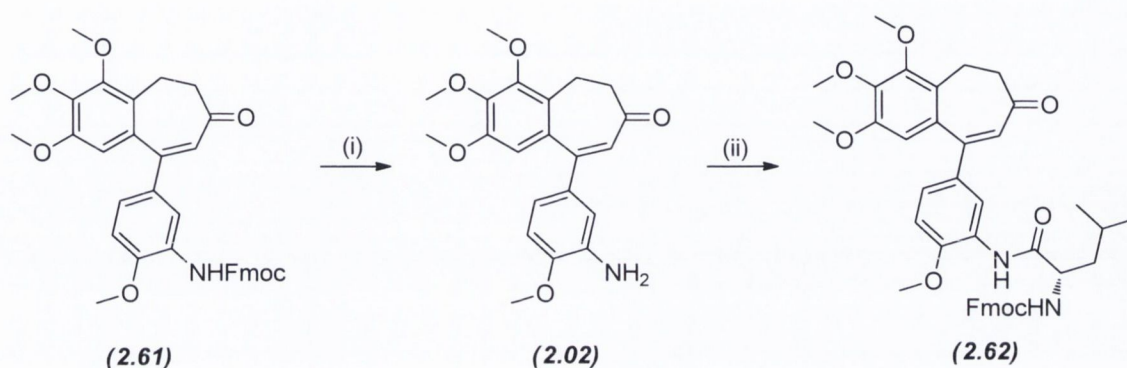
(i) 1M TBAF in THF, THF, 0 °C, 30 min (ii) N-Fmoc Leucine, PyBrop, DIPEA, DCM, 0 °C, 6 h, 86%

Scheme 2.20: Conjugation of *(2.02)* to Fmoc-Leucine.

Following the isolation of the ketones *(2.59)* and *(2.62)*, they were reacted with (O-carboxymethyl) hydroxylamine hemihydrochloride using the same oximination procedure as previously described to yield oxime ethers *(2.63)* and *(2.64)*. After their conversion to activated PFP esters *(2.65)* and *(2.66)*, they were reacted with $NH_2OH.HCl$ over 1 h in H_2O/EtOH to introduce the hydroxamate functionality. Final compound *(2.03)* was afforded via the deprotection of the Boc protecting group using a 1:1 mixture of TFA in DCM. After 2 min reaction time, the hydroxamic acid with the free aniline was isolated in yield of 58%. As *(2.62)* is Fmoc protected, a different deprotection strategy was required, using the same TBAF approach as used in the deprotection of *(2.61)*. This transformation furnished *(2.53)* in 54% yield.

R=Boc, (2.59)
R=Fmoc-Leu (2.62)

R=Boc, (2.63)
R=Fmoc-Leu (2.64)

R=Boc, (2.65)
R=Fmoc-Leu (2.66)

R=Boc, (iv)
R=FmocLeu, (v)

R=Boc, (2.67)
R=Fmoc-Leu (2.68)

R=H, (2.06)
R=Leu (2.53)
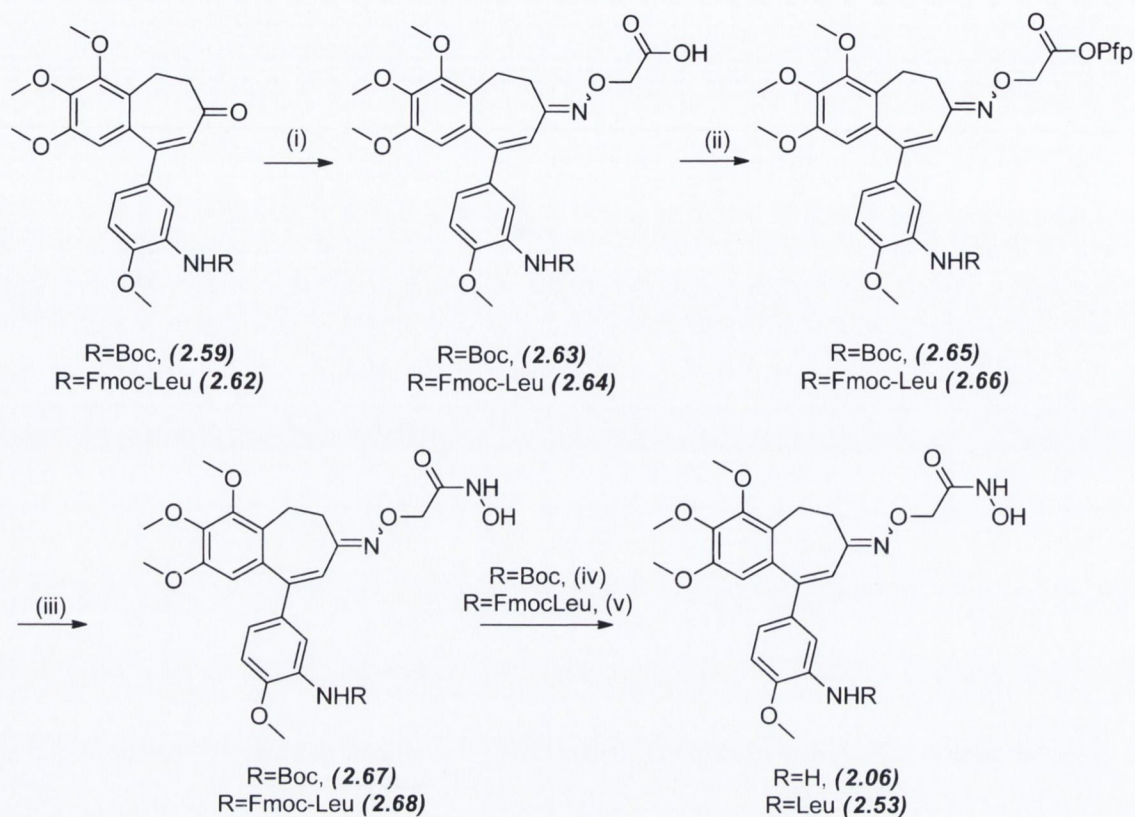
(i) (O-carboxymethyl) hydroxylamine hemihydrochloride, NaOAc, EtOH/H_2O, 24 h
(ii) PFPOH, DCC,DCM, 1 h (iii) $NH_2OH.HCl$, NaOAc, EtOH/H_2O, 30 min
(iv) 1:1 TFA/DCM, 0 °C, 2 min, 58% (v) TBAF, THF, 15 min, 0 °C, 54%.

Scheme 2.21: Final synthesis of compounds (2.06) and (2.53).

The spectra of compound (2.06) showed distinct similarities with those observed for compounds (2.03) to (2.05) with particular closeness observed to that of (2.03), the phenol bearing the same chain length in the oxime ether side chain with its only CH_2 signal observed as broad singlet at 4.57 ppm. The spectra show the similar doubling of peaks as previously observed. The NMR spectra of (2.53) show the similarities to that of (2.06), the side chain protons appearing at 4.51 ppm as a split singlet. There is the added complexity of the leucine side chain, manifesting itself with 3 peaks in the furthest upfield region representative of the leucine portion of the conjugate; a doublet at 0.95 ppm, a multiplet at 1.5 ppm integrating to two protons and a multiplet at 1.75

ppm corresponding to the aliphatic leucine protons. Additionally, a broad peak at 8.30 ppm suggests the presence of the amide bond supporting the structure of *(2.53)*.
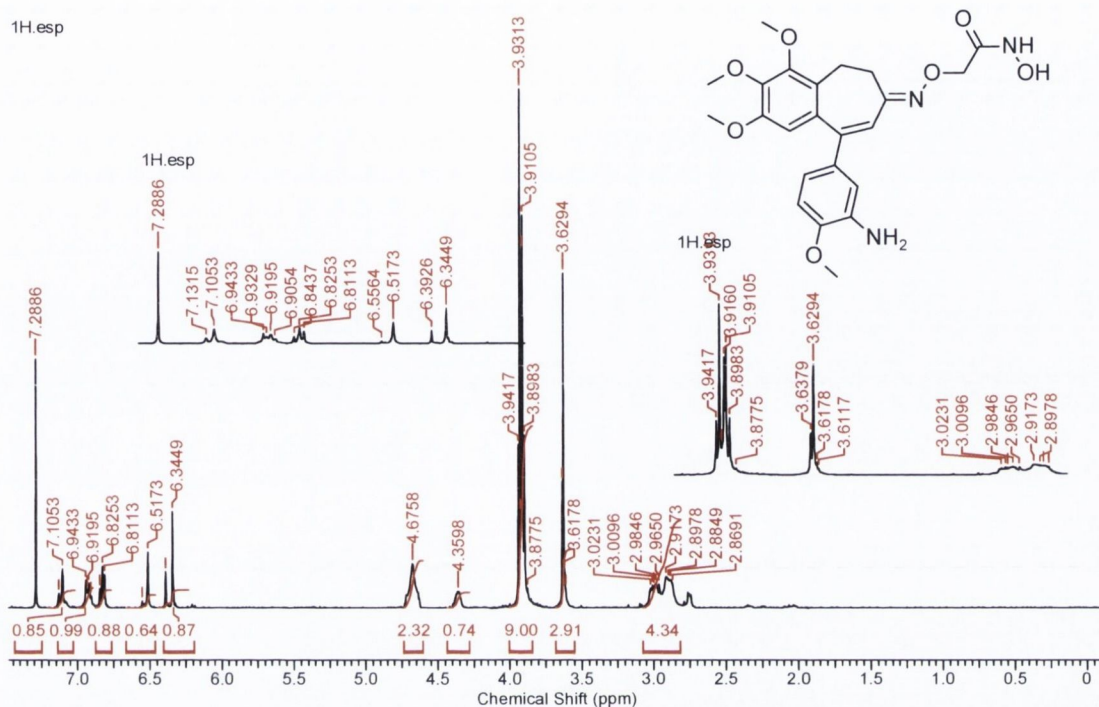
Figure 2.11: ¹H NMR of *(2.06)*.
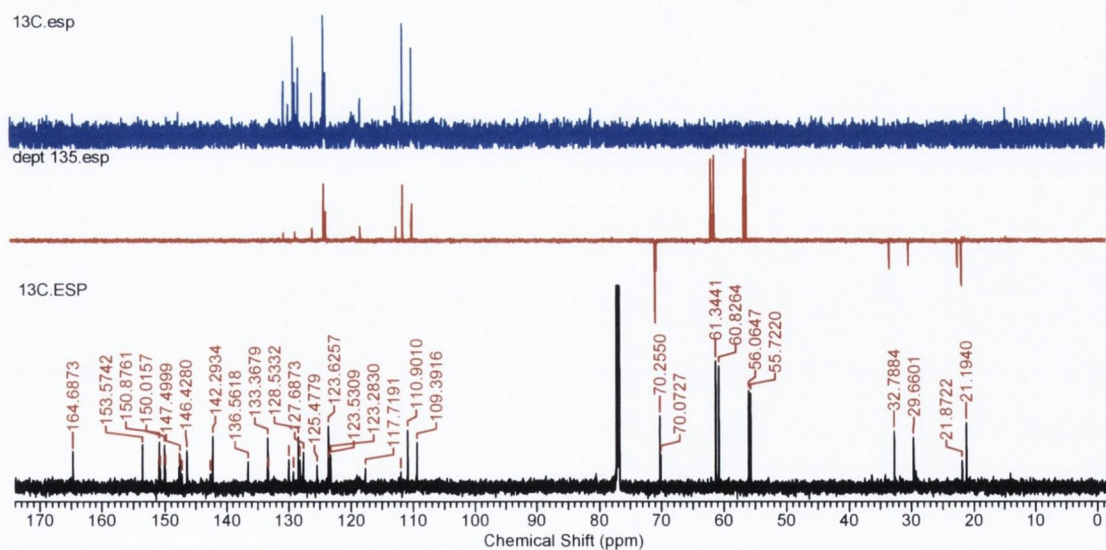
Figure 2.12: ¹³C NMR spectrum of *(2.06)*.
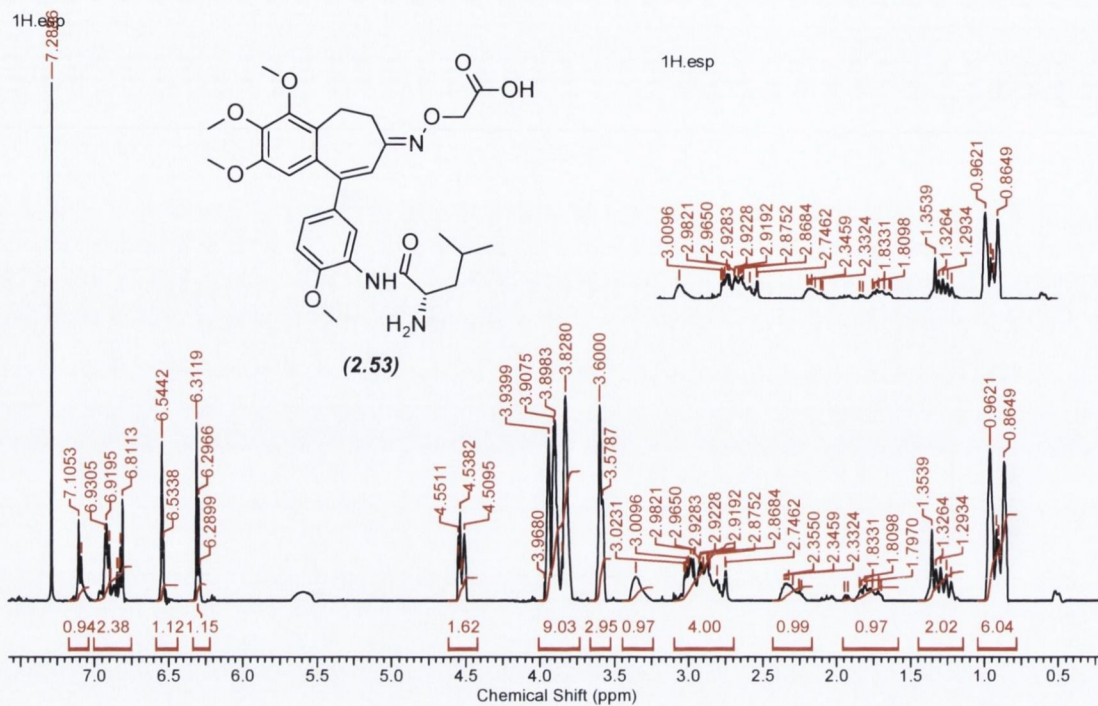
Figure 2.13: ^{1}H NMR spectrum of *(2.53)*.
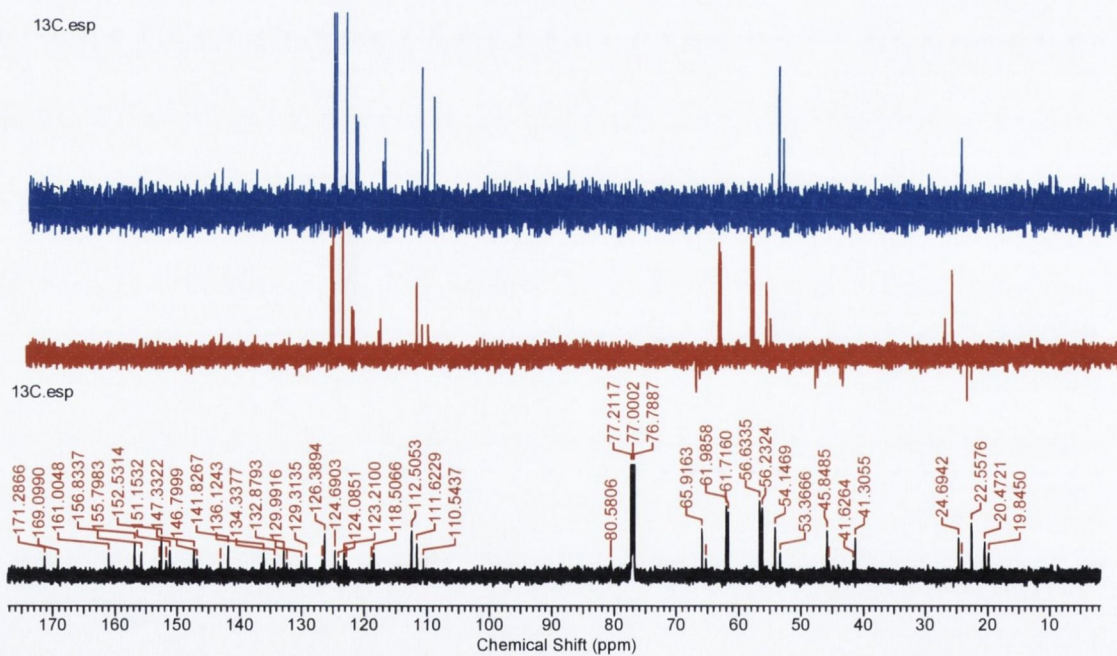
Figure 2.14: ^{13}C NMR spectrum of *(2.53)*.

2.6 Biological Evaluation of Compounds Synthesised in Chapter 2.

The biological activity of the compounds synthesised within this chapter was evaluated using three assay protocols. As stated in the introduction to this chapter these are the APN inhibition assay,[135b] the MTT cell proliferation assay[212] and the cell migration assay.[213] In total, nine compounds whose synthesis is described within this chapter were evaluated and are grouped as follows;

Group 1: The three hydroxamic acid DMLs with the phenolic C-ring *(2.03)*, *(2.04)* and *(2.05)* in addition to the oxime *(2.32)*, Group 2: The two aniline containing hydroxamic acid DMLs *(2.06)* and *(2.53)* and Group 3: The three carboxylic acids *(2.50)*, *(2.51)* and *(2.52)*.

2.6.1 APN Inhibition Assay.

APN inhibition was determined using the spectrophotometric assay originally described by Melzig.[135b] By measurement of the compound's effect on the hydrolysis of the known APN substrate L-leucine-*p*-nitroanilide *(2.69)* to its yellow pigmented *p*-nitroaniline *(2.70)* over a range of concentrations including a dimethylsulfoxide (DMSO) blank in a 96 well plate using the Fluorstar Optima plate reader, the percentage inhibition at each concentration was calculated using the formula:

APN inhibition% = 100 – [(absorbance of test sample/absorbance of DMSO blank)]*100.

(2.69)   **(2.70)**
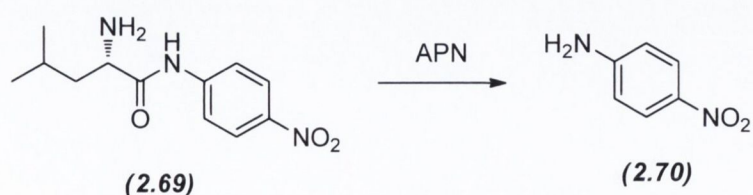
Scheme 2.22: The APN mediated hydrolysis of substrate L-leucine-*p*-nitroanilide.

Non-linear regression analysis of the plot of log concentration versus normalised percentage inhibition was performed using GraphPad Prism 5™ software to calculate the IC_{50} values in μM for each of these compounds, the results of which are tabulated in Table 2.1. The IC_{50} were measured relative to that of a control compound, bestatin whose APN inhibitory IC_{50} was calculated as 32.55±1.40 μM SEM.

Compound	APN inhibition (μM)	SEM
(2.03)	8.70	±1.10
(2.04)	62.49	±1.05
(2.05)	36.97	±1.05
(2.32)	> 400	n/a
(2.06)	18.00	±1.08
(2.53)	78.22	±1.09
(2.50)	> 400	n/a
(2.51)	> 400	n/a
(2.52)	>400	n/a
Bestatin	32.55	±1.40

Table 2.1: IC_{50} (μM) values of test compounds synthesised within this chapter's work measured using the APN inhibition assay.

Graph 2.1 shows a representative example of the graphs produced using the Prism software illustrating the effect of *(2.03)*, the highest performing compound in the assay. The graph shows the percentage inhibition of the enzyme over a range of log concentration of the compound versus normalised percentage inhibition.
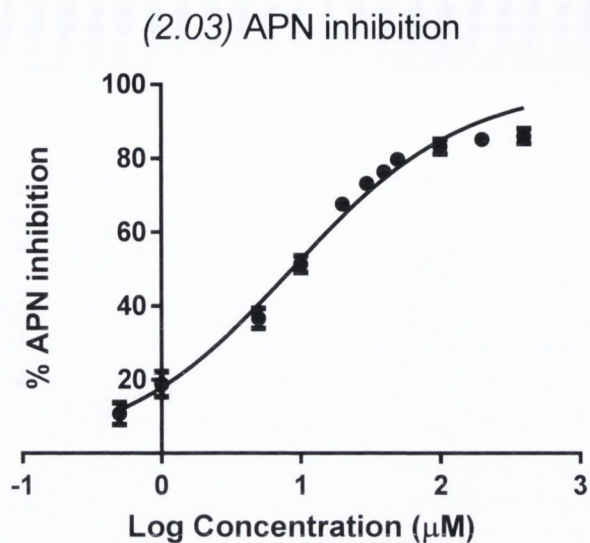
(2.03) APN inhibition

Graph 2.1: APN inhibition of *(2.03)*.

2.6.2 MTT Cell Proliferation Assay

The MTT assay is a colourimetric assay used to measure the activity of the living cells following their treatment with the compounds from Groups 1, 2 and 3. The procedure, first reported by Mosmann[212] measures the mitochondrial reduction of the yellow pigmented tetrazolium salt 3-(4,5-dimethylthiazol-2-yl)-2,5-diphenyltetrazolium bromide (MTT) *(2.70)* following incubation of various concentrations of drug compounds at 37 °C for 72 h. After this time an MTT solution in cell medium is added to each well, effecting a mitochondrial reductase cleavage of the tetrazolium ring to form the dark blue formazan crystals *(2.71)* inside the living cells, but not the dead cells.

(2.70)　　　　　　　　　　　　*(2.71)*
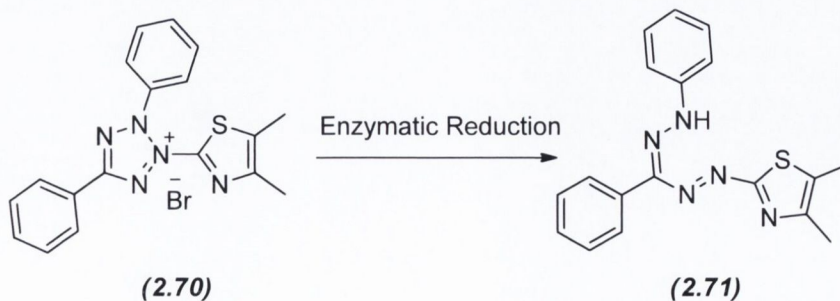
Scheme 2.23: Cleavage of the tetrazolium ring observed in the MTT assay

77

Following the reconstitution of these crystals in suitable solvents,[237] the quantification of the formazan's purple absorbance can be performed using the Fluostar Optima 96 well plate reader. The sensitivity of this protocol means that only a relatively low cell density is required for this measurement allowing the use of 96 well plates facilitating measurement of the effect on cell proliferation of many compounds in a short amount of time. Other tetrazolium salts including XTT and MTS have been developed to introduce greater sensitivity to the assay and in the case of the water soluble MTS, a stock solution of this salt can be added directly to cell medium meaning there is no requirement to replace the cell medium after the 72 h incubation period,[238] however this would not be ideal in our case as the F-12K medium employed in our protocol is coloured, it would have a notable effect on the measurement's sensitivity. The assay has shown wide usage in the measurement of cancer cell proliferation[239] and has long been used on prostate cancer cell lines including PC-3, the cell line used in measurement of these compound's anti-proliferative activity.[240]

Measurement of the absorbance of each well at 485 nm, corresponding to a range of drug concentrations and a 0.1% DMSO blank in triplicate, allows calculation of the percentage inhibition of cellular activity using the formula:

$$100-[(\text{absorbance of sample})/(\text{absorbance of DMSO blank sample})]*100.$$

Following statistical analysis of the data obtained using GraphPad Prism, IC_{50} values were obtained using a non-linear regression of the log concentration versus normalised percentage inhibition plot. The results of these assays are detailed in Table 2.2. The IC_{50} of a control compound used to evaluate the activities, Combretastatin A-4 was measured as 20.44 ± 1.69 nM SEM.

Compound	IC_{50} (PC-3 Cells) (nM)	SEM
(2.03)	108.7	±1.10
(2.04)	189.3	±1.14
(2.05)	116.1	±1.17
(2.32)	19.6	±1.12
(2.06)	291.0	±1.08
(2.53)	576.3	±1.10
(2.50)	97.94	±1.16
(2.51)	375.1	±2.5
(2.52)	648.1	±3.05
CA-4	20.44	±1.69

Table 2.2: The IC_{50} (nM) values of test compounds synthesised within this chapter's work measured using the MTT assay after 72h incubation period.

2.6.3 Cell Migration Assay

A number of methods have been used to experimentally evaluate the migration potential of cells using complex sets of apparatus, the most common of which is the Boyden chamber.[241] However a relatively inexpensive method to evaluate cell migration has been developed[213] and achieved widespread use as a dependable method to this end.[133, 242] This assay, commonly known as the "scratch assay" involves the growth of a confluent monolayer of cells before creating a scratch in the cell monolayer using a 200 μL pipette tip. Taking images of the size of the cellular breach over a period of time allows the measurement of the relative cell migration potential of the PC-3 cells following treatment with test compounds. One drawback associated with this assay is the requirement to manually measure the open wound area by inspection of each of the series of images acquired. This is a tedious task, however a computer program Tscratch, developed by the CSE lab in the Swiss Federal Institute of technology in Zurich, has enabled a more automated approach towards these measurements achieving comparable results to those calculated manually in drastically reduced times[243] showing widespread acceptance for

completion of this analysis since its introduction.[244] This software was accordingly used in the analysis of the images taken during the course of our migration assay protocol.

Images were acquired at four time points (0 h, 24 h, 36 h and 48 h) using an Olympus CKX41 inverted microscope and its associated Cell[A] software before analysis using Tscratch. Initially each compound was evaluated at 5 μM, 10 μM and 20 μM final concentrations to determine the highest performing compounds. After this initial screening, the compounds *(2.03)*, *(2.06)*, *(2.51)* and *(2.32)* were tested in triplicate allowing measurement of one compound from each of the groups outlined as above at these concentrations, with the exception of *(2.03)* which showed a high degree of toxicity to cells at 20 μM. However after showing anti-migratory activity at lower concentrations, this compound was evaluated at 2.5 μM, 5 μM and 10 μM. Both combretastatin A-4, in final concentrations of 5 μM, 10 μM and 20 μM, and bestatin in concentrations of 40 μM and 80 μM were used as experimental control compounds.

At 24 h, 36 h and 48 h, the spontaneous migration distances were measured as 147.91 nm, 231.51 nm and 270.55 nm showing near complete closure of the wound. The spontaneous migration distances for each test compound, CA-4, 80 μM bestatin and 0.1% DMSO blank are detailed in Table 2.3 below.

Compound	Conc	Cell Migration (nm) 24 h	Cell Migration (nm) 36 h	Cell Migration (nm) 48 h
(2.03)	2.5 μM	158.66±26.79	196.81±25.30	245.08±17.20
	5 μM	128.01±3.41	140.11±14.22	186.94±10.80
	10 μM	101.45±7.96	104.89±14.74	124.00±12.63
(2.06)	5 μM	178.43±12.41	232.65±4.67	242.68±9.40
	10 μM	143.61±5.49	192.14±7.55	197.66±10.18
	20 μM	141.35±20.33	158.97±20.72	197.36±28.62
(2.51)	5 μM	138.22±16.42	158.80±2.96	188.86±16.99
	10 μM	133.90±15.28	176.61±3.40	206.57±14.60
	20 μM	125.61±20.36	173.95±20.91	188.71±28.63
(2.32)	5 μM	146.76±28.10	184.27±9.75	200.32±18.98
	10 μM	112.40±5.72	164.21±8.12	193.85±1.32
	20 μM	99.27±13.84	150.08±20.73	165.39±1.072
CA-4	5 μM	114.93±7.17	137.90±16.27	167.74±7.96
	10 μM	108.05±8.53	133.05±4.82	159.58±14.74
	20 μM	81.37±3.60	122.12±10.26	150.95±12.64
(2.01)	5 μM	127.92±9.99	181.39±21.32	234.09±38.30
	10 μM	102.67±17.17	155.35±13.75	172.04±16.76
	20 μM	89.99±23.89	140.05±23.69	156.42±10.75
Bestatin	80 μM	142.52±6.29	188.61±7.40	208.70±8.88
0.1% DMSO		176.02±8.51	240.93±7.21	277.30±12.09

Table 2.3: The measured cell distances for tested compounds (±SEM).

The highest performing compounds at this concentration was the hydroxamic acid *(2.03)* with migration distances of 101.45 nm, 104.89 nm and 124 nm at 10 μM concentration showing significant inhibition of the migration over DMSO blank and CA-4 at this concentration over 48 h in particular. DMLs *(2.32)* and *(2.51)* also displayed an anti-migratory effect relative to the DMSO blank at all concentrations, whereas the aniline hydroxamic acid displayed an effect only at concentrations of 10 μM and above in contrast with its phenolic counterpart *(2.03)* which was the highest performing compound under these conditions. It is not currently understood as to why there would be such a deviation in activity between these two compounds. At 20 μM, the oxime *(2.32)* showed a large anti-migration effect over the first 24 h performing

similarly to CA-4, however the effect is not as strong over the second 24 h period, with *(2.03)* showing a longer lasting effect. Parent compound *(2.01)* showed higher anti-migratory effect over the first 24 h than *(2.03)*, however the effect associated with the hydroxamic acid was evidenced to be longer lasting.

From this data which is detailed in photographic form in Figure 2.15 below, it is seen that *(2.03)* has the greatest effect on migration of the compounds studied, followed by that of *(2.32)* which shows slightly reduced activity relative to the performance of CA-4 under the same conditions. It is only at the higher concentrations and towards the end of the experimental timeframe where there is an antimigratory effect relative to that seen in CA-4 in the remaining two compounds studied *(2.51)* and *(2.06)*.
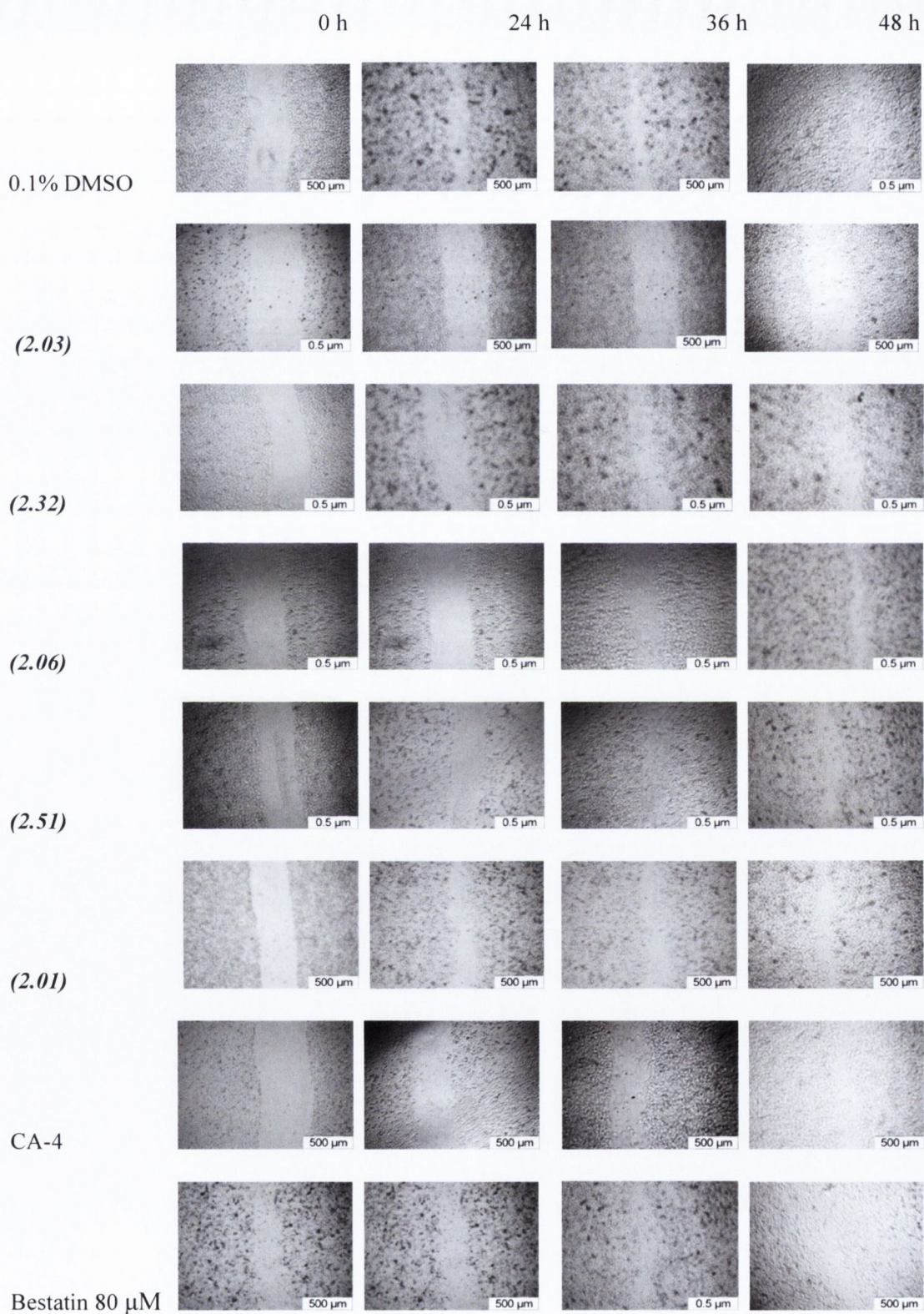
Figure 2. 15: Inhibition of PC-3 cell migration by test compounds at a concentration of 10 μM at 0 h, 24 h, 48 h and 72 h.

(2.03)
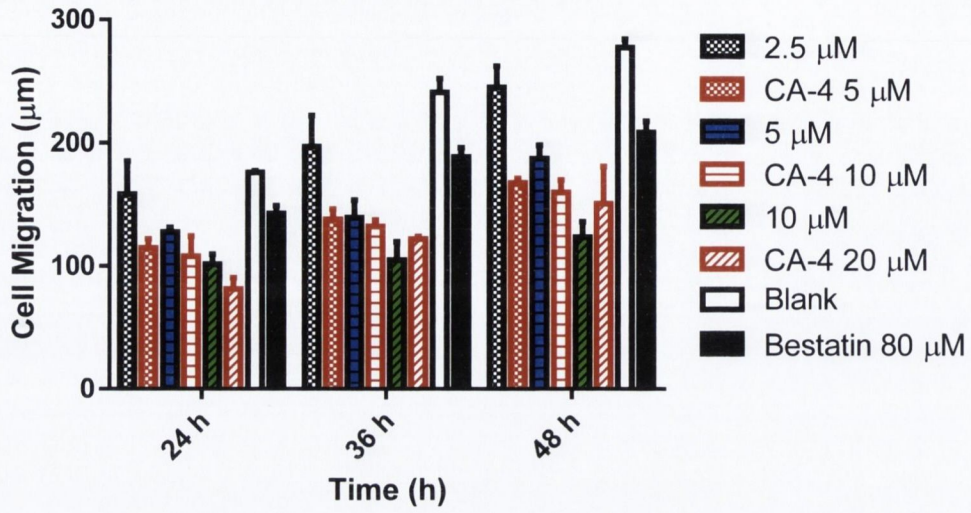
Graph 2.2: Cell migration distance measured for *(2.03)* over 24 h, 36 h and 48 h.

(2.06)
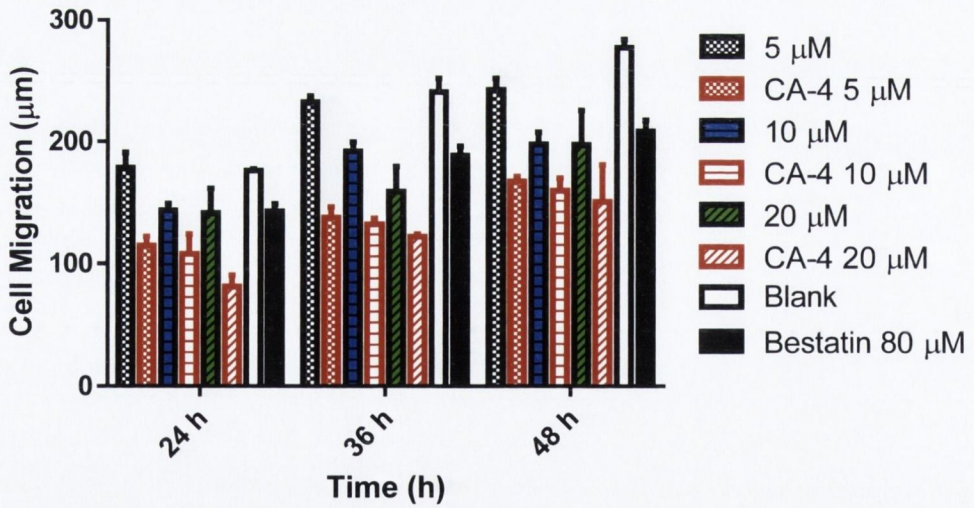
Graph 2.3: Cell migration distance measured for *(2.06)* over 24 h, 36 h and 48 h.

(2.51)
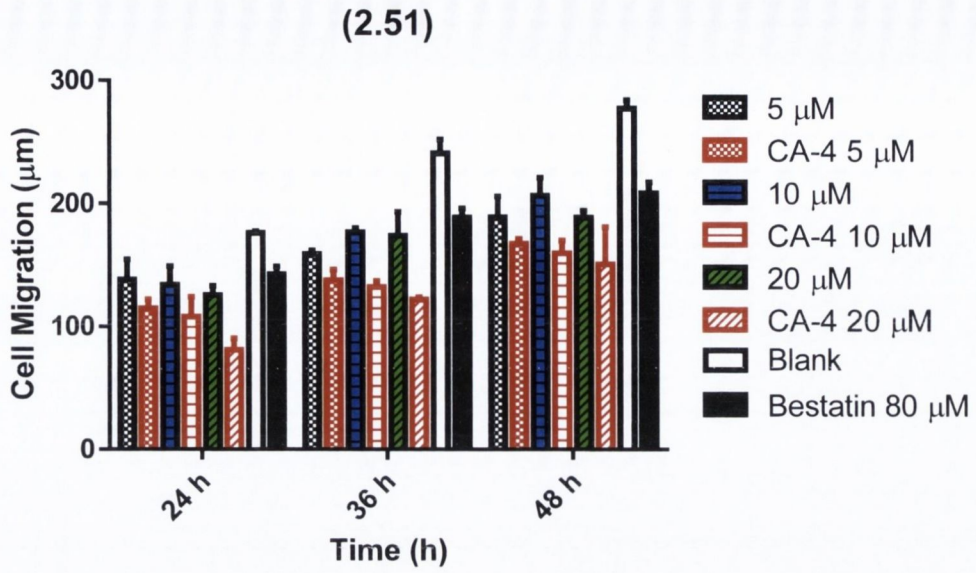
Graph 2.4: Cell migration distance measured for *(2.51)* over 24 h, 36 h and 48 h.

(2.32)
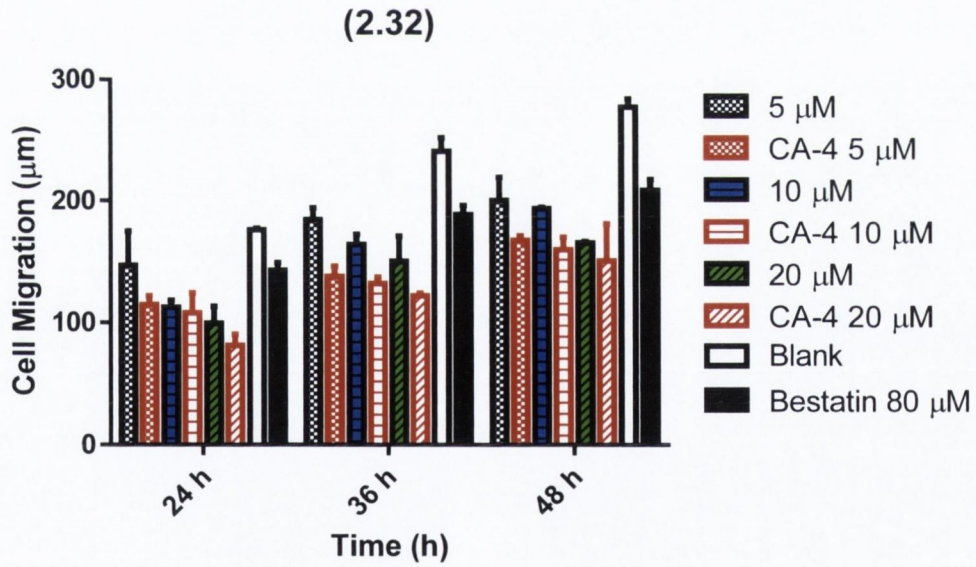
Graph 2.5: Cell migration distance measured for *(2.32)* over 24 h, 36 h and 48 h.

2.7 Discussion and Conclusion

The work described in this chapter outlines the successful synthesis of a series of novel dual targeting APN and tubulin inhibiting agents. These compounds contain the hydroxamic acid functionality which is known to effectively target peptidases implicated in invasion metastasis and angiogenesis in the proliferation of cancers including APN and LTA_4H. The effect of the carbon chain linking the hydroxamic acid to the microtubule targeting component of the compound was investigated by synthesis of compounds *(2.04)* and *(2.05)*. Additionally aniline compound *(2.06)* and its leucine conjugated adduct *(2.53)* were synthesised to illustrate the effect of a nitrogen bearing C-ring on anti-proliferative, antimigratory and anti-APN activity.

Firstly, the APN inhibition data shows the effect of the hydroxamic acid moiety in the in vitro inhibition assay. The highest performing compound observed using the protocol outlined by Melzig was hydroxamic acid *(2.03)* with its IC_{50} of 8.70 μM registering a significant 4-fold increase in APN relative to the control compound bestatin with a measured IC_{50} of 32.55 μM.

While extension of the carbon chain in the oxime ether linker unit did not completely attenuate activity, it did lead to diminished activity relative to the lead compound *(2.03)*. No discernable trend was observed with compound *(2.05)* possessing the three carbon linker unit displaying greater inhibitory effect over that observed by *(2.04)*. On a similar set of oxime ether linked hydroxamic acids, there was also no observable link between carbon chain length and APN inhibitory activity.[136] In fact the only other compound showing activity greater than that observed for bestatin was aniline *(2.06)* also bearing the simplest oxime ether linker. As detailed in chapter 2, the Zn^{2+} centred binding site of APN possesses hydrophobic pockets either side of the metal centre. A potential inhibitor therefore would exert its greatest effect when possessing a hydrophobic group nearest to its zinc binding group (ZBG). In our systems, the tricyclic

structure contains two aromatic rings which could function in such hydrophobic interactions. The result of extending the carbon chain could be to separate the hydrophobic component of the compound from its desired binding site diminishing the strength of interactions required for the APN inhibitory effect.

With the extension of the chain, there is however greater potential to further characterise the side chain with the required hydrophobicity. The chapter details a robust synthetic method whereby hydroxylamines can be added to *(2.07)* via an oximation condensation reaction. By derivatisation of this chain with bulky aliphatic or aromatic groups, to be located near the hydroxamic acid, the hydrophobic character of the compound could be suitably increased.

The chain length extension could alternatively be achieved using a phosphinic acid functionality could be introduced in place of the hydroxamic acid. The phosphorous in the ZBG has a higher valency that nitrogen, allowing it more subsituents attached to its centre to potentially possess hydrophobic chains either side of the ZBG to strengthen interactions with the host enzyme.[154b] Using this functional group could be a preferred method to enhance activity than a simple carbon chain extension.

The importance of the hydroxamic acid in APN inhibition is evident as the carboxylic forms *(2.50)-(2.52)* show no inhibition of the enzyme at high concentrations. The importance of the hydroxamic acid moiety is further seen resulting from the ineffectiveness of oxime *(2.32)* in APN inhibition, showing the increase in anti-APN effect is not due to the oxime group. The inactivity of oxime and carboxylic acid derivatives is established to result from their incapability to form a five membered chelated ring.[96, 136]

In contrast to its fortunes in the APN inhibition assay, oxime *(2.32)* showed the greatest anti-proliferative effect in the MTT assay displaying an IC_{50} of 19.6 nM, positively comparable to

control compound CA-4 (IC_{50} 20.44 nM), but showing slightly lower activity than *(2.01)*. The other compounds in the series all display nanomolar activity with carboxylic acid *(2.50)* and hydroxamic acid *(2.03)* and *(2.06)* displaying IC_{50}s in the region of 100 nM. Leucine conjugate *(2.53)* displays the weakest effect on cell proliferation with an IC_{50} of 648.1 nM. This is surprising as other aniline compounds such as *(2.02)* exhibit strong anti-proliferative effects and the treatment of the compound in medium for 72 h should grant sufficient time for cleavage of the amide to yield the active compound *(2.06)*. However, *(2.06)* itself doesn't exhibit the same anti-proliferative effect as its phenolic counterpart *(2.03)*.

The migration assay illustrates the anti-migratory effects of the test compounds over concentrations ranging between 5 µM and 20 µM relative to the untreated cells and cells treated with 80 µM bestatin. Compounds *(2.03)* and *(2.32)* exhibiting the greatest effect over the 2 day timescale. DML *(2.03)* exhibits a long lasting effect, with a slowdown in migration rate at high concentrations over the second 24 h period. This could be due to the observed *(2.01)* following the hydrolytic cleavage of the oxime bond in the assay conditions.

In conclusion, this chapter describes the synthesis of a series of novel compounds which are proven to inhibit cell proliferation and cell migration. With further development, these compounds could function as potential new lead compounds in cancer chemotherapy.

Chapter 3

3.1   Introduction

Following the encouraging cell proliferation and migration data generated with both *(2.03)* and *(2.32)* in particular, it was decided to expand upon the pharmacophore already described in Section 2.1. Accordingly, it was envisaged that the migration of the carbonyl functional group from the 7-position to the neighbouring carbon would result from a simple modification to the synthesis of RS180 yielding the novel compounds, phenol *(3.01)* and its aniline analogue *(3.02)*. One reason for interest in such migration of the carbonyl functional group is the resultant breakage of conjugation throughout the molecule. Certain reactions in the synthetic pathway toward RS180 have shown to be problematic owing to the potential formation of additional conjugation throughout the molecule as has been noted most clearly in the side reaction during the TBAF deprotection of alcohol *(2.25)* where elimination of the protected alcohol functions to yield a conjugated diene derivative. In compound *(3.01)*, the extra separation between the alkene and carbonyl groups should prevent any such elimination from happening to the related intermediate in its own synthesis, serving to protect the target structure's integrity. The removal of conjugation is also expected to improve the efficiency of any subsequent substitution reactions at the carbonyl position by inhibiting any possibility of side reactions including the Michael addition[245] to the alkene centre of the enone moiety.

Thus, it is hypothesised that this simple alteration to our already established scaffolds could be very valuable from a number of viewpoints. Firstly, being the creation of an entirely new family of compounds exhibiting potential anti-proliferative activity and secondly by doing so in a fashion that improves on the efficiency of the synthesis of these compounds over the related series based on RS180, by way of prevention of the potential conjugation of the compound to act as a driving force for side reactions.

Upon successful completion of their synthesis, subsequent modification to the carbonyl group in particular would allow for the creation of a new family of hydroxamic acid based dual inhibitors *(3.03-3.05)*. Likewise, in an analogous manner to the work of White and Breen[235] the C-ring phenolic or anilino groups can be exploited for the direct attachment of APN peptides based on bestatin as represented by *(3.06)*.

(3.01) R=OH,
(3.02) R=NH$_2$

(3.03) n=2,
(3.04) n=3,
(3.05) n=4

(3.06)
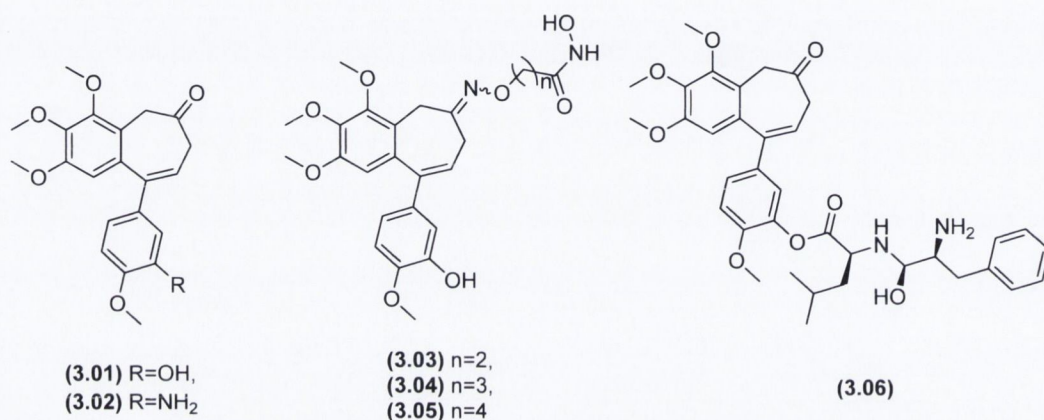
Figure 3.1: A selection of potential new analogues of RS180 that could be synthesised as part of the work outlined in this chapter.

In this chapter the synthetic strategies employed to facilitate the development of this new family of compounds, in particular the efforts taken toward the synthesis of *(3.01)* are discussed.

3.2   Synthesis and Discussion.

3.2.1   Synthetic strategy.

As outlined in Scheme 3.1, our strategy was envisaged to involve the initial reduction of 2,3,4-trimethoxybenzaldehyde with NaBH$_4$, followed by conversion of the resultant alcohol *(3.08)* to its benzyl bromide *(3.09)* using phosphorous tribromide (PBr$_3$) at -10 °C as previously performed by Shah.[209a] Subsequent bimolecular substitution (SN$_2$) of the bromide with sodium cyanide (NaCN) was expected to facilitate the synthesis of the nitrile, 2-(2,3,4-

trimethoxyphenyl) acetonitrile *(3.10)*, which following treatment with allyl magnesium bromide was expected to afford the ketone intermediate *(3.11)*. Its reduction with NaBH$_4$ and protection with TBDPSCl should theoretically furnish the alkene *(3.13)*. It was anticipated that smooth conversion of *(3.13)* to the primary alcohol *(3.14)* could be carried out using the method of Rowan *et al*[246] in their synthesis of macrocycles derived from cinchona alkaloids. This alcohol could be oxidised to the carboxylic acid *(3.15)*, as per the method developed by Corey and Schmidt using pyridinium dichromate in DMF.[247] Subsequent cyclisation in an analogous fashion to that outlined in the previous chapter would form the bicyclic ketone *(3.16)*,[215] whose TBDPS functionality could be removed using TBAF in THF to yield *(3.17)*. Subsequently, the target compound *(3.02)* would then be obtained in a fashion similar to RS180, namely the overnight organolithium addition of *(2.13)* to afford *(3.18)*. Oxidation of the secondary alcohol to the ketone *(3.19)* using DMP, followed by the deprotection of the phenol protecting group using TBAF was expected to yield the target compound, *(3.01)*.
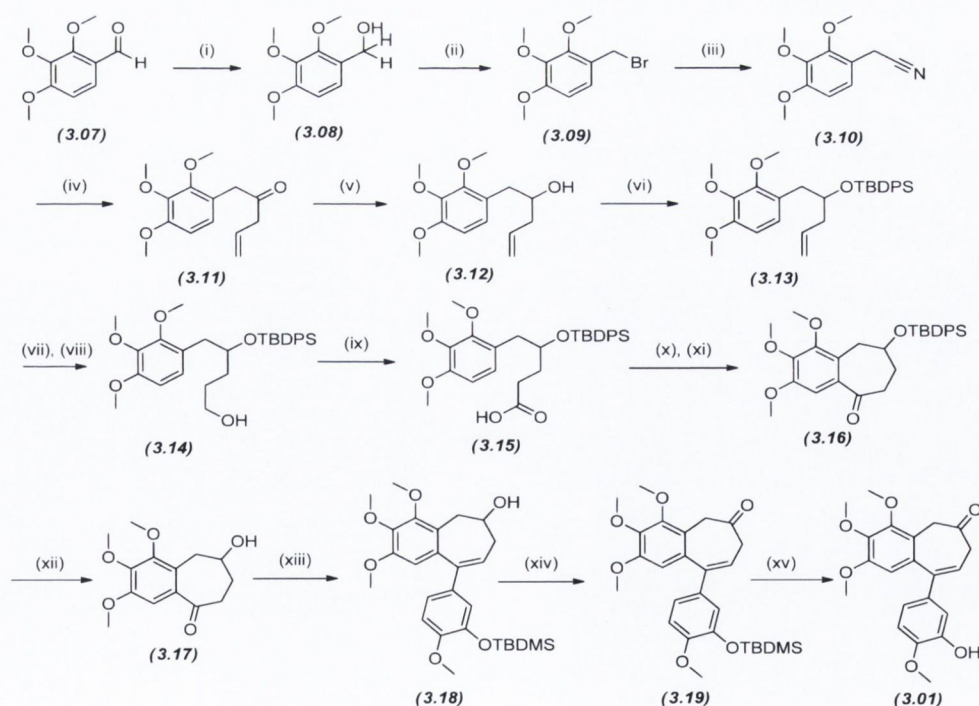
(i) NaBH$_4$, MeOH (ii) PBr$_3$, DCM (iii) NaCN, DMSO (iv) Allyl Bromide, Mg, THF (v) NaBH$_4$, MeOH
(vi) TBDPSCl, Imidazole, DMF (vii) Borane-THF complex, diglyme (viii) Trimethylanilinium
N-oxide dihydrate (ix) PDC, DMF (x) Oxalyl Chloride, DMF, DCM (xi) SnCl$_4$, DCM (xii) TBAF, THF
(xiii) n-BuLi, C-RING, THF (xiv) Dess-Martin periodinane, DCM (xv) TBAF, THF.

Scheme 3.1: Original synthetic strategy towards *(3.01)*.

93

3.2.2 Discussion

As stated in the previous section, the plan was to follow a very similar synthetic approach to that undertaken in the synthesis of RS180, starting with the modification of 2,3,4-trimethoxybenzaldehyde *(2.15)* through a series of reactions to yield the carboxylic acid *(3.15)*. Upon furnishing this compound, the Friedel-Crafts acylation reaction used in the previous chapter would yield the structure with a 7-membered ring fused to the 2,3,4-trimethoxyaryl ring *(3.15)* forming the AB ring structure of our target compound. This reaction and the subsequent C-ring addition would proceed in a manner similar to that observed in the synthesis of RS180.

(3.15)   Acylation   *(3.16)*
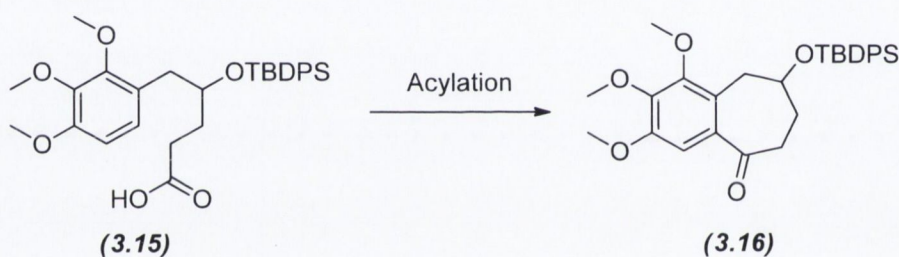
Scheme 3.2: The carboxylic acid intermediate *(3.15)* and the cyclised compound *(3.16)*. Two key intermediate compounds toward the synthesis of *(3.01)*.

The initial objective was to accomplish the synthesis of *(3.15)*. Compound *(3.07)* was reduced to the alcohol *(3.08)* using NaBH$_4$ in methanol (MeOH) at 0 °C over 15 mins in an almost quantitative yield. The two subsequent reactions, namely the bromination of *(3.08)* to compound *(3.09)* using PBr$_3$ in dichloromethane (DCM) at -10 °C and its subsequent room temperature SN$_2$ reaction with NaCN in DMSO to yield nitrile *(3.10)* were more complicated than anticipated, with care needed to ensure optimal reaction yields.

The bromination step proved, as expected, to be quite exothermic, requiring a low reaction temperature and dropwise addition of PBr$_3$ to prevent an overvigorous reaction leading to

generation of multiple undesirable products. Reaction times of longer than 90 min also led to the breakdown of the product, limiting the optimal reaction time to 1 h. No attempt was made to purify this compound using column chromatography, as previous attempts to do so resulted in its degradation on silica.[209b] It was therefore directly reacted with NaCN to form the nitrile *(3.10)*. The best results for this reaction were obtained when the benzyl bromide *(3.09)* was added dropwise to a stirred solution of NaCN in DMSO. This procedure yielded *(3.10)* with conversion rates as high as 80% over the two reactions from the alcohol, whereas the reverse order utilised in the work of Shah[209a] showed much diminished yield (*circa* 40%) obtained, representing a very costly loss of compound at such an early stage of this synthesis.

(3.07)   *(3.08)*   *(3.09)*   *(3.10)*

(i) NaBH$_4$, MeOH, 0 °C, 98%, (ii) PBr$_3$, DCM, -10 °C, (iii) NaCN, DMSO, 20 °C, 80% (over two steps).
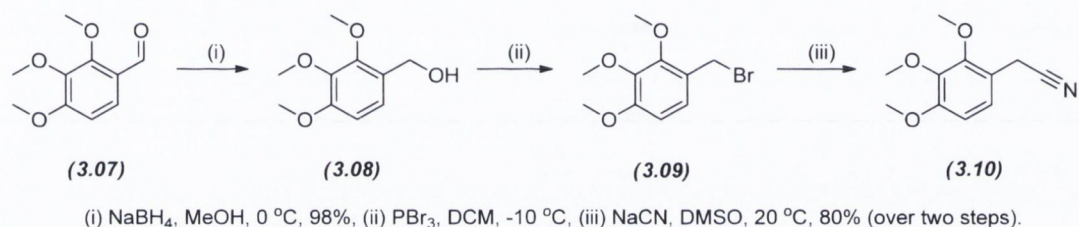
Scheme 3.3: The synthetic pathway toward compound *(3.10)*.

Problems were encountered in the subsequent stage of the synthesis, where it was initially envisaged that the Grignard reaction[248] of the nitrile *(3.10)* with allyl magnesium bromide would yield the ketone *(3.11)*. Unfortunately, this method provided zero conversion of the starting material over the course of several days, under various conditions including activation at increased temperatures up to 100 °C and the use of 1,2-diiodoethane. A literature search showed Weiberth *et al* achieved this desired transformation with the addition of copper (I) salts to the reaction mixture,[249] however our attempts showed no improvements in the progress of the reaction. A number of alternative procedures for the elaboration of the nitrile to yield *(3.11)* were subsequently considered as outlined in Scheme 3.4.
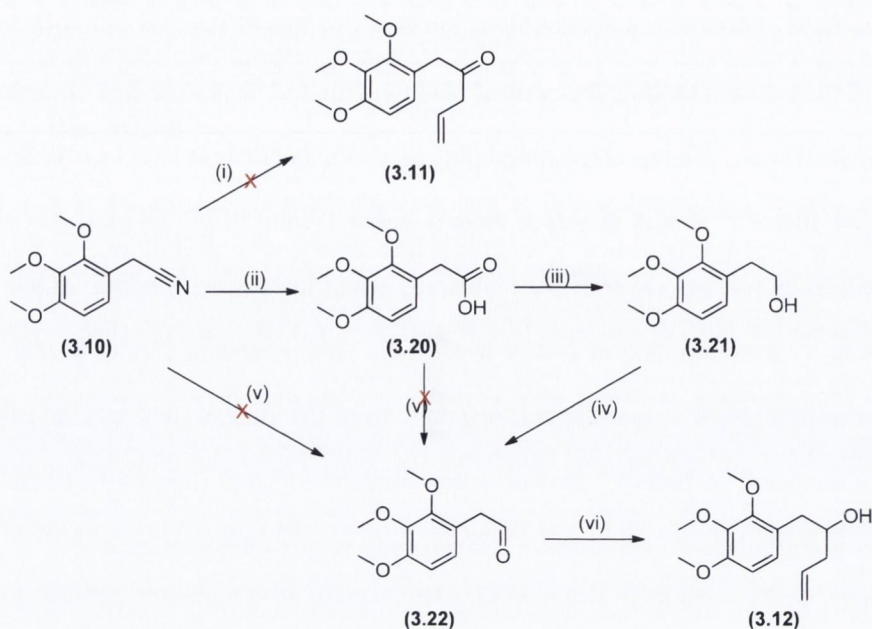
(i) Mg, Allyl Bromide, Cu(I)Br, THF, 3 days, 80 °C, (ii) 2.5 M NaOH, MeOH, 25 °C, 68%, (iii) LiAlH$_4$, THF, -20 °C, 75% (iv) PDC, DCM, 0 °C, 70% (v) DIBAL, THF, -78 °C, N$_2$ (vi) Mg, Allyl Bromide, THF, 6 h, 75%.

Scheme 3.4: of initial attempts to convert the nitrile to alcohol *(3.12)*.

There are reports in the literature suggesting the possibility of the conversion of the nitrile *(3.10)* to the corresponding aldehyde *(3.22)* using diisobutylaluminium hydride (DIBAL).[250] It was anticipated that the Grignard reaction could easily convert this aldehyde to *(3.12)*, allowing further advancement of the synthesis. Unfortunately our attempts using DIBAL at -78 °C in THF under N$_2$, failed to secure the aldehyde *(3.22)*.

It was thus decided to pursue a slightly longer synthetic pathway beginning with the basic hydrolysis of the nitrile *(3.10)* by reflux with an aq. 2.5 M NaOH in MeOH over the course of 3 days to yield the carboxylic acid *(3.20)*. Attempts to furnish the aldehyde *(3.22)* directly at this stage using the same DIBAL method as previously outlined had a similar outcome, necessitating the reduction of the carboxylic acid to alcohol *(3.21)* using LiAlH$_4$ at -20 °C and its subsequent oxidation using pyridinium dichromate (PDC) in DCM to give the aldehyde *(3.22)*. Subsequently, the Grignard reaction furnished the alcohol *(3.12)* in a yield of 75%.

However, it was clear at this stage there were drawbacks to this procedure. Firstly the length of time required to proceed to this relatively early stage in a long synthesis wasn't particularly desirable, as the basic hydrolysis step required 3 days for completion of reaction. There was also a significant increase in the number of steps required compared to the original plan and this manifested itself in the poor overall yield of *(3.12)*, with just 0.35 g of this compound retrieved from 10.00 g of 2,3,4-trimethoxybenzaldehyde. As this represented a total yield of just 2.7% at such an early stage in the synthesis, it was clear that other methods should be pursued in order to maximise the amount of given intermediates going forward.

One further attempt to reduce *(3.10)* to *(3.22)* using NaBH$_4$ in MeOH following a procedure previously used by McHugh[251] did function albeit in the rather low yield of just 10% and thus not functioning as an improvement on our previous results.

3.2.3   Synthesis of *(3.21) via* a Wittig reaction

The Wittig Reaction[252] is a commonly used and reliable method for the conversion of carbonyl compounds (mainly aldehydes or ketones) to alkenes by their reaction with a phosphonium ylide. An ylide is a reactive species containing both a positive charge and a negative charge on adjacent atoms (as seen in Figure 3.2) and phosphonium ylides are formed using a suitable base to deprotonate the relatively acidic proton neighbouring the phosphorous atom. This reaction has found wide use in many multistep syntheses proving to be a reliable synthetic tool to the organic chemist.[253] The key step of the reaction mechanism involves a transition state where a four membered ring intermediate collapses to produce the desired alkene and a by product which possesses the strong P=O bond, the formation of which acts as the driving force behind this reaction.[254]
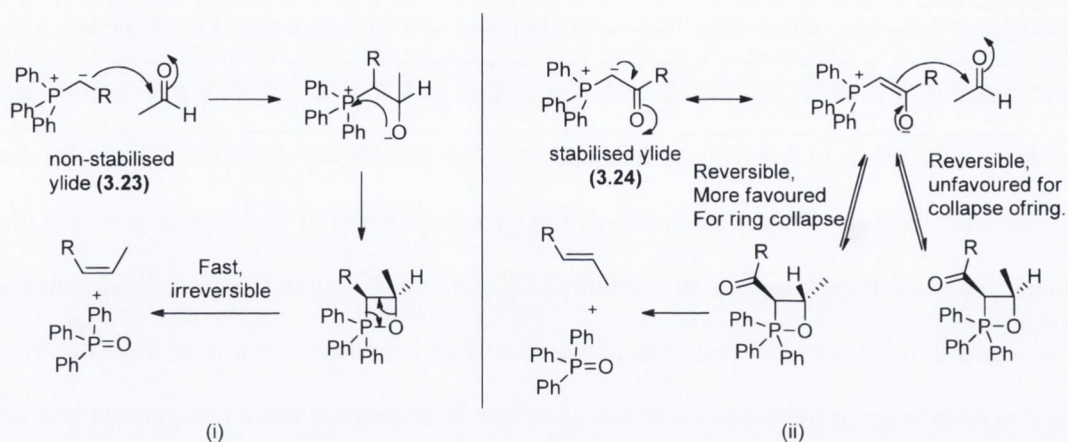
Figure 3.2: General mechanism for the Wittig reaction for (i) non stabilised and (ii) stabilised phosphonium ylides.

Another reason for the Wittig reaction finding such wide usage is due to the generally reliable prediction of the stereochemistry of the alkene product. Reactions effected using non stabilised ylides, represented by *(3.23)*, react to form Z alkenes acting via kinetic control. By contrast stabilised phosphonium ylides, represented by *(3.24)*, which have the ability to stabilise the negative charge on the reactive carbon undergo slower reactions to form the E alkene via thermodynamic control.[255] Neighbouring electron withdrawing groups such as carbonyls commonly function to stabilise this charge. Other variations to the reaction conditions can also be used to influence the stereoselectivity. The exclusion of lithium salts,[256] lower reaction temperature and use of polar aprotic solvents favour the formation of Z alkenes.[257] A drawback of this reaction is the formation of triphenylphospine oxide, which tends to be difficult to remove from reaction mixtures. Modifications such as the Horner-Wadsworth-Emmons[255] reaction use phosphonate salts that yield a water soluble by-product that is more easily removed upon aqueous work-up.

At this point in our investigations, the Wittig reaction was used to furnish the alkene *(3.25)* from the starting material, 2,3,4-trimethoxybenzaldehyde and the ylide of methyltriphenylphosphonium bromide as previously reported by Kiesele *et al.*[258] This reaction

proceeded in a near quantitative yield, over 2 days in contrast to the reported 6 h. Subsequent hydroboration of the alkene product using a complex of borane in THF (BH$_3$.THF) in diglyme at 0 °C and oxidation of this organoborane complex upon its reflux with TMANO at 100 °C over 2 h yielded the primary alcohol (3.21).[246] This alcohol was subsequently oxidised to the aldehyde (3.22) using PDC in 70% yield before its conversion to (3.12) as performed previously. While this pathway showed an observable improvement, it was limited by the relatively low amount of starting material that could be used with a limit seemingly reached at 4 g of 2,3,4 trimethoxybenzaldehyde compared to 10 g in the original pathway's initial borohydride reduction step to yield (3.09). The amount yielded at the alcohol stage was the highest using this approach where the Grignard reaction was attempted on (3.22). Ultimately this approach was superseded by the following method described, which used the same number of synthetic steps without relying on a 2 day Wittig reaction, affording a larger amount of (3.16) in less time.

(3.25)   **(3.21)**
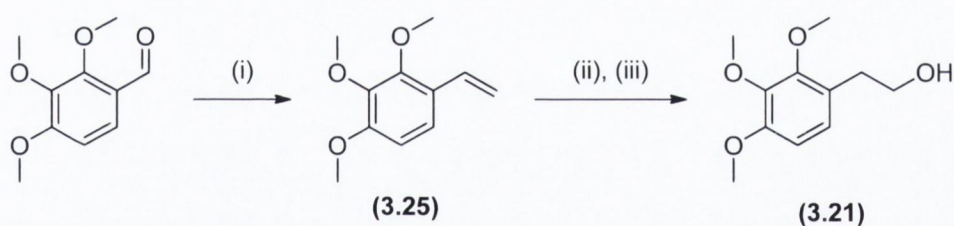
(i) methyltriphenylphosphonium bromide, 18-crown-6, K$_2$CO$_3$, THF, N$_2$, 80 °C, 2 days, 96%
(ii) BH$_3$-THF, diglyme, 0 °C, 1 h (iii) TMANO dihydrate, 100 °C, 70%

Scheme 3.5: Synthesis of alcohol (3.21) using Wittig approach.

Although this approach yielded higher amounts of the alcohol (3.12), we felt alternative chemistry on the nitrile (3.10) might serve as a convenient way to synthesise this intermediate. The chemistry involved was inspired by the work of Lee and Lin[259] who performed the addition of allyl bromide to 2-phenylacetonitrile using a Lewis acid catalysed, zinc promoted Barbier-style reaction. This method proved to be the most successful thus far with a particular progress made due to the very swift fashion in which the reaction proceeded. After a 30 min reaction

time, the desired compound *(3.11)* was obtained directly from *(3.10)* using allyl bromide, zinc dust and a catalytic amount of AlCl$_3$ in a relatively high yield of 82%.

(3.10)   (3.11)
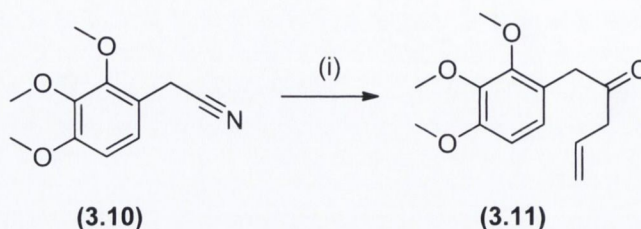
(i) Allyl Bromide, Zn dust, AlCl$_3$, THF, 0 °C, 82%

Scheme 3.6: Approach used to successfully synthesise *(3.11)*.

There was one major problem with this reaction step however, resulting from the incorrect work-up procedure being used leading to the acid catalysed isomerisation of the product to the enone *(3.12a)* which appears as a spot slightly below that of the target compound on TLC. The formation of *(3.12a)* was shown as it had the same mass as that of *(3.12)*, while its NMR spectra showed a new signal integrating to three protons, corresponding to that of the terminal methyl group, with the associated absence of any CH$_2$ peaks in the ^{13}C NMR spectrum. The reaction was initially quenched using 2 M aq. HCl, however as it was clear the acid played a part in the undesired isomerisation, its concentration was subsequently reduced to a 1 M solution. A speedy work-up procedure was also required, lowering the time the acid and product would be associated with one another, while washing the combined organic extracts twice with water before subjecting them to column chromatography. Following these steps carefully allows the complete diminishment of this undesired side reaction, which has the potential to destroy the entire yield of this reaction step. Prevention of this also resulted in a much simplified purification procedure due to these two compounds having similar R$_f$s.

(3.11)   **(3.11a)**
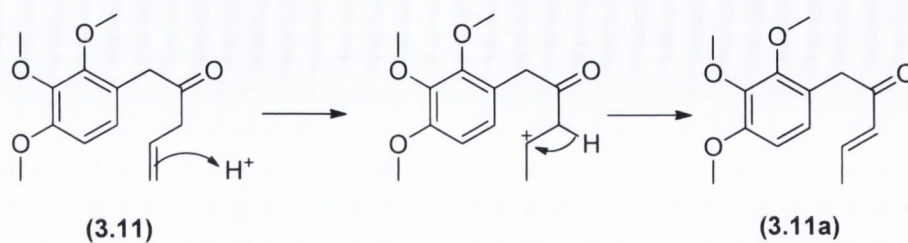
Scheme 3.7: The acid catalysed isomerisation of (3.11).

Reduction of *(3.11)* with NaBH$_4$ in MeOH at 0 °C yielded the alcohol *(3.12)* within 20 min in near quantitative yield. Subsequent protection of the alcohol with TBDPSCl was achieved following overnight reaction catalysed by imidazole in 93% yield. In order to furnish the primary alcohol *(3.14)* in a satisfactory yield, the oxidative hydroboration reaction using a BH$_3$-THF complex to furnish an organoborane intermediate which was subsequently hydrolysed using trimethylanilinium N-oxide (TMANO) dihydrate as following the same procedure used within this group[260] and by Rowan *et al*[246] in their synthesis of macrocycles derived from cinchona alkaloids. The stability of other protecting groups promoted as being stable to the conditions of the hydroboration reaction,[261] namely an acetate protecting group *(3.26)* and a trifluoroacetate (TFA) group *(3.27)* were also investigated. Unfortunately the progress of the hydroborations of these compounds was minimal, with their complete deprotection being observed, leaving only the TBDPS group as a viable option for the completion of this synthesis.

Pyridium dichromate, or the Cornforth reagent,[262] has commonly found use as a selective reagent for the oxidation of primary alcohols to aldehydes using aprotic solvents, mainly DCM, to prevent further oxidation to the carboxylic acid and enables oxidation of acetals to esters.[263] As reported by Corey and Schmidt, it is however possible to promote oxidation of alcohols to carboxylic acids using the correct solvent. In this scenario, this is achieved using DMF as solvent and duly yielded *(3.15)* in a yield of 70%,[247] under conditions milder than those seen when using the similarly chromium based Jones' reagent.

(3.11)   **(3.12)**   **(3.13)** R = TBDPS
(3.26) R = Ac
(3.27) R = CF₃C=O

(3.14)   **(3.15)**
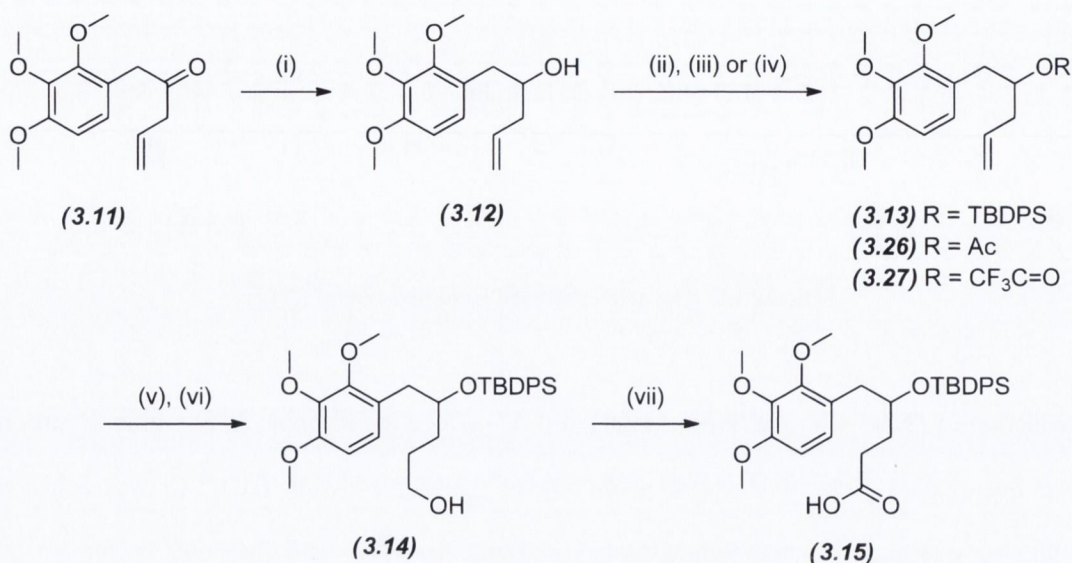
(i) NaBH₄, MeOH, 0 °C, 97% (ii) TBDPSCl, Imidazole, DMF, 13 h, 93% (iii) Ac₂O, NEt₃, DMAP, DCM, 85% (iv) trifluoroacetic anhydride, DCM, -10 °C, 79% (v) BH₃-THF, Diglyme, 0 °C (vi) TMANO dihydrate, 100 °C, diglyme, 70% (vii) PDC, DMF, 75%.

Scheme 3.8: Final synthetic pathway towards (3.15).

3.2.4   Attempted cyclisation of *(3.15)*.

Cyclisation of *(3.15)* was expected to occur using the identical method as that employed for the synthesis of *(2.25)* as detailed in chapter 2. However following multiple reaction attempts, TLC analysis appeared to show only minimal reaction progress under a variety of conditions following the addition of SnCl₄. Closer inspection showed significant deprotection, resulting in formation of *tert*-butyldiphenylsilanol (TBDPSOH), represented by a higher spot on the plate and there was also a new spot with a similar R_f to the starting material. After work up and purification of the reaction mixture by flash column chromatography, NMR analysis of the lower compound on TLC showed it to be that of the 5-membered lactone *(3.28).* Only trace amounts of the desired product **(3.16)** was isolated from the crude mixture.
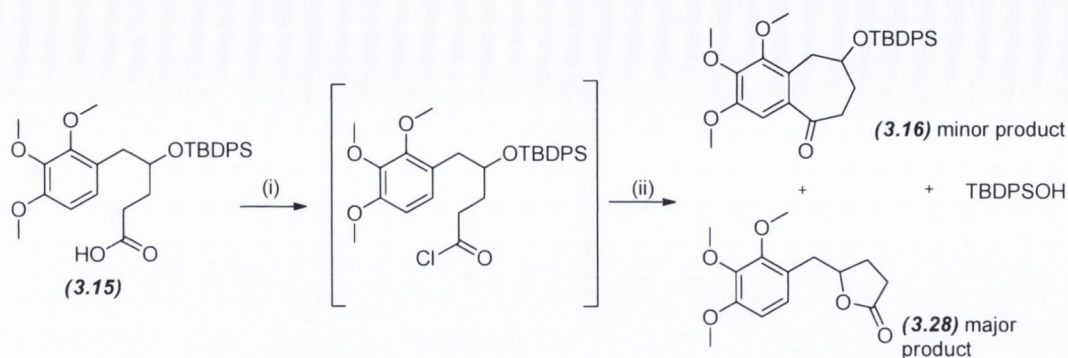
(i) Oxalyl chloride, DMF, DCM, 0 °C, 2 h (ii) tin (IV) chloride, DCM, Range of temperatures from -78 °C to 0 °C, 1 h.

Scheme 3.9: Result of the attempted cyclisation of (3.07) to form 5-membered lactone (3.28).

While the progress of the reaction was monitored closely, TLC showed that the formation of the acyl halide intermediate proceeded as expected, evidenced by the evolution of CO_2 gas as oxalyl chloride was added dropwise to the reaction. Removal of the solvents at this stage also yielded a similarly yellow oily residue to that obtained in the analogous step for the synthesis of *(2.25)*.

This suggests that the problem occurs upon addition of the $SnCl_4$ to the mixture where the Lewis acid catalyst should function by association with the chlorine atom of the acyl halide (i), before the elimination of the tin complex via donation of lone pairs from the keto-oxygen. This forms $[SnCl_5]^-$, which subsequently regenerates to $SnCl_4$ and a chloride ion while simultaneously forming a positively charged acylium ion (iii) that reacts with the electron rich aryl ring in a nucleophilic aromatic substitution reaction. The free chloride ion acts as a base to complete the cyclisation, restoring aromaticity to the system as illustrated in Scheme 3.10.
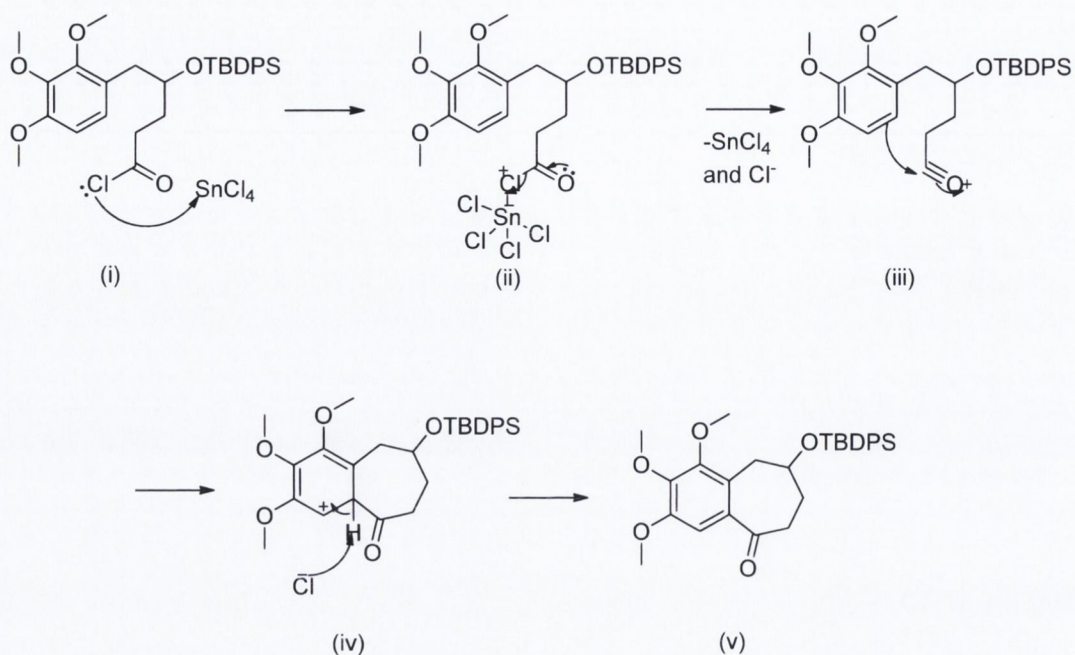
Scheme 3.10: Expected mechanism for successful Friedel-Crafts acylation of (3.15).

In order for the lactone to form, there must be some interaction between the oxygen bound to the TBDPS group and the forming acylium ion. Although it would seem unlikely that the bulky protecting group would disintegrate so easily, the acylium ion[264] is a very strong electrophile and there are free lone pairs of electrons on the oxygen that would be close enough to interact with the ion to form the 5 membered ring structure as shown above. The chloride ion that should be present to restore aromaticity in fact promotes the removal of the TBDPS group completing the formation of the lactone product. This also confirms the origin of TBDPSOH as it forms upon hydrolysis during the reaction's aqueous work up.
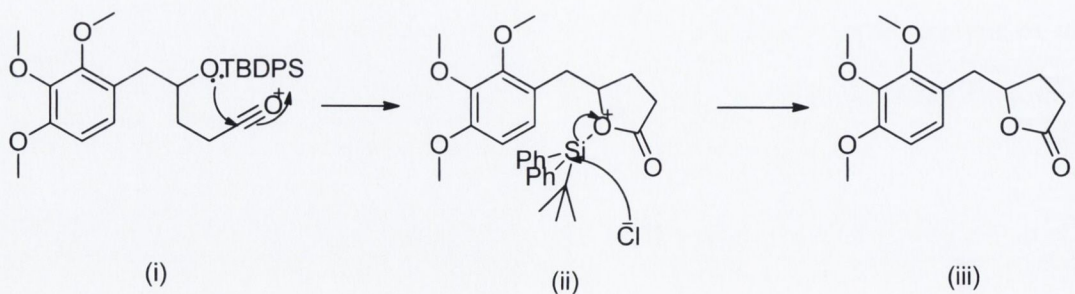
Scheme 3.11: Mechanism of formation of (3.28).

104

Upon examination of the differences between the differing fates of the two structures when undergoing this reaction, it is evident why this side reaction did not occur when conducting this transformation during the synthesis of RS180. As shown in Scheme 3.12, the theoretical intermediate formed would be a four membered lactone. In this case, the bond angle between the four atoms in the ring is 90°, which deviates from the desired angles of 109.57° for tetrahedral carbons and 120° in the case of the carbon at the centre of the carbonyl group. The bulkiness of the TBDPS group also serves to repel the completion of this bond formation.[265] Such strain results in the swift collapse of the lactone bond before the chloride mediated cleavage of the O-Si bond. The resultant 7-membered ring structure that forms as required is free from strain and is much more stable thermodynamically than the potential competing product.
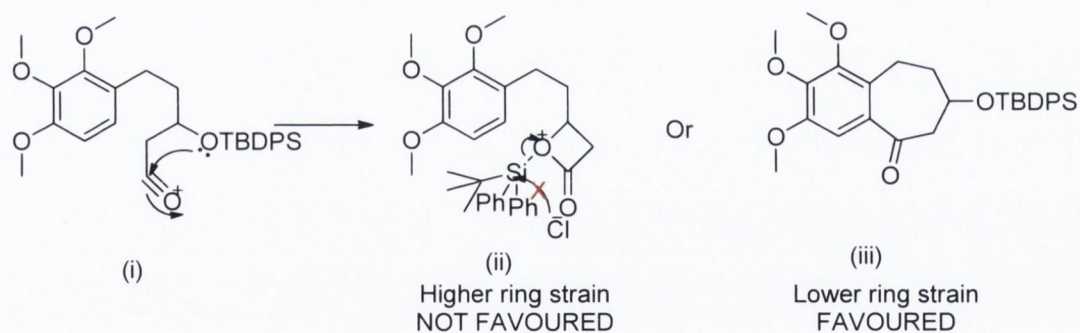
Scheme 3.12: Effects of ring strain preventing the lactone forming in RS180 synthesis.

However in the case of the more recently attempted cyclisations, it is seen that a 5 membered lactone is formed. Unlike its 4 membered counterpart, there is not as much associated ring strain, bestowing enough stability on the newly forming ring to remain until completion of its formation by chloride attack at the silicon centre. Five-membered rings have in general been shown to form the quickest,[266] as a result of the proximity of the atoms central to the reaction to each other. In principle, Scheme 3.11 above suggests how closely the orbitals of the oxygen and acylium ion overlap, suggesting the ease with which the electron exchange occurs. Finally,

these observations are in accordance with Baldwin's rules of cyclisation where the 4-exo-dig cyclisation in Scheme 3.12 is disfavoured while the 5-exo-dig cyclisation of *(3.28)* is favoured.[267]

In spite of these problems, it was attempted to prevent the deprotection from happening by using lower amounts of Lewis acid, thus potentially slowing down the reaction and hopefully encouraging formation of the desired 7-membered ring. Unfortunately, no reaction occurred at all when less than 0.20 molar equivalents of tin (IV) chloride was used. Raising this amount to 0.25 molar equivalents resulted in the total formation of *(3.28)* albeit with a longer reaction time required to effect this transformation.

Increased reaction temperature also showed no improvement on the progress of the reaction towards the desired 7-membered ring compound. At -78 °C, no reaction occurred, however, once the temperature was raised to -40 °C, deprotection and lactonisation was favoured once more.

Having attempted this reaction on several occasions, there was at least sufficient quantities of *(3.08)* generated, to enable its structure to be elucidated spectroscopically and to complete the deprotection of the TBDPS group, using 1 M tetrabutylammonium fluoride (TBAF) in THF at 0 °C, to afford the alcohol *(3.17)* over 3 h.

(3.08)   (3.17)

(i) 1M TBAF in THF, THF, N$_2$, 0 °C, 3 h.
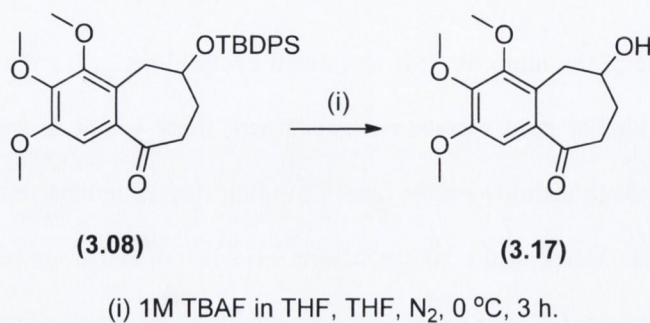
Scheme 3.13: Completion of the synthesis of (3.17).

3.2.5 Structural Elucidation of *(3.17)*.

As a key intermediate in the desired synthesis of these compounds it was necessary to ensure the correct identity of this compound before proceeding further. Firstly the MS spectrum showed an m/z at 267.1213 under positive ionisation conditions correlated to the mass of the protonated species of *(3.17)*.
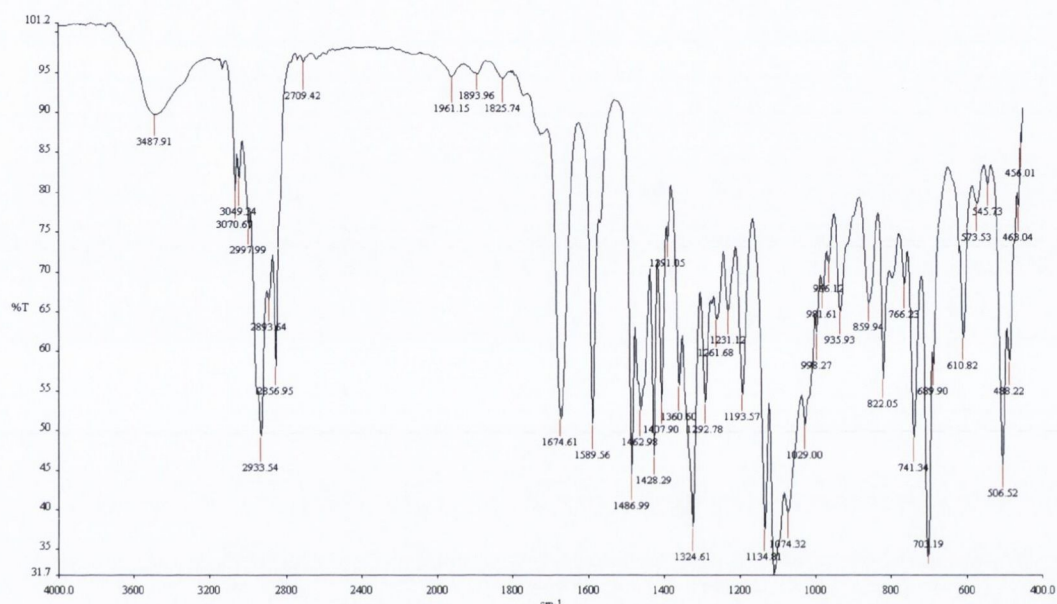
Figure 3.3: IR spectrum of *(3.17)*.

The IR spectrum showed a strong broad peak at 3487 cm^{-1} indicative of the presence of an alcohol functional group, while the strong peak at 1674 cm^{-1} suggests the presence of a carbonyl group. The low frequency of vibration correlates to a carbonyl in conjugation with a neighbouring aromatic group.

The ^{1}H NMR spectrum shows the characteristic elements observed in the spectrum of the analogous compound in the synthesis of RS180. There are 6 protons in the region between 2 ppm and 3 ppm, correlating to the 3×CH$_2$ groups in the B-Ring of the molecule. Three singlets integrating to 9 protons in the region between 3.93 ppm and 4.03 ppm correspond to the three methoxy groups attached to the A-ring in a similar fashion to its related compound. At 4.40

ppm, there is a multiplet signal that integrates to 1 proton, being the proton attached to the same carbon that is attached to the hydroxyl group. Finally a singlet peak at 7.04 ppm is seen to be the aromatic hydrogen in the A-Ring. This peak suggests that the cyclisation reaction previous to this deprotection did proceed as intended. Before this point there was the appearance of the two doublets in the aromatic region. After cyclisation, one of these signals disappeared as expected due to its substitution by the carbonyl group. Overall the ^{1}H NMR spectrum is consistent with that expected of *(3.17)*, while showing similarities to the spectra of the corresponding analogue in the synthesis of RS180.
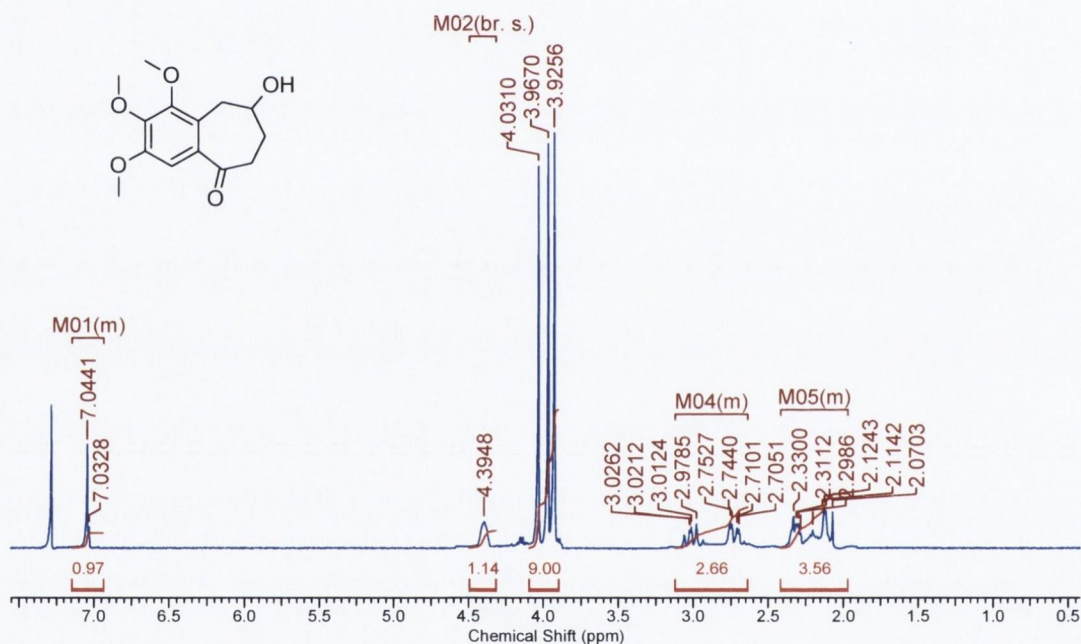
Figure 3.4: ^{1}H NMR Spectrum of *(3.17)*.

The ^{13}C NMR spectrum and its associated DEPT 135 and DEPT 90 spectra also show no anomalies regarding the identity of *(3.17)*. On first look at the ^{13}C NMR spectrum it does however appear that there are only 13 signals. In the DEPT 135 spectrum however, it is clear that one of the signals caused by tertiary carbon at 76.2 ppm was masked by the chloroform peaks. There are 5 quaternary peaks between 128.8 ppm and 151.4 ppm with an additional one that can be seen at 205.3 ppm suggesting the presence of a ketone and 5 quaternary aromatic

carbons in the compound. 2 tertiary carbons appear: the aforementioned one at 76.2 ppm relates to the aliphatic CH unit attached to the hydroxyl group, while the signal at 109.4 ppm correlates to the aromatic CH. Three secondary carbons resonate at the most upfield region of the spectrum between 16 ppm and 34 ppm correlating to the aliphatic CH_2 units in the B-ring. Three CH_3 signals between 55 ppm and 62 ppm correlate to the three methoxy groups attached to the A-ring. When taken into consideration together, this evidence all points toward the identity of the compound being that of *(3.17)*.
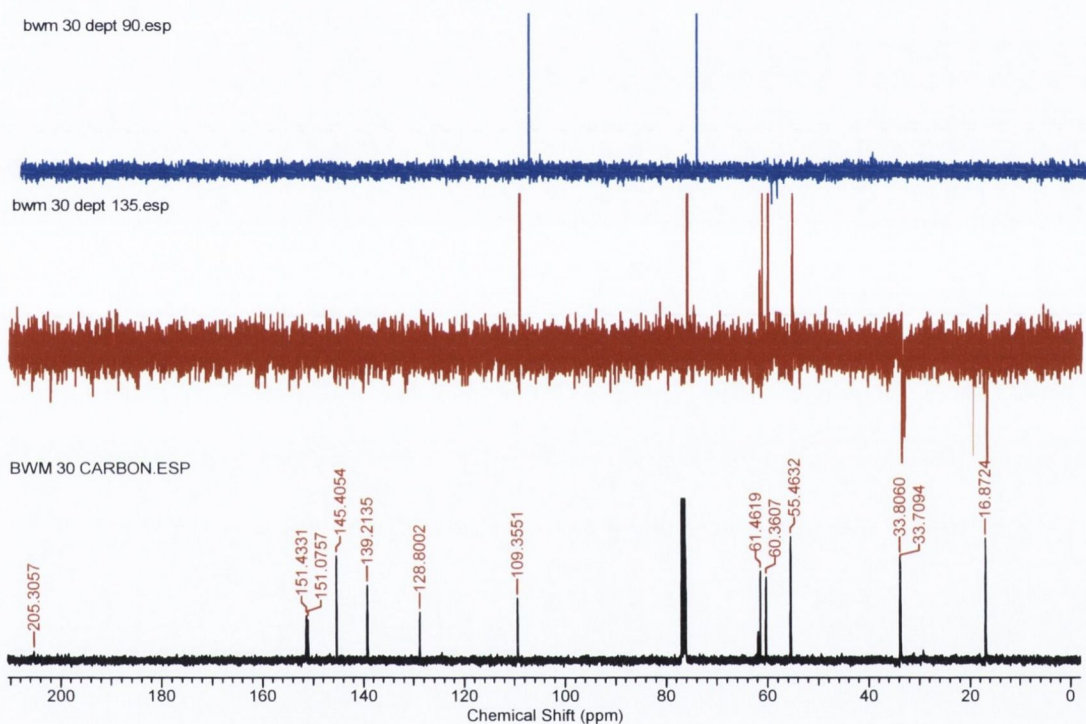
Figure 3.5: ^{13}C NMR of *(3.17)*.

3.3 Introduction of the hydroxyl group after cyclisation

Although we had been successful in synthesising this intermediate, it was of too low a yield to allow further elaboration towards *(3.01),* our target compound. Numerous attempts had been made to obtain this compound, yet the highest amount of compound obtained from the start of the synthesis was still too little for further synthetic manipulation. In total, the yield up to this stage was 3 mg (0.011 mmol) from 10 g (51.71 mmol) of 2, 3, 4 - trimethoxybenzaldehyde starting material, giving an overall yield of 0.2% up to this relatively early stage of the

synthesis. As a result, other methods were investigated, hopefully leading to improvements in the yield to enable further progress. A new synthetic approach was attempted, focussing on the introduction of the hydroxyl functionality to a pre-cyclised compound.

3.3.1   Initial attempts to circumvent the cyclisation issue.

During the course of his work, McCormack[268] was able to introduce a bromine to the benzylic position of the B-ring. This followed from a few steps starting with the PPA mediated cyclisation of carboxylic acid *(3.29)* to yield the annulone compound *(3.30)*. Subsequently, a radical bromination reaction of the aryl ring *(3.31)* using N-bromosuccinimide (NBS), which serves as a mild source of molecular Br_2 and initiated by ultraviolet (UV) light and the radical initiator 1,1'-azobis(cyclohexanecarbonitrile) (ACN) was used to effect the transition.

Unfortunately, despite the high yields reported for this transformation, only minimal reaction progress was observed during our attempts (Scheme 3.14). Had this transformation been successful and the subsequent bromination of the benzylic position followed without problems, the procedure used by Zhang[269] in his doctoral thesis would have been adopted to this work whereby an alkene functionality would have been introduced starting from the benzylic position. If this alkene was epoxidised using MCPBA and the resulting epoxide treated to catalytic hydrogenation conditions, it should have been possible to furnish *(3.17)* without facing the problematic Friedel-Crafts acylation step.
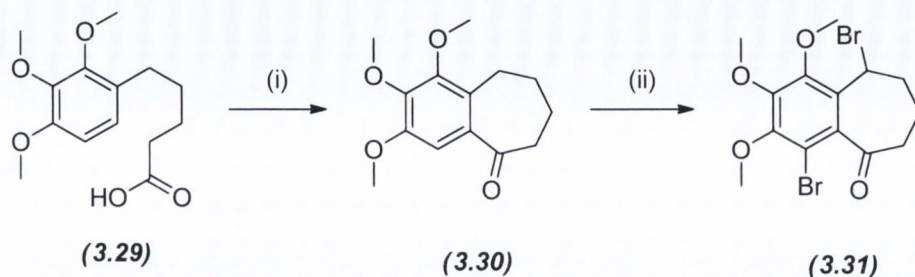
(i) PPA, heat, 1 h. (ii) NBS, ACN, alpha, alpha, alpha-trifluorotoluene, UV light

Scheme 3.14: Attempted synthesis of *(3.31)* via radical bromination.[268]

In combination with the previous work relating to the Wittig reaction these studies did inspire a new perspective regarding the direction of our work. Heretofore, the work hinged on the alcohol functionality being built into the molecule before the cyclisation step, whereas after this point it was recognised that there was potential for the introduction of the hydroxyl group subsequent to cyclisation. It was however dependent on devising a suitable procedure for insertion of the alkene functionality at the benzylic position to facilitate the subsequent epoxidation step.

3.3.2 Using the Wittig reaction towards the synthesisis of *(3.34)*.

A solution to this problem would be to revisit the Wittig reaction, to allow introduction of an alkene as per the synthesis of compound *(3.25)*. In this case a more complicated phosphonium salt, (3-carboxypropyl)triphenylphosphonium bromide *(3.32)*, was used in an attempt to synthesise the unsaturated carboxylic acid *(3.33)* in one step from 2,3,4-trimethoxybenzaldehyde *(2.07)*.

As previously declared, an unstabilised ylide such as that formed by its deprotonation with sodium bis(trimethylsilyl)amide (NaHMDS) would be expected to form the Z alkene selectively. This would be desirable as this isomer "locks" the alkene in close proximity to the aryl ring facilitating progression of the Friedel-Crafts cyclisation. When *(3.33)* is an E-alkene,

the desired reaction between aryl group and acyl halide will only happen in an intermolecular fashion as the two reaction centres are too far away to interact with each other.

Unfortunately studies by Maryanoff *et al*[257] report that a reversal of the expected stereochemistry is noted with this particular ylide due to a "stereochemical drift" in the transition state. This is due to the presence of the carboxylic acid which ionises in the basic conditions required for ylide generation, appearing to have a stabilising effect on the intermediates, preventing its immediate collapse, facilitating a stereochemical shift, eventually allowing the E isomer to form preferentially as illustrated in Figure 3.2.

In spite of this report, it was attempted to promote the formation of the Z isomer using the conditions that are conventionally more favourable to its formation, namely keeping the reaction temperature low (-78 $^{\circ}$C rising to 0 $^{\circ}$C), using an Na^{+} salt and not one with an Li^{+} counter cation as a base and using THF as a solvent in order to overcome the "stereochemical drift".

Unfortunately these attempts failed to operate as desired, leading exclusively to the production of the E isomer *(3.33E)*, as identified by measuring the coupling constant in the ^{1}H NMR for the benzylic alkene proton. As it neighbours only one proton it should resonate as a doublet, doing so with a large coupling constant of 16.04 Hz. It is possible to distinguish between cis and trans alkenes using the coupling constants, as the protons in trans alkenes interact more strongly with each other leading to larger coupling constants in the region of 11-18 Hz, while cis alkenes exhibit lower J values in the area between 6-15 Hz.

Despite this, an attempt at the Friedel-Crafts acylation of this compound was made, using the same procedure as that for the attempted synthesis of *(3.16)*, in the hope that interaction between the alkene and the acidic SnCl$_4$ would lead to a formation of a tin complex with the alkene reverting its stereochemistry to that required for the cyclisation, as illustrated in Scheme

3.15. Unfortunately, this modification to the alkene didn't proceed, leading to the retrieval of starting material upon work up.

(i) NaHMDS, THF, -70 °C (ii) Oxalyl chloride, DMF, DCM, 0 °C (iii) SnCl$_4$, DCM, -10 °C
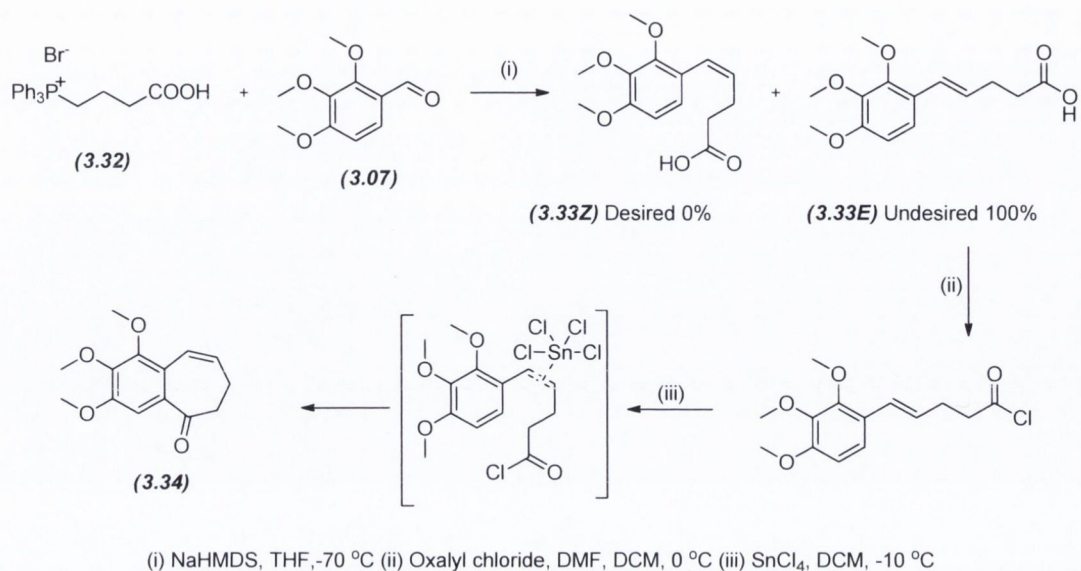
Scheme 3.15: Synthesis of *(3.27E)* and its subsequent use in the first attempt to synthesise *(3.34)*.

To overcome this problem, it was decided to methylate *(3.32)* to yield the ester phosphonium salt *(3.35)*. Reaction of this reagent with 2,3,4-trimethoxybenzaldehyde would theoretically yield the Z-isomer of the methyl ester of *(3.33)* as the ester functionality serves to mask the carboxylic acid moiety, preventing charged side chain participation in the stabilisation of the transition state reverting the condition to being under kinetic control to yield the Z alkene as is most common.

Dissolution of the phosphonium salt in MeOH followed by the bubbling of dry HCl gas, generated using Kipp's apparatus,[270] through the solution yielded *(3.35)* efficiently in 3 h. The product was purified by work up between aqueous sodium bicarbonate (NaHCO$_3$) and DCM removing any unwanted starting material. In a similar fashion to above, this compound underwent the Wittig procedure to yield *(3.36)* in a high yield.

Although this reaction was originally performed at -78 °C in order to ensure stereoselectivity, it was observed that this temperature impeded reaction progress. Increase of the temperature to 0 °C furnished the desired Z alkene in 2 h as determined using the coupling constants. The lower J value of 11.36 Hz for the doublet at 6.47 ppm is indicative of there being a cis alkene.

A drawback with this reaction was the difficulty in obtaining the product in pure form as it possessed a similar R_f to the starting benzaldehyde and the reaction never proceeded to 100% completion. As a result, it was realised that using 0.75 equivalents of the benzaldehyde relative to the 1 equivalent of ylide was the optimal ratio between the two reactants. This allowed easier purification, however if there was some starting material remaining, this could be simply removed in the next step. Within 1 h, the hydrolysis of the ester of *(3.36)* to the acid *(3.33Z)* was completed using aqueous 2.5 M aq. NaOH in THF, with a simple acid-base extraction being sufficient for high purity.
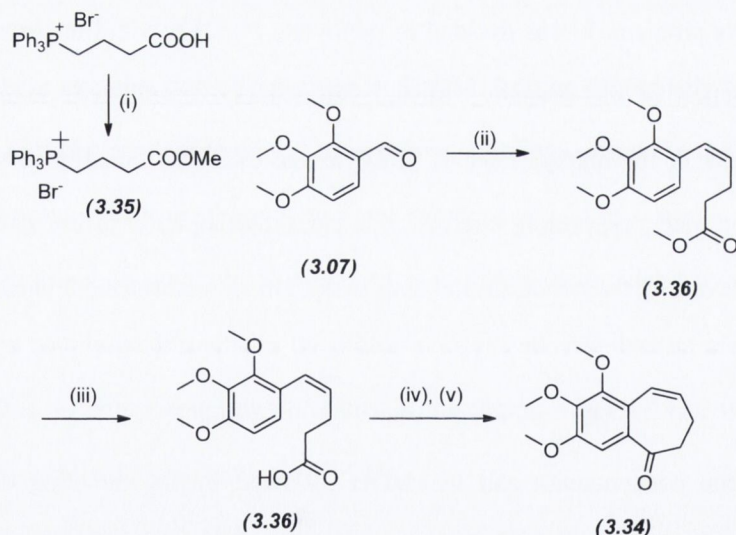
(i) MeOH, HCl, 3 h, 65% (ii) NaHMDS, 0 °C, 2 h, 75 % (iii) Oxalyl Chloride, DMF, DCM, 0 °C, 2 h (iv) SnCl$_4$, -10 °C, DCM, 1 h, 63%

Scheme 3.16: Synthetic pathway towards *(3.34)*.

As seen in Figure 3.6, comparison of the NMRs of (i) *(3.33E)* and (ii) *(3.33Z)* show the difference in the coupling constants of the alkene signals and that the stereochemistry of the Z

alkene was conserved after the ester's hydrolysis. Subsequent cyclisation of this acid using standard Friedel-Crafts acylation yielded *(3.34)*.
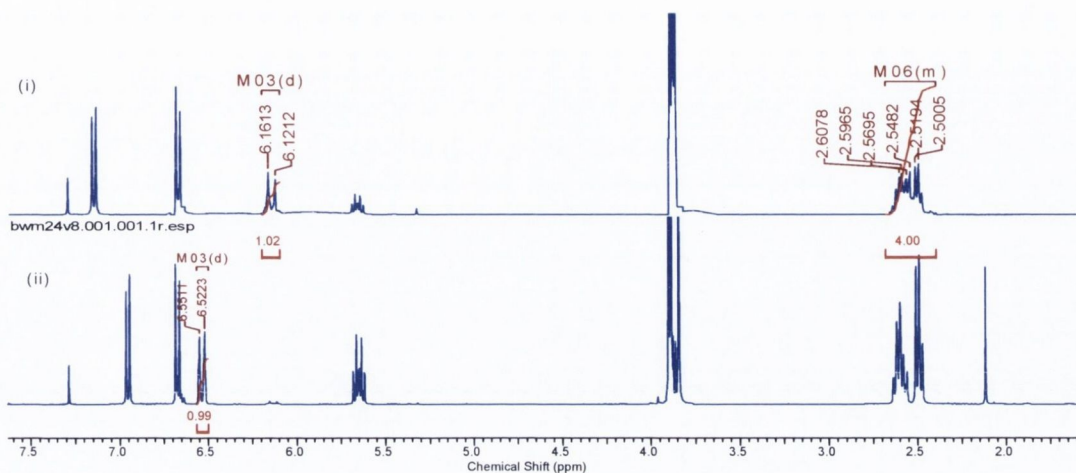
Figure 3.6: Comparison of NMRs for (i) *(3.33E)* and *(3.33Z)*. The benzylic proton's signals remain labelled. In (ii) it is seen to have a lower coupling constant indicating the major presence of a trans alkene.

Although relatively high yields of 63% had been achieved for this transformation, there were also times when there would be as little as 10% conversion. It was difficult to determine the explain why this was the case. This step did prove to often be problematic and while it has functioned it proved to be a bottleneck in this synthetic pathway.

After successfully furnishing *(3.34)*, it was attempted to use the same hydroboration step as before[260] to selectively oxidise the alkene to the desired alcohol *(3.17)* in one step. However, this didn't proceed as expected, yielding a complex mixture of products presumably due to side reactions involving the borane reduction of the carbonyl as has been shown to occur with pinacolone in THF.[271]

To furnish the alcohol it was thus decided to follow Zhang's procedure[269] by treating the alkene with MCPBA in DCM and subsequently hydrogenating the resulting epoxide *(3.35)* to selectively yield *(3.17)* as illustrated in Scheme 3.17.

(3.34)   *(3.37)*   *(3.17)*
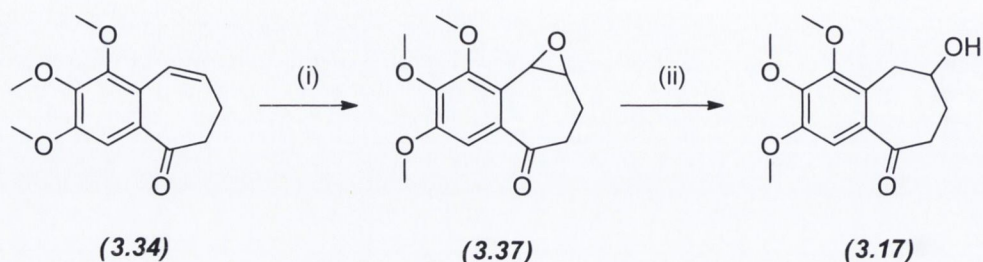
(i) MCPBA, DCM, 0 °C (ii) H₂, 10% Pd/C, 10 h.

Scheme 3.17: Planned synthesis of (3.17).

However, when the reaction was attempted, it appears that the electron rich trimethoxyaryl ring had a detrimental effect on this reaction as opposed to the unfunctionalised ring in Zhang's work, as the two key side reactions namely the Baeyer-Villiger reaction[272] and nucleophilic acid catalysed epoxide ring opening[273] functioned in tandem to form the lactone *(3.38)* (Scheme 3.18). It is not known precisely which order these reaction steps occur, however it is likely that it is arbitrary, depending simply on the instantaneous position of the reaction centres to each other. In the scheme outlined above, it suggests that the peroxyacid MCPBA attacks the ketone directly, forming the unstable tetrahedral intermediate. Upon collapse of this intermediate, the alkyl bond between the carbonyl carbon and the aryl ring breaks, while simultaneously bonding to the positively charged oxygen formed after the nucleophilic attack. This in turn breaks the O-O single bond, generating 3-chlorobenzoic acid, which protonates the oxygen in the epoxide weakening the bond between it and the carbon priming it for nucleophilic attack by the chlorobenzoate anion to furnish *(3.38)*.

Initially it was assumed that the ¹H NMR spectrum was unclean as there were aromatic peaks symptomatic of the presence of 3-chlorobenzoic acid (3-CBA), a by-product of the desired

epoxidation which is commonly known to be difficult to remove from reaction mixtures. Washing with aq. Na$_2$CO$_3$ multiple times usually proves sufficient enough to purge the mixture of the 3-CBA. However, the peaks remained in the ^{1}H NMR spectrum after numerous washes in a 1:1 mixture with the rest of the peaks on the molecule, suggesting conjugation of chlorobenzoic acid to the bicyclic ring system. There was also a lack of a ketonic carbonyl peak in the ^{13}C NMR spectrum suggesting the absence of the ketone in the desired product. The appearance of an unexpected peak at 164.7 ppm suggests the formation of the lactone via Bayer-Villiger reaction. After studying the MS confirmed that the compound isolated had a mass of 459.0632 which correlates to the mass of the sodium adduct of *(3.38)* thus confirming its identity as that of the undesired product.
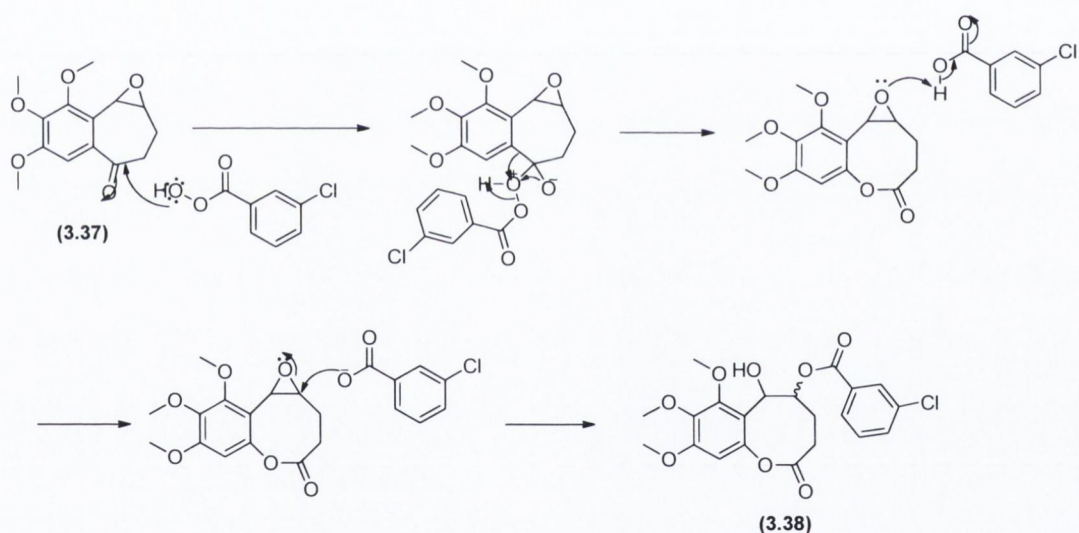
Scheme 3.18: Mechanisms of the Baeyer-Villiger and 3-CBA mediated ring opening of the epoxide resulting in the formation of *(3.38)*.

Consultation with the literature[273-274] showed that this phenomenon had been documented previously. In order to prevent the side reactions from happening it was required that a base was used to buffer the solution scavenging any acid remaining in the mixture. A 10% solution of aq. Na$_2$CO$_3$ was used for this purpose also creating a biphasic reaction which would enable the desired product *(3.37)* to remain in the organic layer separate from the chlorobenzoic acid in the

aqueous preventing occurrence of the undesired side reactions. The desired compound *(3.37)* was obtained in a moderate yield of 54%. Subsequent catalytic hydrogenation using a 10% Pd/C functioned to yield *(3.17)* in a moderate yield of 74%. However these results were not replicable, resulting from the trace amounts always afforded upon repetition of the problematic cyclisation of *(3.34)*. As there were other areas of the research that were starting to show better results and a significant amount of time had been placed on this area of research with low or inconsistent returns, it was decided at this point to direct our attention towards other aspects of the work with the intention of revisiting this molecule at a future stage.

3.4   Conclusions

At the onset of this project it was intended to expand the pharmacophore of our compounds in what originally appeared to be a relatively simple modification of the pre-existing scaffold. What transpired in actuality was a series of challenging barriers ranging from unfavourable thermodynamic conditions to more simple problems such as the acidic nature of the reaction. Ultimately regardless of the approaches taken toward the synthesis, there was a point at which it was impossible to proceed any further due to a lack of available compound to advance the synthesis. This point appeared to arrive just as the synthesis of compound *(3.17)* was completed utilising the two most successful synthetic pathways. It is unfortunate that not enough of this compound was furnished after all the exhaustive efforts, as we were quite near to completing the primary goal of synthesising compound *(3.01)*, which would have enabled us to evaluate at least its activity as a VTA, if not facilitate syntheses of novel hydroxamic acid containing DMLs.

However, reaching this far through the synthetic pathway does show that there is potential for the synthesis of this compound to be completed. Following on from compound *(3.17)* there are a series of steps that are analogous to those performed in Chapter 2 to yield RS180.

Further to this, there is the realisation that a better way to furnish *(3.22)* must be found. However many of our options have already been exhausted. TBDPS protection of alcohols is one of the most stable methods of restricting an alcohol's reactivity. The O-Si bond tends to be stable facing even the most coarse reaction conditions,[261] so to have faced a situation like this proved to be quite an unexpected challenge.

The replacement of the protecting group at this stage to one capable of diminishing the nucleophilic effect of oxygen's electronic charge could end up being useful to overcome this problem. To this end it was considered using the trifluoroacetate group to act as such, however its failure to resist the conditions presented by hydroboration step meant it was unlikely to remain intact after the Friedel-Crafts cyclisation.

One solution that was left unexplored through the course of the research was the possibility of using acetal or dithiane protecting groups.[261, 275] The use of these would be advantageous through the perspective of the carbonyl functionality already being tied up in a stable 5 or 6 membered ring structure, thus preventing a reaction similar to the lactone formation. While there is this clear advantage over any other protecting group mentioned thus far, the major drawback is the notorious difficulty in their selective removal, traditionally requiring harsh conditions such as $HgCl_2$.[276] Milder methods for their removal have been devised in recent times including Dess-Martin periodinane[277], H_2O_2[278] and NBS.[276b] During his work, Shah[209a] however did look at this type of protection achieving success at the cyclisation stage. The drawback in this situation was there being no method efficient enough with which to effect its deprotection. If it were possible to discover a mild method for this deprotection, it could lead to a very efficient pathway towards the target compound.

Potentially, a cyclic acetal could also be useful to inhibit the lactonisation reaction. However these would be less stable towards the reactions conditions than their dithiane counterparts, meaning the chances of their survival in the Friedel-Crafts conditions is not expected to be high.

The work undertaken in this chapter is still not completely resolved, but there is still potential for a satisfactory conclusion at some point. The work described here highlights several potential drawbacks, should the synthesis to ever be revisited.

Chapter 4

4.1 Introduction

The objectives of the work detailed in this chapter are to synthesise DMLs of the RS180 series of compounds detailed in Chapter 2 in combination with curcumin (diferuloylmethane) *(4.01)*, the principal curcuminoid isolated from the Indian spice *Curcuma longa* (turmeric), known commonly as a flavourant in Indian curry dishes but also for displaying a range of positive biological effects including anti-bacterial[279], chemopreventive,[280] anti-oxidant and anti-inflammatory effects.[281] This is in addition to an ever expanding array of evidence suggesting it could have a very important role in the modulation of various pathways implicated in carcinogenesis including arachidonic acid metabolism,[282] angiogenesis,[283] TNF-α mediated apoptotic pathways,[284] NF-κβ transcription resulting in down regulation of many cell control **oncogenes including c-Myc and cyclin D1,[285] HIF 1-α[286] and downregulation of MMPs.[287] A** recent report has also shown the recognition of curcumin and a number of synthetic analogues at a distinct binding site in tubulin, 32 Å from the colchicine-binding site, functioning to prevent tubulin assembly.[288] Additionally, curcumin has been shown to inhibit APN activity following its irreversible binding.[135a]

In Chapter 1, it is seen that cancer is a complex process implicating the mutation of several biological pathways in tandem towards the rapid uncontrolled proliferation of cells.[35] A compound possessing the ability to target multiple pathways can therefore be seen as advantageous to single targeting agents. Resulting from the wide ranging pleiotropic effects of curcumin, it has been identified as a potentially beneficial addition to the RS180 scaffold in order to generate a powerful novel anti-cancer DML amalgamating the anti-proliferative, anti-angiogenic,[283] anti-migratory[287], anti-invasive and anti-tubulin[209, 288] effects of the two component compounds.

123

The structure of curcumin *(4.01)* is very interesting, displaying an array of functional groups postulated to be responsible for its effects. The compound is in effect a dimer of two aromatic *o*-methoxyphenol rings linked via a fully conjugated linker unit containing a central β-diketone functionality. The phenolic groups have been suggested to be responsible for its anti-oxidant activities via free radical scavenging.[289] The β-diketone functionality in the conjugated bridge between aromatic rings displays tautomerisation to an enol form *(4.01a)*. Both tautomeric forms have been shown to interact with enzymes in a number of distinct modes *in vitro* and *in silico*. These include chelation of the both forms to Cu^{2+} and Fe^{2+},[290] reaction at the carbonyl centres, covalent association with sulfur containing residues of enzymes via Michael reactions,[291] and hydrogen bonding interactions with local enzymes.[292] As the binding affinity of the compound to Zn^{2+} complexes is diminished relative to Cu^{2+} and Fe^{2+} complexes[290] and the nature of its binding to APN is irreversible,[135a] it is likely that covalent interactions are observed in the case of its APN inhibitory activity.

(4.01)   **(4.01 a)**
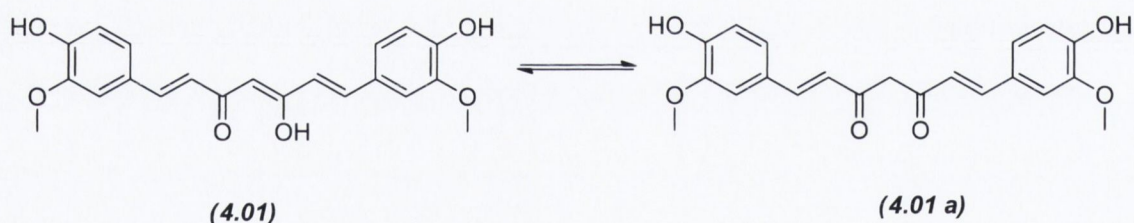
Figure 4.1: The tautomeric structures of the β-diketone functionality of curcumin responsible for its vastly varied activity *(4.01)*.

4.1.1   The bioavailability of curcumin.

In spite of its promiscuous biological effects, curcumin has been shown to be well tolerated in vivo, with clinical trials data showing a tolerance towards treatment with high doses of 12 g per day.[293] Additionally, lower rates of gastrointestinal cancers in areas of the world, including

India, where curcumin dishes form a major part of the diet suggest the beneficial chemopreventive effect associated with daily intake of curcumin[294]. The most disadvantageous property of curcumin inhibiting its clinical use is that of its poor bioavailability resulting from its poor absorption and rapid metabolism[295]. In studies where up to 12 g of curcumin is ingested orally per day, it was seen peak plasma levels of 0.41-1.75 μM were achieved just 1 h after the dosing.[293] This low observable amount of curcumin in the system clearly prevents it from exerting the positive effects observed in *in vitro* as in clinical trials into the use of curcumin for treatment of colorectal cancer showed insufficient systemic concentrations to effect the inhibition of hepatic metastasis from this cancer phenotype.[296]

In accordance with the wide range of functional groups exhibited in curcumin, the possibility for metabolism through a number of pathways is observed. These can be seen through the phenolic group's conjugation to glucuronide sugars *(4.02)* typically observed in first pass metabolism, or through the reduction of the enones in the structure's bridge between phenols to the less active dihydrocurcumin *(4.03)* and tetrahydrocurcumin *(4.04)*, facilitating its swift removal from the system.

(4.02)

(4.03)

(4.04)
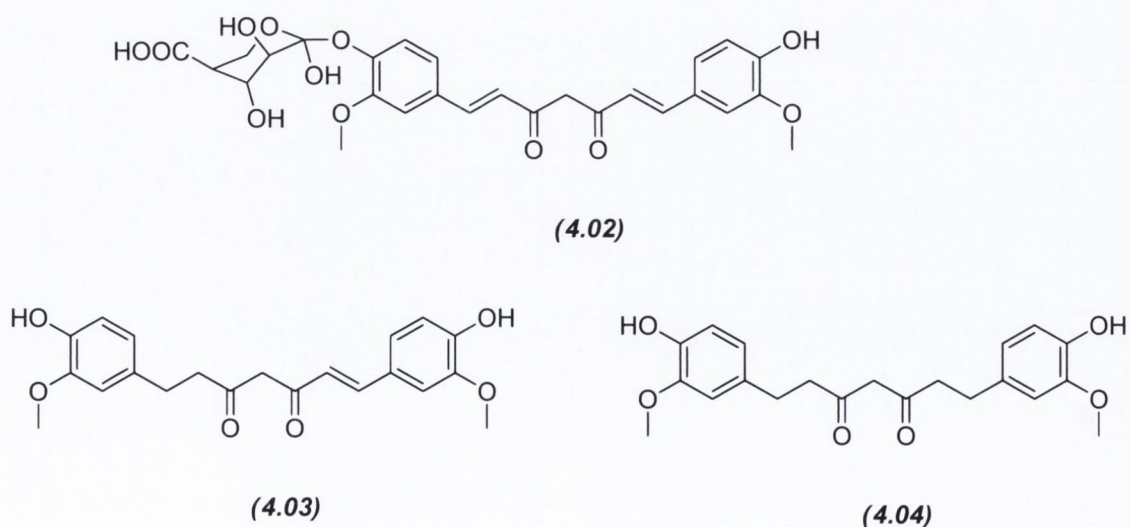
Figure 4.2: Metabolites of curcumin

125

4.1.2 Improved Delivery of Curcumin.

Numerous approaches have been investigated to increase the observed levels of curcumin in the plasma and tissue. The co-administration of curcumin with piperine,[297] a constituent of black pepper shown to inhibit the metabolic enzymes P-glycoprotein and CYP3A4,[298] decreased the elimination halflife of curcumin resulting in an increase of 154% in its bioavailability. Similarly co-administration of curcumin with naringenin has been shown to increase the life span of Ehrlic ascites carcinoma mice by 87.5%.[299] Considering the minute intrinsic bioavailability of curcumin in the system, the increase of curcumin levels observed upon the co-administration of these compounds still does not lead to the required amounts of systemic curcumin to exploit fully its potential biological activity. The use of other delivery systems such as the use of curcumin nanoparticles (NPs)[300] and micellular curcumin[301] for the improved treatment of colon cancer is currently being investigated.

For example, studies have been undertaken investigating the possibility of conjugating curcumin to Fe_3O_4 NPs using a citrate linker which resulted in increased tumour suppression activity relative to curcumin alone.[302] In another approach used to increase cellular uptake, the emulsion diffusion evaporation of the solubilisation polymer polylactic-coglycolic acid (PLGA) has formed uniform sized spherical NPs of curcumin, increasing the bioavailability of curcumin 26-fold, showing a 9-fold increase on the results obtained with the co-administration of curcumin with piperine.[303] Nanoemulsions of curcumin with paclitaxel have also shown effective intracellular delivery of the compounds with SKOV3 and SKOV3TR human ovarian adenocarcinoma cells, suggesting the potential use of this technology for the direct targeted delivery of curcumin to cancer cells.[304]

4.1.3 Synthetic Derivatives of Curcumin.

In addition to these approaches, a number of synthetic derivatives have been synthesised in order to improve upon both its activity and distribution profile. Hydrazinocurcumin *(4.05)* is a derivative formed by the simple reaction of hydrazine with curcumin displaying 30-fold decrease in the proliferation of bovine endothelial aortic cells (BAECs) relative to curcumin,[305] its observed IC_{50} of 0.52 µM comparing favourably to 15 µM in the case of curcumin. Recently it has been shown to exhibit potent activity against the proliferation of breast cancer cells, showing decreased cell migration, increased apoptosis, decreased invasion and a depression in colony formation while showing an enhanced pharmacological profile relative to curcumin.[306] Its anti-APN activity has also been measured, however its IC_{50} of >100 µM suggests no interaction with this enzyme. By comparison, curcumin shows greater potency with an IC_{50} of 10 µM, relative to that of 2.5 µM measured for bestatin. Another curcumin derivative isolated from *Curcuma longa* preserving the β-diketone moiety, demethoxycurcumin *(4.06)*, itself shown to downregulate expression of MMP-9 in HUVEC cells to exhibit an anti-angiogenic effect,[307] possesses an IC_{50} of 20 µM in the same investigations, suggesting its requirement in the interaction with APN.[135a] However, in contrast to hydrazine derivative *(4.05)*, neither *(4.06)* nor *(4.01)* displayed activity against breast cancer cell proliferation.[135a]

(4.05)   *(4.06)*
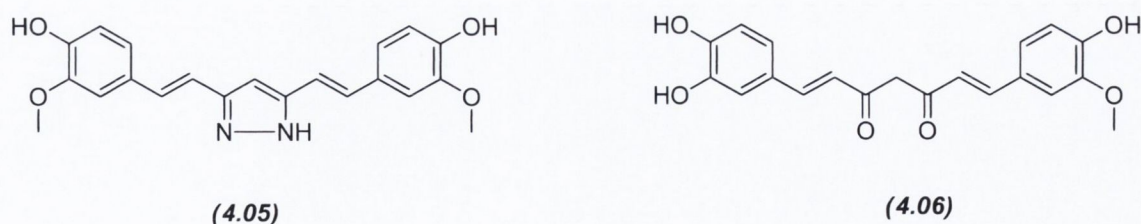
Figure 4.3: Curcumin derivatives hydrazinocurcumin *(4.05)* and demethoxycurcumin *(4.06)*.

Curcumin interacts with a binding site near the colchine tubulin site and has been shown to inhibit the assembly of microtubules with an IC_{50} of 20 µM.[288, 308] Other derivatives of curcumin including *(4.05)* and *(4.07)* display IC_{50} values of 23 µM and 16 µM respectively, with

compound *(4.07)* showing improved anti-proliferative and pro-apoptotic effects against HeLa cells relative to curcumin.[288] The hydrogenated derivative of *(4.07)*, C086 *(4.08)* demonstrated 5-fold to 7-fold more effective anti-proliferative activity against six colon cancer cell lines over curcumin. This derivative also downregulated the expression of NF-κβ, VEGF and MMP-9 in a range of cell lines. It also showed an effect similar to that of 5-FU on tumour growth in SW480 tumour bearing mice.[309]

(4.07)   *(4.08)*
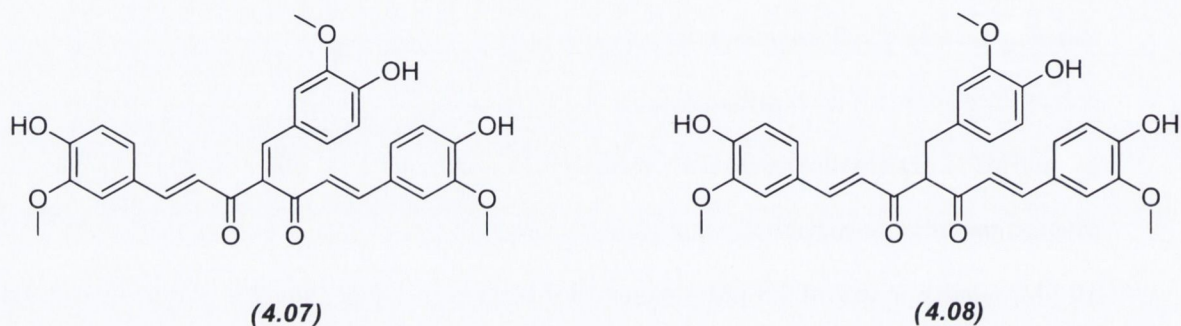
Figure 4.4: Synthetic derivatives of curcumin, *(4.07)* and C086 *(4.08)*.

Other derivatives with varied substituents on the aromatic rings as exemplified by *(4.09)* and *(4.10)*, displayed anti-angiogenic effects perhaps mediated through their effects on the downregulation of the expression of MMP-9 and VEGF.[287]

(4.09)   *(4.10)*
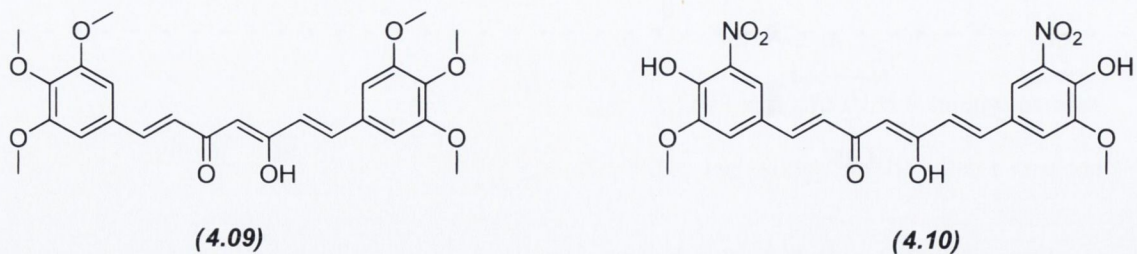
Figure 4.5: Compounds *(4.09)* and *(4.10)*, both bearing additional substituents in the phenol rings.

More radical curcumin derivatives with carbon chain lengths reduced to 5 *(4.11)* and 3 *(4.12)* carbons between the two aromatic rings inhibited angiogenesis and proliferation of SVR cells. However, resulting from the high degree of truncation and lack of phenolic character, it is reasonable to be sceptical about the status of these compounds, *(4.11)* in particular, as being described as being true curcumin derivatives.[310]

(4.11)   *(4.12)*
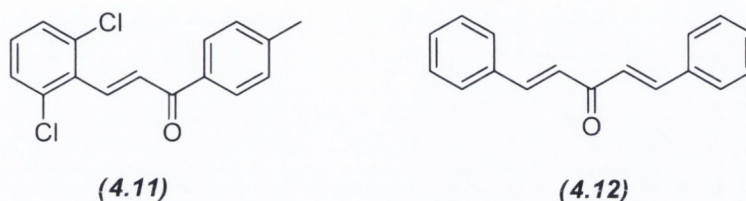
Figure 4.6: Truncated curcumin derivatives *(4.11)* and *(4.12)*.

Other groups have truncated the linker unit, with their screening results suggesting higher activity from a multitude of compounds containing a 5 carbon linker unit and alkylation of the phenol group, while retaining a degree of freedom around the central carbonyl (i.e tethering at this position using rings diminished activity). Several of these compounds showed increased anti-proliferative activity with up to 50-fold lower IC_{50} values than curcumin observed in a wide range of tumour cell lines including DLD-1, SW620 and HCT116 cell lines, while reducing gene expression resulting from the NF-κβ signalling pathway and cell cycle arrest in the G2-M phase.[311] The most active of this family of compounds were GO-Y030 *(4.13)* and GO-Y031 *(4.14)*.

(4.13)   *(4.14)*
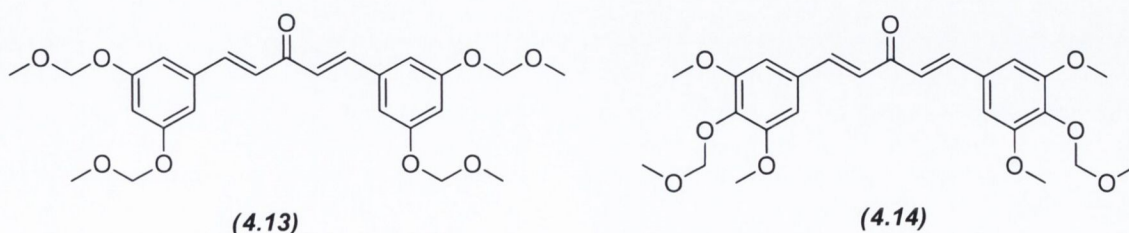
Figure 4.7: Curcumin derivatives GO-Y030 *(4.13)* and GO-Y031 *(4.14)*.

129

Other modifications to the structure include the use of the fluorine substituents and pyridine rings in the derivatives, EF-24 *(4.15)* and EF-31 *(4.16)*. Interestingly in these examples, there is a ring structure around the central carbonyl group, which maintains activity conversely to a previous report which stated a ring at this position would be detrimental to activity.[311] EF-31 showed almost complete inhibition of tumour growth in mice bearing Tu212 xenografts at concentrations of 25 mg kg^{-1} and both showed high anti-proliferative activity against this cell line *in vitro*.[312] Moreover, a greatly enhanced pharmacokinetic profile was witnessed relative to curcumin with plasma levels of drug being witnessed after 6 hours.[312]

(4.15)   *(4.16)*
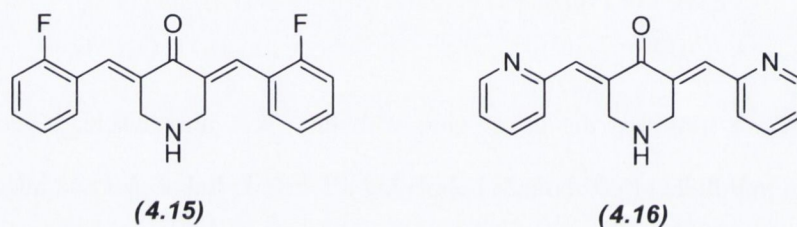
Figure 4.8: Structures of EF-24 and EF-31

4.2 Synthetic Strategy

While mindful of the fact that many of the curcumin derivatives synthesised have not been tested for APN activity, inspection of our compounds structure suggests that the B-ring in particular could be judiciously modified to allow for APN binding by incorporating structural features similar to that contained on the curcumin structure. As our compounds bearing the aromatic rings contain both the alkoxy and phenol substituents in their A and C-rings respectively and are effectively bridged together by an enone methylene strap on the B-ring, our compounds already show some similarities to that of curcumin. Further modifications to the B-ring should allow for the inclusion of the Zn^{2+} chelating β-diketone group to increase further their curcuminic character. This could be introduced by modifications during the synthesis of

the compounds to include the β-diketone moiety within the ring or subsequent to the synthesis of *(2.07)* by acylation at the carbon centre α to the carbonyl carbon to give compounds *(4.17)* and *(4.18)* respectively.

(4.17)　　　　　　　　*(4.18)*
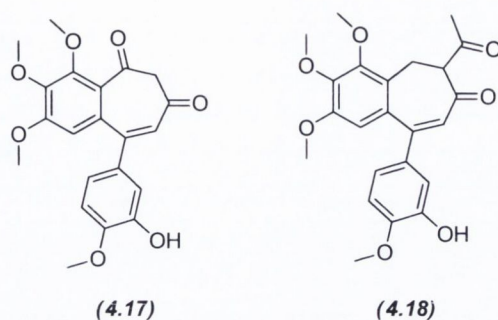
Figure 4.9: Synthetic targets *(4.17)* and *(4.18)*.

4.2.1　Synthesis of *(4.18)*.

Our strategy towards the synthesis of these two DMLs was to use *(2.07)* as the starting point. In principle we felt that we could exploit the benzylic position for the synthesis of *(4.17)* and the relative acidity of the hydrogens adjacent to the carbonyl group for the synthesis of *(4.18)*.

(2.07)　　　　　　　*(4.19)*　　　　　　　*(4.17)*
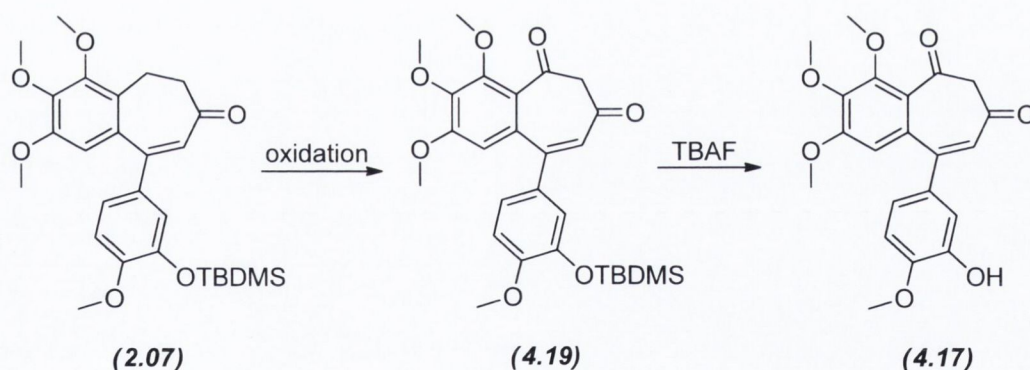
Scheme 4.1: Original attempts to synthesis curcumin hybrid *(4.17)*.

Benzylic methylenes are known to be susceptible towards oxidation, and exploitation of this property could theoretically form *(4.19)*, following the addition of just one oxidative step at this position, subsequent to the established synthesis of **(2.07)**. However, due to the presence of the alkene in *(2.07)*, a compatible oxidation technique must be identified to prevent its undesired

oxidation as the loss of unsaturation at this position has proven detrimental to these compounds activity. As this alkene, however, has shown stability towards PDC it was first decided to effect this transformation using a large excess of this chromium based reagent over a prolonged period of time. The reaction was frequently monitored over a period of seven days by TLC. However, even after this prolonged reaction time the only substance isolated was the unchanged starting material. Changing the oxidant to Jones' reagent, a stronger chromium based reagent did little to enhance the rate of the reaction resulting again in recovery of the starting material. Subsequent to these, other methods were sought including the use of activated MnO_2 and using MnO_2 as a solid support for $KMnO_4$ as per the method employed by Shabaani et al.[313] These methods yielded similar returns as the chromium mediated oxidations. A final attempt to effect this transformation employed the use of SeO_2[314] but this reagent resulted in the breakdown of the starting material to a complex mixture of products. Having exploited most of the standard oxidants for this transformation without success our efforts changed towards the synthesis of *(4.18)*.

It was decided to adopt a new approach towards the synthesis of this novel DML, whereby the 1,3 diketone functionality would be elaborated external to the B-ring using a well established procedure similar to the Claisen reaction.[315] Hydrogens attached to carbons adjacent to carbonyls are electron deficient lending an acidic character at this position to allow the formation of the enolate anion upon treatment with a base of suitable strength. This trait is exploited in the Claisen reaction leading to the formation of 1, 3-diketones from the reaction of a ketone and an ester. Enolate anions have found use in a variety of reactions in total synthesis of natural products.[316]

It was thus postulated that acylation of *(2.07)* at the carbon centre α to the existent ketone in the 7 position via a Claisen style reaction would theoretically yield compound *(4.20)*, which following phenol deprotection would yield the desired compound *(4.18)*. The key addition

reaction should be guided towards this product exclusively as the other carbon neighbouring the ketone forms part of the conjugated enone system negating its acidic character and disallowing it from participation in undesired side reactions often commonplace with enolation processes. Another consideration in preventing side reactions is to prevent the possibility of symmetrical aldol condensation of the starting material.[317] This should be overcome by using a strong base to ensure complete formation of the enolate anion in a short period of time. Strong non-nucleophilic bases such as NaHMDS and lithium diisopropylamide (LDA) have traditionally proven to be effective in the selective direction of the reaction towards one carbonyl group.[318]
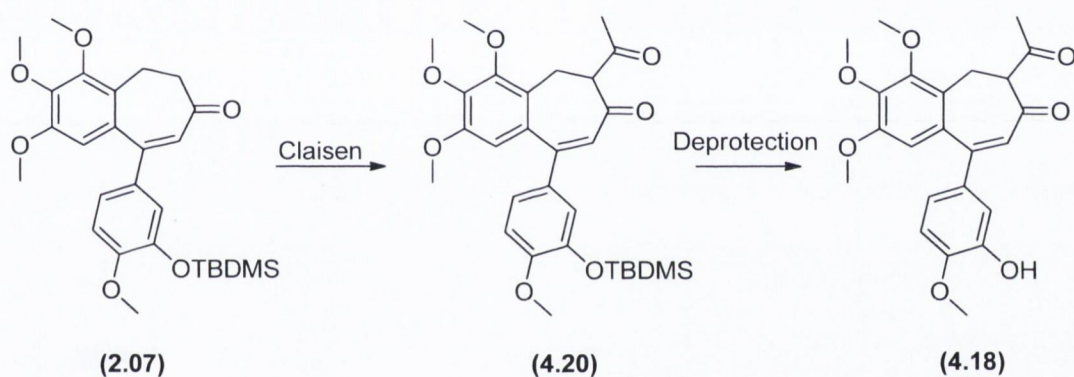
Scheme 4.2: Synthetic pathway towards DML *(4.18)*.

This modification to our existing scaffold at this position could be very advantageous as it would be expected to exhibit firstly a wide array of effects owing to the presence of the curcuminoid character, while the addition of a the sterically unchallenging acetyl ketone functionality would not be expected to diminish the anti-tubulin polymerisation activity inherent with the RS180 series of compounds. Furthermore, upon discovery of a robust synthetic method for the introduction of a second ketone group, subsequent modifications could realistically be made to increase the chain length external to the B-ring, facilitating the simple development of a number of synthetic derivatives from this parent structure, thus potentially creating a new series of compounds capable of exhibiting anti-cancer activity against multiple targets.

133

4.2.2 Results and Discussion

Initial attempts at the acylation reaction involved the generation of the enolate anion of *(2.07)* via deprotonation at the carbon α to the enone using a 0.25 M solution of lithium diisopropylamide (LDA), prepared in situ at -78 °C by the standard reaction of equimolar equivalents of diisopropylamine with butyllithium (BuLi) in THF. The dropwise addition of this solution to compound *(2.07)* at -78 °C in THF yielded a dark red solution within 20 min, suggesting the formation of the enolate anion of *(2.07)*. Attempts to form the acylated product using acetyl chloride showed the immediate quenching of the enolate anion as the distinct colour dissipated. However no reaction progress was observed by TLC (hexane/EtOAc 3:1). The literature reported that attempts by other groups to use acetyl chloride as a means to form a methyl ketone in this manner were also unsuccessful.[319] Similar results were observed when attempting this synthesis with other acylating reagents such as acetic anhydride.

The desired transformation was ultimately furnished using pyruvonitrile as the acylating reagent of the enolate in the same manner as del Mar Rey *et al.*[319] The transformation proved very efficient yielding the desired compound *(4.20)* following 1 h reaction at -78 °C. Subsequent deprotection of the phenol yielded the target compound *(4.18)* in 10 mins in 90% yield.
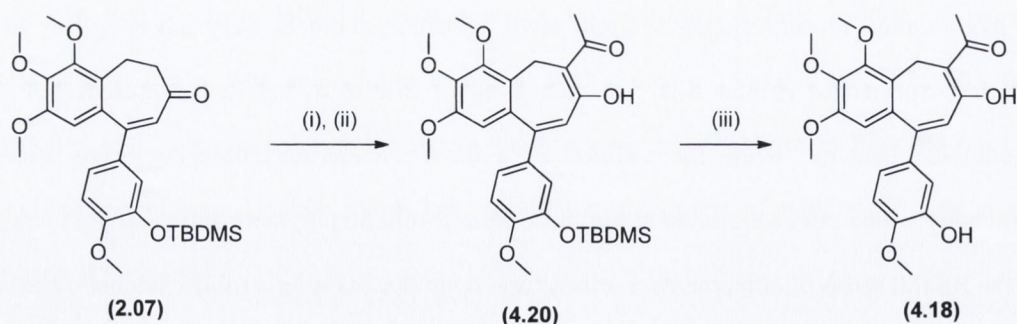
(i) LDA, THF, -78 °C, 10 min (ii) pyruvonitrile, -78 °C, THF, 1 h, 79% (iii) 1M TBAF, THF, 0 °C, 10 min, 90%.

Scheme 4.3: Synthesis of the curcumin derived DML *(4.18)*.

4.2.3 Structural Elucidation of compound *(4.20)*.

As mentioned in the chapter's introduction, curcumin exists in tautomeric forms due to the hydrogen bonding mediated stabilisation of the enol form of this compound. It would be expected that *(4.20)* would similarly adopt all three tautomeric forms illustrated in Figure 4.10, complicating the resultant IR and NMR spectra. Investigations into the structure of this compound were required before completing the synthesis via the deprotection step outline in Scheme 4.3.

(4.20 a)   *(4.20 b)*   *(4.20 c)*
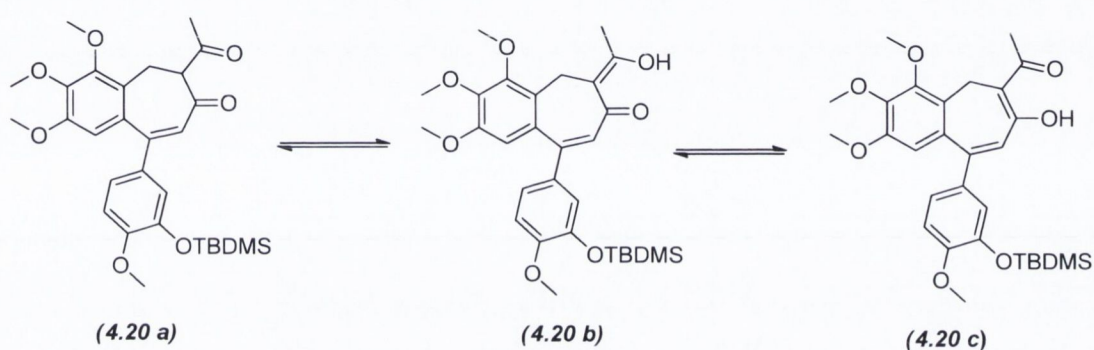
Figure 4.10: The potential tautomeric forms of compound (4.20).

In reality, these spectra appeared relatively clean and the appearance of only one product on TLC during reaction monitoring suggested that just one of these tautomers was produced, the spectral evidence suggesting the formation of *(4.20 c)*. The most interesting peaks in the ^{1}H NMR spectrum include that at 15.62 ppm, a singlet integrating to one proton. Peaks in the range of 14 ppm to 16 ppm can be attributed to the characteristic resonance of a proton attached to an enol oxygen.[320] As tautomer *(4.20 a)* does not possess an enol proton, this can be discounted as the form which the product ultimately adopts. The CH proton alpha to both carbonyls would be expected to resonate more upfield at 4 ppm. The other interesting peak in this spectrum indicating the formation of *(4.20 c)* is that of the singlet integrating to three protons resonating at 2.52 ppm, which are representative of the terminal CH$_3$ neighbouring the carbonyl outside the ring. The analogous protons for *(4.20 b)* would be observed slightly more upfield at around 2

ppm. The ^{13}C NMR spectrum shows adoption of the enol form in the 1,3-diketone functionality as evidenced by the appearance of a single carbonyl peak at 197.4 ppm and an enol peak at 174.8 ppm The methyl group outside the ring is seen at 25.9 ppm, in addition to the expected methoxy resonances between 55 ppm and 62 ppm. The 4 aromatic primary carbons and 1 signal for the alkene carbon are witnessed in the range between 100 ppm and 125 ppm, with 8 aromatic quaternary carbons seen between 127 ppm and 155 ppm. The TBDMS peaks are seen upfield at 1.02 ppm, 18.5 ppm and 25.7 ppm.
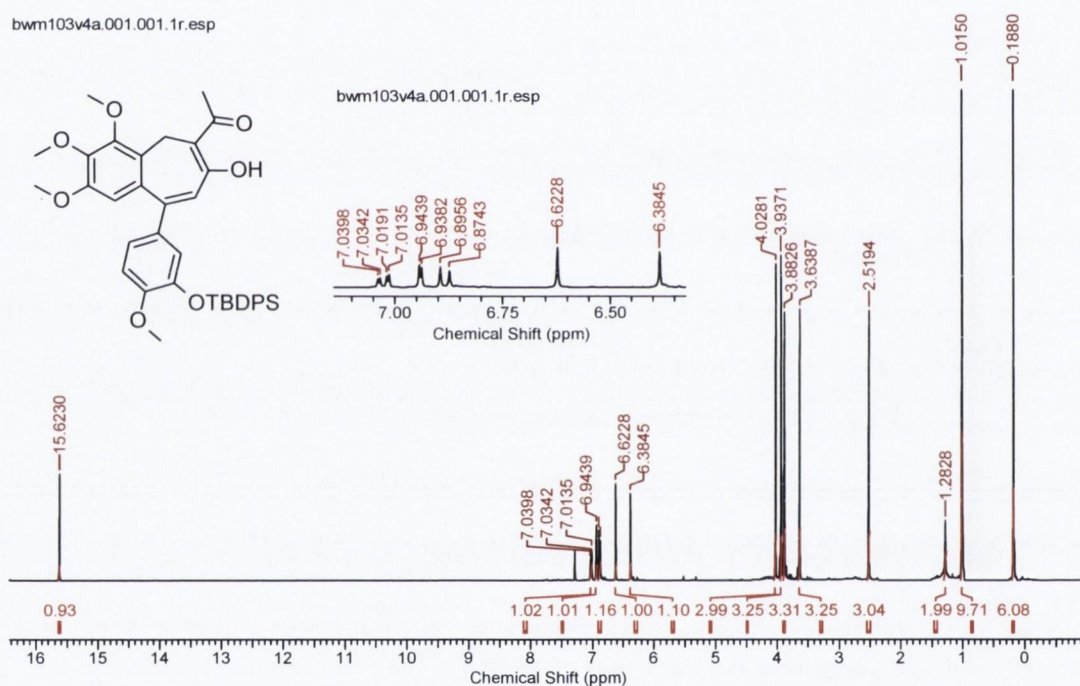
Figure 4.11: ^{1}H NMR spectrum of *(4.20)*.

bwm103v4a.015.001.1r.esp

bwm103v4a.014.001.1r.esp

bwm103v4a.013.001.1r.esp

197.3929
174.8345
151.6540
150.8085
148.6897
144.6853
143.6259
135.0146
132.0794
127.6669
123.4001
123.0113
121.8548
111.4843
110.6970
109.2974
61.3814
60.8469
55.9581
55.4332
25.9061
25.7020
23.6220
18.4611
1.0247
4.5444

Chemical Shift (ppm)

180   160   140   120   100   80   60   40   20   0
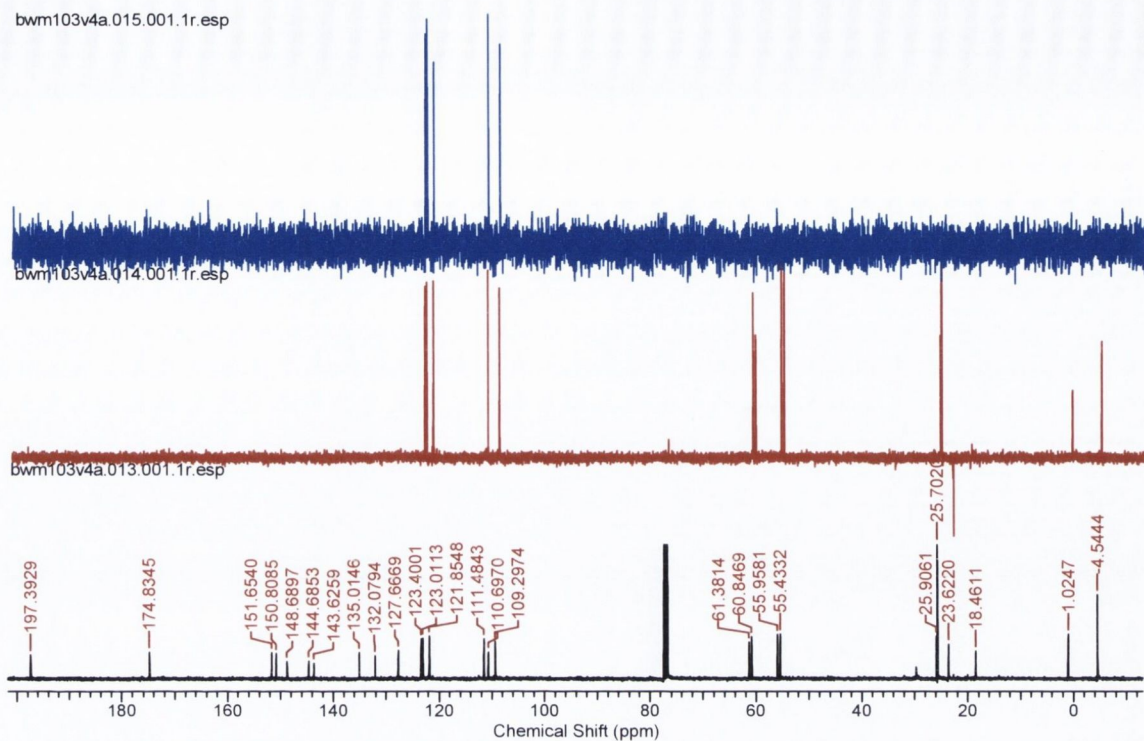
Figure 4.12: ^{13}C NMR spectra of *(4.20)*

The IR spectrum shows a stretch at 1711 cm^{-1}, which supports the identity of the compound being *(4.20 c)*. As there is a lower degree of conjugation around the carbonyl centre, it would be expected to show the stretching frequency at a higher wavelength than that seen in *(4.20 b)*, which falls under the influence of two neighbouring double bonds. The stretching vibration at 3400 cm^{-1} is indicative of the enol hydroxyl group.

The stability of this structure can be further rationalised by the high degree of conjugation bestowed upon it throughout the tricyclic ring structure. The increased double bond character inside the B-ring strengthens the compound's structure, with the potential for aromaticity through the molecule should a charged species similar to a tropylium cation form.[321]

Upon deprotection, the spectra for *(4.18)* are very similar to its precursor compound with the expected disappearance of the two singlet peaks of the TBDMS protecting group at 0.18 ppm

and 1.01 ppm to be replaced with a singlet integrating for the phenol proton at 5.69 ppm. In the ^{1}H NMR, the peak at 15.57 ppm is conserved showing the enol functional group remains intact. The remainder of the spectrum supports the structure with 4 singlets integrating to 12 total protons in the region between 3.65 ppm and 4.01 ppm showing the 12 methoxy protons contained in the compound. The peak at 2.51 ppm shows the acetyl protons, while the 4 aromatic protons and B-ring alkenyl proton are seen resonating between 6.40 ppm and 7.02 ppm.
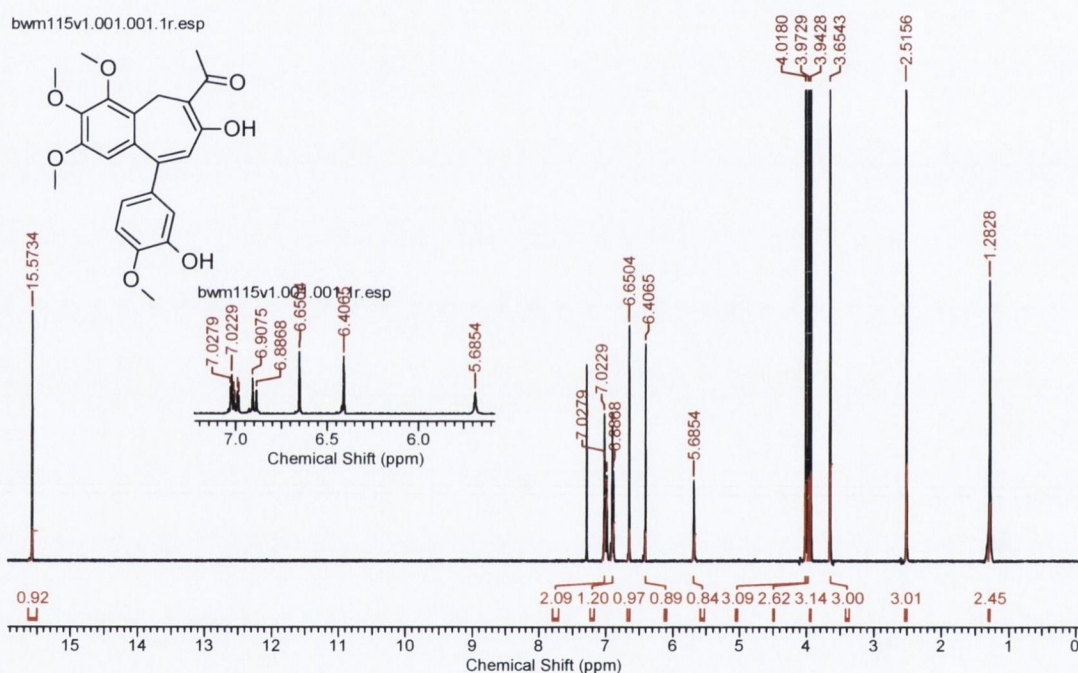
Figure 4.13: ^{1}H NMR spectrum of (4.18)

The first signals to be noted in the ^{13}C NMR spectrum are those at 197.5 ppm and 174.8 ppm showing the presence of the carbonyl carbon and the enol carbon respectively. There is a CH$_2$ peak at 23.9 ppm, showing the presence of the benzylic carbon in the B-ring. The four methoxy signals are seen between 56 ppm and 61 ppm. The fifth methyl group in this compound is seen at 25.9 ppm showing the one belonging to the acetyl group exo to the β-diketone. Between 109 ppm and 121 ppm, 5 peaks are seen corresponding to the aromatic and alkene carbons in (4.18).

There are 9 additional quaternary carbons in the region between 127 ppm and 151 ppm corresponding to the amount expected in the compound. The m/z of 411.1495 matches the m/z expected from the (M-H)⁻ ion, suggesting the completed synthesis of the target compound.
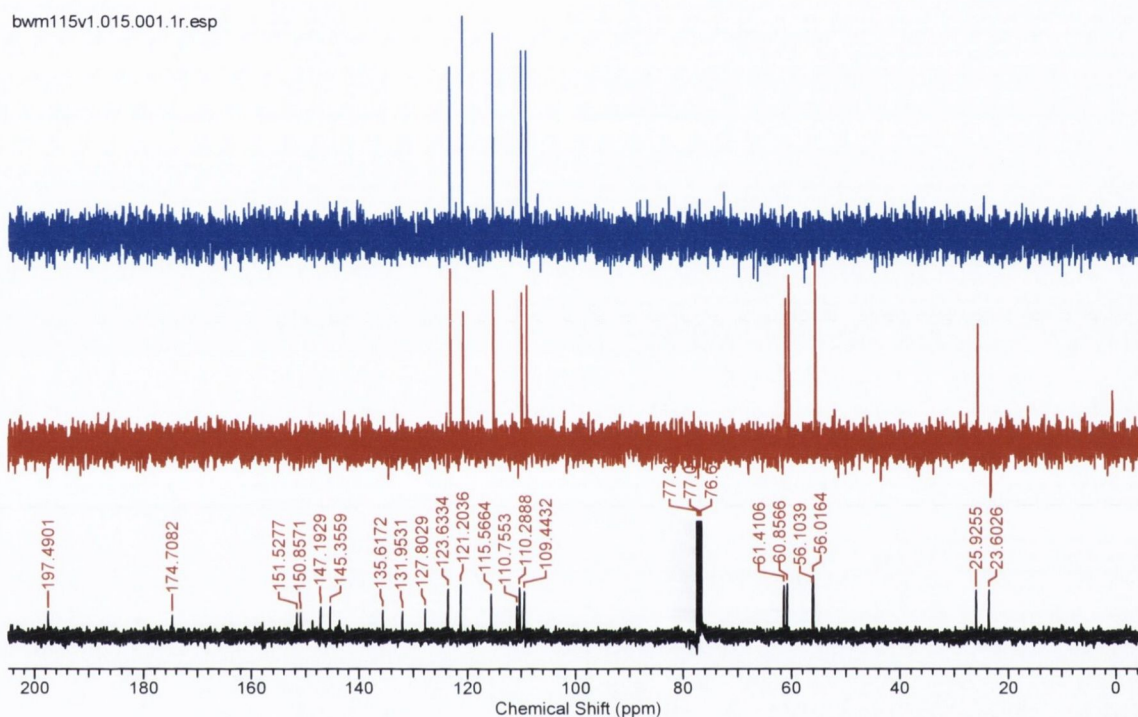
Figure 4.14: ¹³C NMR spectrum of (4.18)

4.3   Biological Evaluation of compound (4.18).

Following the successful synthesis of (4.18), its anti proliferative, APN inhibitory and anti-migratory effects were measured using the three assays used to evaluate the activity of the series of compounds outlined in Chapter 2.

4.3.1   APN Activity of (4.18).

Anti-APN activity was measured using the same approach as used for the compounds previously described in Chapter 2[135b] requiring a modification to factor interference resulting

from the distinctive yellow colour of the compound *(4.18)* into the results. Whereas the colouration resulting from the hydrolysed substrate was measured only once after a time period of 2 h in the standard assay, the change in absorbance was measured in the plate reader at 100 time points over this period. The slope of the line was determined using linear regression and the percentage of enzyme inhibition relative to the DMSO blank was calculated using the formula:

% inhibition = 100-(slope of test sample)/(slope of DMSO blank)*100

The IC_{50} value of 79.56 μM ±1.03 SEM was calculated following the plot of log concentration versus normalised percentage inhibition. The control compound bestatin was measured as possessing an IC_{50} of 32.55 μM ±1.40 SEM.

Compound	APN inhibition (μM)	SEM
(4.03)	79.56	±1.03
Bestatin	32.55	±1.40

Table 4.1: IC_{50} of APN inhibition for both *(4.18)* and bestatin.

APN Inhibition *(4.18)*

The graph shows % APN Inhibition (y-axis, 0 to 100) versus Log concentration (µM) (x-axis, -1 to 3).
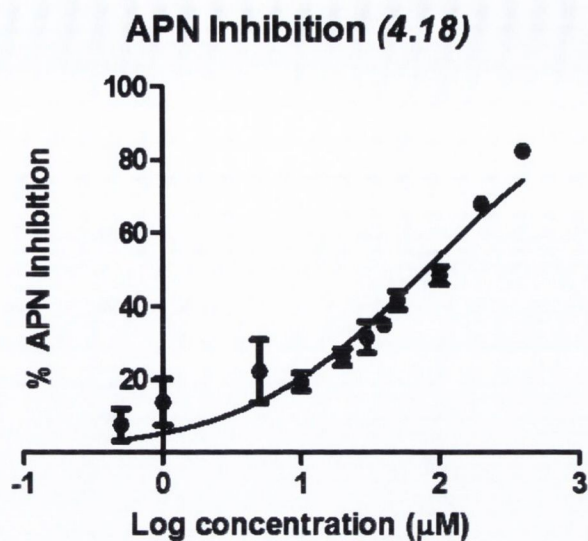
Graph 4.1: Percentage inhibition of APN versus log concentration of *(4.18)*

4.3.2 MTT Assay results.

The proliferation of PC-3 cells was measured using the same procedure as outlined in Chapter 2.[212] The IC_{50} calculated was 335.9 nM ±1.12 SEM, comparing unfavourably to the control compound CA-4 which exhibited an IC_{50} of 20.44 nM ± 1.69 SEM.

Compound	IC_{50} (PC-3 Cells) (nM)	SEM
(4.18)	335.9	±1.12
CA-4	20.44	±1.69

Table 4.2: IC_{50} of *(4.18)* and CA-4 obtained from the MTT cell proliferation assay.

4.3.3 Cell Migration Assay Results.

Compound *(4.18)* showed a marked effect on cell migration at concentration of 5 µM, 10 µM and 20 µM showing a halving of the spontaneous migration rate over the time period. At 24 h, it showed comparable activity to that of CA-4, with a longer lasting effect illustrated by the migration distance witnessed after 48 hours especially at the high concentrations where cell migration was observed as half that of the control compound. The APN inhibitor bestatin

showed an effect at 80 µM concentration less than that observed at any of these concentrations showing that the anti-migratory effect is not mediated by its anti-APN effect. The results of this assay are tabulated in Table 4.3 detailed in photographic form in Figure 4.16 as in Chapter 2.

Compound	Conc	Cell Migration (nm) 24 h	Cell Migration (nm) 36 h	Cell Migration (nm) 48 h
(4.18)	5 µM	110.02±17.92	164.63±39.08	167.81±14.81
	10 µM	87.85±16.15	108.92±3.62	169.59±27.93
	20 µM	95.16±20.76	103.98±6.30	188.04±6.91
CA-4	5 µM	114.93±7.17	137.90±16.27	167.74±7.96
	10 µM	108.05±8.53	133.05±4.82	159.58±14.74
	20 µM	81.37±3.60	122.12±10.26	150.95±12.64
(2.01)	5 µM	127.92±9.99	181.39±21.32	234.09±38.30
	10 µM	102.67±17.17	155.35±13.75	172.04±16.76
	20 µM	89.99±23.89	140.05±23.69	156.42±10.75
Bestatin	80 µM	142.52±6.29	188.61±7.40	208.70±8.88
0.1% DMSO		176.02±8.51	240.93±7.21	277.30±12.09

Table 4.3: Cell migration assay results (±SEM) for *(4.18)*.
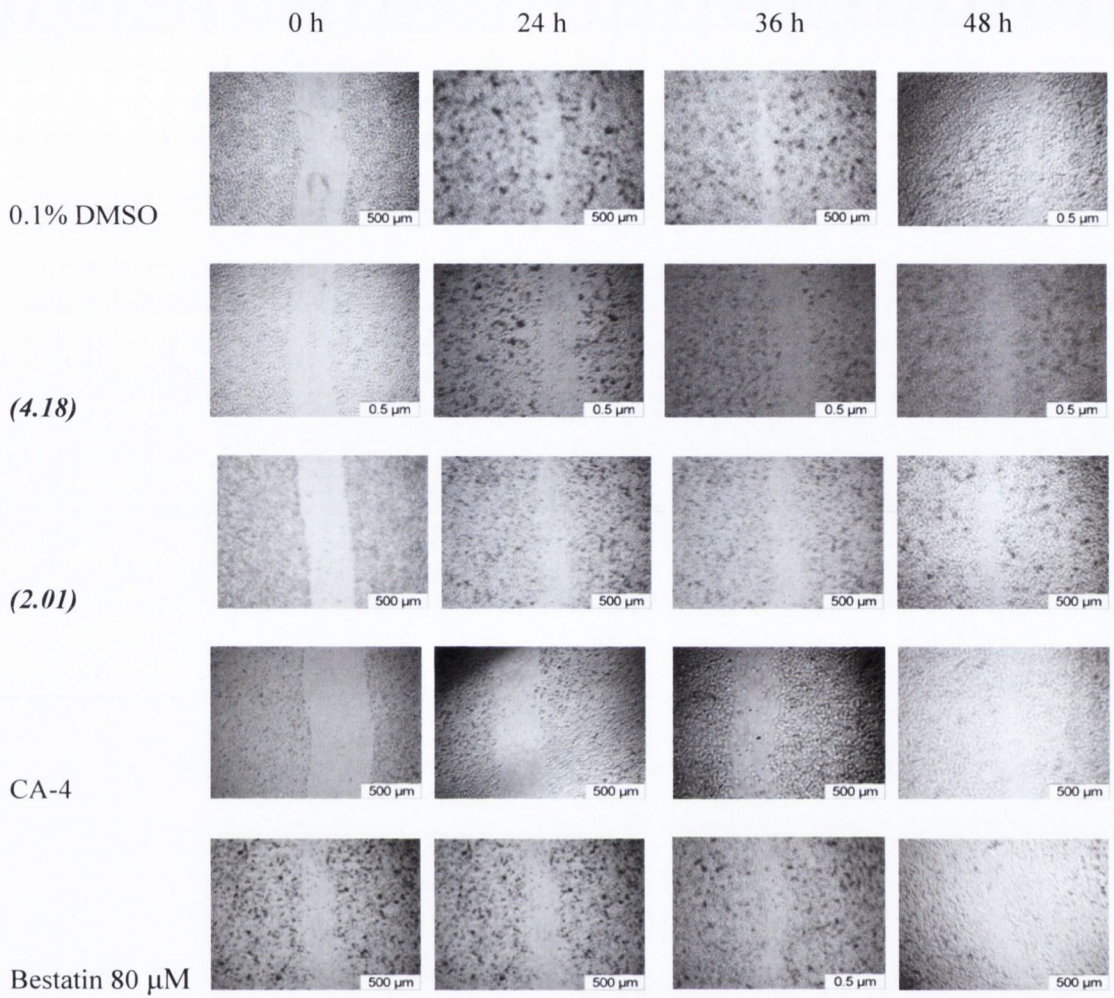
Figure 4. 15: Observed cell migration following treatment of PC-3 cells with *(4.18)* at 10 µM measured over 24, 48 and 72 h.

143

(4.18)
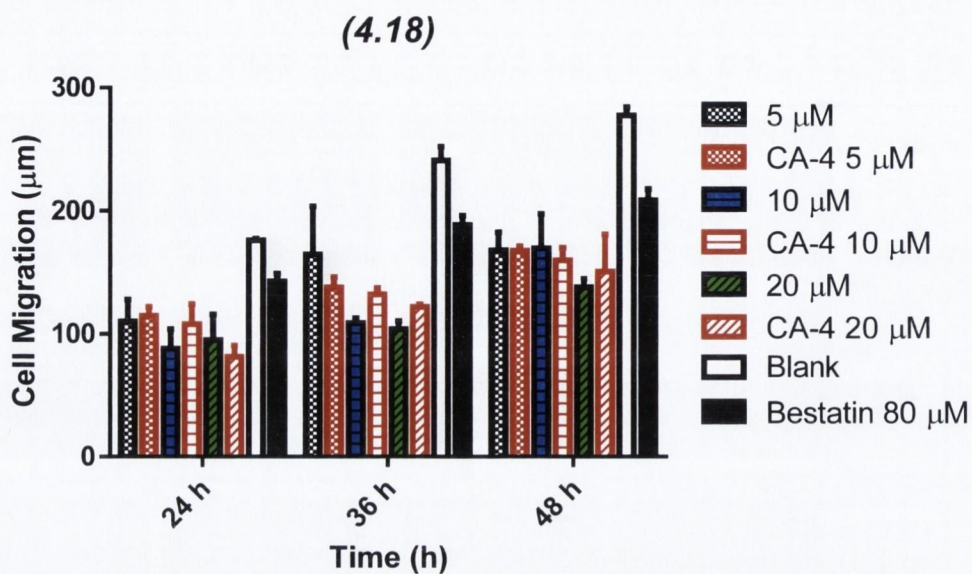
Graph 4.2: Cell migration distance measured for *(4.18)* over 24 h, 36 h and 48 h.

4.4 Discussion and Conclusion

The integration of a β-diketone into the structure of *(2.01)* was achieved following one additional reaction step prior to its final deprotection. The compound *(4.18)* could theoretically form the basis of a new series of compounds as the elaboration *(2.07)* in this manner could be achieved relatively simply. At the outset of the investigations, it was fully intended to keep the added alkyl substituent of the β-diketone as small as possible to prevent the diminishing of biological activity due to steric bulk crowding the important carbonyl functionality. However, now that theoretically the enol ketone structure has been proven active in APN inhibition, larger groups can be used to investigate the effect, if any, their added bulk could have in interactions with the biological targets. For example, as stated in Section 2.7, the binding site in APN possesses hydrophobic pockets ready for exploitation using bulkier side chains than the methyl group in *(4.18)*. Such modifications could lead to further improvements in the series' APN inhitory effect. The activity of *(4.18)*, while promising, is much diminished from control compound bestatin (IC_{50} 32.55 μM) and *(2.03)* (IC_{50} 8.70 μM).

Cell proliferation is inhibited in the nanomolar range as exemplified by the MTT assay results (Section 4.3.2) and the cell migration assay shows a greater anti-migratory activity than that of CA-4 over the range of concentrations. In addition, the anti-migratory effect of the compound is greater than that observed in the parent compound *(2.01)*, suggesting the benefit of added curcuminic character for anti-cancer activity.

Together, the biological data prove the synthesis of a novel compound with the potential to target multiple facets implicated in cancer spread. In future work, perhaps work could be done in order to solubilise the compound using phosphate ester pro-drugs similar to that of CA-4 phosphate, providing a manner for the introduction of the important 1,3-diketone in a more clinically reliable manner. The phosphate ester of *(2.01)* has already been synthesised, suggesting the easy modification of *(4.18)* in this way. As mentioned in the introduction to this chapter, much of the investigations into the anti-cancer effect of curcumin is orientated towards improvement of its bioavailability, which could realistically be achieved using this approach.

Chapter 5

5.1 Introduction

Artemisinin *(5.01)* is a sesquiterpenene lactone containing a 1,2,4-trioxane ring, isolated from the Chinese herb, *Artemesia annua*.[322] This herb was traditionally used in Chinese medicine for the treatment of fever.[323] More recently, following the isolation of its principal active constituent, artemisinin, this compound and derivatives thereof have found widespread clinical use in the treatment of malaria. Indeed, in many instances they have replaced the more traditionally used anti-malarial agents such as quinine and chloroquine.[324] However owing to reports implicating the onset of resistance[325] towards the treatment with artemisinin in isolation, the World Health Organisation(WHO) has discouraged monotherapy of artemisinin,[326] recommending its administration in combination therapy with other anti-malarial compounds including mefloquine and piperaquine. Artemisinin and its derivatives are known to selectively target the *Plasmodium* parasite showing little toxicity to normal host tissues. Its mode of action is unclear and still a cause of much debate,[327] however one major argument suggests the opening of the trioxane ring upon interaction with high levels of Fe^{3+} in the parasite's digestive vacuole generates highly reactive carbon centred radical intermediates, alkylating an array of parasitic proteins necessary for parasitic survival.[328]

Two major disadvantages inherent with the drug are the need to isolate it from a natural source and its inherently low bioavailabilty. In redressing the first point, total syntheses have been reported as far back as 1982.[329] As total syntheses of such large complex compounds are challenging procedures, these are rarely produced at large scales due to cost constraints. Consequently several methods have been devised to generate precursor compounds in culture, with a very recent report[330] showing the development of a *Saccharomyces cerevisiae* strain

capable of generating almost 16 times the amount of precursor compound artemisinic acid *(5.02)* relative to previous reported procedures.[331]

This large scale production of artemisinic acid permits the generation of semi-synthetic derivatives of artemisinin displaying greater water-solubility. The most common semi-synthetic derivatives are modifications of the reduced form of artemisinin, dihydroartemisinin (DHA) *(5.03)*, an active metabolite of artemisinin. These include the lipophilic artemether *(5.04)*, and the water-soluble succinate ester of DHA, artesunate *(5.05)*. The generation of this water-soluble form of artemisinin has resulted in a much more favourable pharmacokinetic profile than the parent compound.[332]

(5.01)   *(5.02)*   *(5.03)*

(5.04)   *(5.05)*
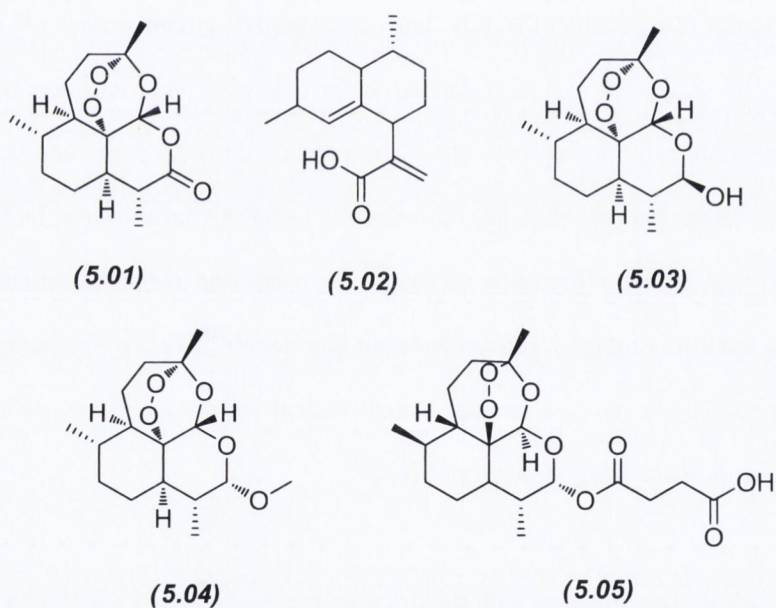
Figure 5.1: The structures of artemisinin *(5.01)*, artesmisinic acid *(5.02)*, DHA *(5.03)* and the semisynthetic derivatives artemether *(5.04)* and artesunate *(5.05)*.

5.1.1 The use of artemisinin and its derivatives for treatment of cancer.

In addition to its clinical use in the treatment of malaria, significant research has suggested the potential use of artemisinin and its derivatives for the treatment of solid tumours. It has been shown to induce apoptosis[333] in resistant cell lines,[334] inactivate NF-κβ,[335] upregulate death

receptor 5 (DR5)[335], inhibit angiogenesis[336] and cell proliferation in a range of cell lines including those of pituitary,[337] leukaemia,[338] hepatic,[339] and prostate[340] cancer phenotypes.

One of the mechanisms underpinning its anti-cancer effects is similar to its anti-malarial mode of action. In developing tumours, there is a requirement for heightened levels of iron relative to normal cells to enable further advancement of the cell cycle.[341] As the endoperoxide bridge of artemisinin is known to be highly tolerated *in vivo* and generates carbon centred radicals in the presence of iron, it has been postulated that artemisinin can selectively target cancer cells by generating these reactive species inside cancer cells only.[342] It has been shown to induce apoptosis in T47D and MDA-MB-231 breast cancer cells through this mechanism.[343] In fact, studies have shown the potential beneficial effect of conjugation of artemisinin to a range of iron containing compounds including transferrin and holotransferrin already shows benefits associated with its selective targeting of cancer cells containining increased levels of iron.[344]

In vivo, artesunate has been shown to inhibit the invasion and metastasis of NSCLCs, inhibiting the expression of multiple targets involved in these processes including K-cadherin (CDH6), fibroblast growth factor receptor 4, Myc, transforming growth factor beta 1 (TGFβ1) and MMPs 2 and 7.[345] Artemether has already shown beneficial results in the treatment of a patient with pituitary adenoma[346] while artesunate has been shown as effective in the reduction of a laryngeal squamous cell carcinoma by 70% over two months treatment suggesting these compound's potential clinical benefits in the treatment of many cancer types.[347]

Artemisinin displays an anti-migratory effect on human melanoma cell lines and has been shown to down-regulate important markers in the development of cancer including MMP-9 and the $\alpha_v\beta3$ integrin.[348] Similar effects have been noted with DHA in murine lymphatic endothelial cells in addition to the upregulation of pro-apoptotic gene bax and downregulation of the anti-

apoptotic bcl-2 with diminished levels of VEGFR-3 measured, further displaying the anti-angiogenic, anti-lymphangiogenic and anti-apoptotic effects of artemisinin.[349]

As shown in Figure 5.1, the majority of modifications to the structure of artemisinin involves its functionalisation at the C-12 carbonyl. However, there have also been investigations towards the simplification of the structure that replace the trioxane ring with a tetraoxane ring to generate a series of compounds containing the core cholic acid backbone that are more stable relative to artemisinin, even in acidic conditions with pH as low as 1.6.[350] The stability of the tetraoxane functional group allows for harsher modifications not possible in the trioxane ring structure including functional group reduction with LiAlH$_4$. The cholic acid derived 1,2,4,5-tetraoxanes *(5.06)* and *(5.07)*, bridged by the tetraoxane group, have shown similar antiproliferative activity against both HeLa and Fem-X cells to that of cisplatin. Likewise, the tetraoxane *(5.08)* was also highly effective against the proliferation of both melanoma (LOX IMVI) and ovarian cancer (IGROV1) cell lines displaying LC$_{50}$ values in the range of 60 nM for both cell lines.

X=NH$_2$ *(5.06)*
X=OH *(5.07)*

(5.08)
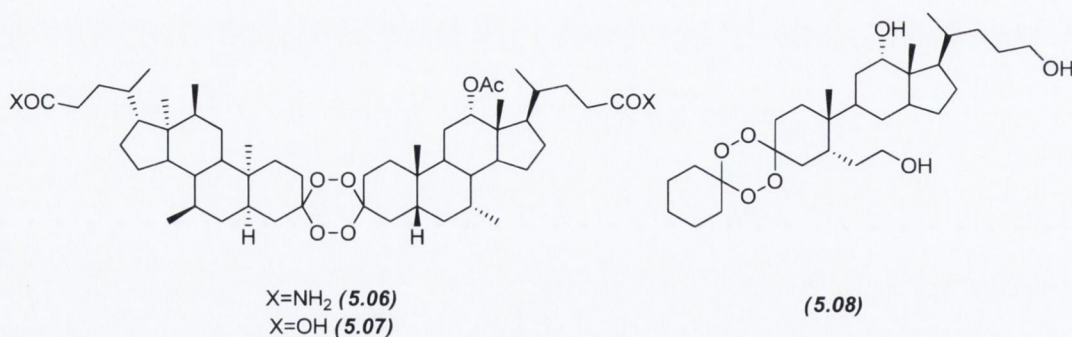
Figure 5.2: Semisynthetic tetraoxane artemisinin derivatives *(5.06-5.08)*.

It is in adjuvant treatment that artemisinin has been shown to operate best. As examples, it has shown particularly promising effects in combination with γ-radiotherapy against glioma cells.[351] Furthermore these studies also showed the additive effect of co-administration with transferrin, further supporting the role of iron in the mechanism of artemisinin's anti-cancer action. DHA

has been shown to amplify the effect of gemcitabine towards pancreatic cancer cells both *in vitro* and *in vivo*.[335] Based on the promising anti-angiogenic data and observation that artemisinin type compounds show a degree of selectivity for iron-rich prostate cancer cells, this pharmacophore presents itself as the ideal partner to combine with our lead vasculature disrupting agents. There are many ideal partners from our suite of compounds, but our primary focus here will be on RS180 *(2.01)* and RS176 *(5.12)* to generate these hybrid forms.

5.2   The synthesis of RS180-Artemisinin conjugates.

Previously within the group the synthesis of a novel conjugate of artemisinin and quinine was accomplished, displaying superior activity against both drug susceptible and resisistant strains of *Plasmodium falciparum* over artemisinin or quinine alone.[260]

In the first instance, the strategy adopted was to utilise the phenolic group on *(2.01)* to couple artesunate *(5.05)*, ultimately providing us with a hybrid where the tubulin component of the design is presented in pro-drug from, but is expected to generate slowly the individual components again following hydrolysis. Using the coupling methodology employed by Horwedel *et al* in their synthesis of betulin-artemisinin hybrids,[352] the conjugate *(5.09)* was formed using 1-ethyl-3-(3-dimethylaminopropyl)carbodiimide (EDCI) as a coupling reagent.[353] Although EDCI functions in much the same way as DCC, the advantages of using this coupling reagent results from the increased solubility in water of its urea side product relative to that seen in DCC coupling, thus facilitating the simpler purification of the desired products.
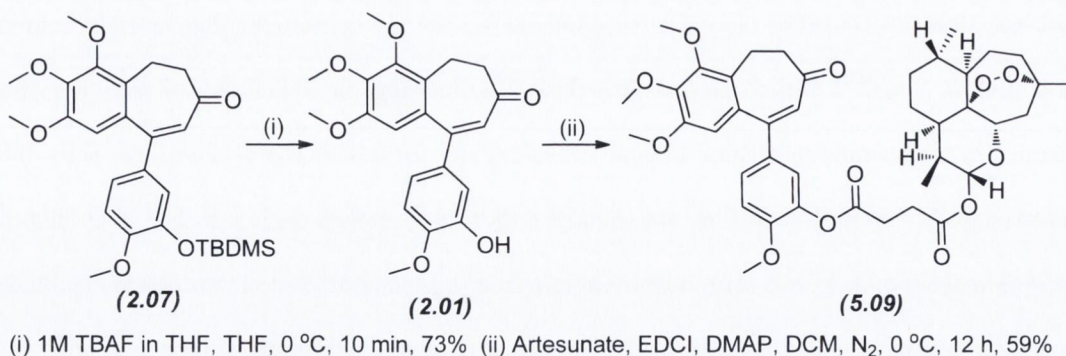
Scheme 5.1: Synthesis of novel RS180-artemisinin hybrid (5.09)

(i) 1M TBAF in THF, THF, 0 °C, 10 min, 73% (ii) Artesunate, EDCI, DMAP, DCM, N$_2$, 0 °C, 12 h, 59%

5.2.1 The synthesis of *(5.09)*.

Following the synthetic scheme outlined in Scheme 5.1, the phenol *(2.01)* was generated in a moderate yield of 73% upon its deprotection with 1 M TBAF in THF at 0 °C over 10 mins. This phenol was reacted with the activated ester formed between EDCI and artesunate for 12 h in DCM using DMAP as an acylation catalyst to afford compound *(5.09)* as expected, in a modest yield of 59%.

Notable in this reaction step is the appearance of the product *(5.09)* at a very similar R$_f$ to that of the starting material *(2.01)* on TLC using hexane/EtOAc (1:1) as the mobile phase. The product could be visualised upon spraying with vanillin/H$_2$SO$_4$ solution as a red spot of similar pigmentation to that exhibited by artesunate which itself appeared on the baseline of the plate. A solution of aq. Na$_2$CO$_3$ was used in the work up to remove any amounts of the acidic artesunate and RS180 facilitating a simpler purification of *(5.09)* by column chromatography.

5.2.2 Structural Elucidation of *(5.09)*.

A complete spectroscopic study on *(5.09)* was carried out using a variety of NMR spectra including ^{1}H, ^{13}C, and DEPT spectra in addition to Total Correlation Spectroscopy (TOCSY),

Heteronuclear Multiple-Bond Correlation (HMBC) and Heteronuclear Single Quantum Correlation (HSQC) NMR spectra as well as IR and HRMS spectra.

Although it is seemingly a very complex compound at first glance, it is made up of two building blocks whose spectra are already known. Dividing the task into two, where first the peaks in the RS180 section of the compound were studied before those of the artemisinin component makes assignment of signals a simpler task. The following numbering scheme was used (Figure 5.3)
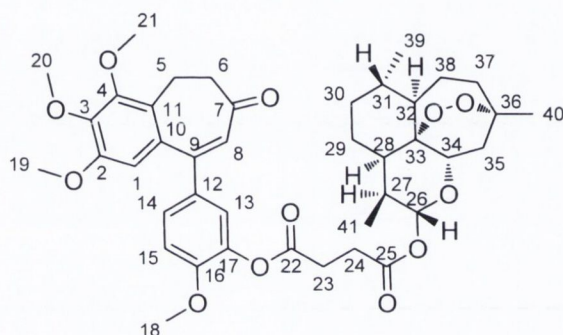
Figure 5.3: Atomic labelling system used for compound (5.09).

The mass spectrum in positive ionisation mode was consistent with the sodium adduct of compound *(5.09)*, with a given m/z of 759.3032. The IR spectrum shows stretching vibrations at 1700 cm $^{-1}$ and 1734 cm^{-1} which are indicative of those of the enone and ester functionality respectively on *(5.09)*. In addition to this, the ^{1}H NMR spectra showed a total of 50 protons while there were 41 signals in the ^{13}C NMR spectrum, in agreement with the postulated structure.
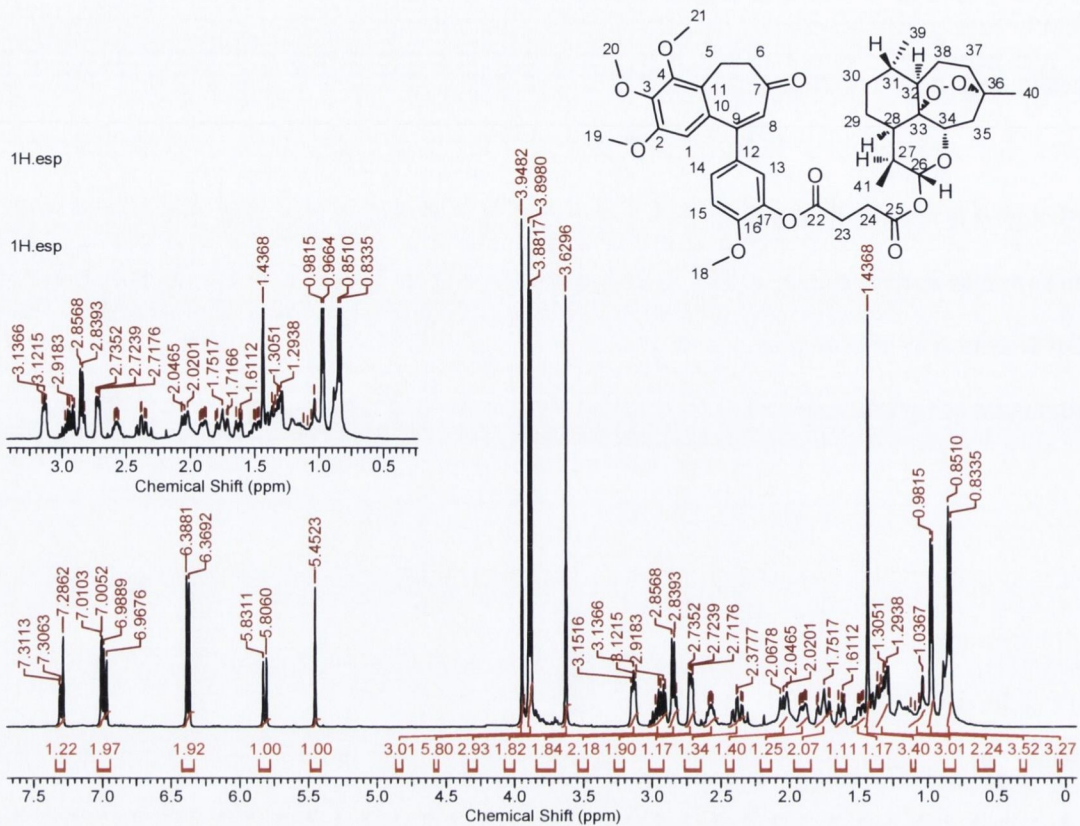
Figure 5.4: ^{1}H NMR of compound *(5.09)*.
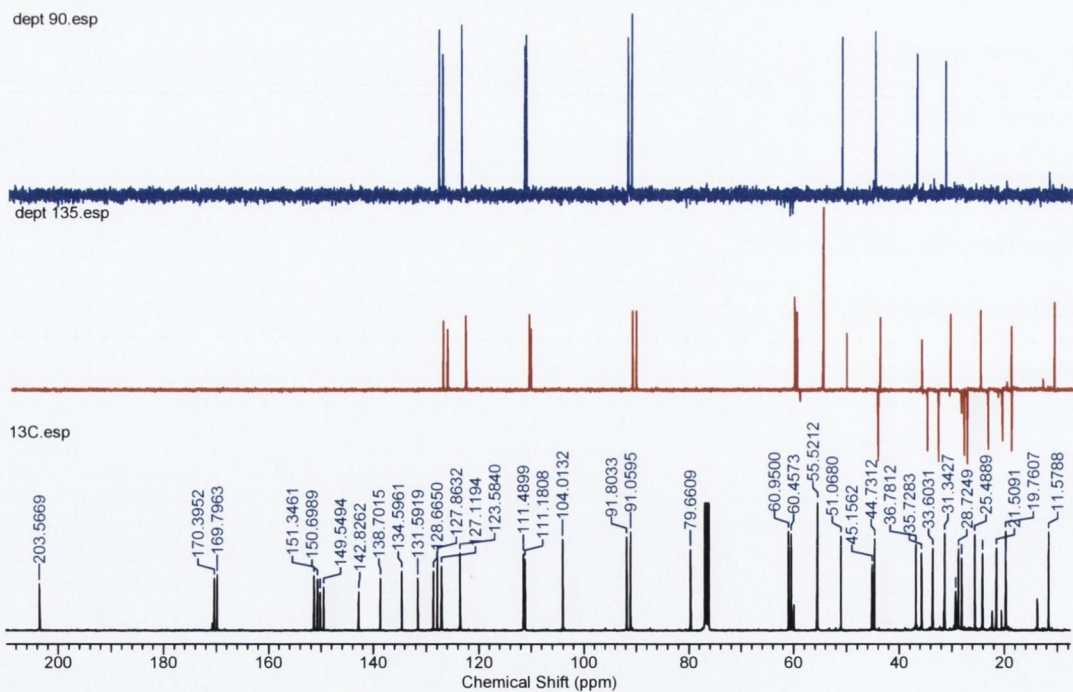
Figure 5.5: ^{13}C, DEPT 135 and DEPT 90 NMR spectra of compound *(5.09)*.

In the carbon NMR, the peak at 203.3 ppm stands out as the carbonyl peak at C-7. In the HMBC spectrum, correlations with protons at 3.14 ppm and 2.72 ppm are evident, correlating to those on C-6 and C-5 respectively. Using the HSQC, these proton resonances are shown to correlate to carbon signals resonating at 45.2 ppm and 19.7 ppm with C-6 resonating further downfield relative to C-5, resulting from its proximity to the carbonyl. Similarly, H-5 shows more correlations in the HMBC to the aromatic proton of the A-ring due to its closeness to this aromatic ring. In addition to the quaternary carbon at 128.7 ppm, H-5 also interacts with carbon resonances at 131.6 ppm and 150.2 ppm representing carbons 4, 10 and 11. As H-6 also correlates to 128.7 ppm, this resonance is assigned to C-11. The higher shift at 150.2 ppm would suggest this carbon falls under the influence of an electronegative group. Correlation to a singlet at 3.89 ppm integrating to 3H shows that this peak is responsible for the resonance of C-4, while identifying the peak at 3.89 ppm as the methoxy group at C-21, whose corresponding ^{13}C resonance is found at 61.0 ppm. C-11 shows an association with a proton at 6.37 ppm, a singlet integrating to one proton. Only the aromatic proton at C-1 is within the three bonds at which HMBC functions optimally, the corresponding carbon of which is seen at 111.2 ppm. H-1 further couples to carbons with resonances of 142.8 ppm and 150.7 ppm. These carbons also correlate to methoxy groups at 3.94 ppm and 3.63 ppm respectively. Although it is not possible to distinguish between these signals using the spectra obtained, it is known that due to the existence of resonance, the methoxy peak for the hydrogens at C-20 are shifted further upfield allowing the peak at 3.63 ppm to be assigned at this position, and that at 3.94 to be given to H-19. HSQC shows their respective ^{13}C chemical shifts to be at 55.5 ppm and 60.5 ppm respectively. Furthermore, the quaternary carbons C-2 and C-3 can be definitively identified as those at 142.8 ppm and 150.7 ppm. Within the fused AB ring structure there are now only two atoms without resonances assigned to them, being those associated with C-8 and C-9. H1 shows long range coupling to the carbon at 134.6 ppm, indicating the chemical shift of C-9. This

carbon shows long range interactions with the aromatic protons at 6.98 ppm and 7.00 ppm, while also correlating to the singlet appearing slightly upfield of the aromatic region at 6.39 ppm which is attributable to the alkene CH at position 8. The peak at 7.00 ppm couples with a J value of 2 Hz to the signal at 7.31 ppm suggesting a meta relationship between protons, whereas the larger J value of 8.5 Hz between the peaks at 7.31 ppm and 6.98 ppm suggest a ortho relationship, consistent with the assignment of the doublet at 7.00 ppm as H-13, the doublet at 6.98 ppm as H-14 and the double doublet at 7.31 ppm as H-15. Using the HSQC enables identification of their respective carbons resonating at 123.6 ppm, 111.5 ppm and 127.1 ppm.
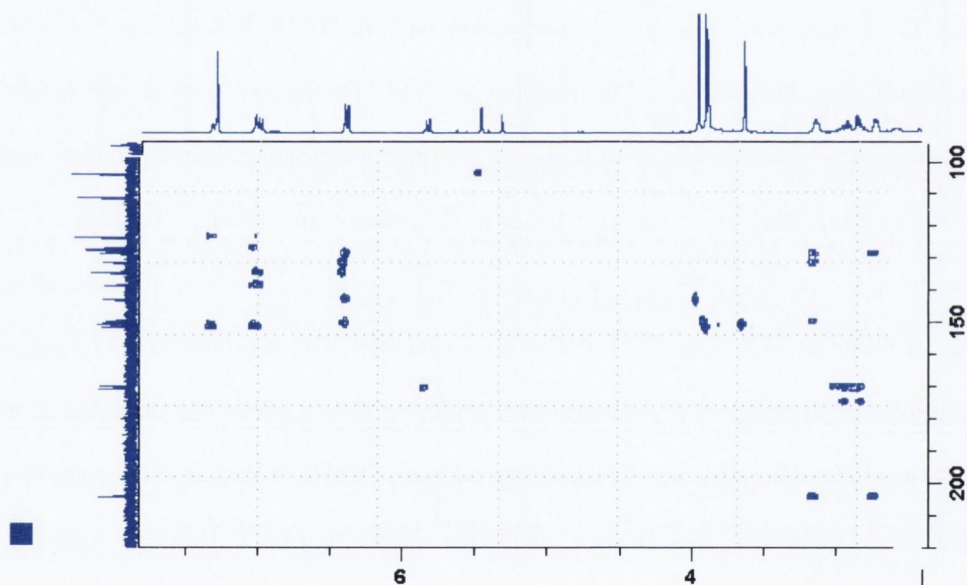
Figure 5.6: Expansion of the HMBC spectrum

There remains only one methoxy group to be assigned, that at position C-18, whose protons can therefore be seen as resonating at 3.88 ppm and carbon at 55.5 ppm. This proton resonance is seen to interact with C-16 at 151.8 ppm. Final inspection of the aromatic region on the HMBC shows coupling of H-13 and H-14 to a carbon at 138.7 ppm and H-13 and H-15 showing interaction with a carbon at 149.6 ppm. Checking the structure of the molecule identifies C-12 as being the peak with the resonance at 138.7 ppm and C-17 as resonating at 149.6 ppm.

Examining the remainder of the molecule, there are two functional groups which instantly stand out, namely the two ester carbonyls which have resonances at 168.9 ppm and 170.4 ppm and the positioning of C-26 between two oxygen atoms which should shift the ^{1}H resonance closer to 6 ppm than the case where only one oxygen atom is seen. Using the HMBC spectrum again, the ester at 170.4 ppm is shown to correlate to a hydrogen resonating as a doublet at 5.81 ppm. This differentiates the carbonyls as only C-25 is capable of this interaction and determines the location of H-26 on the ^{1}H NMR spectrum. Both carbonyls also interact with the multiplet signals between 2.82-2.86 ppm and 2.91-2.95 ppm, both of which integrate to 2H and reasonably correlate to the signal expected for the succinate linker. Reference to the HSQC shows their carbons to resonate at 28.1 ppm and 28.7 ppm respectively with C-26 seen to resonate at 91.8 ppm. Using the H-H COSY, H-26 is seen to couple to a multiplet, integrating to one proton at 2.57 ppm as expected for H-27. This proton in turn couples to the most upfield doublet in the spectrum at 0.83 ppm representing the resonance of the CH$_3$ protons at C-41. Additionally, H-27 couples to the multiplet at 1.6 ppm integrating for one hydrogen, corresponding to H-28. In turn H-28 couples to a multiplet integrating for the two C-29 protons at 1.76 ppm. Using the HSQC spectrum, C-29 resonates at 21.5ppm, with C-27 and C-28 resonating at 31.3 ppm and 44.7 ppm respectively. Using the HMBC spectrum again identifies the quaternary carbon C-33 as the peak resonating at 79.7 ppm. This in turn correlates on HMBC spectrum to ^{1}H resonances at 5.45 ppm and 1.32 ppm. Owing to the different chemical environments in which both atoms are situated it is easy to distinguish between these peaks as the proton at position 34 is adjacent to one oxygen atom, shifting it downfield towards 5.45 ppm. H-32 is then identified as the signal at 1.32 ppm.

H-34 couples through HMBC to the quaternary carbon at 104.0 ppm representing the resonance of C-36 whose identity is confirmed as it couples to the singlet at 1.44 ppm integrating for 3H belonging to C-40, whose Carbon's resonance in turn is observed at 25.5 ppm. The multiplet at 1.25 ppm is shown to couple to C34, identifying it as H-35, showing a resonance in the ^{13}C

NMR spectrum at 29.2 ppm. The final CH₃ group to be accounted for is seen at 0.96 ppm and can be attributed to H-39, with its carbon resonance appearing at 19.8 ppm. This couples to the final CH proton at 1.2 ppm (H-31) by HMBC correlation. H-39 is also seen correlating to the ^{13}C peak at 33.7 ppm. Two peaks associated to this resonance are observed due to their position in different chemical environments resulting from their being locked in position within the ring structure. These are seen at 1.00 ppm and 1.72 ppm. The final signals to be identified were those of the ring CH₂ units found at position 37 and 38. H-37 exhibits long range H-C coupling to C-40 with multiplets at 1.70 ppm and 2.36 ppm each integrating to 1H. The final ^{13}C signal resonates at 24.1 ppm while the protons attached to this carbon are seen to resonate at 1.48 and 1.88 ppm.
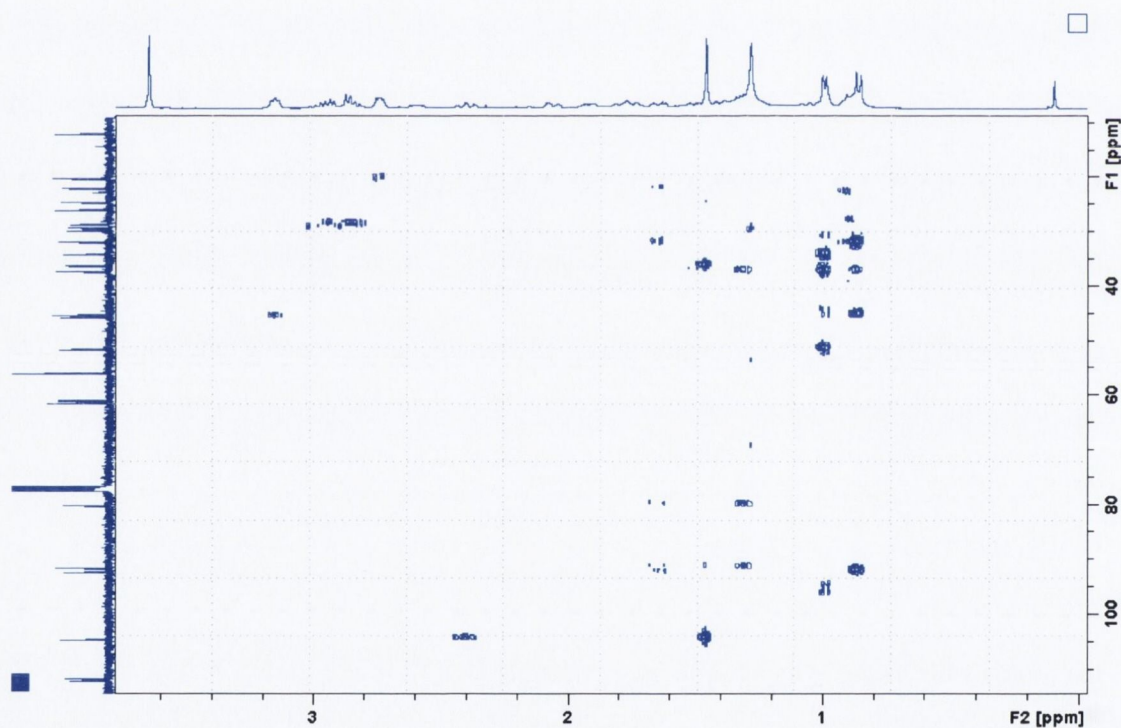
Figure 5.7: Expansion of aliphatic region of HMBC of *(5.09)*
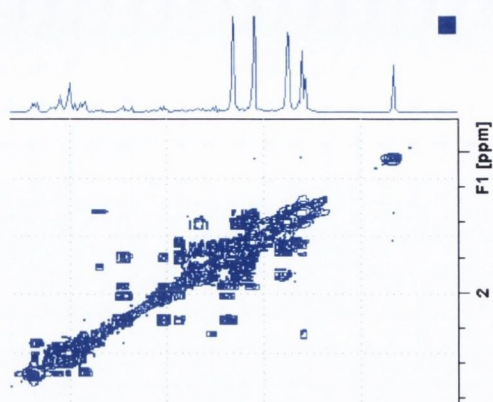
Figure 5.8: Expansion of the H-H COSY of *(5.09)*.
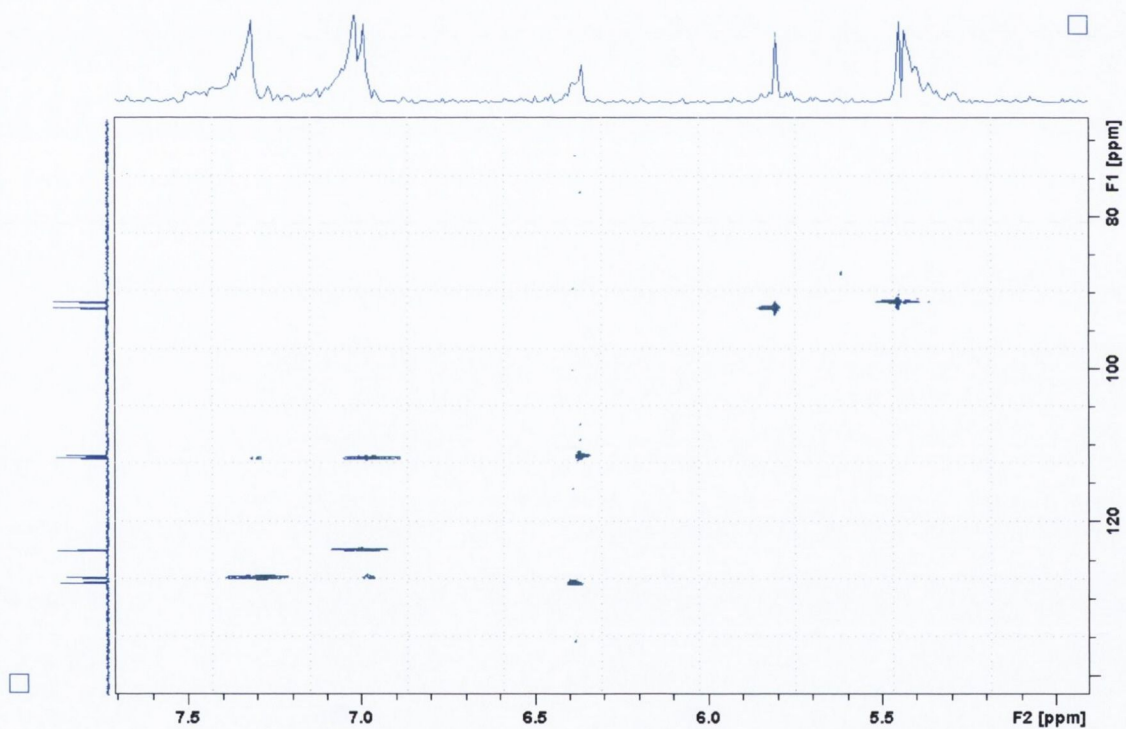
Figure 5.9: Expansion of the Aromatic region in the HSQC of *(5.09)*.
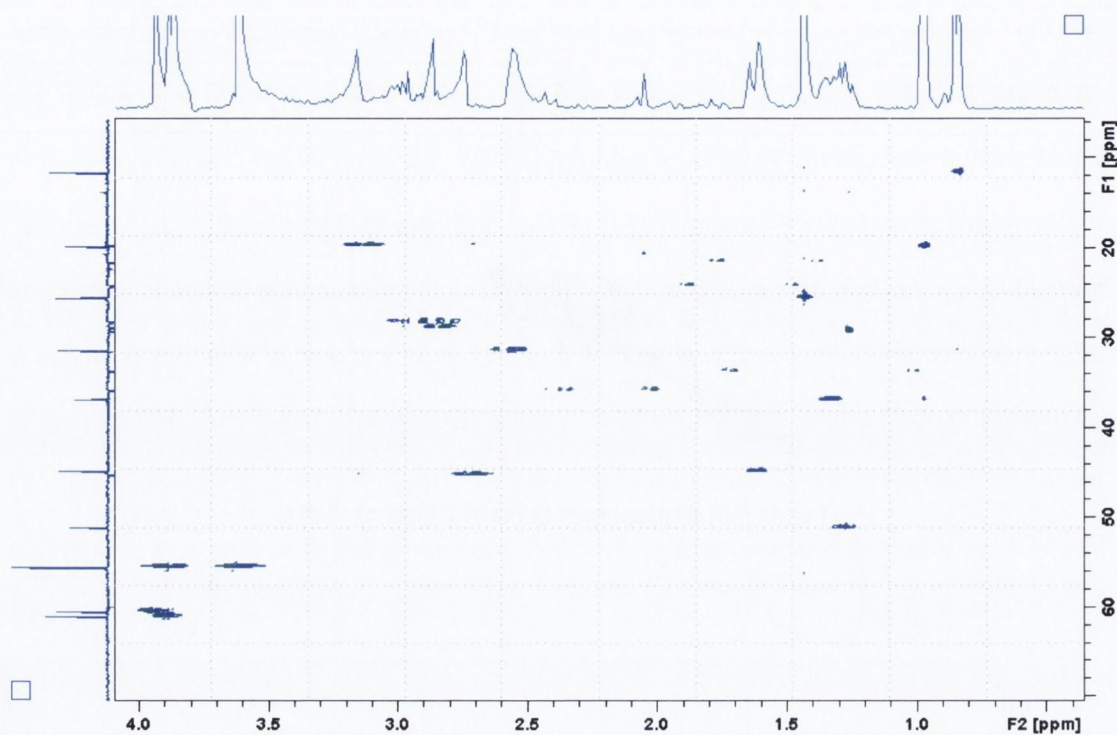
Figure 5.10: Expansion in the aliphatic region for the C-H COSY of *(5.09)*.

5.2.3 **Synthesis of hybrid *(5.11)*.**

We know from previous studies by Breen that the C-7 position of alcoholic form of *(2.01)* (RS176) is particularly amenable to the placement of substituents on it without drastically affecting the overall activity of the tubulin component of the design. Thus, with the synthesis of our second hybrid in this sequence, both components of the hybrid are presented in active form.

One important parameter to consider here in choosing the starting material is the greater nucleophilicity of the phenoxide anion over than that of C-7 secondary alcohol. Therefore, if RS176 was used instead of its silyl protected precursor there would be two potential points at which conjugation could occur and the reaction at the phenol centre would strongly dominate over that at the C-7 position. It is necessary for the protected form of RS176 *(2.07)* to undergo the coupling reaction prior to the deprotection of the C-Ring TBDMS group in order to best furnish the target compound *(5.11)*.

160

As planned, these two reactions proceeded to afford our second artemisinin conjugate. As expected during the synthesis of *(5.10)*, the reactivity of the hydroxyl group was diminished in comparison to that of the C-ring phenol requiring a longer reaction time at higher temperature to proceed as far as 46% completion after stirring for 7 days. As it was noted that there was not much additional conversion of starting material after 48 h, subsequent attempts at this reaction were quenched after this time. The deprotection of *(5.10)* to yield final compound *(5.11)* proceeded swiftly in 92% yield.
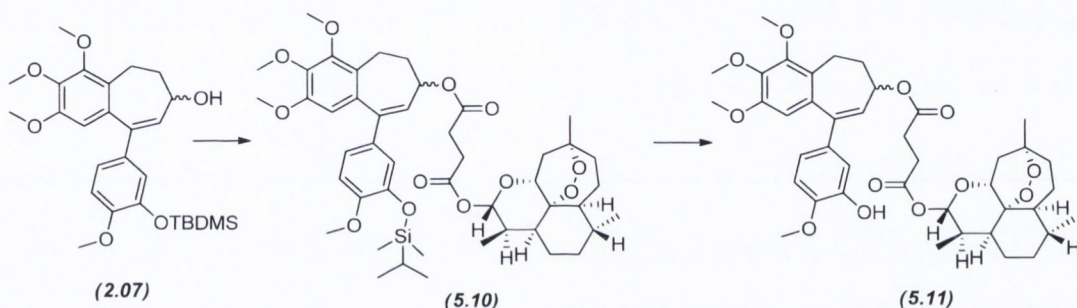
(i) Artesunate, EDCI, DMAP, DCM, N$_2$, rt, 48 h, 46% (ii) 1M TBAF in THF, 0 °C, 92%

Figure 5.11: Synthesis of novel RS176-artemisinin conjugate *(5.11)*.

5.3   Structural elucidation of compound *(5.11)*.

Following the detailed description of the spectra undertaken previously within this chapter for compound *(5.09)*, the majority of the peaks in this compound have already been explained, as the artesunate component retains the majority of the features witnessed previously. There are however a number of key differences associated between the spectra of these two compounds. Firstly, the number of hydrogens in the ^{1}H NMR spectrum has increased to 52 as a result of the degree of saturation increasing at the C-7 position. This manifests itself with the addition of two new peaks resulting from the extra proton at C-7 and the free phenol group in the C-ring. These appear as a double double doublet with J values of 10.4 Hz, 7.7 Hz and 5.0 Hz at 5.13 ppm and

a broad singlet at 5.67 ppm respectively. In the ^{13}C NMR spectrum, the carbonyl peak at 203 ppm is replaced with a CH peak at 72.5 ppm.
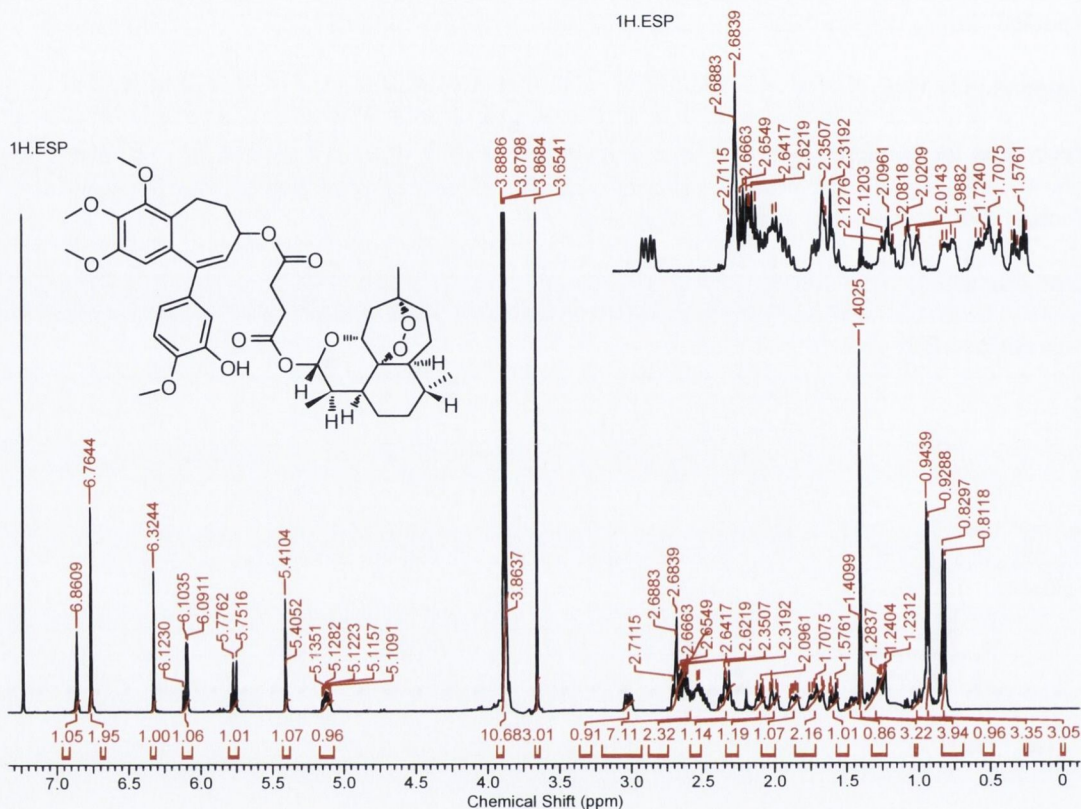
Figure 5.12: ^{1}H NMR spectrum of *(5.11)*.
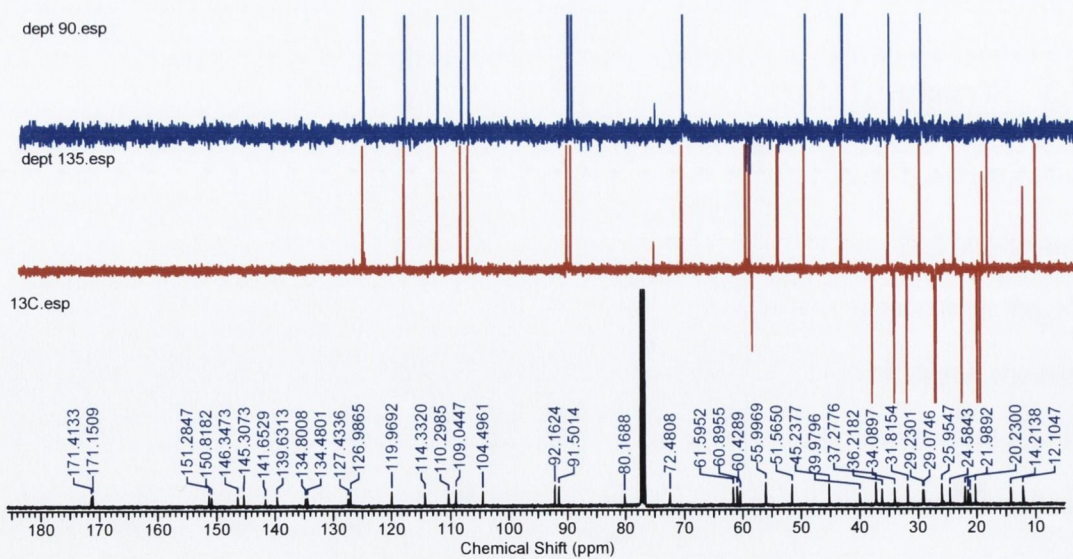
Figure 5.13: ^{13}C NMR spectrum of *(5.11)*.

162

5.4 Synthesis of *(5.14)*.

Upon synthesis of the two conjugates it was attempted to further use this methodology to introduce the artemisinin component of these compounds at both of the hydroxyl positions of RS176 to form an artemisinin dimer using *(5.12)* as a rigid linker to study if the effect of doubling the relative concentration of artemisinin was beneficial to overall anti-cancer activity. Horwedel has reported a synthesis of a dimeric artemisinin compound linked with betulin using 2 molar equivalents of artesunate,[352] and it was thought that adopting a similar approach would furnish compound *(5.13)* from RS176. Prior to the conjugation reaction, the silyl protecting group of *(2.07)* was removed using the standard TBAF methodology in 87% yield. Upon reaction of *(5.12)* with two equivalents of artesunate, the product of the reaction was isolated after 72 h and the mass spectrum of the retrieved major compound suggested the formation of a different compound.

(2.07) *(5.12)* *(5.13)*
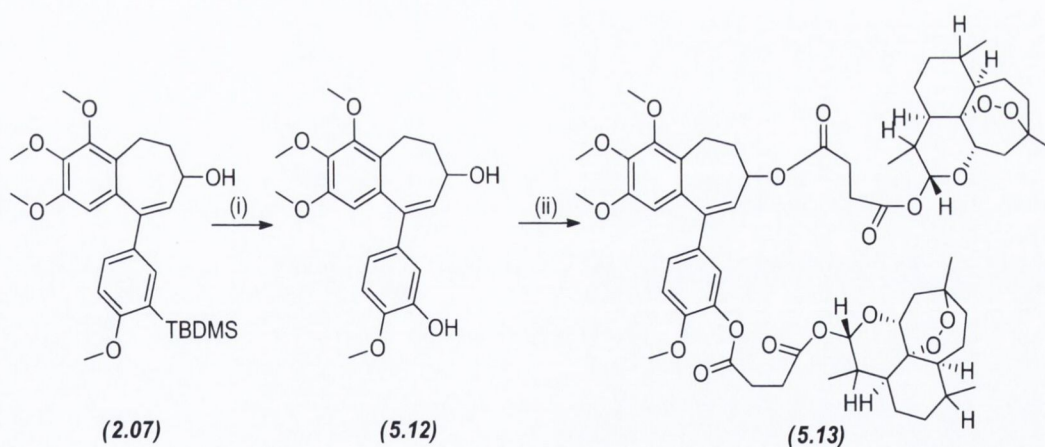
(i) 1M TBAF in THF, THF, 0 °C, 10 min, 87% (ii) 2.5 Eq artesunate, DMAP, DCM, N$_2$, rt, 72 h

Scheme 5.2: Attempted synthesis of *(5.12)* linked artemisinin dimer *(5.13)*.

Whereas compound *(5.13)* would be expected to show a m/z of 1101.5417 under positive ionisation conditions correlating to the (M+H)$^+$ ion, the mass spectrum exhibited a dominant peak with an m/z of 737.3547, similar to the mass observed in both *(5.09)* and *(5.11)*, suggesting the conjugation to just one molecule of artemisinin. Revisiting previous

considerations regarding the increaseded nucleophilicity of phenol compared to that of secondary alcohols, it was immediately considered the alternative isomer of compound *(5.14)* had formed as depicted in Scheme 5.3.
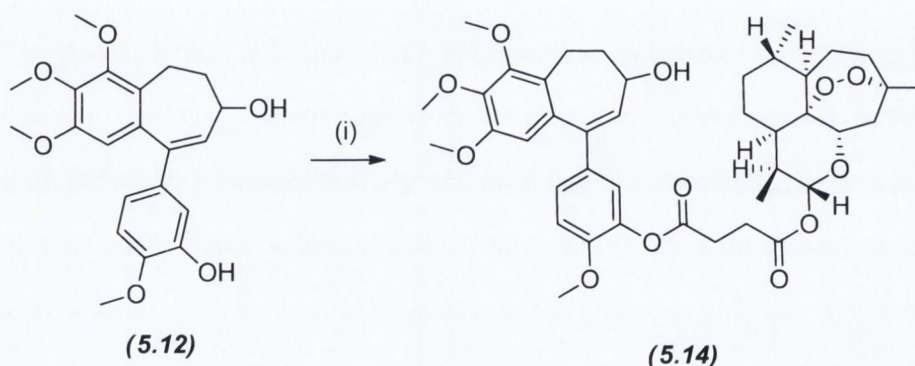
(i) 2.5 Eq artesunate, EDCI, DMAP, DCM, N_2, rt, 72 h

Scheme 5.3: Synthesis of compound *(5.14)*.

It is likely that the increased steric bulk of the compound derived upon addition of artesunate to the phenol position serves to hinder the addition at the C-7 position of the second artesunate equivalent by blocking the hydroxyl group from participating in the reaction. Considering the steric bulk of the electrophile in question, it is fair to assume that the reaction centres do not approach each other to the required proximity for the reaction to progress. Although the synthesis of the initial target compound *(5.14)* was unsuccessful, nevertheless the hybrid that formed was deemed a suitable comparator for future studies with *(5.11)*.

5.4.1   Structural Elucidation of *(5.14)*.

In the ^{1}H NMR spectrum of *(5.14)* the region between 0 to 3 ppm is dominated by the peaks seen from the artemisinin component of the compound, similar as expected to that observed with hybrids *(5.09)* and *(5.11)*. Relative to *(5.11)* the most noticeable difference is the upfield multiplet at 4.15 ppm for H-7, as it no longer falls under the influence of the ester carbonyl of

(5.11). The ^{13}C NMR shows a similar shift slightly upfield of the signal at C-7 to represent a CH peak at 69.8 ppm. As expected there is no signal at ~200.0 ppm for the carbonyl seen in the original hybrid, *(5.09)*. In conclusion, this fact alongside the disappearance of the phenolic hydroxyl group in the ^{1}H NMR spectrum and the similar mass as that obtained for compound *(5.11)*, supports the formation of the hybrid *(5.14)*.
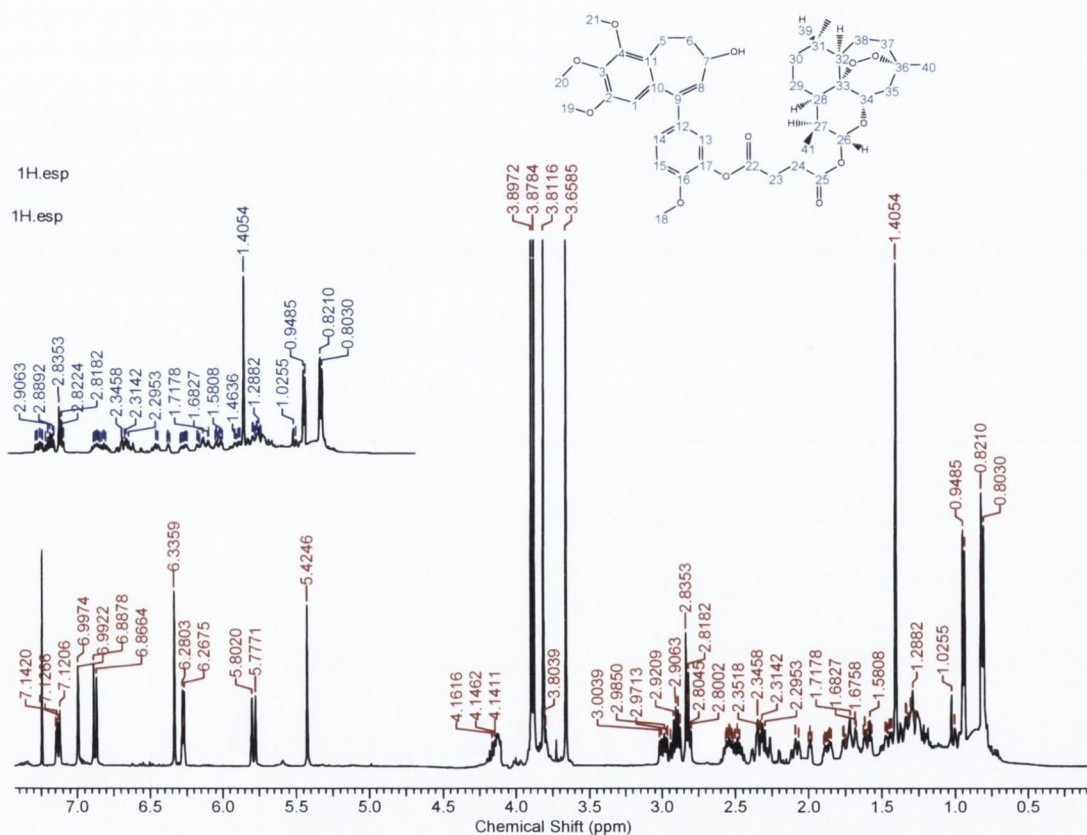
Figure 5.14: ^{1}H NMR spectrum of *(5.14)*.
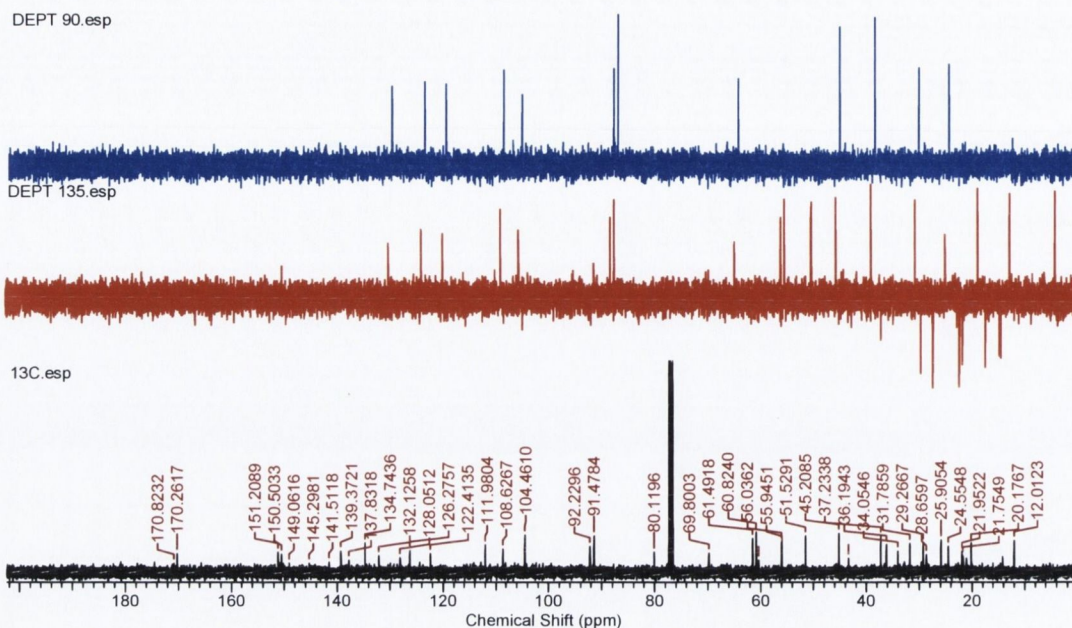
Figure 5.15: ^{13}C NMR spectra of *(5.14)*.

5.5 Biological Evaluation of Compounds *(5.09)*, *(5.11)* and *(5.14)*.

The biological activity of the compounds synthesised within this chapter were evaluated using the MTT cell proliferation[212] assay and the cell migration assay using the same methods as outlined in Chapter 2.

5.5.1 MTT Assay.

The IC$_{50}$ values (nM) for the three compounds are as tabulated in Table 5.1.

Compound	Cell proliferation IC$_{50}$ (nM)	SEM
(5.09)	40.55	±1.13
(5.11)	177.5	±1.11
(5.14)	97.94	±1.16
CA-4	20.44	±1.69

Table 5.1: IC$_{50}$ values calculated for compounds *(5.09)*, *(5.11)* and *(5.14)* for the MTT cell

proliferation assay.

5.5.2 Cell migration assay

The "scratch assay" was employed as described in Chapter 2 to measure the effect of these compounds on cell migration potential using 5 µM, 10 µM and 20 µM of test compounds over 24-48 hours. Following an initial screening run the highest performing compounds namely *(5.09)* and *(5.11)* were evaluated in triplicate. As shown in Table 5.2, both compounds exerted a significant anti-migratory effect on PC-3 cells relative to those treated with a blank control and 80 µM of bestatin. The effect of *(5.11)* on migration is shown to be almost comparable to that of CA-4 across the range of concentrations. However, the effect shown by *(5.09)* is the greatest out of all the compounds presented in this thesis, showing migration distances of 97 nm, 115 nm and 121 nm at 10 µM at concentration at 24 h, 36 h and 48 h respectively relative to CA-4 with measured distances of 108 nm, 133 nm and 159 nm. The results are presented in Table 5.2 and shown in photographic form in Figure 5.13.

Compound	Conc	Cell Migration (nm) 24 h	Cell Migration (nm) 36 h	Cell Migration (nm) 48 h
(5.09)	5 µM	110.61±9.21	124.27±5.52	143.37±6.88
	10 µM	97.36±5.12	114.88±3.55	121.42±9.50
	20 µM	92.12±6.21	112.90±12.39	111.26±3.08
	5 µM	116.51±5.63	162.62±0.73	189.35±10.52
	10 µM	108.33±9.78	160.41±19.31	176.76±15.10
	20 µM	109.34±14.06	137.88±13.26	160.84±17.73
CA-4	5 µM	114.93±7.17	137.90±16.27	167.74±7.96
	10 µM	108.05±8.53	133.05±4.82	159.58±14.74
	20 µM	81.37±3.60	122.12±10.26	150.95±12.64
(2.01)	5 µM	127.92±9.99	181.39±21.32	234.09±38.30
	10 µM	102.67±17.17	155.35±13.75	172.04±16.76
	20 µM	89.99±23.89	140.05±23.69	156.42±10.75
Bestatin	80 µM	142.52±6.29	188.61±7.40	208.70±8.88
0.1% DMSO		176.02±8.51	240.93±7.21	277.30±12.09

Table 5.2: Cell migration distances measured for *(5.09)* and *(5.11)* (±SEM).

| | 0 h | 24 h | 36 h | 48 h |

0.1% DMSO

(5.09)

(5.11)

(2.01)

CA-4

Bestatin 80 μM
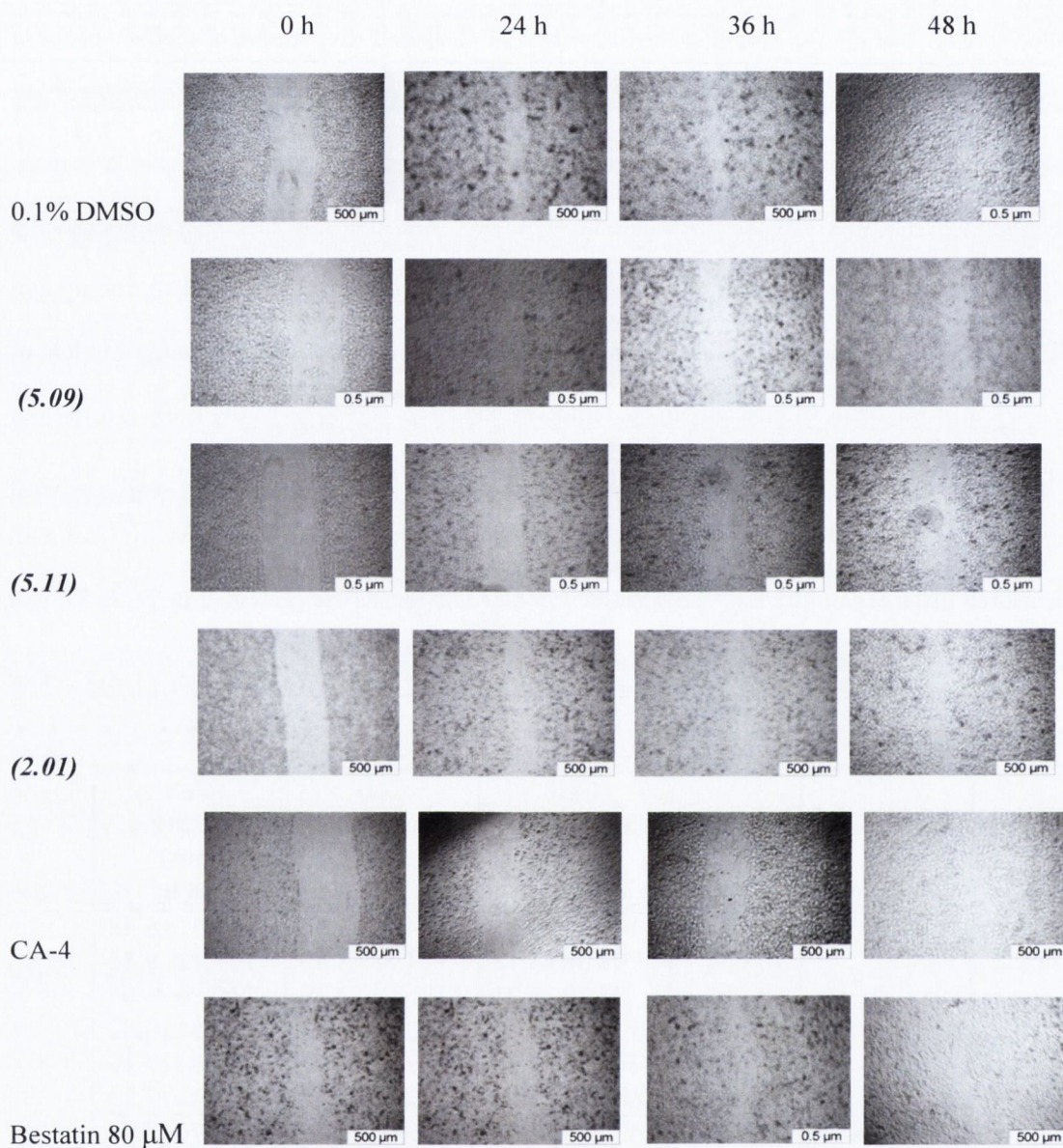
Figure 5. 16: Images acquired upon treatment with 10 M of test compounds at 0 h, 24 h, 36 h and 48 h.

(5.09)
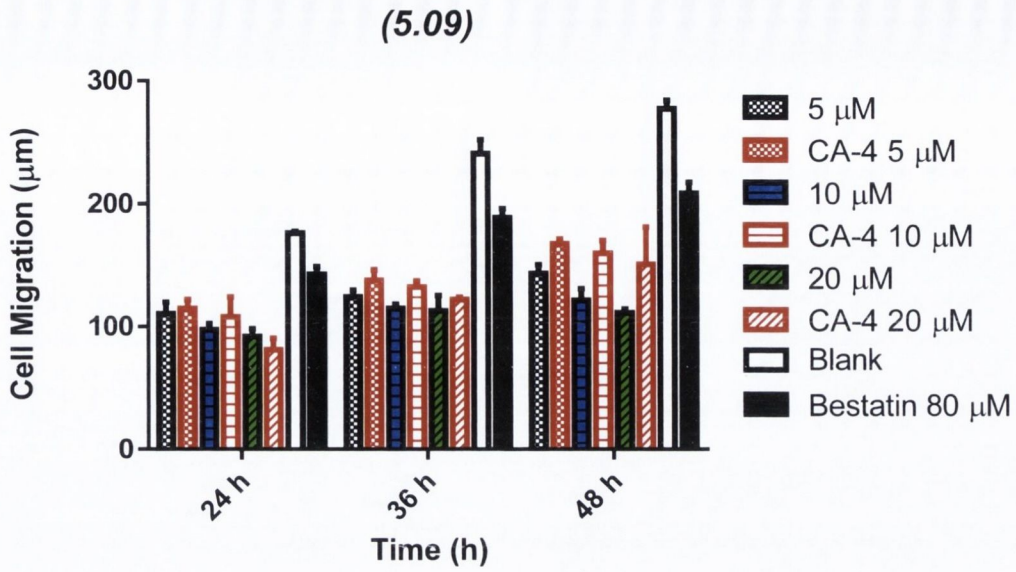
Graph 5.1: Cell migration distance measured for *(5.09)* over 24 h, 36 h and 48 h.

(5.11)
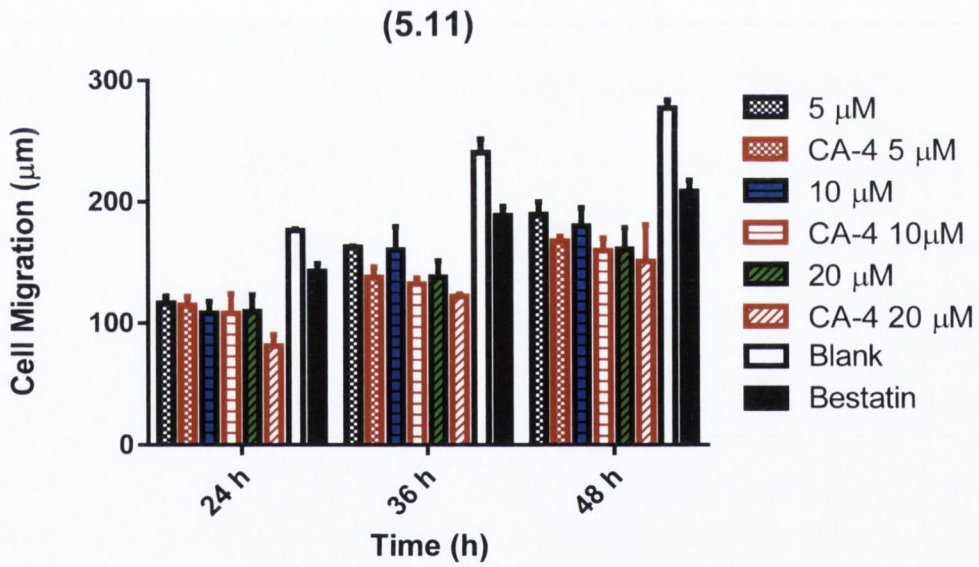
Graph 5.2: Cell migration distance measured for *(5.11)* over 24 h, 36 h and 48 h.

169

5.6 Conclusion

The adaptation of artemisinin into the scaffold of *(2.01)* was successfully achieved via exploitation of the succinate ester linkage of artemisinin as intended at the outset of this work. The three hybrids in this novel family of compounds each showed inhibition of the proliferative activity of PC-3 prostate cancer cells in the MTT assay, with IC_{50} values in the low nanomolar range recorded for each of them.

The highest performing compound in the cell proliferation assay was *(5.09)*, formed between *(2.01)* and artesunate, while the second highest performing compound was *(5.14)*, the hybrid of artesunate and *(5.12)* also at the phenolic position. Their inhibitory potential was approximately 4-fold and 2-fold more pronounced than that obtained by *(5.11)*, the C-7 linked hybrid of *(5.12)* and artesunate. While not being conclusive, this does suggest that the phenolic ester in both *(5.09)* and *(5.14)* are both cleaved more rapidly than the alcoholic ester in *(5.11)* in the medium. Cleavage of this bond frees either *(2.01)* or *(5.12)* in addition to DHA permitting both components of the hybrid to exert their individual anti-proliferative effects. The ester at the C-7 position would likely cleave at a later stage, tethering the more active anti-proliferative agent *(5.12)* for a longer time, diminishing its potential anti-proliferative over the assay timescale.

Notable is the observed IC_{50} of 40.55 nM for *(5.09)*, showing significantly less than that of free *(2.01)*, exhibiting an IC_{50} of 8.72 nM.[214] This suggests the artemisinin component and *(2.01)* do not function synergistically to exert an enhanced anti-proliferative effect. However these compounds are among the highest active synthesised in this thesis' work showing their potential as lead compounds of their own.

As stated in the introduction to this chapter, artemisinin has been shown to exert an anti-migratory effect by downregulation and deactivation of proteins and integrins implicated in this process.[348] The cell migration assay proved the anti-migratory effect of artemisinin remained

intact, particularly in *(5.09)* which showed a greater effect than CA-4 over all the concentrations the all observed time points suggesting an additive effect on activity by the artemisinin and RS180 components.

Ultimately, the work detailed in this chapter could find its most important function in the targeted delivery of anti-tumour drugs to the tumour. The low toxicity of artemisinin in addition to its reported specificity towards cancer cells containing heightened levels of iron[344] suggests that this family of compounds potentially be used in this way. The cleavage of both the artemisinin peroxide bridge and ester linkage in tandem within the tumour mass could be of huge potential benefit. A wider series of similar compounds could be synthesised in many ways to this end. For example, the amide *(5.15)* contains the more stable peptide bond and can be synthesised using an analogous route from the anilino derivatives of *(2.01)* exhibiting different pharmacokinetics to that of the compounds synthesised already synthesised.
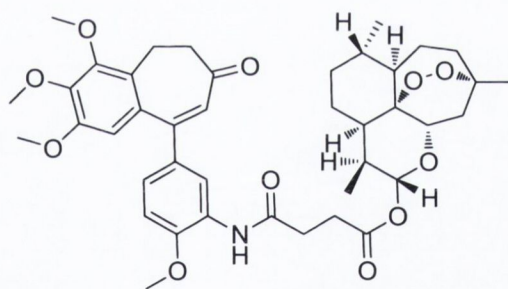
(5.15)

Figure 5.17: Potential novel amide derivative of *(5.09)*.

No studies have been performed on the hydrolysis of these compounds as of yet, however it would be interested to note the rate of ester bond cleavage. Modification at the C-12 alcoholic position of DHA could introduce a variety of linker units between the two components opening up an interesting area for future work in the development of targeted anti-tumour agents.

Chapter 6: Chemistry Experimental

Melting points were determined using an Electrothermal® melting point apparatus and were uncorrected.

Starting materials were obtained from Sigma-Aldrich Ireland and were not characterised prior to use.

Infra-red (IR) spectroscopy was performed using a Perkin Elmer FT-IR spectrophotometer Paragon 1000.

Nuclear Magnetic Resonance (NMR) spectroscopy were performed using Bruker Avance 400 NMR, Bruker Avance III 400 NMR and Bruker Avance II 600 NMR machines. All compounds were dissolved in $CDCl_3$ prior to analysis unless otherwise stated. ^1H NMR were irradiated at 400 MHz and at 100.71 MHz for ^{13}C NMR unless otherwise stated. NMR spectra were analysed using Bruker Topspin and ACD/NMR Processor Academic Edition Version 12.01. Peak positions were assigned relative to $CHCl_3$ resonances at 7.28 ppm for ^1H NMR and 75.20 ppm, 76.90 ppm and 78.16 ppm for ^{13}C NMR. Abbreviations used: s = singlet, d = doublet, t = triplet, q = quartet, dd = double doublet, dt = double triplet, m = multiplet, br = broad, Q = quaternary carbon.

High Resolution Mass Spectrometry (HRMS) was performed using the Fischer Thermoscientific LTQ-Orbitrap Discovery. Analysis of samples was performed using its associated Xcalibur software.

Column Chromatography was carried out using silica gel 60 (230-400 mesh) and thin layer chromatography with silica gell GF-254 precoated aluminium sheets (Merck Laboratories).

Compounds were visualised using UV at 254 nm and an array of spray reagents including vanillin/H$_2$SO$_4$, ninhydrin and KMnO$_4$ solutions.

Anhydrous DCM was prepared by distilling over CaH$_2$ for 24 h. Upon collection for reaction, the first 5% was rejected.

Anhydrous THF was prepared by refluxing over LiAlH$_4$ for 24 h, before collecting the distillate in a flask containing sodium metal and benzophenone indicator. The resulting mixture was refluxed until acquiring an intense purple colour. The first 5% of the obtained distillate was rejected before use.

Anhydrous DMF was purchased from Sigma-Aldrich Ireland.

6.1   Chapter 2 Synthesis

6.1.1   Synthesis of (Z)-3-(2,3,4-trimethoxyphenyl)acrylic acid *(2.16)*.

To a stirred solution of 2, 3, 4 trimethoxybenzaldehyde *(2.15)* (26.23 g, 133.70 mmol) in pyridine (90 mL) and piperidine (2 mL) was added malonic acid (27.82 g, 267.30 mmol). The mixture was heated under reflux for 5 h and then at room temperature overnight. The mixture was acidified using 2 M HCl (200 mL) and washed with DCM (300 mL). The DCM layer was further washed with aq. HCl (2×150 mL, 1×100 mL). The DCM extract was dried over MgSO$_4$ and concentrated *in vacuo* to give the product as a colourless solid.

Yield: 30.25 g, 127.00 mmol, 95%.

^{1}H NMR (CDCl$_3$, 400MHz) δ$_H$ ppm: 3.90 (s, 3H, C$\underline{H}_3$), 3.93 (s, 3H, C$\underline{H}_3$), 3.96 (s, 3H, C$\underline{H}_3$), 6.46 (dd, J1 = 16 Hz, J2 = 2.36 Hz, 1H, Alkene C$\underline{H}$), 6.73 (d, J = 8.72 Hz, Ar$\underline{H}$), 7.32 (d, J = 8.72 Hz, 1H, Ar$\underline{H}$), 8.02 (d, J = 16 Hz, 1H, Alkene C$\underline{H}$).

¹³C NMR (CDCl₃, 100.71 MHz) δc ppm: 55.6 (CH₃), 60.5 (CH₃), 61.0 (CH₃), 107.1 (CH), 115.6 (CH), 120.7 (Q), 123.1 (CH), 141.6 (CH), 141.9 (Q), 153.1 (Q), 155.5 (Q), 172.4 (Q, COOH).

HRMS (+ESI): Calculated 238.0841. Found 237.0772 (M-H)⁻.

Vmax (DCM)/cm⁻¹: 3387, 2978, 2942, 2832, 2571, 1678, 1589, 1497, 1425, 1285, 1271, 1170, 1010, 922, 795, 676, 566, 492.

Melting point: 160-162 °C.

6.1.2 **Synthesis of 3-(2,3,4-trimethoxyphenyl)propanoic acid *(2.17)*.**

(2.16) (15.00 g, 63.50 mmol) was dissolved in a 1:1 mixture of EtOH (150 mL) and EtOAc (150 mL). A catalytic amount of palladium (10% on carbon) was added to the flask. A septum was fitted and the flask was equipped with a H₂ filled balloon. The mixture was stirred for 48 h with sporadic replacement of the H₂ balloon. At this time, the solvents were removed *in vacuo*, yielding the product as a colourless solid.

Yield: 15.30 g, 63.50 mmol, 100%.

¹H NMR (CDCl₃, 400MHz) δH ppm: 2.63 (t, J = 7.44 Hz, 2H, CH₂), 2.91 (t, J= 7.54 Hz, 2H, CH₂), 3.86 (s, 3H, CH₃), 3.89 (s, 3H, CH₃), 3.92 (s, 3H, CH₃), 6.62 (d, J = 8.48 Hz, ArH, 1H), 8.87 (d, J= 8.48 Hz, ArH, 1H).

¹³C NMR (CDCl₃, 100.71 MHz) δc ppm: 24.7 (CH₂), 34.4 (CH₂), 55.5 (CH₃), 60.3 (CH₃), 60.4 (CH₃), 106.6 (CH), 123.3 (CH), 125.6 (Q), 141.7 (Q), 151.4 (Q), 152.0 (Q).

HRMS (+ESI): Calculated 240.0998. Found 239.0915 (M-H)⁻.

Vmax (DCM)/cm⁻¹: 3486 (OH stretch), 2940, 2836, 2648, 1709 (C=O stretch), 1603, 1467, 1418, 1275, 1051, 1015, 801.

Melting point: 65-67 °C.

6.1.3 Synthesis of 5-(3-(2,3,4-trimethoxyphenyl)propanoyl)-2,2-dimethyl-1,3-dioxane-4,6-dione (2.19).

(2.17) (15.30 g, 64.22 mmol) was dissolved in DCM (40 mL) under anhydrous conditions and DMF (3 drops) was added to this stirred solution which was placed under N_2 at 0 °C. A solution of oxalyl chloride (2 M in DCM, 48.0 mL, 96.0 mmol) was added dropwise to the flask and reacted at this temperature for 2 h, at which time the solvents were removed under high vacuum for 3 h. A solution of DMAP (15.69 g, 128.44 mmol) and Meldrum's acid (9.26 g, 64.22 mmol) in DCM (70 mL) was then added to the formed acyl halide *(2.18)* by syringe. The resulting brown mixture was stirred for 1 h at 0 °C before consumption of the *(2.18)* had been completed. DCM (200 mL) was added to the mixture which was washed with 2 M aq. HCl. (3×250 mL). The organic extracts were dried over $MgSO_4$ yielding *(2.19)* as a black solid. No further attempts were made to purify this compound which was used directly in the next step.

^{1}H NMR (CDCl$_3$, 400MHz) δ_H ppm: 1.74 (s, 6H, 2×C$\underline{H}_3$), 2.98 (t, J= 7.32 Hz, 2H, C$\underline{H}_2$), 3.32-3.41 (m, 2H, C$\underline{H}_2$), 3.87 (s, 3H, C$\underline{H}_3$), 3.89 (s, 3H, C$\underline{H}_3$), 3.93 (s, 3H, C$\underline{H}_3$), 6.61 (d, J= 8.52 Hz, 1H, Ar$\underline{H}$), 6.89 (d, J = 8.52 Hz, 1H, Ar$\underline{H}$).

^{13}C NMR (CDCl$_3$, 100.71 MHz) δ_c ppm: 25.8 ($\underline{C}H_2$), 26.3 ($\underline{C}H_3$), 36.2 ($\underline{C}H_2$), 55.5 ($\underline{C}H_3$), 60.3 ($\underline{C}H_3$), 60.5 ($\underline{C}H_3$), 91.2 (Q), 104.4 (Q), 106.6 ($\underline{C}H$), 123.5 ($\underline{C}H$), 125.1 (Q), 141.7 (Q), 151.5 (Q), 152.1 (Q), 159.7 (Q), 160.6 (Q), 170.0 (2×$\underline{C}$=O ester), 196.6 ($\underline{C}$=O ketone).

HRMS (+ESI): Calculated 366.1315. Found 365.1247 (M-H)$^-$.

V$_{max}$ (DCM)/cm^{-1}: 2938, 2853, 1714, 1646, 1602, 1495, 1467, 1277, 1089, 1017, 798.

6.1.4 Synthesis of methyl 5-(2,3,4-trimethoxyphenyl)-3-oxopentanoate (2.20).

(2.19) (19.78 g, 53.99 mmol) was dissolved in toluene (400 mL) and MeOH (100 mL) and the mixture was heated under reflux for 3 h. The solvent was removed in vacuo yielding a black oil which was purified using FCC with hexane / EtOAc (5:1) as the mobile phase. The product was afforded as an oil with a slight yellow colour.

Yield: 15.53 g, (52. 4 mmol, 82.5% from *(2.17)*).

^{1}H NMR (CDCl$_3$, 400MHz) δ_H ppm: 2.84 (s, 4H, 2×CH$_2$), 3.47 (s, 2H, CH$_2$), 3.74 (s, 3H, CH$_3$), 3.85 (s, 3H, CH$_3$), 3.88 (s, 3H, CH$_3$), 3.89 (s, 3H, CH$_3$), 6.60 (d, J = 8.44 Hz, 1H, ArH), 6.84 (d, J = 8.44 Hz, 1H, ArH).

^{13}C NMR (CDCl$_3$, 100.71 MHz) δ_c ppm: 23.7 (CH$_2$), 43.4 (CH$_2$), 48.6 (CH$_2$), 51.9 (CH$_3$), 55.5 (CH$_3$), 60.3 (CH$_3$), 60.4 (CH$_3$), 106.65 (CH), 123.5 (CH), 125.8 (Q), 141.8 (Q), 151.4 (Q), 152.0 (Q), 167.2 (COOMe), 201.8 (C=O).

HRMS (+ESI): Calculated 296.1260. Found 319.1168 (M+Na)$^+$.

V$_{max}$ (DCM)/cm^{-1}: 2940, 2836, 1747, 1717, 1602, 1498, 1497, 1314, 1233, 1050, 1017, 901, 800.

6.1.5 **Synthesis of methyl 3-hydroxy-5-(2,3,4-trimethoxyphenyl)pentanoate *(2.21)*.**

To a stirred solution of *(2.20)* (15.03 g, 50.72 mmol) in MeOH (200 mL) at -10°C was added NaBH$_4$ (0.64 g, 16.91 mmol) over a period of 5 min. The mixture was stirred on ice for 90 min, and at room temperature for a further 90 min at which time H$_2$O (250 mL) was used to quench the reaction. The MeOH was then removed *in vacuo* and the aqueous layer was washed with Et$_2$O (3×100 mL). The combined organic extracts were dried over MgSO$_4$ and concentrated to yield the product as a colourless oil.

Yield: 12.56 g, 42.1 mmol, 83%.

^{1}H NMR (CDCl$_3$, 400MHz) δ_H ppm: 1.64 – 1.84 (m, 2H, CH$_2$), 2.47 – 2.53 (m, 2H, CH$_2$), 2.67 – 2.74 (m, 2H, CH$_2$), 3.2 (br s, 1H, OH), 3.71 (s, 3H, CH$_3$), 3.85 (s, 3H, CH$_3$), 3.87 (s, 3H, CH$_3$), 3.89 (s, 3H, CH$_3$), 3.96 – 4.03 (m, H, CHOH), 6.63 (d, J = 8.52 Hz, 1H, ArH), 6.85 (d, J = 8.52 Hz, 1H, ArH).

^{13}C NMR (CDCl$_3$, 100.71 MHz) δ_c ppm: 25.1 (CH$_2$), 37.2 (CH$_2$), 40.7 (CH$_2$), 51.3 (CH$_3$), 55.5 (CH$_3$), 60.3 (CH$_3$), 60.6 (CH$_3$), 66.7 (CHOH), 106.9 (CH), 123.5 (CH), 126.9 (Q), 141.7 (Q), 151.3 (Q), 151.6 (Q), 172.8 (Q, COOMe).

HRMS (+ESI): Calculated 298.1416. Found 321.1327 (M+Na)$^+$.

V_{max} **(DCM)/cm^{-1}:** 3488 (OH stretch), 2939, 2836, 1735 (C=O stretch), 1602, 1495, 1432, 1278, 1232, 1199, 1164, 1036, 901, 801, 683.

6.1.6 Synthesis of methyl 3-((tert-butyldiphenylsilyl)oxy)-5-(2,3,4-trimethoxyphenyl) pentanoate *(2.22)*.

(2.21) (12.00 g, 40.22 mmol) and imidazole (6.85 g, 100.55 mmol) were stirred in dry DMF (80 mL) under an atmosphere of N$_2$. To this solution was added slowly *tert*-butylchlorodiphenylsilane (13.27 g, 12.55 mL, 48.26 mmol) and the mixture was stirred overnight at room temperature. The product was isolated in crude form following partition between H$_2$O (100 mL) and Et$_2$O (1×100 mL, 2×50 mL). The combined organic extracts were dried over MgSO$_4$ and concentrated to give a colourless oil. Following purification by column chromatography using hexane/EtOAc (50:1) as a mobile phase, the product was isolated as a colourless viscous oil.

Yield: 16.03 g, 29.86 mmol, 75%.

^{1}H NMR (CDCl$_3$, 400MHz) δ$_H$ ppm: 1.10 (s, 9H, ^{t}Bu), 1.75-1.84 (m, 2H, C$\underline{H}_3$), 2.44-2.63 (m, 4H, 2×C$\underline{H}_2$), 3.58 (s,3H, C$\underline{H}_3$), 3.80 (s, 3H, C$\underline{H}_3$), 3.86 (s, 3H, C$\underline{H}_3$), 3.87 (s, 3H, C$\underline{H}_3$), 4.229 - 4.34 (m, 1H, C$\underline{H}$OH), 6.56 (d, J=8.52 Hz, 1H, Ar$\underline{H}$), 6.63 (d, J=8.56 Hz, 1H, Ar$\underline{H}$), 7.38-7.49 (m, 6H, Ar$\underline{H}$), 7.69-7.79 (m, 4H, Ar$\underline{H}$).

^{13}C NMR (CDCl$_3$, 100.71 MHz) δ$_c$ ppm: 19.4 (Q), 25.1 (C$\underline{H}_2$), 27.0 (C$\underline{H}_3$), 38.3 (C$\underline{H}_2$), 41.8 (C$\underline{H}_2$), 51.4 (C$\underline{H}_3$), 56.0 (C$\underline{H}_3$), 60.7 (C$\underline{H}_3$), 60.8 (C$\underline{H}_3$), 70.4 (C$\underline{H}$), 107.2 (C$\underline{H}$), 123.5 (C$\underline{H}$), 127.5 (C$\underline{H}$), 127.6 (C$\underline{H}$), 129.6 (C$\underline{H}$), 129.6 (C$\underline{H}$), 134.0 (Q), 135.9 (C$\underline{H}$) 136.0 (C$\underline{H}$), 142.2 (Q), 151.8 (Q), 151.9 (Q), 171.9 (Q).

HRMS (+ESI): Calculated 536.2594. Found 559.2534 (M+Na)$^+$.

V_{max} (DCM)/cm^{-1}: 3071, 2933, 2857, 1739, 1602, 1494, 1466, 1273, 1199, 1150, 1042, 1018, 822, 741, 703, 508.

6.1.7 **Synthesis of 3-((tert-butyldiphenylsilyl)oxy)-5-(2,3,4-trimethoxyphenyl)pentanoic acid** *(2.23).*

(2.22) (16.00 g, 29.80 mmol) was dissolved in MeOH (150 mL) and THF (115 mL) and stirred on an ice bath at 0 °C. To this solution was added carefully over 10 min, a 2.5 M aq. NaOH solution (60 mL). After 1 h the solution was removed from the ice bath and the reaction was allowed to proceed for a further 13 h before the starting material had been consumed. 2 M aq. HCl (70 mL) was used to quench reaction and the organic solvents were subsequently removed *in vacuo*. The product was extracted by washing the aqueous layer with Et$_2$O (2×100 mL, 2×50 mL). The combined organic extracts were dried over MgSO$_4$ to yield the product in crude form as a colourless solid. The product was purified by column chromatography to yield a colourless solid.

Yield: 13.45 g, 25.73 mmol, 86.3%.

^{1}H NMR (CDCl$_3$, 400MHz) δ_H ppm: 1.07 (s, 9H, ^{t}Bu), 1.73-1.82 (m, 2H, C$\underline{H}_3$), 2.39-2.55 (m, 2H, C$\underline{H}_2$), 2.58 (d, J = 6.04 Hz, 2H, C$\underline{H}_2$), 3.75 (s, 3H, C$\underline{H}_3$), 3.82 (s, 3H, 2×C$\underline{H}_3$), , 4.23 (t, J=5.68 Hz, 1H, C$\underline{H}$OSi), 6.52 (d, J=8.48 Hz, 1H, Ar$\underline{H}$), 6.60 (d, J=8.48 Hz, 1H, Ar$\underline{H}$), 7.36-7.43 (m, 6H, Ar$\underline{H}$), 7.67-7.72 (m, 4H, Ar$\underline{H}$).

^{13}C NMR (CDCl$_3$, 100.71 MHz) δ_c ppm: 18.9 (Q), 24.6 ($\underline{C}$H$_2$), 26.5 ($\underline{C}$H$_3$), 37.5 ($\underline{C}$H$_2$), 55.5 ($\underline{C}$H$_3$), 60.2 ($\underline{C}$H$_3$), 60.4 ($\underline{C}$H$_3$), 69.8 ($\underline{C}$H), 106.7 ($\underline{C}$H), 123.1 ($\underline{C}$H), 127.1 ($\underline{C}$H), 129.3 ($\underline{C}$H), 133.3 (Q), 134.3 ($\underline{C}$H), 135.5 ($\underline{C}$H), 141.7 (Q), 151.2 (Q), 151.4 (Q).

HRMS (+ESI): Calculated 522.2438. Found 545.2393 (M+Na)$^+$.

HRMS(-ESI): 521.2383 (M-H)$^-$.

V$_{max}$ (DCM)/cm^{-1}: 3070, 3048, 2997, 2933, 2857, 1709 (C=O stretch), 1660, 1601, 1590, 1495, 1466, 127, 1041, 941, 822, 703, 611, 506.

Melting point: 110-112 °C.

6.1.8 Synthesis of 7-((tert-butyldiphenylsilyl)oxy)-1,2,3-trimethoxy-6,7,8,9-tetrahydro-5H-benzo[7]annulen-5-one (2.25).

A solution of *(2.23)* (10.38 g, 19.96 mmol) in dry DCM (50 mL) was stirred in an atmosphere of N_2 at 0 °C. To this was added DMF (1 mL). After 5 min, a 2 M solution of oxalyl chloride in DCM (49.64 mL, 99.29 mmol) was added slowly over 10 min. The mixture was stirred on ice for a further 30 min, before removal of the ice bath and subsequent stirring for 90 min at room temperature. The solvents were then removed under high vacuum and allowed to dry under these conditions for 3 h. Following this period, the acid chloride *(2.24)* was reconstituted in DCM (65 mL) under an atmosphere of N_2 and stirred in an ice/NaCl bath at -15 °C. A 1 M solution of SnCl₄ (19.56 mL, 19.56 mmol) was added and the mixture was stirred for 1 h. The reaction was quenched by addition of brine (50 mL) and the product was extracted by washing the aqueous layer with Et₂O (3×50 mL). The combined organic extracts were then washed with H_2O (100 mL) and dried with MgSO₄ before being concentrated to a colourless oil *in vacuo*. The product was afforded in pure form following column chromatography (hexane/EtOAc 6:1) as a colourless solid.

Yield: 5.66 g, 10.82 mmol, 55.3%.

¹H NMR (CDCl₃, 400MHz) δ_H ppm: 1.05 (s, 9H, ᵗBu), 1.80 - 2.05 (m, 2H, C$\underline{H}_2$), 2.88 - 2.98 (m, 2H, C$\underline{H}_2$), 3.85 (s, 3H, C$\underline{H}_3$), 3.89 (s, 6H, C$\underline{H}_3$), 3.95 (s, 6H, C$\underline{H}_3$), 4.28-4.36 (m, 1H, C$\underline{H}$OSi), 7.16 (s, 1H, Ar$\underline{H}$), 7.37-7.49 (m, 6H, Ar$\underline{H}$), 7.62-7.71 (m, 4H, Ar$\underline{H}$).

¹³C NMR (CDCl₃, 100.71 MHz) δ_c ppm: 18.9 (Q), 20.5 ($\underline{C}H_2$), 26.4 (Q), 35.9 ($\underline{C}H_2$), 49.8 ($\underline{C}H_2$), 55.5 ($\underline{C}H_3$), 60.4 ($\underline{C}H_3$), 60.7 ($\underline{C}H_3$), 67.8 ($\underline{C}H$), 107.0 ($\underline{C}H$), 127.2 (CH), 127.2 ($\underline{C}H$), 129.3 ($\underline{C}H$), 129.3 ($\underline{C}H$), 130.4 (Q), 133.3 (Q), 133.5 (Q), 134.2 (Q), 135.3 ($\underline{C}H$), 135.4 ($\underline{C}H$), 145.0 (Q), 150.6 (Q), 150.9 (Q), 199.3 ($\underline{C}$=O).

HRMS (+ESI): Calculated 504.2332. Found 527.2264 (M+Na)⁺.

V$_{max}$ (DCM)/cm⁻¹: 2933, 2856, 1671, 1590, 1486, 1407, 1324, 1193, 1110, 1074, 1028, 821, 740, 703, 611, 506.

Melting point: 69-73 °C.

6.1.9 Synthesis of 6,7,8,9-tetrahydro-7-hydroxy-1,2,3-trimethoxybenzo[7]annulen-5-one *(2.12)*.

To a stirred solution of *(2.25)* (1.12 g, 2.22 mmol) in THF (7 mL) at 0 °C under an atmosphere of N_2, was added a 1 M solution of TBAF in THF (2.22 mL, 2.22 mmol). The mixture was allowed to reach room temperature after 1 h and subsequently stirred at this temperature for a further 6 h until TLC had shown that the starting material had been consumed. The solvent was removed by the bubbling of N_2 through it. The product was then obtained in a pure form as a yellow oil using column chromatography (hexane/EtOAc 2:1).

Yield: 0.45 g, 1.69 mmol, 76%.

^{1}H NMR (CDCl$_3$, 400MHz) δ_H ppm: 2.14-2.23 (m, 2H, C$\underline{H}_2$), 2.94-3.13 (m, 2H, C$\underline{H}_2$), 3.85 (s, 3H, C$\underline{H}_3$), 3.89 (s, 3H, C$\underline{H}_3$), 3.94 (s, 3H, C$\underline{H}_3$), 4.36 (m, 1H, C$\underline{H}$OH), 7.17 (s, 1H, Ar$\underline{H}$).

^{13}C NMR (CDCl$_3$, 100.71 MHz) δ_c ppm: 20.6 ($\underline{C}H_2$), 35.4 ($\underline{C}H_2$), 49.9 ($\underline{C}H_2$), 55.5 ($\underline{C}H_3$), 60.5 ($\underline{C}H_3$), 60.7 ($\underline{C}H_3$), 66.7 ($\underline{C}H$), 107.0 ($\underline{C}H$), 130.5 (Q), 133.6 (Q), 145.3 (Q), 150.7 (Q), 151.1 (Q), 199.3 ($\underline{C}$=O).

HRMS (+ESI): Calculated 504.2332. Found 527.2281 $(M+Na)^+$.

V_{max} (DCM)/cm^{-1}: 3401 (-OH stretch), 2933, 2854, 1726 (C=O stretch), 1580, 1596, 1490, 1453, 1314, 1165, 1107, 1041, 998, 736.

6.1.10 Synthesis of 5-bromo-2-methoxyphenol (2.28)

5-Bromo-2-methoxybenzaldehyde *(2.26)* (5.00 g, 23.2 mmol) was dissolved in DCM (250 mL) at 0 °C. To this solution was added drop-wise a solution of MCPBA (6.2 g, 28 mmol) in DCM (100 mL) over 10 min. The ice bath was removed after 1 h and the mixture was allowed to stir for a further 24 h. The by-product 3-chlorobenzoic acid was removed by filtration, washing the filter paper with DCM. The DCM solution was washed with saturated aq. NaHCO$_3$ (5×100 mL), H$_2$O (3×100 mL) and brine (2×100 mL). This was dried over MgSO$_4$ and concentrated *in vacuo* to yield 5-bromo-2-methoxyphenyl formate as a yellow oil. This oil was placed in solution with

MeOH (45 mL) and THF (35 mL). After stirring for 10 min at 0 °C, 2 M aq. NaOH (13 mL) was added dropwise and the mixture was stirred for 30 min. The ice bath was removed and the reaction proceeded for a further 3 h. 2 M aq. HCl (50 mL) was used to quench the reaction before the MeOH and THF were removed *in vacuo*. The acidic layer was washed with Et_2O (3×50 mL). The combined organic extracts were washed with 2 M aq. NaOH (3×50 mL). The aqueous layer was neutralised with 2 M aq. HCl, before the product was finally extracted with Et_2O (3×50 mL). The organic solution which resulted from this extraction was dried over $MgSO_4$ and concentrated to a yellow oil *in vacuo*. Using a 3:1 mixture of hexane/EtOAc, the product was obtained as a colourless solid.

Yield: 3.75 g, 18.5 mmol, 80%.

^{1}H NMR (CDCl$_3$, 400MHz) δ_H ppm: 3.89 (s, 3H, C$\underline{H}_3$), 5.68 (s, 1H, ArO$\underline{H}$), 6.73 (d, J=8.56Hz, 1H, Ar$\underline{H}$), 6.9 (dd, J=8.52Hz, 2.32Hz, 1H, Ar$\underline{H}$), 7.09 (d, J=2.12Hz, 1H, Ar$\underline{H}$).

^{13}C NMR (CDCl$_3$, 100.71 MHz) δ_c ppm: 55.6 ($\underline{C}H_3$), 111.1 ($\underline{C}H$), 112.8 (Q), 117.3 ($\underline{C}H$), 122.3 ($\underline{C}H$), 145.4 (Q), 146.0 (Q).

HRMS (ESI): Calculated mass 201.9629. Found 202.8221 $(M+H)^+$.

V_{max} (DCM)/cm^{-1}: 3502 (-OH), 3072, 3007, 2941, 2840, 1697, 1591, 1480, 1260, 1217, 1125, 1024, 887, 792, 621.

Melting point: 60-62 °C.

6.1.11 Synthesis of (5-bromo-2-methoxyphenoxy)(tert-butyl)dimethylsilane *(2.13)*

(2.28) (3.75 g, 18.5 mmol), imidazole (3.14 g, 46.05 mmol) and *tert*-butyl dimethylsilylchloride (3.47 g, 23.02 mmol) were dried under vacuum in a three necked round bottom flask. The reaction vessel was filled with nitrogen at 0 °C before dry DMF (10 mL) was added. The mixture was stirred for 30 min at 0 °C before the temperature was allowed to rise to room temperature and stirred overnight. After 14 h, the reaction was quenched with H_2O (20 mL) and the product was extracted with Et_2O (3×30 mL). The combined organic extracts were dried over

MgSO$_4$ and concentrated to a mobile oil. The product was isolated as a colourless oil after column chromatography (hexane/EtOAc 10:1).

Yield: 5.20 g, 16.49 mmol, 89%.

^{1}H NMR (CDCl$_3$, 400MHz) δ$_H$ ppm: 0.18 (s, 6H, 2×CH$_3$), 1.02 (s, 9H, ^{t}Bu), 3.81 (s, 3H, OMe), 6.73 (d, J=8.56Hz, 1H, ArH), 7.00-7.03 (m, 2H, 2×ArH).

^{13}C NMR (CDCl$_3$, 100.71 MHz) δ$_c$ ppm: -5.1 (CH$_3$), 17.9 (Q), 25.2 (CH$_3$), 55.1 (CH$_3$), 111.8 (Q), 112.7 (CH), 123.6 (CH), 123.9 (CH), 145.4 (Q), 149.9 (Q).

HRMS (ESI): Calculated mass 316.0494. Found 317.8089 (M+H)$^+$.

V$_{max}$ (DCM)/cm^{-1}: 2954, 2930, 2857, 1585, 1496, 1471, 1463, 1441, 1269, 1225, 1132, 934, 831, 784.

6.1.12 Synthesis of 9-(3-(((tert-butyldimethylsilyl)oxy)-4-methoxyphenyl)-2,3,4-trimethoxy-6,7-dihydro-5H-benzo[7]annulen-7-ol *(2.14)*.

To a stirred solution of (5-bromo-2-methoxyphenoxy)(tert-butyl)dimethylsilane *(2.13)* (6.43 g, 20.27 mmol) in dry THF (15 mL) under N$_2$ at -78 ^{o}C in a cool bath of acetone and dry ice was added 2.5 M BuLi (8.1 mL, 20.27 mmol) dropwise over 10 min. This mixture was stirred for a further 20 min with further addition of THF used if a colourless precipitate formed. After this time, *(2.13)* (1.80 g, 6.75 mmol) in THF (10 mL) was added dropwise and stirred for 2 h at this temperature. The solution was allowed to 0 ^{o}C and was stirred overnight. Upon completion of the reaction, it was quenched using 1 M HCl solution (50 mL) and stirred for 5 min. The product was extracted using Et$_2$O (3×50 mL). The combined organic extracts were washed with H$_2$O (50 mL) before being dried over MgSO$_4$ and concentrated *in vacuo*. The product was obtained in pure form following column chromatography (hexane/EtOAc 2:1) as a viscous yellow oil.

Yield: 1.98 g, 3.95 mmol, 58.5%.

¹H NMR (CDCl₃, 400MHz) δ_H ppm: 0.17 (d, J=5.26 Hz, 6H, 2×C_H₃), 1.00 (s, 9H, ᵗBu), 2.07-2.19 (m, 1 H, C_H₂), 2.31-2.61 (m, 2H, C_H₂), 2.98-3.12 (m, 1H), 3.69 (s, 3H, C_H₃), 3.84 (s, 3H, C_H₃), 3.93 (s, 6H, 2×C_H₃), 4.14 - 4.25 (m, 1 H, C_HOH), 6.27 (d, J=4.68 Hz, 1 H, Ar_H), 6.36 (s, 1H, C=C_H), 6.78 - 6.89 (m, 3H, 3×Ar_H).

¹³C NMR (CDCl₃, 100.71 MHz) δ_c ppm: -5.0 (_CH₃), 0.6 (_CH₃), 21.2 (_CH₂), 25.3 (_CH₃), 43.0 (_CH₂), 55.1 (_CH₃), 55.5 (_CH₃), 60.4 (_CH₃), 61.1 (_CH₃), 69.4 (_CH), 108.2 (_CH), 111.1 (_CH), 120.2 (_CH), 121.1 (_CH), 127.5 (Q), 130.7 (_CH), 133.5 (Q), 134.9 (Q), 138.2 (Q), 141.0 (Q), 144.2 (Q), 150.1 (Q), 150.6 (Q).

HRMS (-ESI): Calculated 486.2438. Found 485.2445 (M-H).

V_max (DCM)/cm⁻¹: 3499, 2934, 1643, 1488, 1453, 1407, 1343, 1266, 1117, 1030, 749.

6.1.13 Synthesis of 9-(3-((tert-butyldimethylsilyl)oxy)-4-methoxyphenyl)-2,3,4-trimethoxy-5H-benzo[7]annulen-7(6H)-one (2.07).

To a solution of *(2.14)* (0.50 g, 1.03 mmol) in DCM (10 mL) stirred at room temperature was added quickly Dess-Martin periodinane (0.87 g, 2.06 mmol). After 5 min of stirring the reaction mixture was observed to have turned a reddish colour and monitoring of the reaction using TLC (hexane/EtOAc 3:1) had shown it reached completion. Extraction of the product between Et₂O (3×30 mL) and 5% aq. NaHCO₃ solution (30 mL) furnished the product in its crude form. Following purification by column chromatography (hexane/EtOAc 3:1), the product was obtained as an oil with a slight yellow colouration.

Yield: 0.45 g, 0.90 mmol, 87.4%.

¹H NMR (CDCl₃, 400MHz) δ_H ppm: 0.13 (s, 6H, 2×C_H₃ silyl), 0.96 (s, 9H, ᵗBu silyl), 2.67-2.70 (m, 2H, C_H₂), 3.10-3.13 (m, 2H, C_H₂), 3.58 (s, 3H, C_H₃), 3.85 (s, 3H, C_H₃), 3.89 (s, 3H, C_H₃), 3.94 (s, 3H, C_H₃), 6.32 (s, 2H, 1×Ar_H, 1×C=C_H), 6.79-6.82 (m, 2H, 2×Ar_H), 6.87-6.90 (m, 1H, Ar_H).

¹³**C NMR (CDCl₃, 100.71 MHz) δ_c ppm:** -4.5 (2×<u>C</u>H₃), 18.4 (Q), 20.2 (<u>C</u>H₂), 25.7 (3×<u>C</u>H₃), 45.6 (<u>C</u>H₂), 55.4 (<u>C</u>H₃), 55.9 (<u>C</u>H₃), 60.9 (<u>C</u>H₃), 61.4 (<u>C</u>H₃), 111.3 (<u>C</u>H), 111.8 (<u>C</u>H), 121.7 (<u>C</u>H), 122.9 (<u>C</u>H), 127.9 (<u>C</u>H), 128.3 (Q), 129.0 (Q), 129.3 (Q), 132.6 (Q), 135.3 (Q), 143.2 (Q), 144.6 (Q), 149.9 (Q), 151.0 (Q), 151.8 (Q), 204.1 (<u>C</u>=O).

HRMS (+ESI): Calculated 507.2179, Found 508.2233 (M+Na)⁺.

V_{max} (DCM)/cm⁻¹: 2933, 2856, 2095, 1653, 1509, 1405, 1284, 1117, 809.

6.1.14 Synthesis of 9-(3-((tert-butyldimethylsilyl)oxy)-4-methoxyphenyl)-2,3,4-trimethoxy-5H-benzo[7]annulen-7(6H)-one oxime (2.31).

To a stirred solution of *(2.07)* (0.20 g, 0.42 mmol) in EtOH (4 mL) and H₂O (1 mL), was added NH₂OH.HCl (0.04 g, 0.46 mmol) and sodium acetate (0.06 g, 0.66 mmol). The resultant mixture was stirred at room temperature for 1 h, until complete consumption of the starting material was observed using TLC (hexane/EtOAc 3:1). The mixture was diluted in H₂O (10 mL) and the product was extracted using Et₂O (3×15 mL). The product was isolated as a 2:1 mixture of isomers by column chromatography using hexane/EtOAc (6:1) as the mobile phase, in the form of a yellow oil.

Yield: 0.16 g, 0.32 mmol, 76%.

¹**H NMR (CDCl₃, 400MHz) δ_H ppm:** 0.16 (s, 6H, 2×C<u>H</u>₃), 0.99 (s, 9H, ^t<u>Bu</u>), 2.95-3.03 (m, 4H, 2xC<u>H</u>₂), 3.61 (s, 3H, OC<u>H</u>₃), 3.87 (s, 3H, OC<u>H</u>₃), 3.92 (s, 6H, 2×OC<u>H</u>₃), 6.31 (s, 1H), 6.55 (s, 1H), 6.83 (m, 2H), 6.95 (m, 1H).

¹³**C NMR (CDCl₃, 100.71 MHz) δ_c ppm:** -5.0 (<u>C</u>H₃), 13.7 (Q), 20.8 (<u>C</u>H₂), 25.3 (<u>C</u>H₃), 29.3 (<u>C</u>H₂), 55.0 (<u>C</u>H₃), 55.4 (<u>C</u>H₃), 60.5 (<u>C</u>H₃), 61.0 (<u>C</u>H₃), 110.0 (<u>C</u>H), 111.0 (<u>C</u>H), 121.2 (<u>C</u>H), 122.0 (<u>C</u>H), 123.7 (<u>C</u>H), 128.2 (Q), 133.1 (Q), 136.2 (Q), 141.7 (Q), 144.0 (Q), 144.7 (Q), 149.6 (Q), 150.4 (Q), 150.4 (Q).

HRMS (+ ESI): Calculated Mass 499.2390 Found 500.1702 (M+H⁺).

V_{max} (DCM)/cm⁻¹: 3482 (OH stretch), 1651 (C=N stretch), 1261, 1117, 1028, 750, 471.

6.1.15 Synthesis of 9-(3-hydroxy-4-methoxyphenyl)-2,3,4-trimethoxy-5H-benzo[7]annulen-7(6H)-one oxime (2.32).

To a stirred solution of *(2.32)* (0.02 g, 0.04 mmol) in THF (1 mL) was added 1 M TBAF (0.04 mL, 0.04 mmol). The mixture was stirred for 20 min after which TLC (hexane/EtOAc 1:1) showed complete consumption of starting materials. The solvents were removed *in vacuo* and the remaining residue was placed directly on a column. The product was isolated as a brown solid using a mobile phase system of hexane/EtOAc (2:1).

Yield: 0.01 g, 0.039 mmol, 97%.

^{1}H NMR (CDCl$_3$, 400MHz) δ_H ppm: 2.93-3.02 (m, 4H, 2×C$\underline{H}_3$), 3.62 (s, 3H, OC$\underline{H}_3$), 3.91 (s, 3H, OC$\underline{H}_3$), 3.93 (s, 3H, OC$\underline{H}_3$), 3.96 (s, 3H, OC$\underline{H}_3$), 6.34 (s, 1H), 6.57 (s, 1H), 6.84 (d, J=8.35Hz, 1H, Ar$\underline{H}$), 6.89 (d, J=8.92Hz, 1H, Ar$\underline{H}$), 6.95 (1H, s, Ar$\underline{H}$).

^{13}C NMR (CDCl$_3$, 100.71 MHz) δ_c ppm: 21.3 ($\underline{C}H_2$), 29.8 ($\underline{C}H_2$), 56.0 (2x$\underline{C}H_3$), 60.9 ($\underline{C}H_3$), 61.5 ($\underline{C}H_3$), 110.2 ($\underline{C}H$), 110.6 ($\underline{C}H$), 115.3 ($\underline{C}H$), 120.8 ($\underline{C}H$), 124.4 ($\underline{C}H$), 128.8 (Q), 133.5 (Q), 137.3 (Q), 142.3 (Q), 145.0 (Q), 146.5 (Q), 150.1 (Q), 150.9 (Q).

HRMS (+ ESI): Calculated Mass 385.1525 Found 386.1598 (M+H$^+$).

V$_{max}$ (DCM)/cm^{-1}: 3487, 2941, 2929, 1579, 1509, 1492, 1452, 1405, 1368, 1275, 1110, 1030, 801, 763.

Melting point: 97-103 ^{o}C.

6.1.16 Synthesis of 2-(((9-(3-((tert-butyldimethylsilyl)oxy)-4-methoxyphenyl)-2,3,4-trimethoxy-5H-benzo[7]annulen-7(6H)-ylidene)amino)oxy)acetic acid (2.09).

To a stirred solution of *(2.07)* (0.07 g, 0.14 mmol) in EtOH (4 mL) and H$_2$O (1 mL), was added (O-carboxymethyl) hydroxylamine hemi-hydrochloride (0.02 g, 0.16 mmol) and NaOAc (0.02 g, 0.23 mmol). The resultant mixture was stirred at room temperature for 4 h, until complete

consumption of the starting material was observed using TLC (hexane/EtOAc 1:1). The mixture was diluted in H_2O (10 mL) and the product was extracted using Et_2O (3×15 mL). The product was isolated as a 2:1 mixture of isomers by column chromatography using EtOAc/MeOH (6:1) as the mobile phase, in the form of a yellow oil.

Yield: 0.06 g, 0.11 mmol, 76%.

^{1}H NMR (CDCl$_3$, 400MHz) δ_H ppm: 0.16 (s, 6H, 2×C$\underline{H}_3$), 0.99 (s, 9H, ^{t}Bu), 2.75-3.05 (m, 4H, 2×C$\underline{H}_2$), 3.61 (s, 3H, OC$\underline{H}_3$), 3.86 (s, 3H, OC$\underline{H}_3$), 3.89 (s,3H, OC$\underline{H}_3$), 3.91 (s, 3H, OC$\underline{H}_3$), 4.71 (d, 2H, OC$\underline{H}_2$), 6.33 (s, 1H), 6.50 (s, 1H), 6.81-6.85 (m, 2H), 6.93-6.96 (m, 1H).

^{13}C NMR (CDCl$_3$, 100.71 MHz) δ_c ppm: -5.0 ($\underline{C}H_3$), 0.58 ($\underline{C}H_3$), 14.8 ($\underline{C}H_3$), 18.0 (Q), 20.7 ($\underline{C}H_2$), 21.4 ($\underline{C}H_2$), 25.3 ($\underline{C}H_3$), 29.8 ($\underline{C}H_3$), 32.5 ($\underline{C}H_2$), 36.1 ($\underline{C}H_2$), 54.9 ($\underline{C}H_3$), 55.4 ($\underline{C}H_3$), 60.5 ($\underline{C}H_3$), 60.9 ($\underline{C}H_3$), 65.4 ($\underline{C}H_2$ minor isomer), 69.8 ($\underline{C}H_2$ major isomer), 110.0 ($\underline{C}H$), 110.9 ($\underline{C}H$ major isomer), 111.1 (CH minor isomer), 117.0 ($\underline{C}H$), 121.1 ($\underline{C}H$ major isomer), 121.4 ($\underline{C}H$ minor isomer), 122.0 ($\underline{C}H$ major isomer), 122.3 ($\underline{C}H$ minor isomer), 122.6 ($\underline{C}H$ major isomer), 128.0 (Q major isomer), 128.7 (Q minor isomer), 132.9 (Q minor isomer), 133.0 (Q major isomer), 135.0 (Q major isomer), 136.4 (Q minor isomer), 141.8 (Q minor isomer), 142.1 (Q minor isomer), 143.9 (Q major isomer), 146.0 (Q major isomer), 146.6 (Q minor isomer), 149.4 (Q minor isomer)149.6 (Q major isomer), 150.3 (Q minor isomer), 150.4 (Q major isomer), 150.5 (Q major isomer), 150.8 (Q major isomer), 161.8 (Q), 173.8 (Q, C=O).

HRMS (- ESI): Calculated 557.2445 Found 556.2437 (M-H)$^-$.

V_{max} (DCM)/cm^{-1}: 2932, 2857, 1736, 1595, 1572, 1509, 1405, 1367, 1284, 1117, 1029, 925, 880, 783.

6.1.17 Synthesis of perfluorophenyl 2-(((9-(3-((tert-butyldimethylsilyl)oxy)-4-methoxyphenyl)-2,3,4-trimethoxy-5H-benzo[7]annulen-7(6H)-ylidene)amino)oxy) acetate (2.10).

To a stirred solution of *(2.09)* (0.44 g, 0.79 mmol) in DCM (3 mL) under an atmosphere of N_2 at 0 °C was added a solution of pentafluorophenol (0.15 g, 0.79 mmol) in DCM (1.5 mL). This was followed by the subsequent addition of DCC (0.16 g, 0.79 mmol) in DCM (1.5 mL). The solution was stirred for 1 h, after which time the dicyclohexylurea by-product was removed via filtration. The mixture was then washed between H_2O (20 mL) and Et_2O (2 x 20 mL) to yield the product in crude form. Purification using column chromatography yielded the product in a 2:1 mixture of syn- and anti-isomers as a colourless oil.

Yield: 0.51 g, 0.70 mmol, 89%.

^{1}H NMR (CDCl$_3$, 400MHz) δ_H ppm: 0.17 (s, 6H, 2 x C<u>H</u>$_3$), 1.00 (s, 9H, ^{t}Bu), 2.75-2.83 (m, 2H, C<u>H</u>$_2$), 2.93-3.08 (m, 2H, C<u>H</u>$_2$), 3.61 (s, 2H, OC<u>H</u>$_3$ major isomer), 3.62 (s, 1H, OC<u>H</u>$_3$ minor isomer), 3.91 (s, 2H, OC<u>H</u>$_3$ major isomer), 3.92 (s, 2H, OC<u>H</u>$_3$ major isomer), 3.93 (s, 1H, OC<u>H</u>$_3$ minor isomer), 3.94 (s, 1H, OC<u>H</u>$_3$ minor isomer), 4.17 (s, 1H, C<u>H</u>$_2$ minor isomer), 5.01 (s, 1H, C<u>H</u>$_2$ major isomer), 6.31 (s, 1H, Ar<u>H</u> major isomer), 6.36 (s, 1H, Ar<u>H</u> minor isomer), 6.52 (s, 1H, Ar<u>H</u> major isomer), 6.81-6.87 (m, 2H), 6.93-6.98 (m, 1H), 7.03 (s, 1H, minor isomer).

^{13}C NMR (CDCl$_3$, 100.71 MHz) δ_c ppm: 0.6 (<u>C</u>H$_3$), 18.0 (Q), 20.7 (<u>C</u>H$_2$ major isomer), 21.40 (<u>C</u>H$_2$ minor isomer), 25.2 (<u>C</u>H$_3$), 32.5 (<u>C</u>H$_2$ major isomer), 36.1 (<u>C</u>H$_2$ minor isomer), 55.0 (<u>C</u>H$_3$), 55.4 (<u>C</u>H$_3$), 60.4 (<u>C</u>H$_3$), 61.0 (<u>C</u>H$_3$), 69.3 (<u>C</u>H$_2$ minor isomer), 69.5 (<u>C</u>H$_2$ major isomer), 110.0 (<u>C</u>H), 110.9 (<u>C</u>H major isomer), 111.0 (<u>C</u>H minor isomer), 117.1 (<u>C</u>H), 121.1 (<u>C</u>H major isomer), 121.5 (<u>C</u>H minor isomer), 122.0 (<u>C</u>H major isomer), 122.3 (<u>C</u>H minor isomer), 122.6 (<u>C</u>H), 128.0 (Q), 128.7 (Q), 132.9 (Q), 133.0 (Q), 136.0 (Q), 136.4 (Q), 141.8 (Q), 142.1 (Q), 144.0 (Q), 146.0 (Q), 146.3 (Q), 149.5 (Q minor isomer), 149.6 (Q major isomer), 150.3 (minor isomer), 150.4 (Q major isomer), 150.5 (Q major isomer), 150.8 (Q minor isomer), 158.4 (Q), 161.9 (Q, <u>C</u>=N), 165.7 (Q, <u>C</u>=O major isomer), 165.8 (Q, <u>C</u>=O minor isomer).

HRMS (+ ESI): Calculated mass 723.2287. Found 724.2301 (M+H)$^+$.

V_{max} **(DCM)/cm^{-1}:** 2931, 2857, 1732, 1596, 1572, 1493, 1367, 1284, 1263, 1117, 1030, 880, 783.

6.1.18 Synthesis of 2-(((9-(3-((tert-butyldimethylsilyl)oxy)-4-methoxyphenyl)-2,3,4-trimethoxy-5H-benzo[7]annulen-7(6H)-ylidene)amino)oxy)-N-hydroxyacetamide (2.11).

A solution of *(2.10)* (0.0997 g, 0.138 mmol), $NH_2OH.HCl$ (0.105 g, 0.151 mmol) and DIPEA (0.019 g, 0.151 mmol) in DMF (2 mL) under N_2 was stirred at room temperature for 30 min. At this time, the product was extracted by washing between 0.5 M HCl (15 mL) and Et_2O (3 x 15 mL). The combined organic extracts were washed with H_2O (15 mL) and dried over $MgSO_4$. Following concentration *in vacuo*, the product was purified as a mixture of syn- and anti-isomers using column chromatography with EtOAc as the mobile phase as an oil with a yellowish colouration.

Yield: 0.0419 g, 0.074 mmol, 53.5%.

^{1}H NMR (CDCl$_3$, 400MHz) δ_H ppm: 0.17 (s, 6H, 2xC$\underline{H}_3$), 1.00 (s, 9H, ^{t}Bu), 2.72-2.93 (m, 2H, C$\underline{H}_2$), 2.96-3.08 (m, 2H, C$\underline{H}_2$), 3.63 (s, 3H, OC$\underline{H}_3$), 3.86 (s, 2H, OC$\underline{H}_3$ major isomer), 3.87 (s, 1H, OC$\underline{H}_3$ minor isomer), 3.91 (s, 1H, OC$\underline{H}_3$ minor isomer), 3.93 (s, 2H, OC$\underline{H}_3$ major isomer), 3.93 (s, 2H, OC$\underline{H}_3$ major isomer), 3.94 (s, 1H, OC$\underline{H}_3$ minor isomer), 4.67 (s, 1H, C$\underline{H}_2$ minor isomer), 4.70 (s, 1H, C$\underline{H}_2$ major isomer), 6.32 (s, 1H, Ar$\underline{H}$ major isomer), 6.37 (s, 1H, Ar$\underline{H}$ minor isomer), 6.49 (s, 1H, Ar$\underline{H}$), 6.80-6.89 (m, 2H), 6.94 (s, 1H, Ar$\underline{H}$ major isomer), 6.96 (s, 1H, Ar$\underline{H}$ minor isomer), 8.72 (br s, 1H, N$\underline{H}$).

^{13}C NMR (CDCl$_3$, 100.71 MHz) δ_c ppm: -4.5 ($\underline{C}H_3OSi$), 1.0 ($\underline{C}H_3OSi$), 18.5 (Q), 21.1 ($\underline{C}H_2$ major isomer), 22.7 ($\underline{C}H_2$ minor isomer), 25.7 (^{t}Bu), 29.7 ($\underline{C}H_2$ major isomer), 33.2 ($\underline{C}H_2$ minor isomer), 55.4 ($\underline{C}H_3$), 55.9 ($\underline{C}H_3$), 60.9 ($\underline{C}H_3$), 61.4 ($\underline{C}H_3$), 71.9 ($\underline{C}H_2$), 109.1 (CH minor isomer), 110.6 (CH major isomer), 111.5 (CH), 121.5 (CH), 121.8 (CH), 122.4 (CH), 122.6 (CH), 128.1 (Q), 129.1 (Q), 133.0 (Q), 133.3 (Q), 136.2 (Q), 136.6 (Q), 142.4 (Q), 144.6 (Q), 147.0 (Q),

147.6 (Q), 150.1 (Q), 150.9 (Q), 151.1 (Q), 151.1 (Q), 151.4 (Q), 154.5 (Q, $\underline{C}$=N), 162.8 (Q, $\underline{C}$=O).

HRMS (- ESI): Calculated Mass 572.7220. Found 571.2495 (M-H)⁻.

V$_{max}$ (DCM)/cm⁻¹: 3212 (OH stretch), 2932, 2857, 1670, 1596, 1493, 1406, 1282, 1117, 1076, 981, 840.

6.1.19 Synthesis of N-hydroxy-2-((((9-(3-hydroxy-4-methoxyphenyl)-2,3,4-trimethoxy-5H-benzo[7]annulen-7(6H)-ylidene)amino)oxy)acetamide (2.03).

To a stirred solution of *(2.11)* (0.0419 g, 0.0732 mmol) in THF (1 mL) at 0 °C under an atmosphere of N$_2$, was added a 1 M solution of TBAF (0.08 mL, 0.08 mmol). The mixture was stirred at this temperature for 30 min. TLC analysis showed that the starting material had been consumed. The solvent was removed by the bubbling of N$_2$ through it. The product was then obtained in a 2:1 mixture of syn and anti isomers as a yellow oil using column chromatography (hexane/EtOAc 2:1).

Yield: 0.029 g, 0.063 mmol, 86.4%.

¹H NMR (CDCl$_3$, 400MHz) δ$_H$ ppm: 2.76-2.78 (m, 1H, C$\underline{H_2}$ ring minor isomer), 2.83-3.00 (m, 3H, mixture of isomers C$\underline{H_2}$ ring), 3.63 (s, 2H, OC$\underline{H_3}$ major isomer), 3.64 (s, 1H, OC$\underline{H_3}$ minor isomer), 3.89 (s, 2H, OC$\underline{H_3}$ minor isomer), 3.91 (s, 2H, OC$\underline{H_3}$ minor isomer), 3.92 (s, 2H, OC$\underline{H_3}$ major isomer), 3.93 (s, 2H, OC$\underline{H_3}$ major isomer), 3.94 (s, 2H, OC$\underline{H_3}$ major isomer), 4.68 (s, 2H, C$\underline{H_2}$ major isomer), 4.87 (s, 2H, C$\underline{H_2}$ minor isomer), 5.87 (br s, 1H, ArO$\underline{H}$), 6.34 (s, 1H, ArC$\underline{H}$ major isomer), 6.53 (s, 1H, ArC$\underline{H}$ minor isomer), 6.82-6.93 (m, 3H, 3×ArC$\underline{H}$), 8.85 (br s, 1H, N$\underline{H}$OH).

¹³C NMR (CDCl$_3$, 100.71 MHz) δ$_c$ ppm: 21.1 ($\underline{C}$H$_2$ major isomer), 21.8 ($\underline{C}$H$_2$ minor isomer), 33.3 ($\underline{C}$H$_2$ major isomer), 36.8 ($\underline{C}$H$_2$ minor isomer), 56.0 (2×$\underline{C}$H$_3$), 61.0 ($\underline{C}$H$_3$), 61.5 ($\underline{C}$H$_3$), 69.0 ($\underline{C}$H$_2$ minor isomer), 71.9 ($\underline{C}$H$_2$ major isomer), 110.2 ($\underline{C}$H alkene), 110.6 ($\underline{C}$H), 111.5 ($\underline{C}$H minor isomer), 115.2 ($\underline{C}$H major isomer), 115.3 ($\underline{C}$H major isomer), 115.4 ($\underline{C}$H minor isomer),

120.8 (CH major isomer), 121.1 (CH minor isomer), 122.8 (CH major isomer), 122.9 (CH minor isomer), 123.4 (Q), 128.2 (Q), 129.0 (Q), 133.0 (Q), 133.1 (Q), 133.2 (Q), 136.7 (Q), 137.0 (Q), 142.3 (Q), 142.4 (Q), 142.7 (Q), 145.1 (Q), 145.2 (Q), 146.3 (Q) 146.7 (Q), 146.9 (Q), 147.0 (Q), 150.1 (Q), 151.1 (Q), 159.3 (Q), 162.7 (Q, C=N), 167.6 (Q, C=O).

HRMS (+ ESI): Calculated Mass 458.1689. Found 459.1778(M+H)$^+$.

V$_{max}$ (DCM)/cm^{-1}: 3425, 2936, 1674, 1509, 1450, 1405, 1371, 1282, 1247, 1109, 1074, 1030, 732.

6.1.20 Synthesis of benzophenone oxime *(2.35).*

To a stirred suspension of benzophenone (9.11 g, 50 mmol) in H_2O (60 mL) and EtOH (20 mL) was added $NH_2OH.HCl$ (5.14 g, 74 mmol) and NaOAc (10.14 g, 125 mmol). Following heating of the mixture for 10 h at 90 ^{o}C, the product was extracted between H_2O (50 mL) and Et_2O (3x50 mL). The combined organic extracts were dried over $MgSO_4$ and concentrated in vacuo. The resultant colourless solid was purified using column chromatography (hexane/EtOAc 4:1) to yield the product as a colourless solid.

Yield: 9.65 g, 48.92 mmol, 98%.

^{1}H NMR (CDCl$_3$, 400MHz) δ$_H$ ppm: 7.33 – 7.43 (m, 4H, 4×ArH), 7.47 – 7.53 (m, 6H, 6×ArH).

^{13}C NMR (CDCl$_3$, 100.71 MHz) δ$_c$ ppm: 127.5 (CH), 127.8 (CH), 127.9 (CH), 128.8 (CH), 128.8 (CH), 129.2 (CH), 132.1 (ArQ), 135.6 (ArQ), 157.6 (C=N).

HRMS (ESI): Calculated 197.0815. Found 196.0722 (M-H)$^-$.

V$_{max}$ (DCM)/cm^{-1}: 3061, 1658, 1598, 1562, 1447, 1317, 1278, 1176, 941, 763, 638.

Melting Point: 137-139 ^{o}C.

6.1.21 Synthesis of ethyl-3-bromopropanoate *(2.40)*.

To a stirred solution of 3-bromopropanoic acid (4.05 g, 26.4 mmol) in EtOH (30 mL) was added a 4N solution of HCl in 1,4-dioxane (5 mL). The mixture was stirred at room temperature for 12 h. Following removal of the EtOH in vacuo, the mixture was diluted with DCM (125 mL). This was then washed with saturated aq. $NaHCO_3$ (100 mL), followed by brine (100 mL). The organic extract was dried using $MgSO_4$ before being concentrated in vacuo to yield the product as a colourless liquid.

Yield: 2.00 g, 11.04 mmol, 48%.

^{1}H NMR (CDCl$_3$, 400MHz) δ_H ppm: 1.24 (t, J = 7.04 Hz, 3H, C$\underline{H}_3$), 2.87 (t, J= 6.56 Hz, 2H, C$\underline{H}_2$), 3.54 (t, J= 7 Hz, 2H, C$\underline{H}_2$), 4.15 (q, J=7.04, 2H, C$\underline{H}_2$).

^{13}C NMR (CDCl$_3$, 100.71 MHz) δ_c ppm: 13.7 ($\underline{C}H_3$), 25.6 ($\underline{C}H_2$), 37.2 ($\underline{C}H_2$), 60.5 ($\underline{C}H_2$), 170.0 ($\underline{C}$=O).

HRMS (ESI): Calculated mass 179.9786. Found 181.0852 (M+H)$^+$.

V$_{max}$ (DCM)/cm^{-1}: 3552 (w), 2982, 2938, 2907, 2874, 1740, 1476, 1446, 1374, 1236, 1210, 1135, 1018, 921, 849, 613.

6.1.22 Synthesis of ethyl-4-chlorobutanoate *(2.41)*.

To a stirred solution of 4-chlorobutanoic acid (3.00 g, 24.4 mmol) in EtOH (30 mL) was added a 4N solution of HCl in 1,4-dioxane (5 mL). The mixture was stirred at room temperature for 12 h. Following removal of the EtOH in vacuo, the mixture was diluted with DCM (125 mL). This was then washed with saturated aq. $NaHCO_3$ (100 mL), followed by brine (100 mL). The organic extract was dried using $MgSO_4$ before being concentrated in vacuo to yield the product as a colourless liquid.

Yield: 1.1 g, 8.97 mmol, 36.7%.

¹H NMR (CDCl₃, 400MHz) δ_H ppm: 1.20 (t, J = 7Hz, 3H, C$\underline{H}_3$), 2.04 (q, J = 6.52 Hz, 2H, C$\underline{H}_2$), 2.43 (t, J = 7 Hz, 2H, C$\underline{H}_2$), 3.54 (t, J = 6.52 Hz, 2H, C$\underline{H}_2$), 4.08 (q, J = 7.04 Hz, 2H, C$\underline{H}_2$).

¹³C NMR (CDCl₃, 100.71 MHz) δ_c ppm: 13.6 ($\underline{C}H_3$), 27.1 ($\underline{C}H_2$), 30.7 ($\underline{C}H_2$), 43.6 ($\underline{C}H_2$), 60.0 ($\underline{C}H_2$), 172.1 ($\underline{C}$=O).

HRMS (ESI+): Calculated 150.0448. Found 151.0521 (M+H)⁺.

V_max (DCM)/cm⁻¹: 2982, 2940, 2875, 1740, 1445, 1419, 1375, 1244, 1209, 1147, 1028, 786, 651.

6.1.23 Synthesis of ethyl 3-((((diphenylmethylene)amino)oxy)propanoate (2.42).

Under an atmosphere of N₂, *(2.35)* (0.40 g, 2.02 mmol) was dissolved in DMF (5 mL). To this solution was added 60% NaH (0.12 g, 3.04 mmol). The mixture was allowed to stir until going a clear yellow colour and cessation of H₂ gas generation was noted. In a separate flask, *(2.40)* (1.25 g, 2.63 mmol) was dissolved in DMF (2 mL) and added to the oxime salt dropwise over 5 mins. The resultant mixture was left to stir overnight at room temperature before the product was extracted between H₂O (20 mL) and Et₂O (3×20 mL). The combined organic extracts were washed with H₂O before drying over MgSO₄ and concentration to yield a colourless solid *in vacuo*. The target compound was furnished in its pure form following flash column chromatography (hexane/EtOAc 9:1) as a colourless oil.

Yield: 0.30 g, 1 mmol, 50%.

¹H NMR (CDCl₃, 400MHz) δ_H ppm: 1.22 - 1.29 (m, 3H, C$\underline{H}_3$), 2.73 - 2.81 (m, 2H, C$\underline{H}_2$), 4.16 (q, J = 7.04 Hz), 4.49 (t, J = 6.52 Hz, 2H, C$\underline{H}_2$), 7.32 – 7.54 (m, 10H, 10×Ar$\underline{H}$).

¹³C NMR (CDCl₃, 100.71 MHz) δ_c ppm: 13.8 ($\underline{C}H_3$), 34.6 ($\underline{C}H_2$), 60.1 ($\underline{C}H_2$), 69.5 ($\underline{C}H_2$), 127.5 ($\underline{C}H$), 127.6 ($\underline{C}H$), 127.8 ($\underline{C}H$), 128.4 ($\underline{C}H$), 128.8 ($\underline{C}H$), 128.9 ($\underline{C}H$), 132.7 (Ar$\underline{Q}$), 136.0 (Ar$\underline{Q}$), 156.8 ($\underline{C}$=N), 171.1 ($\underline{C}$=O).

HRMS (ESI+): Calculated mass 311.1521. Found 334.1250 (M+Na)⁺.

V_max (DCM)/cm⁻¹: 3058, 2981, 2939, 1739, 1444, 1373, 1186, 1042, 1029, 978, 773, 696.

6.1.24 Synthesis of ethyl 4-(((diphenylmethylene)amino)oxy)butanoate *(2.43)*.

Under an atmosphere of N_2, *(2.35)* (0.40 g, 2.02 mmol) was dissolved in DMF (5 mL). To this solution was added 60% NaH (0.12 g, 3.04 mmol). The mixture was allowed to stir until going a clear yellow colour and cessation of H_2 gas generation was noted. In a separate flask, *(2.41)* (0.40 g, 2.63 mmol) was dissolved in DMF (2 mL) and added to the oxime salt dropwise over 5 mins. The resultant mixture was left to stir overnight at room temperature before the product was extracted between H_2O (20 mL) and Et_2O (3×20 mL). The combined organic extracts were washed with H_2O before drying over $MgSO_4$ and concentration to yield a colourless solid *in vacuo*. The target compound was furnished in its pure form following flash column chromatography (hexane/EtOAc 9:1) as a colourless oil.

Yield: 0.27 g, 0.86 mmol, 43%.

^{1}H NMR (CDCl$_3$, 400MHz) δ_H ppm: 1.27 (t, J = 7.04 Hz, 3H, C$\underline{H}_3$), 2.04 – 2.11 (m, 2H, C$\underline{H}_2$), 2.41 (t, J = 7.52 Hz, 2H, C$\underline{H}_2$), 4.14 (q, J = 7.04 Hz, 2H, C$\underline{H}_2$), 4.25 (t, J = 6 Hz, 2H, C$\underline{H}_2$), 7.31 – 7.58 (m, 10H, 10×Ar$\underline{H}$).

^{13}C NMR (CDCl$_3$, 100.71 MHz) δ_c ppm: 13.7 ($\underline{C}H_3$), 24.3 ($\underline{C}H_2$), 30.4 ($\underline{C}H_2$), 59.9 ($\underline{C}H_2$), 73.0 ($\underline{C}H_2$), 127.4 ($\underline{C}H$), 127.6 ($\underline{C}H$), 127.8 ($\underline{C}H$), 128.3 ($\underline{C}H$), 128.8 ($\underline{C}H$), 128.8 ($\underline{C}H$), 132.9 (Ar$\underline{C}$), 136.1 (Ar$\underline{C}$), 156.3 ($\underline{C}$=N), 172.9 ($\underline{C}$=O).

HRMS (ESI): Calculated mass 311.1521. Found 334.1400 (M+Na)$^+$.

V$_{max}$ (DCM)/cm^{-1}: 3058, 2978, 2935, 2874, 1738, 1494, 1444, 1372, 1253, 1179, 1055, 983, 773, 696.

6.1.25 Synthesis of 3-(aminooxy)propanoic acid hydrochloride *(2.33)*.

To a stirred solution of *(2.42)* (0.30 g, 1.00 mmol) in DCM (5 mL), was added concentrated HCl solution (3 mL). The resultant solution was stirred overnight at room temperature after which time the volatile solvents were removed *in vacuo*. Upon reconstitution in Et_2O (5 mL),

the target compound precipitated out as a colourless solid at 0 °C. Filtration of the mixture and repeated washing with Et$_2$O yielded the compound in pure form as a colourless solid.

Yield: 0.10 g, 0.70 mmol, 70%.

^{1}H NMR (CD$_3$OD, 400MHz) δ$_H$ ppm: 2.72-2.81 (m, 2H, C$\underline{H}_2$), 3.33 (br s, 0.5H, N$\underline{H}_2$), 4.36 (d, J = 5 Hz, 2H, C$\underline{H}_2$), 10.37 (br s, 1H, COO$\underline{H}$).

^{13}C NMR (CDCl$_3$, 100.71 MHz) δ$_c$ ppm: 32.0 ($\underline{C}$H$_2$), 69.9 ($\underline{C}$H$_2$), 170.6 ($\underline{C}$=O).

Melting point: 101 °C.

HRMS (ESI): Calculated Mass 105.0426 Found 103.056 (M-H)$^-$.

V$_{max}$ (DCM)/cm^{-1}: 3479, 2918, 1752, 1260, 1275, 764.

.

6.1.26 Synthesis of 4-(aminooxy)butanoic acid hydrochloride (2.34).

To a stirred solution of *(2.43)* (0.30 g, 0.96 mmol) in DCM (5 mL), was added concentrated HCl solution (3 mL). The resultant solution was stirred overnight at room temperature after which time the volatile solvents were removed *in vacuo*. Upon reconstitution in Et$_2$O (5 mL), the target compound precipitated out as a colourless solid. Filtration of the mixture and repeated washing with Et$_2$O (10×5 mL) yielded the compound in pure form as a colourless solid.

Yield: 0.11 g, 0.70 mmol, 73%.

^{1}H NMR (CD$_3$OD, 400MHz) δ$_H$ ppm: 1.95 – 2.05 (m, 2H, C$\underline{H}_2$), 2.41 – 2.53 (m, 2H, C$\underline{H}_2$), 4.06 – 4.14 (m, 2H, C$\underline{H}_2$NH$_3^+$), 4.93 (s, 3H, N$\underline{H}_3^+$).

^{13}C NMR (CD$_3$OD, 100.71 MHz) δ$_c$ ppm: 22.2 ($\underline{C}$H$_2$), 28.8 ($\underline{C}$H$_2$), 73.5 (O$\underline{C}$H$_2$), 174.4 ($\underline{C}$=O).

Melting point: 123-129 °C.

HRMS (ESI): Calculated Mass 119.0582 Found 118.0510 (M-H)$^-$.

V$_{max}$ (DCM)/cm^{-1}: 3583, 3400, 2929, 1751, 1416, 1370, 1260, 1073, 956, 827.

6.1.27 Synthesis of 3-((((9-(3-((tert-butyldimethylsilyl)oxy)-4-methoxyphenyl)-2,3,4-trimethoxy-5H-benzo[7]annulen-7(6H)-ylidene)amino)oxy)propanoic acid.*(2.44)*

To a stirred solution of *(2.07)* (0.07 g, 0.14 mmol) in EtOH (4 mL) and H_2O (1 mL), was added *(2.33)* (0.09 g, 0.51 mmol) and NaOAc (0.06 g, 0.69 mmol). The resultant mixture was stirred at room temperature for 3 h, until complete consumption of the starting material was observed using TLC (hexane/EtOAc 1:1). The reaction was quenched using 1 M aq. HCl (15 mL) and the product was extracted using Et_2O (3×15 mL). The combined organic extracts were dried over $MgSO_4$, filtered and concentrated *in vacuo*. The product was isolated as a mixture of isomers by column chromatography using EtOAc/MeOH (6:1) as the mobile phase, in the form of a yellow oil.

Yield: 0.07 g, 0.12 mmol, 85%.

^{1}H NMR (CDCl₃ 400MHz) δ_H ppm: 0.19 (s, 6H, 2×C_H₃ TBDMS), 0.95 (s, 9H, tBu, TBDMS), 2.51 - 2.58 (m, 2H, C_H₂), 2.84 - 2.90 (m, 2H, ring C_H₂), 2.94 - 3.01 (m, 2H, ring C_H₂), 3.59 (s, 3 H, C_H₃), 3.72 - 3.77 (m, 2H, C_H₂), 3.86 (s, 3H, C_H₃ major isomer), 3.86 (s, 3H, C_H₃ minor isomer), 3.90 (s, 3H, C_H₃ minor isomer), 3.90 (s, 3H, C_H₃ major isomer), 3.92 (s, 3H, C_H₃ major isomer), 3.93 (s, 3H, C_H₃ minor isomer), 6.35 (s, 1H, C=C_H minor isomer), 6.36 (m, 1H, C=C_H major isomer), 6.54 (s, 1H, Ar_H), 6.77 - 6.88 (m, 2H, 2×Ar_H), 6.92 - 7.03 (m, 1H, Ar_H).

^{13}C NMR (CDCl₃, 100.71 MHz) δ_c ppm: 0.5 (C_H₃), 17.6 (Q TBDMS), 20.3 (C_H₂ major isomer), 21.2 (C_H₂ minor isomer), 25.2 (C_H₃, ᵗBu TBDMS), 27.8 (C_H₂ minor isomer), 31.2 (C_H₂ major isomer), 36.2 (C_H₂ major isomer), 36.5 (C_H₂ minor isomer), 55.5 (C_H₃), 55.7 (C_H₃), 60.0 (C_H₃), 60.3 (C_H₃), 65.1 (C_H₂ minor isomer), 67.1 (C_H₂ major isomer), 109.6 (C_H minor isomer), 110.3 (C_H major isomer) 111.1 (C_H major isomer), 111.2 (C_H minor isomer), 117.1 (C_H minor isomer), 119.2 (C_H major isomer), 122.3 (C_H minor isomer), 122.4 (C_H minor isomer), 122.7 (C_H major isomer), 122.8 (C_H major isomer), 124.3 (C_H minor isomer), 125.4 (C_H major isomer), 129.1 (Q major isomer), 129.8 (Q minor isomer), 131.9 (Q minor isomer), 133.0 (Q major isomer), 135.6 (Q minor isomer), 136.5 (Q major isomer), 141.2 (Q

major isomer), 142.2 (Q minor isomer), 144.3 (Q major isomer), 146.1 (Q minor isomer), 148.9 (Q minor isomer), 149.4 (Q major isomer), 150.2 (Q major isomer), 150.2 (Q minor isomer), 151.0 (Q major isomer), 151.4 (Q minor isomer), 157.6 (Q minor isomer), 162.3 (Q, $\underline{C}$=N), 176.2 ($\underline{C}$=O).

HRMS (ESI -): Calculated Mass 571.2601 Found 570.2540 (M-H)⁻.

V$_{max}$ (DCM)/cm⁻¹: 3425, 2933, 1637, 909.

6.1.28 **Synthesis of 4-((((9-(3-((tert-butyldimethylsilyl)oxy)-4-methoxyphenyl)-2,3,4-trimethoxy-5H-benzo[7]annulen-7(6H)-ylidene)amino)oxy)butanoic acid *(2.45)***

To a stirred solution of *(2.07)* (0.08 g, 0.16 mmol) in EtOH (4 mL) and H$_2$O (1 mL), was added *(2.34)* (0.18 g, 1.20 mmol) and NaOAc (0.10 g, 1.21 mmol). The resultant mixture was stirred at room temperature for 16 h, until complete consumption of the starting material was observed using TLC (hexane/EtOAc 1:1). The reaction was quenched with 1 M aq. HCl (20 mL) and the product was extracted using Et$_2$O (3×25 mL). The combined organic extracts were washed with H$_2$O (20 mL), dried over MgSO$_4$, filtered and concentrated *in vacuo*. The product was isolated as a mixture of isomers by column chromatography using EtOAc/ MeOH /formic acid (10:1:0.1) as the mobile phase, in the form of a yellow oil.

Yield: 0.09 g, 0.15 mmol, 93%.

¹H NMR (CDCl₃ 400MHz) δ$_H$ ppm: 0.17 (s, 6H, 2×C$\underline{H}$₃), 1.00 (s, 9H, ᵗBu TBDMS), 1.29 - 1.35 (m, 2H, C$\underline{H}$₂), 2.45 - 2.54 (m, 2H, C$\underline{H}$₂), 2.94 - 3.12 (m, 4H, 2×C$\underline{H}$₂), 3.60 (s, 3H, C$\underline{H}$₃ minor isomer), 3.61 (s, 3H, C$\underline{H}$₃ major isomer), 3.68 - 3.72 (m, 2H, C$\underline{H}$₂), 3.84 (s, 3H, C$\underline{H}$₃ minor isomer), 3.85 (s, 3H, C$\underline{H}$₃ major isomer), 3.90 (s, 3H, C$\underline{H}$₃ major isomer) 3.91 (s, 3H, C$\underline{H}$₃ minor isomer), 3.93 (s, 3H, C$\underline{H}$₃ minor isomer), 3.94 (s, 3H, C$\underline{H}$₃ major isomer), 6.36 (s, 1 H, C=C$\underline{H}$), 6.48 (s, 1H, Ar$\underline{H}$ major isomer), 6.50 (s, 1H, ArH, minor isomer), 6.91 (s, 1 H, Ar$\underline{H}$), 6.96 - 7.01 (m, 2H, Ar$\underline{H}$).

13C NMR (CDCl3, 100.71 MHz) δc ppm: -0.5 (<u>C</u>H3), 16.5 (Q TBDMS), 19.5 (<u>C</u>H2 major isomer), 21.3 (<u>C</u>H2 major isomer), 21.5 (<u>C</u>H2 minor isomer), 23.2 (<u>C</u>H2 minor isomer), 26.0 (<u>C</u>H3, ^tBu TBDMS), 28.8 (<u>C</u>H2 minor isomer), 30.2 (<u>C</u>H2 major isomer), 36.5 (<u>C</u>H2 major isomer), 36.9 (<u>C</u>H2 minor isomer), 55.6 (<u>C</u>H3), 55.8 (<u>C</u>H3), 60.5 (<u>C</u>H3), 61.0 (<u>C</u>H3), 64.3 (<u>C</u>H2 minor isomer), 67.8 (<u>C</u>H2 major isomer), 110.1 (<u>C</u>H minor isomer), 110.9 (<u>C</u>H major isomer) 111.8 (<u>C</u>H major isomer), 112.2 (<u>C</u>H minor isomer), 118.5 (<u>C</u>H minor isomer), 119.2 (<u>C</u>H major isomer), 122.6 (<u>C</u>H minor isomer), 122.8 (<u>C</u>H minor isomer), 122.7 (<u>C</u>H major isomer), 122.9 (<u>C</u>H major isomer), 124.2 (<u>C</u>H minor isomer), 125.1 (<u>C</u>H major isomer), 129.3 (Q major isomer), 129.6 (Q minor isomer), 132.2 (Q minor isomer), 133.0 (Q major isomer), 135.9 (Q minor isomer), 136.5 (Q major isomer), 141.2 (Q major isomer), 142.2 (Q minor isomer), 144.4 (Q major isomer), 145.8 (Q minor isomer), 148.1 (Q minor isomer), 148.4 (Q major isomer), 150.2 (Q major isomer), 150.6 (Q minor isomer), 151.0 (Q major isomer), 151.4 (Q minor isomer), 158.4 (Q minor isomer), 158.9 (Q major isomer) 163.4 (Q, <u>C</u>=N), 177.5 (<u>C</u>=O).

MS (ESI -): Calculated Mass 585.2738. Found 585.2685 (M-H)⁻.

Vmax (DCM)/cm⁻¹: 3372, 2999, 1721, 1641, 1052, 921, 837.

6.1.29 Synthesis of perfluorophenyl 3-(((9-(3-((tert-butyldimethylsilyl)oxy)-4-methoxyphenyl)-2,3,4-trimethoxy-5H-benzo[7]annulen-7(6H)-ylidene)amino)oxy) propanoate. *(2.46)*

To a stirred solution of *(2.44)* (0.101 g, 0.175 mmol) in DCM (3 mL) under an atmosphere of N2 at 0 °C was added a solution of pentafluorophenol (0.034 g, 0.18 mmol) in DCM (1 mL). This was followed by the subsequent addition of DCC (0.037 g, 0.18 mmol) in DCM (1 mL). The solution was stirred for 1 h, after which time the dicyclohexylurea by-product was removed via filtration. The mixture was then washed between H2O (10 mL) and Et2O (3×10 mL) to yield the product in crude form. The combined organic phases were dried using MgSO4, filtered and the solvents were removed under reduced pressure. Purification using column chromatography

yielded the product in a mixture of syn- and anti-isomers as a colourless oil using a 5:1 mixture of hexane/EtOAc as the mobile phase.

Yield: 0.06 g, 0.081 mmol, 46.4%.

^{1}H NMR (CDCl$_3$, 400MHz) δ_H ppm: 0.19 (s, 6H, 2×C$\underline{H}_3$), 0.95 (s, 9H, ^{t}Bu), 2.59 - 2.71 (m, 2H, C$\underline{H}_2$), 2.84 - 3.01 (m, 4H,2×C$\underline{H}_2$), 3.59 (s, 3H, C$\underline{H}_3$), 3.77 (m, 2H, C$\underline{H}_2$), 3.90 (s, 3H, C$\underline{H}_3$ minor isomer), 3.90(s, 3H, C$\underline{H}_3$ major isomer), 3.91(s, 3H, C$\underline{H}_3$ minor isomer), 3.93 (s, 3H, C$\underline{H}_3$ major isomer), 3.94 (s, 3H, C$\underline{H}_3$ major isomer), 3.95 (s, 3H, C$\underline{H}_3$ major isomer), 6.39 (2×s, 1H, C=C$\underline{H}$), 6.60 (d, J=11.54 Hz, 1 H), 6.84 - 6.89 (m, 1 H), 6.91 - 6.99 (m, 2 H).

^{13}C NMR (CDCl$_3$, 100.71 MHz) δ_c ppm: -4.9 ($\underline{C}$H$_3$), 18.3 (Q TBDMS), 20.5 ($\underline{C}$H$_2$ major isomer), 21.0 ($\underline{C}$H$_2$ minor isomer), 25.7 ($\underline{C}$H$_3$, ^{t}Bu TBDMS), 29.3 ($\underline{C}$H$_2$ minor isomer), 30.9 ($\underline{C}$H$_2$ major isomer), 36.6 ($\underline{C}$H$_2$ major isomer), 36.9 ($\underline{C}$H$_2$ minor isomer), 55.6 ($\underline{C}$H$_3$), 55.7 ($\underline{C}$H$_3$), 60.0 ($\underline{C}$H$_3$), 60.2 ($\underline{C}$H$_3$), 64.7 ($\underline{C}$H$_2$ minor isomer), 66.9 ($\underline{C}$H$_2$ major isomer), 110.1 ($\underline{C}$H minor isomer), 110.5 ($\underline{C}$H major isomer) 111.6 ($\underline{C}$H major isomer), 111.9 ($\underline{C}$H minor isomer), 116.8 ($\underline{C}$H minor isomer), 119.2 ($\underline{C}$H major isomer), 120.9 (Q), 122.4 ($\underline{C}$H minor isomer), 122.7 ($\underline{C}$H minor isomer), 122.9 ($\underline{C}$H major isomer), 123.2 ($\underline{C}$H major isomer), 124.3 ($\underline{C}$H minor isomer), 125.4 ($\underline{C}$H major isomer), 127.8 (Q), 129.7 (Q major isomer), 129.9 (Q minor isomer), 131.2(Q), 131.7 (Q), 132.9 (Q minor isomer), 133.3 (Q), 133.5 (Q major isomer), 135.9 (Q minor isomer), 136.8 (Q major isomer), 139.1 (Q), 141.2 (Q major isomer), 142.0 (Q minor isomer), 144.7 (Q major isomer), 146.3 (Q minor isomer), 148.9 (Q minor isomer), 149.7 (Q major isomer), 150.4 (Q major isomer), 150.8 (Q minor isomer), 151.1 (Q major isomer), 151.5 (Q minor isomer), 157.6 (Q minor isomer), 164.3 (Q, $\underline{C}$=N), 169.7 ($\underline{C}$=O).

HRMS (ESI +): Calculated Mass 737.2443. Found 760.2325 (M+Na)$^+$.

V$_{max}$ (DCM)/cm^{-1}: 3012, 2987, 1639, 1052, 939, 671.

6.1.30 Synthesis of perfluorophenyl 4-((((9-(3-((tert-butyldimethylsilyl)oxy)-4-methoxyphenyl)-2,3,4-trimethoxy-5H-benzo[7]annulen-7(6H)ylidene)amino)oxy) butanoate. *(2.47)*

To a stirred solution *(2.45)* (0.20 g, 0.34 mmol) in DCM (3 mL) under an atmosphere of N_2 at 0 °C was added a solution of pentafluorophenol (0.06 g, 0.34 mmol) in DCM (2 mL). This was followed by the subsequent addition of DCC (0.07 g, 0.34 mmol) in DCM (2 mL). The solution was stirred for 1 h, after which time the dicyclohexylurea by-product was removed via filtration. The mixture was then washed between H_2O (20 mL) and Et_2O (3×20 mL) to yield the product in crude form. The combined organic extracts were dried over $MgSO_4$, filtered and concentrated *in vacuo*. Purification using column chromatography with hexane/EtOAc 4:1 as the mobile phase yielded the product in a mixture of syn- and anti-isomers as a colourless oil.

Yield: 0.23 g, 0.31 mmol, 89%.

^{1}H NMR (CDCl$_3$, 400MHz) δ_H ppm: 0.17 (s, 6H, 2×C$\underline{H}_3$), 0.96 (s, 9H, ^{t}Bu), 1.29 - 1.40 (m, 2H, C$\underline{H}_2$), 2.50 (m, 2H, C$\underline{H}_2$), 2.94 - 3.13 (m, 4H, 2×C$\underline{H}_2$), 3.60 (s, 3H, C$\underline{H}_3$), 3.69-3.72 (m, 2H,C$\underline{H}_2$), 3.84 (s, 3H, C$\underline{H}_3$ major isomer), 3.85 (s, 3H, C$\underline{H}_3$ minor isomer), 3.92 (s, 3H, C$\underline{H}_3$ minor isomer), 3.93 (s, 3H, C$\underline{H}_3$ minor isomer), 3.94 ((s, 3H, 2×C$\underline{H}_3$ major isomer), 6.40 (s, 1H, C=C$\underline{H}$ major isomer), 6.41 (s, 1H, C=C$\underline{H}$ minor isomer), 6.47 - 6.58 (m, 1H, Ar$\underline{H}$), 6.72 - 6.86 (m, 1H, Ar$\underline{H}$), 6.90 - 7.07 (m, 2H, Ar$\underline{H}$).

^{13}C NMR (CDCl$_3$, 100.71 MHz) δ_c ppm: -5.1 (C$\underline{H}_3$), 18.6 (Q TBDMS), 20.4 (C$\underline{H}_2$ major isomer), 21.4 (C$\underline{H}_2$ minor isomer), 23.1 (C$\underline{H}_2$ minor isomer), 23.5 (C$\underline{H}_2$ major isomer), 26.0 (C$\underline{H}_3$, ^{t}Bu TBDMS), 28.9 (C$\underline{H}_2$ minor isomer), 31.7 (C$\underline{H}_2$ major isomer), 36.4 (C$\underline{H}_2$ major isomer), 36.8 (C$\underline{H}_2$ minor isomer), 55.4 (C$\underline{H}_3$), 55.6 (C$\underline{H}_3$), 60.1 (C$\underline{H}_3$), 60.4 (C$\underline{H}_3$), 65.3 (C$\underline{H}_2$ minor isomer), 67.1 (C$\underline{H}_2$ major isomer), 110.5 (C$\underline{H}$ minor isomer), 110.6 (C$\underline{H}$ major isomer) 111.3 (C$\underline{H}$ major isomer), 111.8 (C$\underline{H}$ minor isomer), 116.2 (C$\underline{H}$ minor isomer), 119.6 (C$\underline{H}$ major isomer), 121.0 (Q), 122.9 (C$\underline{H}$ minor isomer), 123.1 (C$\underline{H}$ minor isomer), 123.3 (C$\underline{H}$ major isomer), 123.8 (C$\underline{H}$ major isomer), 124.6 (C$\underline{H}$ minor isomer), 125.8 (C$\underline{H}$ major isomer), 127.8 (Q), 129.2 (Q major isomer), 129.7 (Q minor isomer), 131.4 (Q), 131.8 (Q), 132.9 (Q

minor isomer), 133.1 (Q), 133.5 (Q major isomer), 136.0 (Q minor isomer), 136.8 (Q major isomer), 138.7 (Q), 140.9 (Q major isomer), 142.0 (Q minor isomer), 144.7 (Q major isomer), 146.5 (Q minor isomer), 148.9 (Q minor isomer), 149.5 (Q major isomer), 150.6 (Q major isomer), 150.9 (Q minor isomer), 151.3 (Q major isomer), 151.6 (Q minor isomer), 157.8 (Q minor isomer), 164.9 (Q, $\underline{C}$=N), 168.9 ($\underline{C}$=O).

HRMS (ESI +): Calculated Mass 751.2600. Found 774.2486 $(M+Na)^+$.

V_{max} (DCM)/cm^{-1}: 2946, 1732, 1626, 1476, 1298, 1157, 1043, 882, 692.

6.1.31 Synthesis of 3-(((9-(3-((tert-butyldimethylsilyl)oxy)-4-methoxyphenyl)-2,3,4-trimethoxy-5H-benzo[7]annulen-7(6H)-ylidene)amino)oxy)-N-hydroxypropanamide *(2.48)*.

To a stirred solution of the *(2.46)* (0.051 g, 0.071 mmol), in EtOH (2 mL) and H_2O (0.5 mL) was added $NH_2OH.HCl$ (0.0078 g, 0.113 mmol) and NaOAc (0.0129 g, 0.158 mmol). After 1 h, the mixture was diluted in H_2O (5 mL) and the EtOH was removed *in vacuo*. The product was subsequently extracted by washing between H_2O (15 mL) and Et_2O (3×15 mL). The combined organic extracts were washed with H_2O (15 mL) and dried over $MgSO_4$. Following concentration *in vacuo*, the product was purified as a mixture of syn- and anti- isomers using column chromatography with EtOAc/MeOH /formic acid (95:5:1) as the mobile phase as an oil with a yellowish tinge.

Yield: 0.025 g, 0.043 mmol, 60.5%.

^{1}H NMR (CDCl$_3$, 400MHz) δ_H ppm: 0.19 (s, 6H, 2×C$\underline{H}_3$), 1.07 (s, 9H, ^{t}Bu), 2.55 - 2.65 (m, 2H, C$\underline{H}_2$), 2.89 - 3.08 (m, 4H, 2×C$\underline{H}_2$), 3.59 (s, 3H, C$\underline{H}_3$), 3.74 - 3.81 (m, 2H, C$\underline{H}_3$), 3.86 (s, 3H, C$\underline{H}_3$ minor isomer), 3.87 (s, 3H, C$\underline{H}_3$ major isomer), 3.90 (s, 3H, C$\underline{H}_3$ major isomer), 3.91 (s, 3H, C$\underline{H}_3$ minor isomer), 3.92 (s, 3H, C$\underline{H}_3$ minor isomer), 3.93 (s, 3H, C$\underline{H}_3$ major isomer), 6.39 (s, 1 H, C=C$\underline{H}$ major isomer), 6.40 (s, 3H, C=C$\underline{H}$ minor isomer), 6.53 - 6.59 (m, 1H, Ar$\underline{H}$), 6.81 - 6.88 (m, 1H, Ar$\underline{H}$), 6.92 - 7.01 (m, 2H, Ar$\underline{H}$).

^{13}C NMR (CDCl$_3$, 100.71 MHz) δ_c ppm: -5.0 (CH$_3$), 18.0 (Q TBDMS), 20.5 (CH$_2$ major isomer), 21.0 (CH$_2$ minor isomer), 25.7 (CH$_3$, ^{t}Bu TBDMS), 28.3 (CH$_2$ minor isomer), 31.3(CH$_2$ major isomer), 36.1 (CH$_2$ major isomer), 36.8 (CH$_2$ minor isomer), 56.3 (CH$_3$), 56.4 (CH$_3$), 60.9 (CH$_3$), 61.3 (CH$_3$), 64.8 (CH$_2$ minor isomer), 66.9 (CH$_2$ major isomer), 110.6 (CH minor isomer), 110.9 (CH major isomer) 111.2 (CH major isomer), 111.7 (CH minor isomer), 117.1 (CH minor isomer), 120.0 (CH major isomer), 121.3 (CH minor isomer), 121.9 (CH minor isomer), 122.4 (CH major isomer), 122.8 (CH major isomer), 124.6 (CH minor isomer), 125.6 (CH major isomer), 129.0 (Q major isomer), 129.9 (Q minor isomer), 131.6 (Q minor isomer), 133.5 (Q major isomer), 135.6 (Q minor isomer), 136.4 (Q major isomer), 141.0 (Q major isomer), 142.4 (Q minor isomer), 144.6 (Q major isomer), 145.9 (Q minor isomer), 148.6 (Q minor isomer), 148.9 (Q major isomer), 150.2 (Q major isomer), 150.6 (Q minor isomer), 151.2 (Q major isomer), 151.6 (Q minor isomer), 157.6 (Q), 163.9 (Q, C=N), 169.8 (C=O).

HRMS (- ESI): Calculated Mass 586.2710. Found 587.2797 (M+H)$^+$.

V$_{max}$ (DCM)/cm^{-1}: 3276, 2985, 2800, 1675, 1621, 1499, 1180, 1062, 919, 840.

6.1.32 Synthesis of 4-(((9-(3-((tert-butyldimethylsilyl)oxy)-4-methoxyphenyl)-2,3,4-trimethoxy-5H-benzo[7]annulen-7(6H)-ylidene)amino)oxy)-N-hydroxybutanamide *(2.49)*.

To a solution of the *(2.47)* (0.20 g, 0.27 mmol) in EtOH (4 mL), H$_2$O (1 mL) and DCM (1 mL) was added NH$_2$OH.HCl (0.0295 g, 0.42 mmol) followed by NaOAc (0.0460 g, 0.42 mmol). After 1 h, the EtOH was removed *in vacuo*, and the product was extracted between H$_2$O (20 mL) and Et$_2$O (3×25 mL). The combined organic extracts were washed with H$_2$O (15 mL), dried over MgSO$_4$ and filtered. Following concentration *in vacuo*, the product was purified as a mixture of syn- and anti- isomers using column chromatography with EtOAc/ MeOH/formic acid (95:4:1) as the mobile phase and was obtained as a yellow oil

Yield: 0.12 g, 0.20 mmol, 74%

¹H NMR (CDCl₃, 400MHz) δ_H ppm: 0.16 (s, 6H, 2×CH₃), 0.98 (s, 9H, ᵗBu), 1.25 (dt, J=4.89, 2.32 Hz, 2 H, CH₂), 2.31 - 2.44 (m, 2H, CH₂), 2.95 - 3.17 (m, 4H, CH₂), 3.61 (s, 3H, CH₃ major isomer), 3.62 (s, 3H, CH₃ minor isomer), 3.68 - 3.73 (m, 2H, CH₂), 3.84 (s, 3H, CH₃ minor isomer), 3.85 (s, 3H, CH₃ major isomer), 3.87 (s, 3H, CH₃), 3.93 (s, 3H, CH₃ minor isomer), 3.94 (s, 3H, CH₃ major isomer), 6.30 (s, 1H, C=CH minor isomer), 6.32 (s, 1H, C=CH major isomer) 6.44 - 6.52 (m, 1H, ArH), 6.81 - 7.07 (m, 3H, ArH).

¹³C NMR (CDCl₃, 100.71 MHz) δ_c ppm: -4.9 (CH₃), 18.0 (Q TBDMS), 19.9 (CH₂ major isomer), 21.5 (CH₂ major isomer), 21.7 (CH₂ minor isomer), 24.1 (CH₂ minor isomer), 26.9 (CH₃, ᵗBu TBDMS), 28.5 (CH₂ minor isomer), 31.9 (CH₂ major isomer), 35.9 (CH₂ major isomer), 36.7 (CH₂ minor isomer), 56.6 (CH₃), 56.9 (CH₃), 61.0 (CH₃), 61.4 (CH₃), 65.9 (CH₂ minor isomer), 68.9 (CH₂ major isomer), 110.4 (CH minor isomer), 110.9 (CH major isomer) 112.0 (CH major isomer), 112.9 (CH minor isomer), 117.8 (CH minor isomer), 119.8 (CH major isomer), 122.4 (CH minor isomer), 122.7 (CH minor isomer), 122.8 (CH major isomer), 123.5 (CH major isomer), 124.2 (CH minor isomer), 125.8 (CH major isomer), 129.3 (Q major isomer), 129.9 (Q minor isomer), 132.2 (Q minor isomer), 133.4 (Q major isomer), 135.9 (Q minor isomer), 137.5 (Q major isomer), 141.2 (Q major isomer), 142.6 (Q minor isomer), 144.4 (Q major isomer), 145.9 (Q minor isomer), 148.2 (Q minor isomer), 148.4 (Q major isomer), 150.2 (Q major isomer), 150.3 (Q minor isomer), 151.1 (Q major isomer), 151.7 (Q minor isomer), 158.9 (Q minor isomer), 159.1 (Q major isomer) 161.9 (Q, C=N), 168.9 (C=O).

HRMS (- ESI): Calculated Mass 600.2867. Found 599.2812 (M-H)⁻.

V_max (DCM)/cm⁻¹: 3311, 2917, 2822, 1691, 1625, 1122, 1089, 921, 762.

6.1.33 **Synthesis of N-hydroxy-3-((((9-(3-hydroxy-4-methoxyphenyl)-2,3,4-trimethoxy-5H-benzo[7]annulen-7(6H)-ylidene)amino)oxy)propanamide.**

(2.04)

To a stirred solution of *(2.48)* (0.0214 g, 0.036 mmol) in THF (1 mL) at 0 °C under an atmosphere of N_2, was added a 1 M solution of TBAF (0.05 mL, 0.05 mmol). After stirring at this temperature for 15 min, the reaction mixture was diluted in H_2O (15 mL) and then extracted using Et_2O (3×20 mL). The combined organic extracts were dried over $MgSO_4$, filtered and concentrated in vacuo. Following column chromatography using EtOAc/MeOH /formic acid (95:4:1) the product was obtained as a mixture of syn and anti isomers as a yellow oil.

Yield: 0.0123 g, 0.026 mmol, 72.3%.

^{1}H NMR (CDCl$_3$, 400MHz) δ_H ppm: 2.52 - 2.56 (m, 2H, C$\underline{H}_2$), 2.92-3.10 (m, 4H, 2×C$\underline{H}_2$), 3.59 (s, 3H, C$\underline{H}_3$), 3.70 - 3.75 (m, 2H, C$\underline{H}_2$), 3.86 (s, 3H, C$\underline{H}_3$ minor isomer), 3.87 (s, 3H, C$\underline{H}_3$ major isomer), 3.92 (s, 3H, C$\underline{H}_3$ minor isomer), 3.93 (s, 3H, C$\underline{H}_3$ major isomer), 3.94 (s, 3H, C$\underline{H}_3$ major isomer), 3.95 (s, 3H, C$\underline{H}_3$ minor isomer), 5.58 - 5.74 (br s, 1 H, ArO$\underline{H}$), 6.43 - 6.61 (m, 2H, 1×C=C$\underline{H}$, 1×Ar$\underline{H}$), 6.88 (m, 1H, Ar$\underline{H}$), 6.94 - 7.06 (m, 2H, Ar$\underline{H}$).

^{13}C NMR (CDCl$_3$, 100.71 MHz) δ_c ppm: 21.3 ($\underline{C}H_2$ major isomer), 21.5 ($\underline{C}H_2$ minor isomer), 27.6 ($\underline{C}H_2$ minor isomer), 31.2 ($\underline{C}H_2$ major isomer), 35.2 ($\underline{C}H_2$ major isomer), 36.1 ($\underline{C}H_2$ minor isomer), 55.9 ($\underline{C}H_3$), 56.1 ($\underline{C}H_3$), 59.6 ($\underline{C}H_3$), 60.4 ($\underline{C}H_3$), 64.7 ($\underline{C}H_2$ minor isomer), 67.2 ($\underline{C}H_2$ major isomer), 110.3 ($\underline{C}H$ minor isomer), 110.9 ($\underline{C}H$ major isomer) 112.4 ($\underline{C}H$ major isomer), 113.2 ($\underline{C}H$ minor isomer), 117.5 ($\underline{C}H$ minor isomer), 120.0 ($\underline{C}H$ major isomer), 122.3 ($\underline{C}H$ minor isomer), 122.5 ($\underline{C}H$ minor isomer), 123.7 ($\underline{C}H$ major isomer), 123.8 ($\underline{C}H$ major isomer), 124.3 ($\underline{C}H$ minor isomer), 125.4 ($\underline{C}H$ major isomer), 129.1 (Q major isomer), 129.9 (Q minor isomer), 132.0 (Q minor isomer), 133.0 (Q major isomer), 135.2 (Q minor isomer), 136.1 (Q major isomer), 140.7 (Q major isomer), 141.9 (Q minor isomer), 145.3 (Q major isomer), 146.1 (Q minor isomer), 148.8 (Q minor isomer), 149.1 (Q major isomer), 150.2 (Q major isomer), 150.8 (Q minor isomer), 151.2 (Q major isomer), 151.5 (Q minor isomer), 155.6 (Q minor isomer), 164.3 (Q, $\underline{C}$=N), 169.2 (Q, $\underline{C}$=O).

HRMS (+ ESI): Calculated Mass 470.1927. Found 493.1816 (M+Na)$^+$

V$_{max}$ (DCM)/cm^{-1}: 3401, 2982, 1689, 1534, 1332, 1101, 1063, 732.

6.1.34 Synthesis of N-hydroxy-4-(((9-(3-hydroxy-4-methoxyphenyl)-2,3,4-trimethoxy-5H-benzo[7]annulen-7(6H)-ylidene)amino)oxy)butanamide *(2.05).*

To a stirred solution of *(2.49)* (0.051 g, 0.085 mmol) in THF (1 mL) at 0 °C under an atmosphere of N$_2$, was added a 1 M solution of TBAF (0.11 mL, 0.11 mmol). After stirring at this temperature for 15 min, the reaction mixture was diluted in H$_2$O (15 mL) and then extracted using Et$_2$O (3×20 mL). The combined organic extracts were dried over MgSO$_4$, filtered and concentrated in vacuo. Following column chromatography using EtOAc/ MeOH /formic acid (95:4:1) the product was obtained as a mixture of syn and anti isomers as a yellow oil.

Yield: 0.0356 g, 0.073 mmol, 85%.

^{1}H NMR (CDCl$_3$, 400MHz) δ$_H$ ppm: 1.41-1.45 (m, 2H, C$\underline{H}_2$), 2.27 - 2.37 (m, 4H, 2×C$\underline{H}_2$), 2.92-3.06 (m, 4H, 2×C$\underline{H}_2$), 3.61 (s, 3H, C$\underline{H}_3$ major isomer), 3.62 (s, 3H, C$\underline{H}_3$ major isomer), 3.67 - 3.77 (m, 2H, C$\underline{H}_2$), 3.84 (s, 3H, C$\underline{H}_3$ minor isomer), 3.87 (s, 3H, C$\underline{H}_3$), 3.93 (s, 3H, C$\underline{H}_3$ minor isomer), 3.94 (s, 3H, C$\underline{H}_3$ major isomer), 5.70 (br s, 1H, ArO$\underline{H}$), 6.27 - 6.37 (m, 1 H, C=C$\underline{H}$), 6.43 - 6.54 (m, 1H, ArH), 6.79 - 7.07 (m, 3H, Ar$\underline{H}$).

^{13}C NMR (CDCl$_3$, 100.71 MHz) δ$_c$ ppm: 20.2 (C$\underline{H}_2$ major isomer), 21.3 (C$\underline{H}_2$ major isomer), 21.9 (C$\underline{H}_2$ minor isomer), 23.5 (C$\underline{H}_2$ minor isomer), 29.8 (C$\underline{H}_2$ minor isomer), 31.4 (C$\underline{H}_2$ major isomer), 36.0 (C$\underline{H}_2$ major isomer), 37.2 (C$\underline{H}_2$ minor isomer), 56.0 (C$\underline{H}_3$), 56.4 (C$\underline{H}_3$), 61.5 (C$\underline{H}_3$), 61.8 (C$\underline{H}_3$), 64.9 (C$\underline{H}_2$ minor isomer), 68.5 (C$\underline{H}_2$ major isomer), 110.4 (C$\underline{H}$ minor isomer), 111.4 (C$\underline{H}$ major isomer) 112.3 (C$\underline{H}$ major isomer), 112.9 (C$\underline{H}$ minor isomer), 118.5 (C$\underline{H}$ minor isomer), 119.8 (C$\underline{H}$ major isomer), 122.6 (C$\underline{H}$ minor isomer), 122.9 (C$\underline{H}$ minor isomer), 123.6 (C$\underline{H}$ major isomer), 124.8 (C$\underline{H}$ major isomer), 125.2 (C$\underline{H}$ minor isomer), 125.9 (C$\underline{H}$ major isomer), 129.3 (Q major isomer), 129.9 (Q minor isomer), 132.2 (Q minor isomer),

132.9 (Q major isomer), 134.3 (Q minor isomer), 136.5 (Q major isomer), 141.2 (Q major isomer), 142.2 (Q minor isomer), 144.4 (Q major isomer), 144.8 (Q minor isomer), 149.1 (Q minor isomer), 149.3 (Q major isomer), 151.2 (Q major isomer), 151.7 (Q minor isomer), 152.5 (Q major isomer), 153.0 (Q minor isomer), 155.4 (Q minor isomer), 156.9 (Q major isomer), 165.4 (Q, $\underline{C}$=N), 170.1 ($\underline{C}$=O).

HRMS (+ ESI): Calculated Mass 486.2002. Found 485.1911 (M-H)⁻.

V$_{max}$ (DCM)/cm⁻¹: 3389, 1673, 1614, 1523, 1450, 1282, 1109, 1030, 732.

6.1.35 Synthesis of 2-(((9-(3-hydroxy-4-methoxyphenyl)-2,3,4-trimethoxy-5H-benzo[7]annulen-7(6H)-ylidene)amino)oxy)acetic acid *(2.50)*.

To a stirred solution of *(2.09)* (0.05 g, 0.09 mmol) in THF (1 mL) at 0 °C under an atmosphere of N$_2$, was added a 1 M solution of TBAF (0.10 mL, 0.10 mmol). After 15 min, TLC analysis showed that the starting material had been consumed. The solvent was removed under a stream of N$_2$, before the product was obtained in its pure form as a yellow oil.

Yield: 0.03 g, 0.067 mmol, 75%

¹H NMR (CDCl$_3$, 400MHz) δ$_H$ ppm: 2.76-3.05 (m, 4H, 2×C$\underline{H}_2$), 3.61 (s, 3H, OC$\underline{H}_3$), 3.85 (s, 3H, OC$\underline{H}_3$ major isomer), 3.89 (s, 3H, OC$\underline{H}_3$ major isomer), 3.91 (s, 3H, OC$\underline{H}_3$ minor isomer), 3.91 (s, 3H, OC$\underline{H}_3$ major isomer), 3.93 (s, 3H, OC$\underline{H}_3$ minor isomer), 4.55 (s, 2H, C$\underline{H}_2$ minor isomer), 4.59 (s, 2H, C$\underline{H}_2$ minor isomer), 5.68 (s, 1H, Ar-O$\underline{H}$), 6.30 (s, 1H, C=C$\underline{H}$ major isomer), 6.36 (s, 1H, C=C$\underline{H}$ minor isomer), 6.52 (s, 1H, Ar$\underline{H}$), 6.82-6.85 (m, 2H, 2×Ar$\underline{H}$), 6.93-6.97 (m, 1H, Ar$\underline{H}$).

HRMS (- ESI): Calculated Mass 443.1580. Found 442.1495.

V$_{max}$ (DCM)/cm⁻¹: 3412, 2929, 1734, 1644, 1020, 947, 675.

6.1.36 Synthesis of 3-(((9-(3-hydroxy-4-methoxyphenyl)-2,3,4-trimethoxy-5H-benzo[7]annulen-7(6H)-ylidene)amino)oxy)propanoic acid. *(2.51)*

To a stirred solution of *(2.44)* (0.0212 g, 0.04 mmol) in dry THF (1 mL) under an atmosphere of N_2 at 0 °C was added 1 M TBAF in THF (0.15 mL, 0.15 mmol). After stirring for 10 min, the product was extracted using Et_2O (3×10 mL) and H_2O (10 mL). The combined organic extracts were dried using $MgSO_4$, filtered and concentrated *in vacuo*. The resultant residue was purified using flash column chromatography (EtOAc/formic acid 99:1), yielding the product as a yellow solid.

Yield: 0.0145 g, 0.031 mmol, 79%.

^{1}H NMR (CDCl$_3$, 400MHz) δ_H ppm: 2.53 - 2.66 (m, 2 H, C$\underline{H}_2$), 2.85 – 2.90 (m, 2H, C$\underline{H}_2$), 2.94-2.99 (m, 2H, C$\underline{H}_2$), 3.59 (s, 3H, C$\underline{H}_3$), 3.77 (m, 2H, C$\underline{H}_2$), 3.89 (s, 3H, C$\underline{H}_3$ minor isomer), 3.90 (m, 3H, C$\underline{H}_3$ major isomer), 3.92 (s, 3H, C$\underline{H}_3$ minor isomer), 3.93 (s, 3H, major isomer) 3.95 (s, 3H, C$\underline{H}_3$ major isomer), 3.96 (s, 3H, C$\underline{H}_3$ minor isomer), 5.45 (s, 1H, ArO$\underline{H}$), 6.39 (m, 1H, C=C$\underline{H}$), 6.58 (s, 1H, Ar$\underline{H}$ major isomer), 6.62 (s, 1H, Ar$\underline{H}$ minor isomer), 6.84 - 6.89 (m, 1 H, Ar$\underline{H}$), 6.92 - 6.98 (m, 2H, 2×Ar$\underline{H}$).

^{13}C NMR (CDCl$_3$, 100.71 MHz) δ_c ppm: 21.4 ($\underline{C}H_2$ major isomer), 21.8 ($\underline{C}H_2$ minor isomer), 27.9 ($\underline{C}H_2$ minor isomer), 30.9 ($\underline{C}H_2$ major isomer), 34.7 ($\underline{C}H_2$ major isomer), 35.9 ($\underline{C}H_2$ minor isomer), 55.9 ($\underline{C}H_3$), 56.3 ($\underline{C}H_3$), 59.9 ($\underline{C}H_3$), 60.4 ($\underline{C}H_3$), 64.3 ($\underline{C}H_2$ minor isomer), 69.1 ($\underline{C}H_2$ major isomer), 110.3 ($\underline{C}H$ minor isomer), 111.0 ($\underline{C}H$ major isomer) 112.4 ($\underline{C}H$ major isomer), 113.4 ($\underline{C}H$ minor isomer), 117.9 ($\underline{C}H$ minor isomer), 120.3 ($\underline{C}H$ major isomer), 122.4 ($\underline{C}H$ minor isomer), 122.9 ($\underline{C}H$ minor isomer), 124.1 ($\underline{C}H$ major isomer), 124.6 ($\underline{C}H$ major isomer), 125.1 ($\underline{C}H$ minor isomer), 125.8 ($\underline{C}H$ major isomer), 129.1 (Q major isomer), 130.2 (Q minor isomer), 132.2 (Q minor isomer), 133.6 (Q major isomer), 135.7 (Q minor isomer), 136.4 (Q major isomer), 141.0 (Q major isomer), 142.1 (Q minor isomer), 145.3 (Q major isomer), 146.4 (Q minor isomer), 148.8 (Q minor isomer), 149.4 (Q major isomer), 150.4 (Q major isomer), 150.9 (Q minor isomer), 151.5 (Q major isomer), 151.8 (Q minor isomer), 165.1 (Q, $\underline{C}$=N), 178.2 (Q, $\underline{C}$=O).

HRMS (- ESI): Calculated Mass 457.1737. Found 456.1679 (M-H)⁻.

V$_{max}$ (DCM)/cm^{-1}: 3398, 3001, 2001, 1698, 1628, 1040, 913, 736.

6.1.37 Synthesis of 4-(((9-(3-hydroxy-4-methoxyphenyl)-2,3,4-trimethoxy-5H-benzo[7]annulen-7(6H)-ylidene)amino)oxy)butanoic acid. *(2.52)*

To a stirred solution of *(2.45)* (0.07 g, 0.12 mmol) in dry THF (2 mL) under an atmosphere of N$_2$ at 0 °C was added 1 M TBAF in THF (0.20 mL, 0.20 mmol). The reaction was quenched after 10 min by addition of H$_2$O (15 mL) and the product was extracted using Et$_2$O (3×20 mL). The combined organic extracts were dried using MgSO$_4$ and concentrated *in vacuo*. The resultant residue was purified using flash column chromatography, with a mobile phase of EtOAc/formic acid (99:1) yielding the product as a yellow solid.

Yield: 0.04 g, 0.085 mmol, 70%.

^{1}H NMR (CDCl$_3$, 400MHz) δ$_H$ ppm: 1.39 - 1.51 (m, 2H, C$\underline{H}_2$), 2.58 (td, *J*=7.65, 3.26 Hz, 2H, CH$_2$), 2.94 - 3.14 (m, 4H, 2× CH$_2$), 3.61 (s, 1H, C$\underline{H}_3$ major isomer), 3.61 (s, 1H, C$\underline{H}_3$ minor isomer), 3.68 - 3.72 (m, 2H, CH$_2$), 3.85 (s, 3H, CH$_3$), 3.90 (s, 1H, C$\underline{H}_3$ major isomer), 3.91 (s, 1H, C$\underline{H}_3$ minor isomer), 3.94 (s, 1H, C$\underline{H}_3$ minor isomer), 3.95 (s, 1H, C$\underline{H}_3$ major isomer), 5.50 (br s, 1H, ArO$\underline{H}$), 6.36 (s, 1H, C=C$\underline{H}$), 6.48 - 6.50 (m, 1H, Ar$\underline{H}$), 6.92 (m, 1 H, Ar$\underline{H}$), 6.96 - 6.99 (m, 2H, 2×Ar$\underline{H}$).

^{13}C NMR (CDCl$_3$, 100.71 MHz) δ$_c$ ppm: 20.8 ($\underline{C}$H$_2$ major isomer), 21.3 ($\underline{C}$H$_2$ major isomer), 22.7 ($\underline{C}$H$_2$ minor isomer), 23.2 ($\underline{C}$H$_2$ minor isomer), 30.1 ($\underline{C}$H$_2$ minor isomer), 32.4 ($\underline{C}$H$_2$ major isomer), 35.8 ($\underline{C}$H$_2$ major isomer), 36.7 ($\underline{C}$H$_2$ minor isomer), 56.0 ($\underline{C}$H$_3$), 56.2 ($\underline{C}$H$_3$), 61.0 ($\underline{C}$H$_3$), 61.3 ($\underline{C}$H$_3$), 66.7 ($\underline{C}$H$_2$ minor isomer), 69.9 ($\underline{C}$H$_2$ major isomer), 109.8 ($\underline{C}$H minor isomer), 110.9 ($\underline{C}$H major isomer), 111.9 ($\underline{C}$H major isomer), 112.5 ($\underline{C}$H minor isomer), 118.5 ($\underline{C}$H minor isomer), 119.3 ($\underline{C}$H major isomer), 121.6 ($\underline{C}$H minor isomer), 122.9 ($\underline{C}$H minor isomer), 123.8 ($\underline{C}$H major isomer), 124.7 ($\underline{C}$H major isomer), 124.9 ($\underline{C}$H minor isomer), 125.6 ($\underline{C}$H major isomer), 129.3 (Q major isomer), 130.1 (Q minor isomer), 132.2 (Q minor isomer),

132.7 (Q major isomer), 134.9 (Q minor isomer), 136.8 (Q major isomer), 141.4 (Q major isomer), 142.8 (Q minor isomer), 144.9 (Q major isomer), 150.6 (Q minor isomer), 150.7 (Q minor isomer), 150.9 (Q major isomer), 151.3 (Q major isomer), 151.5 (Q minor isomer), 152.5 (Q major isomer), 152.9 (Q minor isomer), 155.1 (Q minor isomer), 156.6 (Q major isomer), 165.4 (Q, $\underline{C}$=N), 179.1 ($\underline{C}$=O).

HRMS (- ESI): Calculated Mass 471.1893. Found 470.1808.

V_{max} (DCM)/cm^{-1}: 3339, 2999, 1712, 1610, 1333, 1079, 737.

6.1.38 Synthesis of 7-((tert-butyldiphenylsilyl)oxy)-2,3,4-trimethoxy-6,7-dihydro-5H-benzo[7]annulen-9-yl trifluoromethanesulfonate (2.54).

To a three-necked round bottomed flask under an atmosphere of N_2 at -78 °C in an acetone/CO_2 cooling bath was added diisopropylamine (1.00 g, 1.40 mL, 10.00 mmol) and dry THF (10 mL). To this was added 2.5 M BuLi in THF (4.00 mL, 10.00 mmol) dropwise. The resultant mixture was stirred for 20 min after which time a solution of *(2.25)* (2.50 g, 5.00 mmol) in THF (10 mL) was added. This mixture was stirred for a further 2 h at this temperature before the addition of a solution of 2-[N,N- bis(trifluoromethylsulfonyl)amino]-5-chloropyridine (2.90 g, 7.50 mmol) in THF (10 mL). Following further stirring for 2 h, the reaction was quenched with the slow addition of 2 M aq. HCl (40 mL). Following extraction of the organic compounds into Et_2O (3×50 mL), the combined organic extracts were washed once with H_2O (50 mL), dried over $MgSO_4$, filtered and concentrated *in* vacuo. The product was purified using column chromatography, eluting using hexane/EtOAc (9:1) to yield a colourless oil.

Yield: 2.89 g, 4.53 mmol, 90.8%.

^{1}H NMR (CDCl$_3$, 400MHz) δ_H ppm: 1.23 (9H, s, C(C$\underline{H}_3$)$_3$), 1.92 (1H, m, C$\underline{H}_2$), 2.27 (1H, m, C$\underline{H}_2$), 2.59 (1H, m, C$\underline{H}_2$), 3.00 (1H, m, C$\underline{H}_2$), 3.76 (3H, s, O$\underline{Me}$), 3.87 (3H, s, O$\underline{Me}$), 3.93 (3H, s, O$\underline{Me}$), 4.30 (1H, m, C$\underline{H}$OSi), 6.13 (1H, d, J=4.7Hz, C=C$\underline{H}$), 6.82 (1H, s, Ar$\underline{H}$), 7.38-7.48 (6H, m, 6×Ar$\underline{H}$) 7.67-7.78 (4H, m, 4×Ar$\underline{H}$).

¹³C NMR (CDCl₃, 400MHz) δ_c ppm: 19.1 (Q, tBu), 20.4 (CH₂), 26.6 (CH₃), 39.7 (CH₂), 56.0 (CH₃), 60.9 (CH₃), 61.5 (CH₃), 68.6 (CHOSi) 106.0 (CH), 126.6 (CH) 127.0 (Q) 127.7 (2×CH), 127.8 (2×ArCH), 129.0 (Q), 129.7 (Q), 133.4 (Q), 133.6 (Q), 134.8 (2×CH), 135.26 (Q), 135.78 (2×CH), 143.54 (Q), 143.88 (Q), 150.89 (Q), 151.52 (Q).

HRMS (+ ESI): Calculated Mass 659.1723. Found 659.1707 (M+Na)⁺.

V_max (DCM)/cm⁻¹: 3482, 3071, 3050, 2999, 2893, 1654, 1595, 1569, 1348, 1267, 943, 838, 803, 636.

Melting Point: 40-43 °C.

6.1.39 Synthesis of tert-butyl 5-bromo-2-methoxyphenylcarbamate (2.57).

To as stirred solution of 5-bromo-2-methoxy aniline (5.1 g, 25.24 mmol) in THF under an atmosphere of N2 was added di-*tert*-butyl dicarbonate (11.02 g, 50.48 mmol). The resulting mixture was stirred under reflux at 90 °C for 12 h. The reaction mixture was quenched by addition of H₂O (50 mL) before removal of THF *in vacuo*. The products were extracted with Et₂O (3×50 mL) and the combined organic extracts were dried over MgSO₄ before filtration and removal of the solvent *in vacuo*. Excess Boc anhydride was removed under high vacuum before the product was isolated in its pure form using hexane\EtOAc 3:1 as the mobile phase.

Yield: 5.20 g, 16.49 mmol, 89%.

¹H NMR (CDCl₃, 400MHz) δ_H ppm: 1.53 (s, 9H, ᵗBu(Boc)), 3.85 (s, 3H, CH₃), 6.70 (d, J=9.00 Hz, 1H, ArH), 7.07 (d, J=10 Hz, 1H, ArH). 7.08 (s, 1H, ArH), 8.29 (br s, 1H, NHBoc).

¹³C NMR (CDCl₃, 100.71 MHz) δ_c ppm: 27.8 (CH₃ (Boc)), 55.4 (CH₃), 84.7 (Q (Boc)), 110.7 (CH), 120.1 (CH), 124.2 (CH), 128.9 (Q), 146.0 (Q), 146.3 (Q), 151.9 (CONH).

MS (ESI): Calculated Mass 200.9789. Found 201.9855 (M+H)⁺.

V_max (DCM)/cm⁻¹: 3440, 2982, 1810, 1730, 1522, 1377, 1235, 1071, 846.

Melting Point: 110 °C.

6.1.40 Synthesis of tert-butyl 2-methoxy-5-(4,4,5,5-tetramethyl-1,3,2-dioxaborolan-2-yl)phenylcarbamate (2.55).

To a stirred solution of *(2.57)* (3.07 g, 10.20 mmol) in DMSO (30 mL) was added KOAc (4.00 g, 40.77 mmol), bis-pinacolatodiboron (4.14 g, 16.31 mmol) and PdCl$_2$(dppf) (0.30 g, 0.03 mmol). The resulting mixture was stirred at 80 °C for 90 min. Upon completion of the reaction, the product was extracted between H$_2$O (50 mL) and Et$_2$O (3×50 mL). The combined organic extracts were subsequently washed with H$_2$O (50 mL) before being dried over MgSO$_4$, filtered and concentrated *in vacuo*. The resulting residue was purified using column chromatography, eluting with a 6:1 mixture of hexane/EtOAc. The combined homogeneous fractions were combined and reduced to yield the product as a colourless solid.

Yield: 3.43 g, 10.08 mmol, 98%.

^{1}H NMR (CDCl$_3$, 400MHz) δ$_H$ ppm: 1.33 (s, 12H, 4×CH$_3$), 1.55 (s, 9H, ^{t}Bu), 3.90 (s, 3H, OMe), 6.86 (d, J=8.03Hz, 1H, ArH), 7.01-7.11 (m, 1H, ArH), 7.42-7.49 (m, 1H, ArH), 8.34-8.57 (m, 1H, NHBoc).

^{13}C NMR (CDCl$_3$, 100.71 MHz) δ$_c$ ppm: 24.4 (CH3), 24.6 (CH$_3$), 55.1 (CH$_3$), 83.1 (Q), 108.8 (CH), 123.6 (Q), 127.0 (CH), 129.3 (CH), 149.6 (Q), 152.2 (Q), 158.9 (C=O Boc).

MS (ESI +): Calculated mass 372.1958, Found 395.1895 (M+Na)$^+$.

V$_{max}$ (DCM)/cm^{-1}: 3443, 2979, 1732, 1604, 1536.

Melting Point: 44 -47 °C.

6.1.41 Synthesis of tert-butyl (5-(7-((tert-butyldiphenylsilyl)oxy)-2,3,4-trimethoxy-6,7-dihydro-5H-benzo[7]annulen-9-yl)-2-methoxyphenyl)carbamate (2.56).

(2.54) (1.40 g, 2.20 mmol), *(2.56)* (1.16 g, 3.30 mmol), K$_2$CO$_3$ (0.91 g, 6.59 mmol) and Pd(PPh$_3$)$_4$ (0.25 g, 0.21 mmol) were combined in a mixture of toluene (18 mL), EtOH (6 mL) and H$_2$O (6 mL) and stirred at 60 °C for 50 min. Following completion of the reaction, monitored by TLC, the product was extracted between 10% aq. NaHCO$_3$ (40 mL) and Et$_2$O

(3×40 mL). The combined organic extracts were washed over MgSO$_4$, filtered and concentrated in vacuo. The resultant residue was purified using Flash Column Chromatography using a 5:1 mixture of hexane/EtOAc as the eluting solvent, affording the product as a yellow oil.

Yield: 1.29 g, 1.81 mmol, 82.7%.

^{1}H NMR (CDCl$_3$, 400MHz) δ$_H$ ppm: 1.32 (s, 9H, <u>t</u>Bu), 1.34 (s, 9H, <u>t</u>Bu), 2.07-2.21 (m, 3H), 2.73-2.81 (m, 1H), 3.60 (s, 3H, C<u>H</u>$_3$), 3.82 (s, 3H, C<u>H</u>$_3$), 3.84 (s, 3H, C<u>H</u>$_3$), 3.90 (s, 3H, C<u>H</u>$_3$), 4.09-4.17 (m, 1H, C<u>H</u>OSi), 6.62 (s, 1H, C=C<u>H</u>), 6.83-6.91 (m, 1H, Ar<u>H</u>), 7.01 (d, J=4.52 Hz, 1H, Ar<u>H</u>), 7.30-7.34 (m, 2H, 2×Ar<u>H</u>), 7.39 (dd, J=18.6 Hz, 7.5Hz, 4H, 4×Ar<u>H</u>), 7.60 (m, 4H, 4×Ar<u>H</u>), 7.74 (d, J=6.53 Hz, 2H, 2×Ar<u>H</u>), 8.41-8.55 (m, 1H, N<u>H</u>Boc).

^{13}C NMR (CDCl$_3$, 100.71 MHz) δ$_c$ ppm: 19.2 (<u>C</u>H$_3$), 21.9 (<u>C</u>H$_2$), 27.0 (<u>C</u>H$_3$), 28.4 (<u>C</u>H$_3$), 43.8 (<u>C</u>H$_2$), 55.8 (<u>C</u>H$_3$), 56.0 (<u>C</u>H$_3$), 60.8 (<u>C</u>H$_3$), 61.5 (<u>C</u>H$_3$), 71.3 (<u>C</u>H), 80.4 (COO<u>C</u>(CH$_3$)$_3$) 108.8 (<u>C</u>H), 109.4 (<u>C</u>H), 118.1 (<u>C</u>H), 122.2 (<u>C</u>H), 127.4 (2×<u>C</u>H), 127.5 (2×<u>C</u>H), 127.8 (Q), 128.0 (Q), 129.4 (<u>C</u>H), 129.4 (<u>C</u>H), 133.0 (<u>C</u>H), 134.2 (Q), 134.4 (Q), 134.4 (Q), 134.5 (Q), 135.7 (2×<u>C</u>H), 135.8 (2×<u>C</u>H), 137.9 (Q), 141.1 (Q), 147.1 (Q), 150.6 (Q), 150.8 (Q), 152.7 (<u>C</u>=O).

HRMS (+ ESI): Calculated Mass 709.3435. Found 710.3508 (M+H)$^+$.

V$_{max}$ (DCM)/cm^{-1}: 3440, 2982, 1810, 1771, 1595, 1522, 1372, 1235, 1071, 846.

6.1.42 Synthesis of tert-butyl 5-((Z)-6,7-dihydro-7-hydroxy-2,3,4-trimethoxy-5H-benzo[7]annulen-9-yl)-2-methoxyphenylcarbamate (2.58).

To a stirred solution of *(2.57)* (1.10 g, 1.54 mmol) in dry THF (4 mL) under a blanket of N$_2$ at 0 °C was added dropwise a 1 M solution of TBAF in THF (1.65 mL, 1.65 mmol). The mixture was allowed to elevate to room temperature over 1 h and allowed to stir for a further 2 h. Upon completion of the reaction, the solvents were removed under a stream of N$_2$ before being purified using column chromatography (hexane/EtOAc 2:1) furnishing the product as a colourless oil.

Yield: 0.59 g, 1.25 mmol, 81.1%.

¹H NMR (CDCl₃, 400MHz) δ_H ppm: 1.53 (s, 9H. tBu), 2.32-2.60 (m, 2H, CH₂), 3.00-3.09 (m, 2H, CH₂), 3.70 (s, 3H, CH₃), 3.90 (s, 3H, CH₃), 3.92 (s, 3H, CH₃), 3.94 (s, 3H, CH₃), 4.13-4.22 (m, 1H, CHOH), 6.36 (d, J=5 Hz, 1H, ArH), 6.39 (s, 1H, C=CH), 6.79 (s, 2H, 2×ArH), 7.09 (s, 1H, ArH), 8.18 (br s, 1H, NHBoc).

¹³C NMR (CDCl₃, 100.71 MHz) δ_c ppm: 21.4 (CH₂), 22.3 (Q, tBu), 27.9 (CH₃ (Fmoc)), 42.9 (CH₂), 55.3 (CH₃), 55.6 (CH₃), 60.4 (CH₃), 61.1 (CH₃), 69.4 (CHOH), 108.4 (CH), 109.0 (ArCH), 117.1 (CH), 122.0 (CH), 127.5 (Q), 127.7 (Q), 131.5 (CH), 133.7 (QC), 134.9 (Q), 138.4 (Q), 140.9 (Q), 147.7 (Q), 150.3 (Q), 150.6 (Q), 152.28 (Q).

HRMS (+ ESI): Calculated mass 494.2155, Found 494.2211.

V_max (DCM)/cm⁻¹: 2066.14, 1643.67, 1528.58, 1488.47, 1406.30.

Melting Point: 180 °C.

6.1.43 Synthesis of tert-butyl 5-((Z)-6,7-dihydro-2,3,4-trimethoxy-7-oxo-5H-benzo[7]annulen-9-yl)-2-methoxyphenylcarbamate (2.59).

To a stirred solution of *(2.58)* (0.50 g, 1.06 mmol) in DCM (10 mL) at 0 °C was added Dess-Martin periodinane (0.90 g, 2.12 mmol) over a period of 2 min. After 10 min, the reaction was quenched by addition of 10% aq. NaHCO₃ (30 mL). Following the extraction of the product using Et₂O (3×30 mL), the combined organic extracts were dried over MgSO₄, filtered and concentrated in vacuo. Purification by column chromatography (hexane/EtOAc 3:1) yielded the product as a colourless oil.

Yield: 0.41 g, 0.87 mmol, 82%.

¹H NMR (CDCl₃, 400MHz) δ_H ppm: 1.51 (s, 9H, tBu), 2.68-2.78 (m, 2H, CH₂), 3.09-3.23 (m, 2H, CH₂), 3.63 (s, 3H, CH₃), 3.90 (s, 3H, CH₃), 3.93 (s, 3H, CH₃), 3.95 (s, 3H, CH₃), 6.40 (s, 1H, C=CH), 6.41 (s, 1H, ArH), 6.85 (d, J=8.03 Hz, 1H, ArH), 6.96 (d, J=7.53 Hz, 1H, ArH), 7.10 (s, 1H, ArH), 8.09 (br s, 1H, NHBoc).

¹³C NMR (CDCl₃, 100.71 MHz) δ_c ppm: 19.8 (C̲H₂), 27.9 (C̲H₃), 45.0 (C̲H₂), 55.3 (C̲H₃), 55.7 (C̲H₃), 60.5 (C̲H₃), 60.9 (C̲H₃), 108.9 (C̲H), 111.7 (C̲H), 118.3 (C̲H), 123.1 (C̲H), 127.4 (Q), 127.9 (C̲H), 128.8 (Q), 132.1 (Q), 135.1 (Q), 142.8 (Q), 147.7 (Q), 149.5 (Q), 150.6 (Q), 151.7 (Q), 152.1 (NHC̲OBoc), 203.54 (C̲=O).

HRMS (+ ESI): Calculated Mass 469.2101. Found 470.2165 (M+H)⁺.

V_max (DCM)/cm⁻¹: 3436, 2975, 1727, 1528, 1364, 1246, 1116, 1030, 810, 765.

6.1.44 Synthesis of (9H-fluoren-9-yl)methyl (2-methoxy-5-(2,3,4-trimethoxy-7-oxo-6,7-dihydro-5H-benzo[7]annulen-9-yl)phenyl)carbamate *(2.61)*.

To a stirred solution of (9H-fluoren-9-yl) methyl (5-(7-hydroxy-2,3,4-trimethoxy-6,7-dihydro-5H-benzo[7]annulen-9-yl)-2-methoxyphenyl)carbamate (0.25 g, 0.42 mmol) in DCM (5 mL) at 0 °C was added Dess-Martin Periodinane (0.27 g, 0.50 mmol). After 10 min, the reaction was quenched by the addition of 10% aq. NaHCO₃ (25 mL) and the product was extracted into Et₂O (3×30 mL). The combined organic extracts were dried over MgSO₄, filtered and concentrated in vacuo to yield a residue which was subsequently purified using flash column chromatography (hexane/EtOAc 3:1) furnishing the product as a colourless oil.

Yield: 0.24 g, 0.41 mmol, 96.4%.

¹H NMR (CDCl₃, 400MHz) δ_H ppm: 2.71-2.78 (m, 2H, C̲H₂), 3.13-3.20 (m, 2H, C̲H₂), 3.63 (s, 3H, C̲H₃), 3.91 (s, 3H, C̲H₃), 3.96 (s, 3H, C̲H₃), 3.97 (s, 3H, C̲H₃), 4.30 (t, J=6.48 Hz, 1H, C̲H (Fmoc)), 4.51 (d, J=7.04 Hz, 2H, C̲H₂ (Fmoc)), 6.39 (s, 1H), 6.42 (s, 1H), 6.90 (d, J=8.04 Hz, 1H, ArH̲), 7.06 (d, J=8.04 Hz, 1H, ArH̲), 7.35 (t, J=7.52 Hz, 2H, ArH̲ (Fmoc)), 7.44 (t, J=7.52 Hz, 2H, ArH̲, (Fmoc)), 7.65 (d, J=7.04 Hz, 2H, ArH̲ (Fmoc)), 7.80 (d, J=7.00 Hz, 2H, ArH̲ (Fmoc)), 8.12 (br s, 1H, NH̲Fmoc).

¹³C NMR (CDCl₃, 100.71 MHz) δ_c ppm: 19.8 (C̲H₂), 45.1 (C̲H), 46.7 (C̲H₂), 55.4 (C̲H₃), 55.7 (C̲H₃), 60.5 (C̲H₃), 60.9 (C̲H₃), 66.6 (C̲H₂), 109.2 (C̲H), 111.6 (C̲H), 119.6 (C̲H), 123.6 (C̲H), 124.6 (C̲H), 126.7 (C̲H), 127.4 (C̲H), 128.1 (C̲H), 128.8 (Q), 132.0 (Q), 135.2 (Q), 140.9 (Q),

142.9 (Q), 143.3 (Q), 147.9 (Q), 149.5 (Q), 150.6 (Q), 151.4 (Q), 152.7 (Q, $\underline{C}$ONHFmoc), 203.5 (C=O ketone).

HRMS (ESI): Calculated Mass 591.2257. Found 592.2339 (M+H)$^+$.

V$_{max}$ (DCM)/cm^{-1}: 2983, 1731, 1701, 1501, 1414, 1231, 1062, 732.

6.1.45 **Synthesis of 9-(3-amino-4-methoxyphenyl)-2,3,4-trimethoxy-5H-benzo[7]annulen-7(6H)-one** *(2.02).*

To a stirred solution of *(2.61)* (0.20 g, 0.34 mmol) in THF (1 mL) under a blanket of N$_2$ at 0 °C was added a 1 M solution of TBAF (0.40 mL, 0.40 mmol). After 5 min, the solvents were removed under a stream of N$_2$ and the product was purified via flash column chromatography as a colourless oil, eluting with a mobile phase of 2:1 hexane/EtOAc.

Yield: 0.12 g, 0.32 mmol, 94%.

^{1}H NMR (CDCl$_3$, 400MHz) δ$_H$ ppm: 2.69-2.78 (m, 2H, C$\underline{H}_2$), 3.11-3.18 (m, 2H, C$\underline{H}_2$), 3.65 (s, 3H, C$\underline{H}_3$), 3.91 (s, 6H, 2×C$\underline{H}_3$), 3.96 (s, 3H, C$\underline{H}_3$), 6.38 (s, 1H, C=C$\underline{H}$), 6.43 (s, 1H, Ar$\underline{H}$), 6.71-6.82 (m, 3H, 3×Ar$\underline{H}$).

^{13}C NMR (CDCl$_3$, 100.71 MHz) δ$_c$ ppm: 19.8 ($\underline{C}$H$_2$), 45.2 ($\underline{C}$H$_2$), 55.1 ($\underline{C}$H$_3$), 55.6 ($\underline{C}$H$_3$), 60.5 ($\underline{C}$H$_3$), 61.0 ($\underline{C}$H$_3$), 109.3 ($\underline{C}$H), 111.5 ($\underline{C}$H), 115.1 ($\underline{C}$H), 119.3 ($\underline{C}$H), 127.3 ($\underline{C}$H), 128.6 (Q), 132.2 (Q), 135.0 (Q), 135.3 (Q), 142.7 (Q), 147.6 (Q), 149.4 (Q), 150.5 (Q), 151.9 (Q), 203.9 ($\underline{C}$=O).

HRMS (ESI+): Calculated 369.1576. Found 370.1627 (M+H)$^+$, 392.1443 (M+Na)$^+$.

V$_{max}$ (DCM)/cm^{-1}: 3583, 2932, 1731, 1531, 1450, 1248, 1099, 901, 703.

6.1.46 Synthesis of (9H-fluoren-9-yl)methyl (1-((2-methoxy-5-(2,3,4-trimethoxy-7-oxo-6,7-dihydro-5H-benzo[7]annulen-9-yl)phenyl)amino)-4-methyl-1-oxopentan-2-yl)carbamate *(2.62)*.

To a stirred solution of *(2.02)* (0.05 g, 0.14 mmol) under an atmosphere of N_2 in dry DCM (5 mL) at 0 °C was added dropwise a solution of N-Fmoc Leucine (0.14 g, 0.41 mmol), PyBrop (0.10 g, 0.20 mmol) and DIPEA (0.10 mL, 0.54 mmol) in dry DCM (2 mL). The reaction temperature was allowed to reach room temperature and stirred for a subsequent 6 h. After quenching with 1 M aq. HCl (15 mL), the product was extracted into Et_2O (3×20 mL). The combined organic extracts were dried over $MgSO_4$, filtered and concentrated in vacuo. The product was purified using flash column chromatography (stationary phase; silica gel 230-240 mesh, mobile phase 2:1 hexane/EtOAc). All homogeneous fractions were collected and the solvents were evaporated to afford *(2.62)* as a yellow oil.

Yield: 0.081 g, 0.12 mmol, 86%.

^{1}H NMR (CDCl$_3$, 400MHz) δ_H ppm: 0.89 (d, J=6.52 Hz, 6H, 2×C$\underline{H}_3$ (Leu)), 1.51-1.54 (m, 1H, C$\underline{H}$ (Leu)), 1.70-1.81 (m, 2H, C$\underline{H}_2$ (Leu)), 2.70-2.77 (m, 1H, C$\underline{H}$), 3.11-3.20 (m, 2H, C$\underline{H}_2$), 3.62 (s, 3H, C$\underline{H}_3$), 3.89 (s, 3H, C$\underline{H}_3$), 3.92 (s, 3H, C$\underline{H}_3$), 3.96 (s, 3H, C$\underline{H}_3$), 4.25 (t, J=6.25 Hz, 1H, C$\underline{H}$ (Fmoc)), 4.46 (d, J=6.5 Hz, 2H, C$\underline{H}_2$ (Fmoc)), 5.29 (d, J=6.5 Hz, 1H, C=C$\underline{H}$), 6.37 (s, 1H, Ar$\underline{H}$), 6.39 (s, 1H, Ar$\underline{H}$), 6.88 (d, J=8.00 Hz, 1H, Ar$\underline{H}$), 7.08 (d, J=7.04 Hz, 1H, Ar$\underline{H}$), 7.32 (t, J=7.28 Hz, 2H, ArH(Fmoc)), 7.42 (t, J=7.52 Hz, 2H, ArH(Fmoc)), 7.61 (d, J=8.12 Hz, 2H, Ar$\underline{H}$(Fmoc)), 7.79 (d, J=8.04 Hz, 2H, Ar$\underline{H}$(Fmoc)), 8.30 (s, 1H, N$\underline{H}$CO), 8.36 (s, 1H, N$\underline{H}$CO).

^{13}C NMR (CDCl$_3$, 100.71 MHz) δ_c ppm: 19.8 ($\underline{C}H_2$), 22.5 ($\underline{C}H_3$), 24.8 ($\underline{C}H$), 41.0 ($\underline{C}H_2$), 45.1 ($\underline{C}H_2$), 46.7 ($\underline{C}H$), 54.0 ($\underline{C}H$), 55.5 ($\underline{C}H_3$), 55.7 ($\underline{C}H_3$), 60.5 ($\underline{C}H_3$), 61.0 ($\underline{C}H_3$), 66.8 ($\underline{C}H_2$), 109.2 ($\underline{C}H$), 111.6 ($\underline{C}H$), 119.6 ($\underline{C}H$), 120.2 ($\underline{C}H$), 124.5 ($\underline{C}H$), 124.8 ($\underline{C}H$), 126.4 (Q), 126.6 ($\underline{C}H$), 127.3 ($\underline{C}H$), 128.2 ($\underline{C}H$), 128.7 (Q), 131.9 (Q), 135.1 (Q), 140.8 (Q), 142.9 (Q), 143.2 (Q), 143.3 (Q), 148.3 (Q), 149.5 (Q), 150.6 (Q), 151.3 (Q), 169.7 ($\underline{C}$ONH Leu), 203.5 ($\underline{C}$=O Ketone).

HRMS (ESI+): Calculated Mass 704.3098. Found 727.2979 (M+H)$^+$.

V_{max} **(DCM)/cm^{-1}**: 3411, 2987, 1731, 1667, 1293, 991, 703.

6.1.47 Synthesis of 2-(((9-(3-((tert-butoxycarbonyl)amino)-4-methoxyphenyl)-2,3,4-trimethoxy-5H-benzo[7]annulen-7(6H)-ylidene)amino)oxy)acetic acid (2.63).

To a stirred solution of **(2.59)** (0.0381 g, 0.081 mmol) in EtOH (2.5 mL) and H_2O (0.5 mL), was added (O-carboxymethyl) hydroxylamine hemi-hydrochloride (0.0115 g, 0.105 mmol) and NaOAc (0.0107 g, 0.129 mmol). The resultant mixture was stirred at room temperature for 4 h, until complete consumption of the starting material was observed using TLC (hexane/EtOAc 1:1). The mixture was diluted in H_2O (10 mL) and the product was extracted using Et_2O (3x15 mL). The product was isolated as a mixture of isomers by column chromatography using EtOAc as the mobile phase, in the form of a yellow oil.

Yield: 0.0307 g, 0.056 mmol, 70%.

^{1}H NMR (CDCl$_3$, 400MHz) δ_H ppm: 1.51 (s, 9H, ^{t}Bu), 2.75-2.79 (m, 1H, C$\underline{H}_2$ minor isomer), 2.90-2.97 (m, 1H, C$\underline{H}_2$ major isomer), 2.97-3.02 (m, 1H, C$\underline{H}_2$ major isomer), 3.02-3.06 (m, 1H, C$\underline{H}_2$ minor isomer), 3.63 (s, 3H, OC$\underline{H}_3$), 3.89 (s, 1H, OC$\underline{H}_3$ minor isomer), 3.90 (s, 2H, OC$\underline{H}_3$ major isomer), 3.91 (s, 2H, OC$\underline{H}_3$ major isomer), 3.92 (s, 1H, OC$\underline{H}_3$ minor isomer), 3.92 (s, 2H, OC$\underline{H}_3$ major isomer), 3.94 (s, 1H, OC$\underline{H}_3$ minor isomer), 4.67 (s, 1H, C$\underline{H}_2$ minor isomer), 4.69 (s, 1H, C$\underline{H}_2$ major isomer), 6.34 (s, 1H, Ar$\underline{H}$ major isomer), 6.38 (s, 1H, Ar$\underline{H}$ minor isomer), 6.55 (s, 1H), 6.80-6.86 (m, 1H, Ar$\underline{H}$), 6.95-7.03 (m, 2H), 7.12 (s, 1H, N$\underline{H}$Boc).

^{13}C NMR (CDCl$_3$, 100.71 MHz) δ_c ppm: 14.2 (Q), 21.3 ($\underline{C}H_2$ major isomer), 21.9 ($\underline{C}H_2$ minor isomer), 28.4 ($\underline{C}H_3$), 29.7 ($\underline{C}H_2$ minor isomer), 30.3 ($\underline{C}H_3$ minor isomer), 32.9 ($\underline{C}H_2$ major isomer), 55.7 ($\underline{C}H_3$), 56.1 ($\underline{C}H_3$), 60.8 ($\underline{C}H_3$), 61.3 ($\underline{C}H_3$), 70.1 ($\underline{C}H_2$ minor isomer), 70.3 ($\underline{C}H_2$ major isomer), 109.4 ($\underline{C}H$), 110.9 ($\underline{C}H$ major isomer), 111.9 ($\underline{C}H$ minor isomer), 123.3 ($\underline{C}H$), 123.5 ($\underline{C}H$), 123.6 ($\underline{C}H$), 127.7 (Q), 128.2 (Q), 128.5 (Q), 130.0 (Q), 133.4 (Q), 136.6 (Q), 142.3 (Q), 146.4 (Q), 147.5 (Q), 150.0 (Q), 162.0 (Q, $\underline{C}$=N), 174.0 (Q, $\underline{C}$OOH).

HRMS: Calculated Mass 542.2264. Found 541.2206 (M-H)⁻.

V_{max} **(DCM)/cm⁻¹**: 3432, 3318, 2930, 1726, 1589, 1490, 1368, 1248, 1077, 1030, 810, 736.

6.1.48 Synthesis of 2-((((9-(3-(2-(((((9H-fluoren-9-yl)methoxy)carbonyl)amino)-4-methylpentanamido)-4-methoxyphenyl)-2,3,4-trimethoxy-5H-benzo[7]annulen-7(6H)-ylidene)amino)oxy)acetic acid *(2.64)*.

To a stirred solution of **(2.62)** (0.0650 g, 0.092 mmol) in EtOH (1.5 mL) and H₂O (0.5 mL), was added (O-carboxymethyl) hydroxylamine hemi-hydrochloride (0.0197 g, 0.18 mmol) and NaOAc (0.0123 g, 0.150 mmol). The resultant mixture was stirred at room temperature for 4 h, until complete consumption of the starting material was observed using TLC (hexane/EtOAc 1:1). The mixture was diluted in H₂O (10 mL) and the product was extracted using Et₂O (3x15 mL). The product was isolated as a mixture of isomers by column chromatography using EtOAc as the mobile phase, in the form of a yellow oil.

Yield: 0.0494 g, 0.064 mmol, 69%.

¹H NMR (CDCl₃, 400MHz) δ_H ppm: 0.93 (d, J=6Hz, 6H, 2×CH₃), 1.19-1.22 (m, 2H, CH₂), 2.01-2.03 (m, 1H, CH), 2.56-2.58 (m, 1H, CH), 2.77-2.80 (m, 1H, 1×CH₂), 2.99-3.06 (m, 3H, 3×CH₂), 3.64 (s, 3H, CH₃ minor isomer), 3.65 (s, 3H, CH₃ major isomer), 3.85 (s, 3H, CH₃ major isomer), 3.86 (s, 3H, CH₃ minor isomer), 3.87 (s, 3H, CH₃ major isomer), 3.88 (s, 3H, CH₃ minor isomer), 3.92 (s, 3H, CH₃ major isomer), 3.93 (s, 3H, CH₃ minor isomer), 4.38 (s, 2H, CH₂ major isomer), 4.39 (s, 1H, CH₂ minor isomer), 4.54-4.55 (m, 2H, CH₂ (Fmoc)), 4.68-2.70 (m, 1H, CH(Fmoc)), 6.40 (s, 1H, C=CH), 6.51 (s, 1H, ArH), 6.87-6.90 (m, 2H, 2×ArH), 6.99-7.01 (m, 1H, ArH), 7.35-7.37 (m, 2H, 2×ArH(Fmoc)), 7.44-7.46 (m, 2H, 2×ArH(Fmoc)), 7.52-7.54 (m, 2H, 2×ArH(Fmoc)), 7.60-7.62 (m, 2H, 2×ArH(Fmoc)), 8.15-8.35 (2×br. S, 2H, 2×CONH).

¹³C NMR (CDCl₃, 100.71 MHz) δ_c ppm: : 19.5 (CH₂ minor isomer), 20.8 (CH₂ major isomer), 22.3 (CH₃ major isomer), 22.9 (CH₃ minor isomer), 24.3 (CH minor isomer), 24.9 (CH major

isomer), 41.1 (CH₂ major isomer), 41.4 (CH₂ minor isomer), 45.2 (CH₂ minor isomer), 45.7 (CH₂ major isomer), 46.5 (CH minor isomer), 46.9 (CH major isomer), 53.1 (CH minor isomer), 54.0 (major isomer), 56.0 (CH₃), 56.4 (CH₃), 61.5 (CH₃), 61.8 (CH₃), 64.9 (CH₂ minor isomer), 65.6 (CH₂ major isomer), 67.9 (CH₂ minor isomer), 68.5 (CH₂ major isomer), 110.4 (CH minor isomer), 111.4 (CH major isomer) 112.3 (CH major isomer), 112.9 (CH minor isomer), 118.2 (CH major isomer), 118.5 (CH minor isomer), 119.4 (CH minor isomer), 119.8 (CH major isomer), 122.6 (CH minor isomer), 122.9 (CH minor isomer), 123.6 (CH major isomer), 123.9 (Q major isomer), 124.1 (Q minor isomer), 124.8 (CH major isomer), 125.2 (CH minor isomer), 125.9 (CH major isomer), 126.6 (CH major isomer), 126.8 (CH minor isomer), 127. 7 (CH major isomer), 128.1 (CH minor isomer), 128.5 (CH minor isomer), 128.7 (CH major isomer), 129.4 (Q major isomer), 130.0 (Q minor isomer), 132.3 (Q minor isomer), 132.8 (Q major isomer), 134.3 (Q minor isomer), 136.5 (Q major isomer), 141.2 (Q major isomer), 142.2 (Q minor isomer), 143.2 (Q major isomer), 143.8 (Q minor isomer), 144.4 (Q major isomer), 144.8 (Q minor isomer), 149.1 (Q minor isomer), 149.3 (Q major isomer), 151.2 (Q major isomer), 151.7 (Q minor isomer), 152.5 (Q major isomer), 153.0 (Q minor isomer), 155.4 (Q minor isomer), 156.9 (Q major isomer), 165.4 (Q, C=N), 173.2 (C=O), 178.1 (C=O).

HRMS: Calculated Mass 777.3261. Found 776.3189.

V_max (DCM)/cm⁻¹: 3532, 3411, 2981, 1731, 1678, 1335, 1057, 1039, 834, 701.

6.1.49 Synthesis of perfluorophenyl 2-(((9-(3-((tert-butoxycarbonyl)amino)-4-methoxyphenyl)-2,3,4-trimethoxy-5H-benzo[7]annulen-7(6H)-ylidene)amino)oxy)acetate (2.65).

To a stirred solution of **(2.63)** (0.0312 g, 0.058 mmol) in DCM (1 mL) under an atmosphere of N₂ at 0 °C was added a solution of pentafluorophenol (0.0116 g, 0.063 mmol) in DCM (0.75 mL). This was followed by the subsequent addition of DCC (0.0137 g, 0.063 mmol) in DCM (0.75 mL). The solution was stirred for 1 h, after which time the dicyclohexylurea by-product

was removed via filtration. The crude DCM residue was then concentrated *in vacuo* to be purified using column chromatography with hexane/EtOAc (7:1) as the mobile phase yielding the desired compound as a colourless oil, in a mixture of syn- and anti- isomers.

Yield: 0.029 g, 0.0412 mmol, 71%.

^{1}H NMR (CDCl$_3$, 600MHz) δ$_H$ ppm: 1.51 (s, 3H, ^{t}Bu minor isomer), 1.52 (s, 3H, ^{t}Bu major isomer), 2.76-2.80 (m, 1H, ring C$\underline{H}_2$ minor isomer), 2.97 (br s, 1H, ring C$\underline{H}_2$ major isomer), 3.00-3.05 (m, 2H, ring C$\underline{H}_2$, mixture of isomers), 3.62 (s, 1H, OC$\underline{H}_3$ minor isomer), 3.63 (s, 2H, OC$\underline{H}_3$ major isomer), 3.90 (s, 1H, OC$\underline{H}_3$ minor isomer), 3.93 (s, 4H, 2 x OC$\underline{H}_3$ major isomers), 3.94 s, 1H, OC$\underline{H}_3$ minor isomer), 4.97 (s, 1H, C$\underline{H}_2$ minor isomer), 5.01 (s, 1H, C$\underline{H}_2$ major isomer), 6.35 (s, 1H major isomer), 6.38 (s, 1H, minor isomer), 6.56 (s, 1H), 6.82-6.86 (m, 1H), 6.94-6.97 (m, 1H major isomer), 6.99-7.02 (m, 1H minor isomer), 7.05 (s, 1H, NHBoc), 7.08 (s, 1H, Ar$\underline{H}$ minor isomer), 7.09 (s, 1H, Ar$\underline{H}$ major isomer).

^{13}C NMR (CDCl$_3$, 151.71 MHz) δ$_c$ ppm: 21.2 ($\underline{C}H_2$ major isomer), 21.9 ($\underline{C}H_2$ minor isomer), 24.8 (Q), 25.4 (Q), 28.3 ($\underline{C}H_3$ minor isomer), 28.3 ($\underline{C}H_3$ major isomer), 32.8 ($\underline{C}H_2$ major isomer), 36.3 ($\underline{C}H_2$ minor isomer), 55.8 ($\underline{C}H_3$), 56.1 ($\underline{C}H_3$), 60.9 ($\underline{C}H_3$), 61.4 ($\underline{C}H_3$), 69.7 ($\underline{C}H_2$ minor isomer), 69.9 ($\underline{C}H_2$ major isomer), 109.4 ($\underline{C}H$), 111.0 ($\underline{C}H$ major isomer), 112.0 ($\underline{C}H$ minor isomer), 117.8 ($\underline{C}H$), 123.3 ($\underline{C}H$), 123.6 ($\underline{C}H$), 127.6 (Q), 127.7 (Q), 129.3 (Q), 133.4 (Q), 136.6 (Q), 137.0 (Q), 138.7 (Q), 142.3 (Q), 142.6 (Q), 146.5 (Q), 147.1 (Q), 147.5 (Q), 147.7 (Q), 149.9 (Q), 150.0 (Q), 150.9 (Q), 152.8 (Q), 158.7 (Q), 162.4 (Q, $\underline{C}$=N), 166.0 (Q, $\underline{C}$=O major isomer), 166.3 (Q, $\underline{C}$=O minor isomer).

HRMS (- ESI): Calculated Mass 723.2287. Found 724.2244 (M+H)$^+$.

V$_{max}$ (DCM)/cm^{-1}: 3005, 1724, 1478, 1275, 1026, 764.

6.1.50 Synthesis of perfluorophenyl 2-((((9-(3-(2-(((((9H-fluoren-9-yl)methoxy)carbonyl)amino)-4-methylpentanamido)-4-methoxyphenyl)-

2,3,4-trimethoxy-5H-benzo[7]annulen-7(6H)-ylidene)amino)oxy)acetate

(2.66).

To a stirred solution of **(2.64)** (0.0401 g, 0.051 mmol) in DCM (1 mL) under an atmosphere of N_2 at 0 °C was added a solution of PFP (0.0105 g, 0.057 mmol) in DCM (0.75 mL). This was followed by the addition of DCC (0.0117 g, 0.057 mmol) in DCM (0.75 mL). The solution was stirred for 1 h, after which time the dicyclohexylurea by-product was removed via filtration. The crude DCM residue was then concentrated *in vacuo* to be purified using column chromatography with hexane/EtOAc (7:1) as the mobile phase yielding the desired compound as a colourless oil, in a mixture of syn- and anti- isomers.

Yield: 0.038 g, 0.0403 mmol, 79%.

¹H NMR (CDCl₃, 600MHz) δ$_H$ ppm: 0.93 (d, J=6.5 Hz, 6H, 2×C$\underline{H}_3$), 1.21-1.27 (m, 2H, C$\underline{H}_2$), 1.81-1.85 (m, 1H, C$\underline{H}$), 2.44-2.47 (m, 1H, C$\underline{H}$), 2.74-2.77 (m, 1H, 1×C$\underline{H}_2$), 2.92-3.05 (3H, 3×C$\underline{H}_2$), 3.60 (s, 3H, C$\underline{H}_3$ minor isomer), 3.62 (s, 3H, C$\underline{H}_3$ major isomer), 3.87 (s, 3H, C$\underline{H}_3$ minor isomer), 3.88 (s, 3H, C$\underline{H}_3$ major isomer), 3.90 (s, 3H, C$\underline{H}_3$ major isomer), 3.91 (s, 3H, C$\underline{H}_3$ minor isomer), 3.95 (s, 3H, C$\underline{H}_3$), 4.31-3.33 (m, 1H, C$\underline{H}$ (Fmoc)), 4.50-4.54 (m, 1H, C$\underline{H}$ (Fmoc)), 4.74 (br. s., 2H, C$\underline{H}_2$), 6.35 (s, 1H, C=C$\underline{H}$), 6.49 (s, 1H, Ar$\underline{H}$), 6.79-6.83 (m, 2H, 2×Ar$\underline{H}$), 6.96-6.98 (m, 1H, Ar$\underline{H}$), 7.39-7.41 (m, 2H, 2×ArH (Fmoc)), 7.50-7.52 (m, 2H, 2×ArH (Fmoc)), 7.59-7.61 (m, 2H, 2×ArH (Fmoc)), 7.75-7.78 (m, 2H, 2×ArH (Fmoc)), 8.28 (br s, 2H, 2×CON$\underline{H}$).

¹³C NMR (CDCl₃, 151.71 MHz) δ$_c$ ppm: 19.8 ($\underline{C}H_2$ minor isomer), 20.5 ($\underline{C}H_2$ major isomer), 22.4 ($\underline{C}H_3$ major isomer), 23.0 ($\underline{C}H_3$ minor isomer), 24.1 ($\underline{C}H$ minor isomer), 24.9 ($\underline{C}H$ major isomer), 41.3 ($\underline{C}H_2$ major isomer), 41.5 ($\underline{C}H_2$ minor isomer), 45.2 ($\underline{C}H_2$ minor isomer), 45.8 ($\underline{C}H_2$ major isomer), 46.4 ($\underline{C}H$ minor isomer), 47.0 ($\underline{C}H$ major isomer), 53.5 ($\underline{C}H$ minor isomer), 54.1 ($\underline{C}H$ major isomer), 56.2 ($\underline{C}H_3$), 56.3 ($\underline{C}H_3$), 61.5 ($\underline{C}H_3$), 61.9 ($\underline{C}H_3$), 65.0 ($\underline{C}H_2$ minor isomer), 65.4 ($\underline{C}H_2$ major isomer), 67.6 ($\underline{C}H_2$ minor isomer), 68.4 ($\underline{C}H_2$ major isomer), 110.0 ($\underline{C}H$ minor isomer), 111.2 ($\underline{C}H$ major isomer) 112.1 ($\underline{C}H$ major isomer), 112.9 ($\underline{C}H$ minor isomer), 118.1 ($\underline{C}H$ major isomer), 118.5 ($\underline{C}H$ minor isomer), 119.5 ($\underline{C}H$ minor isomer), 119.7

(<u>C</u>H major isomer), 122.6 (<u>C</u>H minor isomer), 123.0 (<u>C</u>H minor isomer), 123.6 (<u>C</u>H major isomer), 123.9 (Q major isomer), 124.3 (Q minor isomer), 124.8 (<u>C</u>H major isomer), 125.5 (<u>C</u>H minor isomer), 125.9 (<u>C</u>H major isomer), 126.7 (<u>C</u>H major isomer), 126.9 (<u>C</u>H minor isomer), 127.7 (<u>C</u>H major isomer), 128.1 (<u>C</u>H minor isomer), 128.5 (<u>C</u>H minor isomer), 128.9 (<u>C</u>H major isomer), 129.4 (Q major isomer), 130.0 (Q minor isomer), 130.5 (Q major isomer), 130.7 (Q minor isomer), 130.9 (Q major isomer), 131.3 (Q minor isomer), 131.8 (Q minor isomer), 132.0 (Q major isomer), 132.3 (Q minor isomer), 132.5 (Q major isomer), 132.9 (Q major isomer), 133.3 (Q minor isomer), 133.7 (Q major isomer), 134.0 (Q major isomer), 134.4 (Q minor isomer), 136.7 (Q major isomer), 141.3 (Q major isomer), 142.1 (Q minor isomer), 142.8 (Q minor isomer), 142.9 (Q major isomer), 143.4 (Q major isomer), 143.9 (Q minor isomer), 144.1 (Q major isomer), 144.9 (Q minor isomer), 149.4 (Q minor isomer), 149.7 (Q major isomer), 151.4 (Q major isomer), 151.8 (Q minor isomer), 152.6 (Q major isomer), 153.6 (Q minor isomer), 155.1 (Q minor isomer), 156.2 (Q major isomer), 165.6 (Q, <u>C</u>=N), 173.1 (<u>C</u>=O), 176.1 (<u>C</u>=O).

HRMS (- ESI): Calculated Mass 943.3103. Found 966.2991 (M+Na)$^+$.

V$_{max}$ (DCM)/cm^{-1}: 2929, 1711, 1332, 1110, 1000, 732.

6.1.51 Synthesis of tert-butyl (5-(7-((2-(hydroxyamino)-2-oxoethoxy)imino)-2,3,4-trimethoxy-6,7-dihydro-5H-benzo[7]annulen-9-yl)-2-methoxyphenyl)carbamate (2.67).

A solution of **(2.65)** (0.0292 g, 0.0412 mmol), NH$_2$OH.HCl (0.0029 g, 0.0412 mmol) and NaOAc (0.0034 g, 0.0412 mmol) in EtOH (1 mL) and H$_2$O (0.5 mL) was stirred at room temperature for 30 min. At this time, EtOH was removed *in vacuo* and the product was extracted extraction between 0.5 M aq. HCl (15 mL) and Et$_2$O (3×15 mL). The combined organic extracts were washed with H$_2$O (15 mL) and dried over MgSO$_4$. Following

concentration *in vacuo*, the product was purified using column chromatography with EtOAc as the mobile phase as a yellow oil in a mixture of syn and anti isomers.

Yield: 0.0194 g, 0.0346 mmol, 84.4%.

^{1}H NMR (CDCl$_3$, 400MHz) δ_H ppm: 1.51 (s, 6H, ^{t}Bu major isomer), 1.53 (s, 3H ^{t}Bu minor isomer), 2.74-2.76 (m, 1H, ring C$\underline{H}_2$ minor isomer), 2.98-3.04 (m, 3H, ring C$\underline{H}_2$ + ring C$\underline{H}_2$ major isomer), 3.62 (s, 2H, OC$\underline{H}_3$ major isomer), 3.64 (s, 1H, OC$\underline{H}_3$ minor isomer), 3.89 (s, 1H, OC$\underline{H}_3$ minor isomer), 3.91 (s, 2H, OC$\underline{H}_3$ major isomer), 3.92 (s, 2H, OC$\underline{H}_3$ major isomer), 3.92 (s, 1H, OC$\underline{H}_3$ minor isomer),3.93 (s, 2H, OC$\underline{H}_3$ major isomer), 3.94 (s, 1H, OC$\underline{H}_3$ minor isomer), 4.68 (br s, 2H, C$\underline{H}_2$), 6.35 (s, 1H, ArC$\underline{H}$ major isomer), 6.39 (s, 1H, ArCH minor isomer), 6.51 (s, 1H, Alkene C$\underline{H}$), 6.82 (m, 1H, ArC$\underline{H}$), 6.91-6.94 (m, 1H, ArC$\underline{H}$), 7.10 (s, 1H, ArC$\underline{H}$ major isomer), 7.13 (s, 1H, ArC$\underline{H}$ minor isomer), 8.13 (s, 1H, N$\underline{H}$OH).

^{13}C NMR (CDCl$_3$, 151.71 MHz) δ_c ppm: 14.2 (Q), 21.4 (C$\underline{H}_2$ major isomer), 21.8 (C$\underline{H}_2$ minor isomer), 28.3 (C$\underline{H}_3$ minor isomer), 28.4 (C$\underline{H}_3$ major isomer) 29.8 (C$\underline{H}_2$ minor isomer), 33.0 (C$\underline{H}_2$ major isomer), 55.9 (C$\underline{H}_3$), 56.5 (C$\underline{H}_3$), 60.9 (C$\underline{H}_3$), 61.4 (C$\underline{H}_3$), 70.0 (C$\underline{H}_2$ minor isomer), 70.5 (C$\underline{H}_2$ major isomer), 109.5 (C$\underline{H}$ minor isomer), 110.9 (C$\underline{H}$ major isomer), 111.3 (C$\underline{H}$ major isomer), 111.7 (C$\underline{H}$ minor isomer), 123.5 (C$\underline{H}$ major isomer), 123.6 (C$\underline{H}$ minor isomer), 123.7 (C$\underline{H}$ major isomer), 123.9 (C$\underline{H}$ minor isomer), 125.6 (C$\underline{H}$ major isomer), 125.9 (Q minor isomer), 126.1 (C$\underline{H}$ minor isomer), 126.6 (Q major isomer), 127.5 (Q major isomer), 127.9 (Q minor isomer), 128.6 (Q major isomer), 128.9 (Q minor isomer), 129.5 (Q minor isomer), 130.0 (Q major isomer), 133.5 (Q minor isomer), 133.9 (Q major isomer), 136.7 (Q major isomer), 136.8 (Q minor isomer), 144.5 (Q minor isomer), 145.1 (Q major isomer), 147.1 (Q major isomer), 147.9 (Q major isomer), 162.3 (Q $\underline{C}$=N), 168.4 (Q $\underline{C}$=O).

HRMS (- ESI): Calculated Mass 557.2373. Found 556.2340 (M-H)$^-$.

V$_{max}$ (DCM)/cm^{-1}: 3556, 3005, 1724, 1478, 1275, 1026, 764.

6.1.52 Synthesis of (9H-fluoren-9-yl)methyl (1-((5-(7-((2-(hydroxyamino)-2-oxoethoxy)imino)-2,3,4-trimethoxy-6,7-dihydro-5H-benzo[7]annulen-9-yl)-2-methoxyphenyl)amino)-4-methyl-1-oxopentan-2-yl)carbamate *(2.68)*.

A solution of **(2.66)** (0.035 g, 0.0371 mmol), $NH_2OH.HCl$ (0.00277 g, 0.0400 mmol) and NaOAc (0.0035 g, 0.0422 mmol) in H_2O (1 mL) and EtOH (3 mL) was stirred at room temperature for 30 min. At this time, EtOH was removed *in vacuo* and the product was extracted by washing between 0.5 M aq. HCl (15 mL) and Et_2O (3 x 15 mL). The combined organic extracts were washed with H_2O (15 mL) and dried over $MgSO_4$. Following concentration *in vacuo*, the product was purified using column chromatography with EtOAc as the mobile phase as a yellow oil in a mixture of syn and anti isomers.

Yield: 0.0227 g, 0.0287 mmol, 77.4%.

^{1}H NMR (CDCl$_3$, 400MHz) δ_H ppm: 0.92 (m, 6H, 2×C$\underline{H}_3$), 1.18-1.40 (m, 2H, C$\underline{H}_2$), 1.84 (m, 1H, C$\underline{H}$), 2.30 (m, 1H, C$\underline{H}$), 2.68-3.13 (m, 4H, 2×CH$_2$), 3.57 (s, 3H, C$\underline{H}_3$ major isomer), 3.61 (s, 3H, C$\underline{H}_3$ minor isomer), 3.84 (s, 3H, C$\underline{H}_3$ major isomer), 3.85 (s, 3H, C$\underline{H}_3$ major isomer), 3.91 (s, 3H, C$\underline{H}_3$ minor isomer), 3.93 (s, 3H, C$\underline{H}_3$ major isomer), 4.24 - 4.33 (m, 1H, C$\underline{H}$), 4.46-4.57 (m, 2H, C$\underline{H}_2$), 4.61-4.65 (m, 2H, C$\underline{H}_2$), 6.29 (s, 1H, C=C$\underline{H}$ minor isomer) 6.31 (s, 1 H, C=C$\underline{H}$ minor isomer), 6.54 (s, 1H, Ar$\underline{H}$), 6.79-6.98 (m, 2H, 2×Ar$\underline{H}$), 7.06-7.14 (m, 1H, 2×Ar$\underline{H}$), 7.31-7.40 (m, 2H, 2× Ar$\underline{H}$(Fmoc)), 7.43-7.49 (m, 2H, 2×Ar$\underline{H}$(Fmoc)), 7.51-7.59 (m, 2H, 2×Ar$\underline{H}$(Fmoc)), 7.64-7.73 (m, 2H,2× Ar$\underline{H}$(Fmoc)), 8.23-8.46 (m, 2H, 2×CON$\underline{H}$)).

^{13}C NMR (CDCl$_3$, 151.71 MHz) δ_c ppm: 19.9 ($\underline{C}H_2$ minor isomer), 20.4 ($\underline{C}H_2$ major isomer), 22.4 ($\underline{C}H_3$ major isomer), 22.9 ($\underline{C}H_3$ minor isomer), 24.5 ($\underline{C}H$ minor isomer), 25.0 ($\underline{C}H$ major isomer), 41.3 ($\underline{C}H_2$ major isomer), 41.6 ($\underline{C}H_2$ minor isomer), 45.3 ($\underline{C}H_2$ minor isomer), 45.8 ($\underline{C}H_2$ major isomer), 46.3 ($\underline{C}H$ minor isomer), 46.7 ($\underline{C}H$ major isomer), 53.0 ($\underline{C}H$ minor isomer), 53.7 ($\underline{C}H$ major isomer), 56.1 ($\underline{C}H_3$), 56.4 ($\underline{C}H_3$), 61.3 ($\underline{C}H_3$), 61.5 ($\underline{C}H_3$), 64.4 ($\underline{C}H_2$ minor isomer), 64.6 ($\underline{C}H_2$ major isomer), 68.0 ($\underline{C}H_2$ minor isomer), 68.1 ($\underline{C}H_2$ major isomer), 110.4 ($\underline{C}H$ minor isomer), 111.6 ($\underline{C}H$ major isomer) 112.6 ($\underline{C}H$ major isomer), 113.4 ($\underline{C}H$ minor isomer), 118.1 ($\underline{C}H$ major isomer), 118.6 ($\underline{C}H$ minor isomer), 119.7 ($\underline{C}H$ minor isomer), 119.9

(C̲H major isomer), 122.7 (C̲H minor isomer), 123.2 (C̲H minor isomer), 123.8 (C̲H major isomer), 124.0 (Q major isomer), 124.4 (Q minor isomer), 124.8 (C̲H major isomer), 125.3 (C̲H minor isomer), 126.0 (C̲H major isomer), 126.8 (C̲H major isomer), 127.0 (C̲H minor isomer), 127.7 (C̲H major isomer), 128.3 (C̲H minor isomer), 128.7 (C̲H minor isomer), 128.9 (C̲H major isomer), 129.4 (Q major isomer), 130.1 (Q minor isomer), 132.5 (Q minor isomer), 132.7 (Q major isomer), 134.3 (Q minor isomer), 136.4 (Q major isomer), 141.2 (Q major isomer), 141.9 (Q minor isomer), 143.2 (Q major isomer), 144.5 (Q minor isomer), 149.0 (Q minor isomer), 149.3 (Q major isomer), 151.2 (Q major isomer), 151.4 (Q minor isomer), 152.8 (Q major isomer), 153.0 (Q minor isomer), 155.1 (Q minor isomer), 155.9 (Q major isomer), 165.0 (Q, C̲=N), 170.1 (C̲=O), 173.1 (C̲=O).

HRMS (- ESI): Calculated Mass 792.3370. Found 815.3249 $(M+Na)^+$.

V$_{max}$ (DCM)/cm^{-1}: 3541, 3111, 2991, 1722, 1612,1478, 1026, 764.

6.1.53 Synthesis of 2-(((9-(3-amino-4-methoxyphenyl)-2,3,4-trimethoxy-5H-benzo[7]annulen-7(6H)-ylidene)amino)oxy)-N-hydroxyacetamide (2.06).

Under an atmosphere of N_2, **(2.68)** (0.07 g, 0.12 mmol), was dissolved in DCM (1.5 mL) and stirred for 2 min at 0 °C. TFA (1 mL) was added dropwise to the flask as the solution turn a yellow colour. The mixture was stirred for 15 min, before the removal of the volatile constituents using a stream of N_2 gas. The product was isolated following an extraction between 5% aq. NaHCO$_3$ (10 mL) and Et$_2$O (3×10 mL). The organic layers were combined and washed with H_2O before being dried over MgSO$_4$. Removal of the solvent yielded the product as a yellow solid.

Yield: 0.032 g, 0.07 mmol, 58.3%.

^{1}H NMR (CDCl$_3$, 600MHz) δ$_H$ ppm: 2.73-2.77 (m, 1H, C̲H$_2$), 2.85-3.04 (m, 3H, mixture of ring C̲H$_2$), 3.62 ((s, 3H, C̲H$_3$ major isomer), 3.64 (s, 3H, C̲H$_3$ minor isomer)), 3.89 ((s, 3H, C̲H$_3$ minor isomer), 3.91 (s, 3H, C̲H$_3$ major isomer)), 3.92 ((s, 3H, CH3 major isomer), 3.93 (s, 3H,

CH₃ minor isomer)), 3.93 ((s, 3H, C$\underline{H}$3 major isomer), 3.94 (s, 3H, C$\underline{H}$₃ minor isomer)), 4.36 (br

s, 1H, N$\underline{H}$₂), 4.67 (s, 2H, C$\underline{H}$₂), 6.34 ((s, 1H, C=C$\underline{H}$ major isomer) 6.39 (s, 1H, C=C$\underline{H}$ minor

isomer)), 6.51 ((s, 1H, Ar$\underline{H}$ major isomer), 6.56 (s, 1H, Ar$\underline{H}$ minor isomer)) 6.81-6.85 (m, 1H,

Ar$\underline{H}$ (mixture of isomers)), 6.90-6.96 (m, 1H, ArH (mixture of isomers)), 7.10 ((s, 1H, Ar$\underline{H}$

major isomer), 7.13 (s, 1H, Ar$\underline{H}$ minor isomer)).

¹³C NMR (CDCl₃, 151.71 MHz) δc ppm: 21.2 (C$\underline{H}$₂ major isomer), 21.9 (C$\underline{H}$₂ minor isomer),

29.7 (C$\underline{H}$₂ minor isomer), 32.8 (C$\underline{H}$₂ major isomer), 55.7 (C$\underline{H}$₃), 56.1 (C$\underline{H}$₃), 61.1 (C$\underline{H}$₃), 61.3

(C$\underline{H}$₃), 70.1 (C$\underline{H}$₂ minor isomer), 70.3 (C$\underline{H}$₂ major isomer), 109.4 (C$\underline{H}$ minor isomer), 111.9

(C=C$\underline{H}$), 117.7 (C$\underline{H}$ minor isomer), 123.3 (C$\underline{H}$ minor isomer), 123.5 (C$\underline{H}$ minor isomer), 123.7

(2×C$\underline{H}$ major isomer), 125.4 (C$\underline{H}$), 126.3 (C$\underline{H}$ minor isomer), 126.8 (Q major isomer), 127.6 (Q

major isomer), 127.7 (Q minor isomer), 128.2 (Q minor isomer), 128.4 (Q major isomer), 128.5

(Q major isomer), 129.3 (Q minor isomer), 129.8 (Q minor isomer), 130.5 (Q major isomer),

133.2 (Q minor isomer), 133.4 (Q major isomer), 134.1 (Q major isomer), 136.8 (Q major

isomer), 137.1 (Q minor isomer), 142.3 (Q minor isomer), 142.7 (Q major isomer), 146.4 (Q

major isomer), 147.3 (Q major isomer), 149.9 (Q minor isomer), 150.0 (Q major isomer), 150.7

(Q minor isomer), 150.9 (Q major isomer), 153.6 (Q $\underline{C}$=N), 164.7 (Q $\underline{C}$=O).

HRMS (+ ESI): Calculated Mass 457.1849. Found 458.1907 (M+H)⁺.

V$_{max}$ (DCM)/cm⁻¹: 3583, 2929, 1731, 1463, 1266, 1117, 851, 702.

6.1.54 **Synthesis of 2-amino-N-(5-(7-((2-(hydroxyamino)-2-oxoethoxy)imino)-2,3,4-trimethoxy-6,7-dihydro-5H-benzo[7]annulen-9-yl)-2-methoxyphenyl)-4-methylpentanamide *(2.53)*.**

To a stirred solution of *(2.68)* (0.0200 g, 0.0252 mmol) in dry THF (4 mL) under a blanket of

N₂ at 0 °C was added dropwise a 1 M solution of TBAF in THF (0.04 mL, 0.04 mmol). The

mixture was allowed to elevate to room temperature over 10 min. Upon completion of the

reaction, the solvents were removed under a stream of N_2 before being purified using column chromatography (hexane/EtOAc 2:1) furnishing the product as a colourless oil.

Yield: 0.0777 g, 0.0136 mmol, 54%.

¹H NMR (CDCl₃, 400MHz) δ_H ppm: 0.86-0.96 (m, 6H, 2×C$\underline{H}$₃), 1.22-1.35 (m, 2H, C$\underline{H}$₂), 1.70-1.83 (m, 1H, C$\underline{H}$), 2.24-2.36 (m, 1H, C$\underline{H}$), 2.74-3.02 (m, 4H, 2×C$\underline{H}$₂), 3.36 (br s, 1 H, N$\underline{H}$₂), 3.58 (s, 3H, C$\underline{H}$₃ minor isomer) 3.60 (s, 3H, C$\underline{H}$3 major isomer), 3.82 (s, 3H, C$\underline{H}$₃), 3.89 (s, 3H, C$\underline{H}$₃ major isomer), 3.91 (s, 3H, C$\underline{H}$₃ minor isomer), 3.94 (s, 3H, C$\underline{H}$₃), 6.30 (s, 1H, C=C$\underline{H}$ minor isomer), 6.31 (s, 1H, C=CH major isomer), 6.53 (s, 1H, Ar$\underline{H}$ minor isomer), 6.54 (s, 1H, Ar$\underline{H}$ major isomer), 6.81-6.93 (m, 2H, 2×Ar$\underline{H}$), 7.08 (s, 1H, Ar$\underline{H}$ minor isomer), 7.11 (s, 1H, Ar$\underline{H}$ major isomer).

¹³C NMR (CDCl₃, 100.71 MHz) δ_c ppm: 19.8 ($\underline{C}$H₂ minor isomer), 20.5 ($\underline{C}$H₂ major isomer), 22.5 ($\underline{C}$H₃ major isomer), 24.2 ($\underline{C}$H minor isomer), 24.8 ($\underline{C}$H major isomer), 41.3 ($\underline{C}$H₂ major isomer), 41.6 ($\underline{C}$H₂ minor isomer), 45.5 ($\underline{C}$H₂ minor isomer), 45.9 ($\underline{C}$H₂ major isomer), 53.4 ($\underline{C}$H minor isomer), 54.1 ($\underline{C}$H major isomer), 56.2 ($\underline{C}$H₃), 56.6 ($\underline{C}$H₃), 61.7 ($\underline{C}$H₃), 61.9 ($\underline{C}$H₃), 65.1 ($\underline{C}$H₂ minor isomer), 65.9 ($\underline{C}$H₂ major isomer), 110.5 ($\underline{C}$H minor isomer), 111.6 ($\underline{C}$H major isomer) 112.4 ($\underline{C}$H major isomer), 113.0 ($\underline{C}$H minor isomer), 118.5 ($\underline{C}$H major isomer), 118.9 ($\underline{C}$H minor isomer), 122.9 ($\underline{C}$H minor isomer), 123.2 ($\underline{C}$H minor isomer), 124.1 (Q minor isomer), 124.7 ($\underline{C}$H major isomer), 126.4 ($\underline{C}$H major isomer), 126.8 ($\underline{C}$H minor isomer), 129.3 (Q major isomer), 130.0 (Q minor isomer), 132.4 (Q minor isomer), 132.9 (Q major isomer), 134.3 (Q minor isomer), 136.1 (Q major isomer), 141.9 (Q major isomer), 143.1 (Q minor isomer), 146.8 (Q minor isomer), 147.3 (Q major isomer), 151.2 (Q major isomer), 151.7 (Q minor isomer), 152.5 (Q major isomer), 152.8 (Q minor isomer), 155.8 (Q minor isomer), 156.9 (Q major isomer), 161.0 (Q, $\underline{C}$=N), 169.1 ($\underline{C}$=O), 171.2 (C=O).

HRMS (+ ESI): Calculated mass 570.2690, Found 569.2601.

V_max (DCM)/cm⁻¹: 3314, 3101, 2929, 2016, 1731, 1671, 1638, 1422, 1001, 756.

6.2   Chapter 3 Synthesis

6.2.1   Synthesis of (2, 3, 4 - Trimethoxyphenyl) methanol *(3.08).*

To a stirred solution of 2, 3, 4-trimethoxybenzaldehyde (10.50 g, 532 mmol) in MeOH (150 mL) was added $NaBH_4$ (2.65 g, 70 mmol) at 0 ^{O}C. The progress of the reaction was monitored by Thin Layer Chromatography (TLC) using hexane/EtOAc 4:1 as the mobile phase. After 30 min, the reaction was quenched by the addition of H_2O (100 mL). MeOH was removed from the mixture *in vacuo*. The product was extracted with Et_2O (1×150 mL, 2×75 mL). The organic extracts were combined, dried over $MgSO_4$ and concentrated to a yield the product as a colourless oil.

Yield: 10.25 g, 51.71 mmol, 98%.

^{1}H NMR (CDCl$_3$, 400MHz) δ_H ppm: 3.88 (s, 3H, C$\underline{H}_3$), 3.90 (s, 3H, C$\underline{H}_3$), 3.98 (s, 3H, C$\underline{H}_3$), 4.64 (d, J=6.12 Hz, 2H, C$\underline{H}_2$), 6.66 (d, J=8.44Hz, 1H, Ar$\underline{H}$), 7.00 (d, J = 8.44Hz, 1H, Ar$\underline{H}$).

^{13}C NMR (CDCl$_3$, 100.71 MHz) δ_c ppm: 55.5 ($\underline{C}H_3$), 60.3 ($\underline{C}H_3$), 60.7 ($\underline{C}H_3$), 61.1 ($\underline{C}H_3$), 122.9 ($\underline{C}H$), 126.4 ($\underline{C}H$), 141.4 ($\underline{C}H$), 141.4 (Q), 151.2 (Q), 152.9 (Q).

HRMS (ESI): Calculated Mass 198.0892. Found 221.0775 (M+Na)$^+$.

V_{max} (DCM)/cm^{-1}: 3411, 2939, 2878, 2836, 1602, 1496, 1237, 1017, 896, 804, 688, 509.

6.2.2   Synthesis of 1 - (Bromomethyl) -2, 3, 4 – trimethoxybenzene *(3.09)*

A solution of *(3.08)* (5.00 g, 25.2 mmol) in dry DCM (35 mL) was stirred at -10 ^{o}C in an ice/NaCl bath. After 10 min, PBr$_3$ (13.65 g, 4.75 mL, 50.5 mmol) was added dropwise by syringe. The reaction was monitored by TLC. After 90 min, the reaction was quenched with 10% aq. Na$_2$CO$_3$ (50 mL) in ice H$_2$O and washed with Et$_2$O (75 mL). The organic extract was washed with 10% aq. NaHCO$_3$ (3×50 mL), dried over MgSO$_4$ and concentrated *in vacuo* at a low temperature to prevent degradation of the product. The product was obtained as a colourless oil after being placed under high vacuum for 2 h. The product was not purified and further and was used in directly in the following reaction.

¹H NMR (CDCl₃, 400MHz) δ_H ppm: 3.88 (s, 3H, C$\underline{H}$₃), 3.89 (s, 3H, C$\underline{H}$₃), 4.04 (s, 3H, C$\underline{H}$₃), 4.57 (s, 1H, C$\underline{H}$₂Br), 6.66 (d, J = 8.56Hz, 1H, Ar$\underline{H}$), 7.07 (d, J = 8.56Hz, 1H, Ar$\underline{H}$).

V_max (DCM)/cm⁻¹: 2936, 2827, 1460, 1409, 1067, 1009, 795.

6.2.3 **Synthesis of 2 - (2, 3, 4 - Trimethoxyphenyl) acetonitrile** *(3.10)*

NaCN (2.75 g, 56.1 mmol) was stirred in DMSO (120 mL) at 25 °C for 30 min, ensuring maximum dissolution of the salt in the solvent. To this mixture was added *(3.09)* (4.90 g, 18.7 mmol). The mixture was stirred for 2 h, before TLC (hexane/EtOAc 4:1) had shown that the reaction had proceeded to completion. The mixture was diluted with H₂O (100 mL) and the product was extracted with Et₂O (1×100 mL, 2×50 mL). The combined organic extracts were washed with H₂O (100 mL), dried over MgSO₄ and concentrated *in vacuo* to produce a yellow oil. Column chromatography was used to isolate the product as a colourless solid using a hexane / EtOAc 9:1 mixture as the mobile phase.

Yield: 3.2 g, 15.4 mmol, 62% over 2 steps).

¹H NMR (CDCl₃, 400MHz) δ_H ppm: 3.66 (s, 2H, C$\underline{H}$₂), 3.89 (s, 3H, C$\underline{H}$₃), 3.90 (s, 3H, C$\underline{H}$₃), 3.99(s, 3H, C$\underline{H}$₃), 7.03 (d, J=8.68Hz, 1H, Ar$\underline{H}$), 7.03 (d, J = 8.6Hz, Ar$\underline{H}$).

¹³C NMR (CDCl₃, 100.71 MHz) δ_c ppm: 17.9 ($\underline{C}$H₂), 55.6 ($\underline{C}$H₃), 60.3 ($\underline{C}$H₃), 60.4 ($\underline{C}$H₃), 106.6 (Ar$\underline{C}$H), 115.6 (Q), 115.9 (Q), 123.0 (Ar$\underline{C}$H), 141.6 (Q), 150.9 (Q), 153.5 (Q).

HRMS (ESI): Calculated Mass 208.0968. Found 208.0286 (M+H⁺).

V_max (DCM)/cm⁻¹: 3621 w, 2941 s, 2250 m (C≡N), 1603 s, 1496 s, 1420 s, 1260 s, 1097 s, 801 s, 688 s.

Melting point: 45-47 °C

6.2.4 **Synthesis of 2 - (2, 3, 4 - Trimethoxyphenyl) acetic acid** *(3.20)*

(3.10) (1.18 g, 5.69 mmol) was stirred at room temperature in EtOH (20 mL). A 2.5 M solution of sodium hydroxide was prepared and added to the reaction vessel (30 mL). The solution was heated under reflux for 2.5 days, before TLC (hexane/EtOAc 2:1) had shown that the reaction had proceeded mostly to completion. EtOH was removed by rotary evaporation. The basic

mixture was washed with Et$_2$O (3×20 mL), before acidification with 2 M aq. HCl. The acidic layer was washed with Et$_2$O (3×30 mL). The combined organic extracts were dried over MgSO$_4$ and concentrated *in vacuo* to produce a brown oil. The product was purified using column chromatography to yield a colourless solid.

Yield: 0.88 g, 3.89 mmol, 68%.

^{1}H NMR (CDCl$_3$, 400MHz) δ$_H$ ppm: 3.64 (s, 2H, C$\underline{H}_2$), 3.85 (s, 3H, C$\underline{H}_3$), 3.88 (s, 3H, C$\underline{H}_3$), 3.91 (s, 3H, C$\underline{H}_3$), 6.66 (d, J=8.52Hz, 1H, Ar$\underline{H}$), 6.92 (d, J=8.52, 1H, Ar$\underline{H}$).

^{13}C NMR (CDCl$_3$, 100.71 MHz) δ$_c$ ppm: 55.9 ($\underline{C}$H$_3$), 60.7 ($\underline{C}$H$_3$), 60.8 ($\underline{C}$H$_3$), 107.1 (Ar$\underline{C}$H), 119.8 (Q), 124.9 (Ar$\underline{C}$H), 142.1 (Q), 151.8 (Q), 153.4 (Q), 176.7 ($\underline{C}$OOH).

HRMS (ESI): Calculated Mass 226.0841. Found 225.1121 (M$^-$).

V$_{max}$ (DCM)/cm^{-1}: 3583, 2929, 1707, 1520, 1275, 1002, 764.

Melting point: 87-93 °C.

6.2.5 **Synthesis of 2 - (2, 3, 4 - trimethoxyphenyl) ethanol** *(3.21)*

LiAlH$_4$ (1.34 g, 27 mmol) was added slowly to a round bottomed flask containing THF (20 mL). The mixture was stirred at -25 °C with the assistance of a deep cooler. *(3.20)* (1.75 g, 7.73 mmol) was added slowly to this flask. After 30 min, the temperature was allowed to rise gently to room temperature and the reaction was stirred overnight. The reaction was quenched slowly using 2 M aq. HCl (25 mL). The alcohol was extracted with Et$_2$O (3×30 mL). The combined organic extracts were washed with H$_2$O (50 mL), dried over MgSO$_4$ and the solvent was removed *in vacuo* yielding an off-white oil. This was purified using column chromatography (hexane/EtOAc 3:1) to furnish the product as a colourless mobile oil.

Yield: 1.23 g, 5.79 mmol, 75%.

^{1}H NMR (CDCl$_3$, 400MHz) δ$_H$ ppm: 2.85 (t, J=6.4Hz, 2H, C$\underline{H}_2$), 3.79-3.83 (m, 2H, C$\underline{H}_2$), 3.88 (s, 3H, C$\underline{H}_3$), 3.90 (s, 3H, C$\underline{H}_3$), 3.92 (s, 3H, C$\underline{H}_3$), 6.65 (d, J=8.44Hz, 1H, Ar$\underline{H}$), 6.88 (d, J=8.44Hz, 1H, Ar$\underline{H}$).

^{13}C NMR (CDCl$_3$, 100.71 MHz) δ$_c$ ppm: 33.0 ($\underline{C}$H$_2$), 55.5 ($\underline{C}$H$_3$), 58.5 ($\underline{C}$H$_3$), 60.5 ($\underline{C}$H$_3$), 62.9 ($\underline{C}$H$_2$), 106.8 ($\underline{C}$H), 119.8 (Q), 124.1 ($\underline{C}$H), 141.8 (Q), 151.5 (Q), 152.0 (Q).

HRMS (ESI): Calculated 212.1049. Found 211.0965 (M-H)⁻.

V$_{max}$ (DCM)/cm⁻¹: 3411 (br, -OH), 2936, 2835, 1495, 1466, 1285, 1077, 1057, 1016, 799.

6.2.6   **Synthesis of 2 - (2, 3, 4 - trimethoxyphenyl) acetaldehyde *(3.22).***

PDC (0.68 g, 3.13 mmol) was placed in a dry three necked flask under an atmosphere of N$_2$.

Dry DCM (10 mL) was added to the flask and the suspension was stirred for 5 min at 0 °C. A

solution of *(3.21)* (0.6 g, 2.85 mmol) in DCM (5 mL) was added dropwise to the flask and the

mixture was stirred for 30 min, before being allowed to rise to room temperature. After 90 min,

the reaction mixture was placed through a silica gel plug to remove any chromium salts. The

light green oil that remained after rotary evaporation was subjected to column chromatography.

A 6:1 mixture of hexane and EtOAc was used to isolate the product as a yellowish oil.

Yield: 0.46 g, 2.19 mmol, 70%.

¹H NMR (CDCl$_3$, 400MHz) δ$_H$ ppm: 3.66 (s, 2H, C$\underline{H}_2$), 3.89 (s, 6H, 2×C$\underline{H}_3$), 3.99 (s, 3H,

C$\underline{H}_3$), 6.67 (d, J=8.56Hz, 1H, Ar$\underline{H}$), 6.88 (d, J=8.56Hz, 1H, Ar$\underline{H}$), 9.70 (t, J=2.08Hz, 1H, C$\underline{H}$O).

¹³C NMR (CDCl$_3$, 100.71 MHz) δ$_c$ ppm: 44.3 ($\underline{C}$H$_2$), 55.5 ($\underline{C}$H$_3$), 55.7 ($\underline{C}$H$_3$), 60.3 ($\underline{C}$H$_3$), 106.6

($\underline{C}$H), 124.7 ($\underline{C}$H), 131.1 (Q), 141.7 (Q), 151.6 (Q), 158.6 (Q), 199.5 (Q).

HRMS (ESI +): Calculated Mass 210.0892. Found 211.0957(M+H⁺).

V$_{max}$ (DCM)/cm⁻¹: 3593, 2988, 2961, 28421689, 1591, 1467, 1385, 1299, 1201, 1098, 942, 812.

6.2.7   Synthesis of 2-(2,3,4-trimethoxyphenyl)acetaldehyde (3.22): Attempt 2.

(3.10) (1.05 g, 5.1 mmol) was stirred at 0 °C in MeOH. NaBH$_4$ (0.52 g, 13.7 mmol) powder was

added slowly to avoid an overvigorous reaction. The mixture was stirred for 6 h, showing

negligible product conversion. A further 2 equivalents of NaBH$_4$ was added (0.37 g, 10 mmol).

The reaction was heated under reflux for 3 h, before TLC showed no further reaction progress.

MeOH was removed *in vacuo* after the addition of H$_2$O (30 mL) to quench the reaction. The

aqueous layer was washed with Et$_2$O (3×20 mL). The combined organic extracts were dried

over MgSO$_4$, and concentrated by rotary evaporation. A column isolated a small amount of the

desired product using hexane/EtOAc 7:1 as the mobile phase.

Yield: 0.11 g, 0.54 mmol, 10%.

Characterisation of this compound is previously documented.

6.2.8 Synthesis of 1-(2, 3, 4 - trimethoxyphenyl)pent-4-en-2–ol (3.12) Attempt 1.

To a stirred solution of *(3.22)* (0.40 g, 1.90 mmol) and Mg turnings (0.12 g, 5.00 mmol) in dry THF (10 mL) under an atmosphere of N_2 was added dropwise allyl bromide (0.32 mL, 3.60 mmol). The reaction was monitored using TLC (hexane/EtOAc 4:1) which showed consumption of the starting material after 6 h. The product was extracted between H_2O (30 mL), added slowly to quench any remaining Mg, and Et_2O (3×30 mL). The combined organic extracts were dried with $MgSO_4$, filtered and concentrated *in vacuo*, leaving a colourless oil, which was purified via column (hexane/EtOAc 4:1) to yield the product as a colourless oil.

Yield: 0.36 g, 1.43 mmol, 75%.

^{1}H NMR (CDCl$_3$, 400MHz) δ_H ppm: 2.24-2.35 (m, 2H, C$\underline{H}_2$), 2.67-2.85 (m, 2H, C$\underline{H}_2$), 3.84-3.93 (m, 1H, C$\underline{H}$OH), 3.85 (s, 3H, C$\underline{H}_3$), 3.87 (s, 3H, C$\underline{H}_3$), 3.89 (s, 3H, C$\underline{H}_3$), 5.14-5.19 (m, 2H, Alkene C$\underline{H}_2$), 5.85-5.94 (m, 1H, alkene C$\underline{H}$), 6.65 (d, J=8.44Hz, 1H, Ar$\underline{H}$), 6.88 (d, J=8.48Hz, 1H, Ar$\underline{H}$).

^{13}C NMR (CDCl$_3$, 100.71 MHz) δ_c ppm: 37.0 ($\underline{C}H_2$), 41.0 ($\underline{C}H_2$), 55.5 ($\underline{C}H_3$), 60.3 ($\underline{C}H_3$), 60.4 ($\underline{C}H_3$), 71.0 ($\underline{C}H$), 106.8 ($\underline{C}H$), 117.2 ($\underline{C}H_2$), 123.9 ($\underline{C}H$), 124.7 ($\underline{C}H$), 134.5 (Q), 141.7 (Q), 151.5 (Q), 152.2 (Q).

HRMS (ESI): Calculated Mass 252.1362. Found 251.1298 (M⁻).

V_{max} (DCM)/cm^{-1}: 3434 (br, -OH), 3075, 2935, 2834, 1640, 1494, 1466, 1416, 1257, 1045, 908, 796, 669.

6.2.9 Synthesis of 1,2,3-trimethoxy-4-vinylbenzene (3.25).

A stirred suspension of 2,3,4-trimethoxybenzaldehyde (3.53 g, 18.00 mmol), methyltriphenylphosphonium bromide (7.71 g, 21.59 mmol), K_2CO_3 (11.93 g, 86.36 mmol) and 18-crown-6 was heated under an atmosphere of N_2 at 80 °C for 2 days. The reaction was

monitored by TLC (hexane/EtOAc 4:1) and upon consumption of the starting material the THF was removed *in vacuo*. The residue was diluted in H_2O (50 mL) and extracted into Et_2O (3×50 mL). The organic extracts were combined, washed with H_2O (50 mL), dried over $MgSO_4$, filtered and concentrated in vacuo to yield a colourless oil, from which the product was obtained in pure form using column chromatography hexane/EtOAc 4:1 as the mobile phase as a colourless oil.

Yield: 3.35 g (17.28 mmol, 96%).

^{1}H NMR (CDCl$_3$, 400MHz) δ_H ppm: 3.89 (s, 3H, CH$_3$), 3.90 (s, 3H, CH$_3$), 3.91 (s, 3H, CH$_3$), 5.22 (dd, J=11.00 Hz, J=1.50 Hz, 1H, CH=C$\underline{H}_2$), 5.68 (dd, J=17.70 Hz, J= 1.40 Hz, 1H, CH=C$\underline{H}_2$), 6.70 (d, J= 8.50 Hz, 1H, Ar$\underline{H}$), 6.95 (dd, J=17.70 Hz, J=11.20 Hz, 1H, C$\underline{H}$=CH$_2$), 7.23 (d, J= 8.50 Hz, 1H, Ar$\underline{H}$).

^{13}C NMR (CDCl$_3$, 100.71 MHz) δ_c ppm: 56.0 ($\underline{C}$H$_3$), 60.9 ($\underline{C}$H$_3$), 61.2 ($\underline{C}$H$_3$), 107.6 ($\underline{C}$H), 113.2 ($\underline{C}$H$_2$), 120.6 ($\underline{C}$H), 124.8 (Q), 131.0 ($\underline{C}$H), 142.3 (Q), 151.5 (Q), 153.3 (Q).

HRMS (ESI): Calculated Mass 194.0943. Found 217.0838 (M+Na)$^+$.

V$_{max}$ (DCM)/cm^{-1}: 3583, 2879, 1957, 1595, 1456, 1353, 1289, 1026, 853.

6.2.10 Synthesis of 2 - (2, 3, 4 - trimethoxyphenyl) ethanol (3.21) Method 2

To a stirred solution of *(3.25)* (3.00 g, 15.45 mmol) in diglyme (80 mL) under an atmosphere of N$_2$ was added dropwise a 1 M solution of BH$_3$ in THF (46.4 mL, 46.4 mmol). The resultant mixture was stirred at 0 °C for 1 h after which time the THF was removed under low pressure. To the remaining solution was added Trimethylanilinium N-oxide (8.58 g, 77.25 mmol) and the mixture was stirred at 100 °C for 2 h. The product was extracted by washing with warm H$_2$O (100 mL) and Et$_2$O (3×70 mL). The combined organic extracts were washed with warm H$_2$O (5×100 mL) removing as much diglyme as possible. They were then dried over MgSO$_4$, filtered, concentrated *in vacuo*. Following flash column chromatography using hexane/EtOAc 2:1 as the mobile phase, the title compound was obtained as a colourless oil.

Characterisation of this compound is previously documented.

6.2.11 Synthesis of 1 - (2, 3, 4 - trimethoxyphenyl) pent-4-en-2–one (3.11)

(3.10) (3.00 g, 14.5 mmol) and zinc dust (3.78 g, 58 mmol) was stirred in dry THF THF (45 mL) at 0 °C before dropwise addition of allyl bromide (2.63 g, 1.9 mL, 21.71 mmol). After 10 min, AlCl$_3$ (0.77 g, 5.8 mmol) was added quickly. The mixture was stirred for 20 min at this temperature and stirred for a further hour at room temperature. TLC (hexane/EtOAc 4:1) indicated that the reaction had proceeded to completion. 1 M aq. HCl (75 mL) was added and stirred for 5 min to quench the reaction. The zinc solid was removed by decanting the mixture into a conical flask. The product was extracted by washing with Et$_2$O (3×50 mL), drying the combined organic extracts over MgSO$_4$, and the mixture concentrated to give a dark yellow oil. The compound was isolated as a colourless oil following column chromatography using a 10:1 mixture of hexane/EtOAc as the mobile phase.

Yield: 2.98 g, 11.89 mmol, 82%.

^{1}H NMR (CDCl$_3$, 400MHz) δ_H ppm: 3.22 (d, J=7Hz, 2H, CH$_2$), 3.65 (d, J=9.32Hz, 2H, CH$_2$), 3.79 (s, 3H, CH$_3$), 3.83 (s, 3H, CH$_3$), 3.84 (s, 3H, CH$_3$), 5.08-5.17 (m, 2H, H=CCH$_2$), 5.88-6.20 (m, 1H, alkene C=CH), 6.63 (d, J = 3.24Hz, 1H, ArH), 6.79 (d, J=8.52Hz, 1H, ArH).

^{13}C NMR (CDCl$_3$, 100.71 MHz) δ_c ppm: 43.2 (CH$_2$), 46.4 (CH$_2$), 55.4 (CH$_3$), 60.2 (CH$_3$), 60.2 (CH$_3$), 106.7 (CH), 118.2 (CH$_2$), 120.2 (Q), 124.6 (CH), 126.4 (Q), 130.2 (CH), 141.6 (Q), 151.4 (Q), 206.1 (C=O).

HRMS (ESI): Calculated 250.1278, Found 251.1279 (M+H)$^+$.

V$_{max}$ (DCM)/cm^{-1}: 2941, 2838, 1719 (C=O), 1496, 1468, 1290, 1043, 750.

6.2.12 Synthesis of 1-(2, 3, 4 - trimethoxyphenyl)pent-4-en-2–ol (3.12) Attempt 2.

(3.10) (2.20 g, 8.8 mmol) was stirred at 0 °C in MeOH (40 mL). NaBH$_4$ (0.37 g, 9.68 mmol) was added slowly, and the reaction was stirred for 5 min before removal of the ice bath. TLC (hexane/EtOAc 4:1) showed completion of the reaction within 20 min. H$_2$O (40 mL) was added, and the MeOH was removed by rotary evaporation. The aqueous solution was washed with

Et$_2$O (3×30 mL), the combined organic extracts were dried with MgSO$_4$ and concentrated *in vacuo*, leaving a colourless oil. This was purified via column (hexane/EtOAc 4:1) to give the product as a colourless oil.

Yield: 2.16 g, 8.56 mmol, 97%.

Characterisation of this compound is previously documented.

6.2.13 Synthesis of (1-(2, 3, 4-trimethoxyphenyl) pent-4- en- 2-yloxy) (tert-butyl) diphenylsilane (3.13)

(3.12) (2.45 g, 9.7 mmol) was stirred with imidazole (1.65 g, 24.2 mmol) in dry DMF (10 mL) under N$_2$. *Tert*-butyl diphenylsilylchloride (2.9 mL, 11.1 mmol) was added and the reaction proceeded for 12 h. TLC (4:1 hexane/EtOAc) showed that the reaction had proceeded to completion. Brine (90 mL) was added to quench the reaction. The product was extracted with Et$_2$O (2×90 mL, 2×50 mL). The combined organic extracts were washed with H$_2$O (100 mL), dried over MgSO$_4$ and dried *in vacuo* leaving a colourless oil which was purified via column chromatography using a 50:1 mixture of hexane / EtOAc.

Yield: 4.12 g, 9.02 mmol, 93%.

^{1}H NMR (CDCl$_3$, 400MHz) δ$_H$ ppm: 1.04 (s, 9H, ^{t}Bu), 2.07-2.12 (m, 2H, C$\underline{H}_2$), 2.68-2.8 (m, 2H, C$\underline{H}_2$), 3.66 (s, 3H, C$\underline{H}_3$), 3.83 (s, 3H, C$\underline{H}_3$), 3.85 (s, 3H, C$\underline{H}_3$), 4.05-4.08 (m, 1H, C$\underline{H}$OSi), 4.90-5.02 (m, 2H, C$\underline{H}_2$ alkene), 5.80-5.85 (m, 1H, C$\underline{H}$ alkene), 6.54 (d, J=8.48Hz, 1H, Ar$\underline{H}$), 6.70 (d, J=8.48Hz, 1H, Ar$\underline{H}$), 7.29-7.37 (m, 6H, Ar$\underline{H}$), 7.39-7.44 (m, 2H, Ar$\underline{H}$), 7.54-7.57 (m, 2H, Ar$\underline{H}$).

^{13}C NMR (CDCl$_3$, 100.71 MHz) δ$_c$ ppm: 19.4 (Q), 27.1 ($\underline{C}$H$_3$), 37.4 ($\underline{C}$H$_2$), 40.8 ($\underline{C}$H$_2$), 56.0 ($\underline{C}$H$_3$), 60.6 ($\underline{C}$H$_3$), 60.7 ($\underline{C}$H$_3$), 73.4 ($\underline{C}$H), 106.9 ($\underline{C}$H), 117.0 ($\underline{C}$H$_2$), 125.0 (Q), 125.6 ($\underline{C}$H), 127.4 ($\underline{C}$H), 129.4 ($\underline{C}$H), 134.4 (Q), 134.6 (Q), 135.1 ($\underline{C}$H), 136.1 ($\underline{C}$H), 152.2 (Q), 152.3 (Q).

HRMS (ESI): Calculated Mass 490.7058. Found 513.2427 (M+Na)$^+$.

V$_{max}$ (DCM)/cm^{-1}: 3071, 3047, 2997, 2957, 2931, 2856, 1494, 1466, 1416, 1111, 1044, 822, 702, 507.

6.2.14 Synthesis of 1-(2, 3, 4 - trimethoxyphenyl) pent-4-en-2-yl acetate (3.26)

(3.10) (0.30 g, 1.2 mmol) was stirred in distilled DCM (5 mL) under N_2, followed by addition of triethylamine (NEt_3) (0.4 mL, 1.44 mmol). Acetic Anhydride (0.35 ml, 0.37 g, 3.6 mmol) was added and the mixture was stirred for a further 5 min. DMAP (0.45 g, 3.6 mmol) was then added and the mixture was stirred overnight. After 16 h, TLC (hexane/EtOAc 4:1) showed the reaction had completed. The reaction was quenched with 2 M aq. HCl (20 mL), and the aqueous layer was washed with Et_2O (3×30 mL). The combined organic extracts were washed with H_2O (50 mL), dried over $MgSO_4$ and the solvent was removed *in vacuo*. The product was purified as a colourless oil by column chromatography using a 10:1 mixture of hexane/EtOAc as the mobile phase.

Yield: 0.3 g, 1.02 mmol, 85%.

^{1}H NMR (CDCl$_3$, 400MHz) δ_H ppm: 1.91 (s, 3H, C$\underline{H}_3$), 2.22-2.34 (m, 2H, C$\underline{H}_2$), 2.67-2.85 (m, 2H, C$\underline{H}_2$), 3.78 (s, 3H, C$\underline{H}_3$), 3.85 (s, 3H, C$\underline{H}_3$), 5.01-5.13 (m, 3H, C$\underline{H}_2$ alkene + C$\underline{H}$OH), 5.70-5.80 (m, 1H, C$\underline{H}$ alkene), 6.54 (d, J=8.52Hz, 1H, Ar$\underline{H}$), 6.78 (d, J=8.48Hz, 1H, Ar$\underline{H}$).

^{13}C NMR (CDCl$_3$, 100.71 MHz) δ_c ppm: 20.5 ($\underline{C}$H$_3$), 33.3 ($\underline{C}$H$_2$), 35.4 ($\underline{C}$H$_2$), 55.3 ($\underline{C}$H$_3$), 60.1 ($\underline{C}$H$_3$), 60.2 ($\underline{C}$H$_3$), 72.7 ($\underline{C}$H), 106.2 ($\underline{C}$H), 117.1 ($\underline{C}$H$_2$), 122.3 (Q), 124.4 ($\underline{C}$H), 133.3 ($\underline{C}$H), 141.6 (Q), 151.7 (Q), 152.0 (Q), 169.5 ($\underline{C}$=O).

6.2.15 Synthesis of 4-((tert-butyldiphenylsilyl)oxy)-5-(2,3,4-trimethoxyphenyl)pentan-1-ol *(3.14).*

(3.13) (3.00 g, 6.1 mmol) was stirred in 2-methoxyethyl ether (70 mL) at 0 °C for 10 min under N_2. To this solution, a 1 M solution of BH$_3$-THF (18.3 mL, 18.3 mmol) was added dropwise. After 10 min the ice bath was removed. A further 50 min passed, when the THF was removed by rotary evaporation. Trimethylamine N-oxide dihydrate (4.74 g, 42.7 mmol) was then added to the flask, which was equipped with a reflux condenser. The mixture was heated under reflux for 2 h, by which time the reaction had completed. The reaction mixture was diluted with EtOAc (100 mL) and washed with warm H_2O (100 mL). The organic layer was washed a further 6 times with H_2O (100 mL), dried over $MgSO_4$ and concentrated *in vacuo* to give a

yellow oil. This oil was purified using 3:1 hexane/EtOAc as a mobile phase for the resulting column. This yielded the product as a colourless mobile oil.

Yield: 2.17 g, 4.26 mmol, 70%.

^{1}H NMR (CDCl$_3$, 400MHz) δ_H ppm: 1.57-1.65 (m, 4H, 2×C$\underline{H}_2$), 2.71-2.78 (m, 2H, C$\underline{H}_2$), 3.58-3.6 (m, 2H, C$\underline{H}_2$), 3.68 (s, 3H, C$\underline{H}_3$), 3.82 (s, 3H, C$\underline{H}_3$), 3.84 (s, 3H, C$\underline{H}_3$), 4.02-4.06 (m, 1H, C$\underline{H}$OSi), 6.52 (d, J=8.52Hz, 1H, Ar$\underline{H}$), 6.61 (d, J=8.44Hz, 1H, Ar$\underline{H}$), 7.34-7.45 (m, 6H, Ar$\underline{H}$), 7.59-7.61 (m, 2H, Ar$\underline{H}$), 7.63-7.67 (m, 2H, Ar$\underline{H}$).

^{13}C NMR (CDCl$_3$, 100.71 MHz) δ_c ppm: 13.7 (Q), 18.8 (Q), 26.6 ($\underline{C}$H$_3$), 27.0 ($\underline{C}$H$_2$), 28.6 ($\underline{C}$H$_2$), 36.7 ($\underline{C}$H$_2$), 55.4 ($\underline{C}$H$_3$), 58.5 ($\underline{C}$H$_3$), 60.1 ($\underline{C}$H$_3$), 62.4 ($\underline{C}$H$_2$), 71.4 ($\underline{C}$H), 106.5 ($\underline{C}$H), 124.3 (Q), 124.9 ($\underline{C}$H), 126.9 ($\underline{C}$H), 129.0 ($\underline{C}$H), 133.8 (Q), 135.5 ($\underline{C}$H), 141.6 (Q), 151.5 (Q).

HRMS (- ESI): Calculated Mass 522.2438. Found 521.1628 (M$^-$).

V$_{max}$ (DCM)/cm^{-1}: 3422 (-OH), 3047, 3070, 2997, 2932, 2856, 1602, 1495, 1467, 1416, 1275, 1039, 703.

6.2.16 Synthesis of 4-((tert-butyldiphenylsilyl)oxy)-5-(2,3,4-trimethoxyphenyl)pentanoic acid *(3.15)*.

(3.14) (1.6 g, 3.1 mmol) was dissolved in DMF (2.5 mL). This was added dropwise to a suspension of PDC (3.55 g, 9.45 mmol) in DMF (6.5 mL) and stirred overnight at room temperature. After 21 h, TLC showed that the starting material had been consumed. The reaction was quenched using H$_2$O (50 mL). The product was extracted with Et$_2$O (3×30 mL). The organic extracts were washed with H$_2$O (3×50 mL). Following the washings, it was dried with MgSO$_4$ and the solvent was removed *in vacuo*. The product was purified by column chromatography (3:1 hexane/EtOAc) and obtained as a colourless gel.

Yield: 1.18 g, 2.33 mmol, 75%.

^{1}H NMR (CDCl$_3$, 400MHz) δ_H ppm: 1.14 (s, 9H, ^{t}$\underline{Bu}$), 1.64-1.87 (m, 2H, C$\underline{H}_2$), 2.43-2.59 (m, 2H, C$\underline{H}_2$), 2.73-2.88 (m, 2H, C$\underline{H}_2$), 3.71 (s, 3H, C$\underline{H}_3$), 3.86 (s, 3H, C$\underline{H}_3$), 3.87 (s, 3H, C$\underline{H}_3$),

4.09-4.17 (1H,m,C$\underline{H}$OSi) 6.56 (d, J=8.56 Hz, Ar$\underline{H}$), 6.61 (d, J=8.04 Hz, Ar$\underline{H}$), 7.41-7.49 (m, 6H, Ar$\underline{H}$), 7.72-7.81 (m, 4H, Ar$\underline{H}$).

^{13}C NMR (CDCl$_3$, 100.71 MHz) δ_c ppm: 18.8 (Q), 26.7 ($\underline{C}$H$_3$), 28.9 ($\underline{C}$H$_2$), 29.8 ($\underline{C}$H$_2$), 36.7 ($\underline{C}$H$_2$), 55.5 ($\underline{C}$H$_3$), 60.1 ($\underline{C}$H$_3$), 60.2 ($\underline{C}$H$_3$), 72.3 ($\underline{C}$H), 106.5 ($\underline{C}$H), 123.7 (Q), 124.8 ($\underline{C}$H), 127.1 ($\underline{C}$H), 129.2 ($\underline{C}$H), 133.5 (Q), 135.6 ($\underline{C}$H), 141.6 (Q), 151.6 (Q), 151.9 (Q), 179.9 ($\underline{C}$=O).

HRMS (- ESI): Calculated Mass 522.2438. Found 521.4470 (M$^-$).

V$_{max}$ (DCM)/cm^{-1}: 3505 (br, OH), 1643 (C=O stretch), 1102, 703.

6.2.17 Synthesis of 8-((tert-butyldiphenylsilyl)oxy)-1,2,3-trimethoxy-6,7,8,9-tetrahydro-5H-benzo[7]annulen-5-one *(3.16)*.

(3.05) was stirred in dry DCM (3 mL) at 0 °C under N$_2$ for 5 min. Dry DMF (3 drops) was added, followed by the dropwise addition of 2 M oxalyl chloride solution in DCM (0.34 mL, 0.77 mmol). After 30 min the ice bath was removed and the temperature was gradually allowed to rise to room temperature. After 45 min, the reaction vessel was heated gently for a further 45 min. TLC analysis showed that the carboxylic acid starting material had been consumed. The solvents were removed under high vacuum and the vessel remained under vacuum for 3 h to ensure dryness of the acyl halide. DCM (10 mL) was added and the mixture was stirred in an ice/NaCl bath at -15 °C. SnCl$_4$ (1 M in DCM) was then added dropwise (0.20 mL, 0.20 mmol). The mixture was stirred at this temperature for 1 h. Upon completion, brine (20 mL) was used to quench the reaction. The aqueous layer was washed with Et$_2$O (3×20 mL). The organic extracts were dried over MgSO$_4$ and on the rotary evaporator at room temperature. This yielded a yellow oil which was purified by column chromatography. 3 compounds were isolated. Fraction 1 was seen to be *tert*-butyl silanol by ^{1}H NMR. Fraction two liberated trace amounts of the desired compound *(3.16)*. Fraction three delivered *(3.28)* in high yield.

Side product – Compound *(3.08)*

Yield: 0.015 g, 0.025 mmol, 6.2%

^{1}H NMR (CDCl$_3$, 400MHz) δ_H: 1.04 (s, 9H, ^{t}Bu), 2.71-2.79 (m, 2H), 2.83-2.89 (m, 1H), 2.98-3.03 (m, 1H), 3.72 (s, 3H, CH$_3$), 3.86-3.88 (m, 1H), 3.90 (s, 3H, CH$_3$), 3.94 (s, 3H, CH$_3$), 4.30-4.38 (m, 1H, CHOH), 7.37 (s, 1H, ArH), 7.37-7.47 (m, 6H, ArH), 7.63-7.68 (m, 4H, ArH).

^{13}C NMR (CDCl$_3$, 100.71 MHz) δ_c ppm: 1.0 (Q), 19.1 (Q), 26.8 (CH$_3$), 32.1 (CH$_2$), 47.6 (CH$_2$), 56.0 (CH$_3$), 60.6 (CH$_3$), 60.9 (CH$_3$), 68.3 (CH), 104.6 (CH), 127.6 (CH), 127.7 (Q), 128.3 (CH), 133.5 (Q), 135.7 (CH), 147.5 (Q), 150.9 (Q), 152.1 (Q), 196.1 (Q).

HRMS (+ ESI): Calculated Mass 504.2332. Found 505.2397 (M+H)$^+$.

V_{max} (DCM)/cm^{-1}: 3487, 2933, 1674, 1486, 1486, 1324, 1193, 1154, 1029, 822, 741, 701.

(3.28)

^{1}H NMR (CDCl$_3$, 400MHz) δ_H ppm: 1.96-2.01 (m, 1H), 2.20-2.28 (m, 1H), 2.45-2.49 (m, 2H), 2.84-2.90 (m, 1H), 3.01-3.06 (m, 1H), 3.85 (s, 3H, CH$_3$), 3.88 (s, 3H, CH$_3$), 3.91 (s, 3H, CH$_3$), 4.74 (quintet, J = 6.64Hz, 1H, CH), 6.63 (d, J=8.48Hz, 1H, ArH), 6.89 (d, J=8.48Hz, 1H, ArH).

^{13}C NMR (CDCl$_3$, 100.71 MHz) δ_c ppm: 26.7 (CH$_2$), 28.2 (CH$_2$), 34.7 (CH$_2$), 55.5 (CH$_3$), 60.2 (CH$_3$), 60.4 (CH$_3$), 80.2 (CH), 106.7 (CH), 121.3 (Q), 124.7 (CH), 141.6 (Q), 151.5 (Q), 152.4 (Q), 176.8 (C=O).

HRMS (+ESI): Calculated Mass 266.1152. Found 267.1209 (M+H$^+$).

V_{max} (DCM)/cm^{-1}: 3435, 3071, 2958, 1731, 1710, 1603, 1472, 1360, 1236, 1154, 853, 741, 608.

6.2.18 **Synthesis of 6,7,8,9-tetrahydro-8-hydroxy-1,2,3-trimethoxybenzo[7]annulen-5-one *(3.17)*.**

To a stirred solution of *(3.16)* (0.01 g, 0.02 mmol) in dry THF (0.5 mL) was added TBAF (0.05 mL, 0.05 mmol) under a blanket of N$_2$ at 0 °C. The resultant mixture was stirred for 3 h until TLC analysis had shown complete consumption of the starting material. The solvent was removed and the product was purified as a yellow oil using flash column chromatography (hexane/EtOAc 1:1).

Yield: 0.003 g, 0.011 mmol, 56.3%.

¹H NMR (CDCl₃, 400MHz) δ$_H$ ppm: 2.07-2.12 (m, 2H, C$\underline{H}$₂), 2.28-2.36 (m, 2H, C$\underline{H}$₂), 2.69 - 3.06 (m, 2H, C$\underline{H}$₂), 3.93 (s, 3H, C$\underline{H}$₃), 3.97 (s, 3H, C$\underline{H}$₃), 4.03 (s, 3H, C$\underline{H}$₃), 4.36-4.43 (m, 1 H, C$\underline{H}$OH), 7.04 (s, 1 H, Ar$\underline{H}$).

¹³C NMR (CDCl₃, 100.71 MHz) δ$_c$ ppm: 16.9 ($\underline{C}$H₂), 33.8 ($\underline{C}$H₂), 33.8 ($\underline{C}$H₂), 55.5 ($\underline{C}$H₃), 60.3 ($\underline{C}$H₃), 61.5 ($\underline{C}$H₃), 76.2 ($\underline{C}$H), 109.4 ($\underline{C}$H), 128.8 (Q), 139.2 (Q), 145.4 (Q), 151.1 (Q), 151.4 (Q), 205.3 ($\underline{C}$=O).

HRMS (+ESI): Calculated Mass 266.1152. Found 267.1213 (M+H⁺).

V$_{max}$ (DCM)/cm⁻¹: 3425 (OH stretch), 2938, 1671 (C=O stretch), 1589, 1487, 1454, 1407, 1306, 1231, 1193, 1132, 1093, 1054, 1030, 922.

6.2.19 Synthesis of 6,7,8,9-tetrahydro-1,2,3-trimethoxybenzo[7]annulen-5-one (3.30).

(3.29) (2.90 g, 10.8 mmol) was dissolved in polyphosphoric acid (PPA). The mixture was mildly heated periodically in a H₂O bath, and using the tip of a pasteur pipette was stirred for 1 h. Ice H₂O (200 mL) was used to quench the reaction and this was washed with Et₂O (3×75 mL). The organic layers were combined, dried over MgSO₄ and concentrated by rotary evaporation to yield a yellow oil. The product was isolated from this mixture by column chromatography (hexane/EtOAc 10:1) as a colourless oil.

Yield: 1.61 g, 6.4 mmol, 59.3%.

¹H NMR (CDCl₃, 400MHz) δ$_H$ ppm: 1.79-1.85 (m, 4H, 2x CH₂), 2.72 (t, J=4.8Hz, 2H, CH₂), 2.95 (t, J=5.8Hz, 2H, CH₂), 3.85 (s, 3H, CH₃), 3.89 (s, 3H, CH₃), 3.94 (s, 3H, CH₃), 7.13 (s, 1H, ArH).

¹³C NMR (CDCl₃, 100.71 MHz) δ$_c$ ppm: 20.4 (CH₂), 22.4 (CH₂), 24.5 (CH₂), 40.3 (CH₂), 55.5 (CH₃), 59.9 (CH₃), 60.9 (CH₃), 106.9 (CH), 128.4 (Q), 133.9 (Q), 145.4 (Q), 150.5 (Q), 151.0 (Q), 204.5 (C=O).

HRMS (+ESI): Calculated Mass 250.1205. Found 251.1266 (M+H⁺).

6.2.20 Attempted Synthesis of 4-bromo-6,7,8,9-tetrahydro-1,2,3-trimethoxy benzo[7]annulen-5-one *(3.31)*.

Compound *(3.30)* (0.50 g, 2.00 mmol) was dissolved in α,α,α-trifluorotoluene. *N*-Bromosuccinimide (0.53 g, 3 mmol) and 2, 2 '-azocyclohexanecarbonitrile (0.50 g, 0.2 mmol) were added to the mixture which was stirred at room temperature. A UV light was shone at the flask to initiate the reaction. However TLC showed that nothing had happened. Two 150W lamps were then used to replace the UV light source, and the mixture started turning orange. After 5 mins, it had turned a pale yellow. TLC showed that there were 8 distinct spots. No further effort was made to purify this compound.

6.2.21 Synthesis of (E) 5-(2,3,4-trimethoxyphenyl) pentanoic acid *(3.33E)*.

3-Carboxypropyl triphenylphosphonium Bromide (6.50 g, 15.1 mmol) was stirred in dry THF (15 mL) under N_2. The suspension was stirred at room temperature for 15 min before the addition of a 1 M solution of NaHMDS in THF (30 mL, 30 mmol). This was stirred for a further 30 min resulting in the formation of a red solution. This solution was placed in a cooling bath at -70 °C and allowed 30 min to cool to this temperature. A solution of 2, 3, 4-trimethoxybenzaldehyde (2.55 g, 13.2 mmol) in dry THF (5 mL) was prepared and then added dropwise to the flask over 5 min. The reaction was stirred for 2 h at the low temperature before the temperature of the cooling bath was allowed to rise to 0 °C. At this temperature, the reaction was quenched with 2 M aq. HCl (50 mL). The acidic solution was washed with Et_2O (3×50 mL). The organic layer was washed with 2 M aq. NaOH (3×40 mL) so as to isolate the acidic compound. The basic layer was re-acidified using 2 M aq. HCl to a pH of 4 and the product was extracted using Et_2O (3×50 mL). The combined organic extracts were dried over $MgSO_4$ before being concentrated to a yellow oil. The product was isolated as a colourless solid by column chromatography using hexane/EtOAc 2:1 as the mobile phase.

Yield: 2.37 g, 8.9 mmol, 68%.

^{1}**H NMR (CDCl$_3$, 400MHz) δ_H ppm:** 2.48 -2.61 (m, 4H, 2×C<u>H</u>$_2$), 3.87 (s, 3H, C<u>H</u>$_3$), 3.88 (s, 3H, C<u>H</u>$_3$), 3.89 (s, 3H, C<u>H</u>$_3$), 5.61-5.70 (m, 1H, C<u>H</u> alkene), 6.14 (d, J=16.04 Hz, 1H, C<u>H</u> alkene), 6.67 (d, J=8.8 Hz, 1H, Ar<u>H</u>), 7.13 (d, J=8.5 Hz, 1H, Ar<u>H</u>).

^{13}**C NMR (CDCl$_3$, 100.71 MHz) δ_c ppm:** 27.8 (<u>C</u>H$_2$), 33.4 (<u>C</u>H$_3$), 55.5 (<u>C</u>H$_3$), 60.4 (<u>C</u>H$_3$), 60.6 (<u>C</u>H$_3$), 107.2 (<u>C</u>H), 120.2 (<u>C</u>H), 123.9 (Q), 124.8 (<u>C</u>H), 127.0 (<u>C</u>H), 141.8 (Q), 150.6 (Q), 152.4 (Q), 178.2 (Q).

HRMS (-ESI): Calculated Mass 266.1154. Found 265.1072 (M$^-$).

V$_{max}$ (DCM)/cm^{-1}: 3482 (CO<u>O</u>H stretch), 2937 (CH stretch), 2841 (CH stretch), 1776, 1737 (C<u>O</u>OH stretch), 1595, 1495, 1416, 1291, 1200, 1014, 798, 696.

6.2.22 Synthesis of (3-methoxypropyl) triphenylphosphonium bromide *(3.35)*.

Compound *(3.32)* (10.00 g, 23.3 mmol) was dissolved in MeOH (500 mL) and stirred at room temperature. Hydrogen chloride gas was added to the flask until the pH of the reaction mixture had reached pH 1 before further stirring for 3 h. The MeOH was removed by rotary evaporation to yield a yellow oil. This was reconstituted in DCM (50 mL) and unreacted starting material was removed using a 5% aq. NaHCO$_3$ solution (4×30 mL). The DCM solution was dried over MgSO$_4$ and dried *in vacuo* to yield the product as a colourless solid.

Yield: 6.73 g, 15.2 mmol, 65%.

^{1}**H NMR (CDCl$_3$, 400MHz) δ_H ppm:** 1.95 (broad s, 2H, C<u>H</u>$_2$), 2.67 (broad s, 2H, C<u>H</u>$_2$), 3.13 (broad s, 2H, C<u>H</u>$_2$), 3.67 (s, 3H, O<u>Me</u>), 7.67-7.89 (m, 15H, 15×Ar<u>H</u>).

^{13}**C NMR (CDCl$_3$, 100.71 MHz) δ_c ppm:** 0.5 (<u>C</u>H$_2$), 17.6 (<u>C</u>H$_2$), 32.6 (<u>C</u>H$_2$), 51.3 (<u>C</u>H$_3$), 130.0 (Q), 133.0 (Q), 134.7 (Q), 173.2 (<u>C</u>=O).

^{31}**P NMR (CDCl$_3$) δp:** 25.39 (s).

HRMS: Calculated Mass 442.0697. Found 363.1503 M$^{+=}$.

V$_{max}$ (DCM)/cm^{-1}: 3499 (OH stretch), 1642, 1438, 1190, 1113, 996, 723, 690, 542.

Melting point: 182-189 °C

6.2.23 Synthesis of (Z)-methyl 5-(2,3,4-trimethoxyphenyl)pent-4-enoate *(3.36)*.

Freshly ground *(3.35)* (5.00 g, 11.27 mmol) was stirred in dry THF (10 mL) under N_2. To the resulting suspension was added 1 M NaHMDS in THF (22.5 mL, 22.5 mmol) dropwise, resulting in the formation of a dark red solution. After 30 min, a solution of 2, 3, 4-trimethoxybenzaldehyde (2.21 g, 11.27 mmol) in THF (5 mL) was added dropwise. After 2 h, TLC showed that the reaction had gone to completion. 2 M aq. HCl (50 mL) was added, and the product was extracted by washing with Et_2O (3×50 mL). The combined organic extracts were dried with $MgSO_4$ and concentrated *in vacuo* yielding a yellow oil. Column chromatography was used to isolate the product using a 10:1 hexane/EtOAc mixture as the mobile phase.

¹H NMR (CDCl₃, 400MHz) δ_H ppm: 2.38-2.42 (m, 2H, C__H__₂), 2.53-2.58 (m, 2H, C__H__₂), 3.63 (s, 3H, O__Me__), 3.79 (s, 3H, O__Me__), 3.84 (s, 3H, O__Me__), 3.85 (s, 3H, O__Me__), 5.55-5.62 (m, 1H, alkene C__H__), 6.47 (d, J=11.36Hz, 1H, Alkene C__H__), 6.62 (d, J=8.6Hz, 1H, Ar__H__), 6.92 (d, J=8.6Hz, 1H, Ar__H__).

¹³C NMR (CDCl₃, 100.71 MHz) δ_c ppm: 23.7 (__C__H₂), 28.1 (__C__H₂), 51.1 (__C__H₃), 55.5 (__C__H₃), 60.5 (__C__H₃), 107.1 (__C__H), 120.1 (__C__H), 123.5 (Q), 124.0 (__C__H), 127.3 (__C__H), 141.8 (Q), 150.6 (Q), 152.3 (Q), 173.0 (__C__=O).

HRMS: Calculated Mass 280.1311. Found 279.1334 (M-H)⁻.

V_max (DCM)/cm⁻¹: 2944, 2843, 1736, 1682, 1590, 1495, 1417, 1290, 1115, 1035, 806, 515.

6.2.24 Synthesis of (Z)-5-(2,3,4-trimethoxyphenyl)pent-4-enoic acid *(3.33Z)*.

Compound *(3.36)* was dissolved in MeOH (35 mL). To this mixture, was added 2.5 M aq. NaOH (10 mL). The mixture was stirred for 30 min before TLC showed that the methyl ester had been completely hydrolysed. H_2O (30 mL) was added to the mixture and MeOH was removed *in vacuo.* This aqueous solution was washed with Et_2O (3×30 mL), removing any remaining 2, 3, 4-trimethoxybenzaldehyde. The aqueous layer was thus acidified with 2 M aq.

HCl and washed with Et$_2$O (3×50 mL). The combined organic extracts were dried over MgSO$_4$ and concentrated to yield the product as a colourless oil.

Yield: 1.95 g, 7.33 mmol, 65% over two steps).

^{1}H NMR (CDCl$_3$, 400MHz) δ$_H$ ppm: 2.47-2.51 (m, 2H, C<u>H</u>$_2$), 2.56-2.64 (m, 2H, C<u>H</u>$_2$), 3.85 (s, 3H, C<u>H</u>$_3$), 3.89 (s, 3H, C<u>H</u>$_3$), 3.90 (s, 3H, C<u>H</u>$_3$), 5.62-5.68 (m, 1H, alkene C<u>H</u>), 6.53 (d, J=11.52Hz, 1H, C<u>H</u>$_2$ alkene), 6.67 (d, J=8.6Hz, 1H, Ar<u>H</u>), 6.95 (d, J=8.56Hz, 1H, Ar<u>H</u>).

^{13}C NMR (CDCl$_3$, 100.71 MHz) δ$_c$ ppm: 23.4 (<u>C</u>H$_2$), 33.6 (<u>C</u>H$_2$), 55.5 (<u>C</u>H$_3$), 60.5 (<u>C</u>H$_3$), 106.4 (<u>C</u>H), 123.4 (Q), 123.7 (<u>C</u>H), 124.9 (<u>C</u>H), 129.0 (<u>C</u>H), 141.8 (Q), 151.2 (Q), 152.4 (Q), 178.7 (<u>C</u>=O).

HRMS (+ESI): Calculated Mass 266.1154. Found 265.1031 (M-)$^-$.

V$_{max}$ (DCM)/cm^{-1}: 3482, 2937, 2841, 1776, 1737, 1595, 1495, 1416, 1291, 1200, 1014, 798, 696.

6.2.25 Synthesis of (Z)-6,7-dihydro-1,2,3-trimethoxybenzo[7]annulen-5-one *(3.34)*.

(3.33Z) was dissolved in dry DCM (10 mL) and stirred on ice under a blanket of N$_2$ for 5 min. Dry DMF (3 drop) was then added, followed by the dropwise addition of a 2 M oxalyl chloride solution in DCM (1.4 mL, 2.8 mmol). After 30 min the ice bath was removed and the temperature was gradually allowed to rise to room temperature. After 45 min, the reaction vessel was heated to 45 °C for the next 45 min. The mixture was placed under high vacuum for 3 h. At the end of this period, DCM (15 mL) was added and the mixture was stirred in an ice/NaCl bath at -15 °C. SnCl$_4$ (1 M in DCM) was added dropwise (0.81 mL, 0.81 mmol). The mixture was stirred at this temperature for the next hour. Upon completion, brine (35 mL) was used to quench the reaction. The aqueous layer was washed with Et$_2$O (3×40 mL). The organic extracts were dried over MgSO$_4$ and on the rotary evaporator at room temperature. This yielded a violet oil which was purified by column chromatography (hexane/EtOAc 8:1) to give the product as a colourless oil.

Yield: 0.38 g, 1.53 mmol, 63%.

¹H NMR (CDCl₃, 400MHz) δ_H ppm: 2.47 (dd, J=11.8Hz,J=5.8Hz, 2H, C$\underline{H}_2$), 2.92-2.95 (m, 2H, C$\underline{H}_2$), 3.85 (s, 3H, C$\underline{H}_3$), 3.93 (s, 3H, C$\underline{H}_3$), 3.95 (s, 3H, C$\underline{H}_3$), 6.20-6.25 (m, 1H, alkene C$\underline{H}$), 6.86 (d, J=7.4Hz, 1H, C=C$\underline{H}$), 7.31 (s, 1H, Ar$\underline{H}$).

¹³C NMR (CDCl₃, 100.71 MHz) δ_c ppm: 23.6 ($\underline{C}H_2$), 43.0 ($\underline{C}H_2$), 55.9 ($\underline{C}H_3$), 60.9 ($\underline{C}H_3$), 61.2 ($\underline{C}H_3$), 108.3 ($\underline{C}H$), 123.5 ($\underline{C}H$), 124.3 (Q), 131.7 ($\underline{C}H$), 132.8 (Q), 146.0 (Q), 151.4 (Q), 152.0 (Q), 201.6 ($\underline{C}$=O).

HRMS: Calculated Mass 248.1049. Found 247.0951 (M-H)⁻.

V_max (DCM)/cm⁻¹: 2942, 1732 (C=O), 1657, 1461, 1339, 1115, 667.

6.2.26 Synthesis of 3,4,5,6-tetrahydro-6-hydroxy-7,8,9-trimethoxy-2-oxo-2H-benzo[b]oxocin-5-yl 3-chlorobenzoate *(3.38)*.

(3.34) (0.15 g, 0.6 mmol) was dissolved in DCM (3 mL) and stirred at room temperature for 10 min. To this, a solution of MCPBA (0.14 g, 0.6 mmol) in DCM was added drop-wise. After 13 h, 10% NaHSO₄ (25 mL) was added to quench the reaction. The product was extracted with DCM (3×20 mL) and the combined organic extracts dried over MgSO₄ and concentrated by rotary evaporation. Column (2:1 hexane/EtOAc) isolated the product as a colourless solid.

Yield: 0.09 g, 0.21 mmol, 35%.

¹H NMR (CDCl₃, 400MHz) δ_H ppm: 1.60-1.65 (m, 1H), 1.97-2.01 (m, 2H, C$\underline{H}_2$), 2.26-2.31 (m, 1H), 3.86 (s, 3H, C$\underline{H}_3$), 3.89 (s, 3H, C$\underline{H}_3$), 3.93 (s, 3H, C$\underline{H}_3$), 4.64 (s, 1H, C$\underline{H}$-O), 4.77 (d, J=8.44Hz, 1H), 5.82 (s, 1H), 6.90 (s, 1H), 7.34-7.36 (m, 1H), 7.36-7.38 (m, 1H), 7.98 (d, J=7.8Hz, 1H), 8.08 (s, 1H).

¹³C NMR (CDCl₃, 100.71 MHz) δ_c ppm: 24.4 ($\underline{C}H_2$), 37.4 ($\underline{C}H_2$), 56.0 ($\underline{C}H_3$), 60.7 ($\underline{C}H_3$), 60.9 ($\underline{C}H_3$), 65.8 ($\underline{C}H_2$), 69.3 ($\underline{C}H$), 101.3 ($\underline{C}H$), 103.2 (Q), 115.6 (Q), 128.0 ($\underline{C}H$), 129.6 ($\underline{C}H$), 129.8 ($\underline{C}H$), 132.0 (Q), 133.0 ($\underline{C}H$), 134.5 (Q), 137.8 (Q), 141.5 (Q), 152.9 (Q), 154.6 (Q), 164.7 (Q).

HRMS (+c ESI): Calculated 436.0925. Found 459.0632 (M+Na⁺).

6.2.27 Synthesis of 6,7,8,9-tetrahydro-8,9-epoxy-1,2,3-trimethoxybenzo[7]annulen-5-one *(3.37)*.

(3.34) (0.10 g, 0.4 mmol) was dissolved in DCM (4 mL) and 10% sodium carbonate solution (10 mL). This biphasic mixture was stirred at 0 °C for 10 min. A solution of MCPBA (0.17 g, 0.69 mmol) in DCM was also prepared. This was added dropwise to the biphasic mixture over 5 min. TLC (hexane/EtOAc 4:1) was used to monitor the progress of the reaction. After 2.5 h, DCM (30 mL) and 10% aq. Na_2CO_3 (20 mL) was added and the DCM layer was separated. This was washed with 10% aq. Na_2CO_3 (4×20 mL), 5% aq. $NaHCO_3$ (20 mL) and brine (20 mL). The DCM extract was dried over $MgSO_4$ and concentrated *in vacuo*. The product was isolated using column chromatography (4:1 hexane/EtOAc).

Yield: 0.06 g, 0.216 mmol, 54%.

^{1}H NMR (CDCl$_3$, 400MHz) δ_H ppm: 2.16-2.29 (m, 2H, C$\underline{H}_2$), 2.55-2.62 (m, 1H), 2.83-2.91 (m, 1H), 3.64-3.67 (m, 1H, C$\underline{H}$), 3.89 (s, 3H, C$\underline{H}_3$), 3.94 (s, 3H, C$\underline{H}_3$), 3.97 (s, 3H, C$\underline{H}_3$), 4.29 (d, J=4.28Hz, 1H, C$\underline{H}$), 6.91 (s, 1H, Ar$\underline{H}$).

^{13}C NMR (CDCl$_3$, 100.71 MHz) δ_c ppm: 21.8 ($\underline{C}H_2$), 37.9 ($\underline{C}H_2$), 51.4 ($\underline{C}H$), 55.5 ($\underline{C}H$), 55.9 ($\underline{C}H$), 60.4 ($\underline{C}H_3$), 60.4 ($\underline{C}H_3$), 61.1 ($\underline{C}H_3$), 107.4 ($\underline{C}H$), 120.7 (Q), 129.3 (Q), 144.6 (Q), 152.9 (Q), 153.2 (Q), 203.2 ($\underline{C}$=O).

HRMS (+ESI): Calculated Mass 264.0998. Found 265.1079 (M+H$^+$).

V$_{max}$ (DCM)/cm^{-1}: 2941, 1717, 1590, 1464, 1342, 1290, 1119, 1031, 930, 801.

6.2.28 Synthesis of 6,7,8,9-tetrahydro-8-hydroxy-1,2,3-trimethoxybenzo[7]annulen-5-one *(3.17)*.

6, 7, 8, 9-tetrahydro-8, 9-epoxy-1, 2, 3-trimethoxybenzo [7] annulen-5-one (0.04 g, 0.15 mmol) was dissolved in EtOAc (5 mL). To this stirring solution was added Palladium (5% on Carbon) (catalytic amount). The round bottomed flask was equipped with a Hydrogen balloon and the reaction proceeded for a further 3 h. The palladium was removed by filtration and the filter

paper was washed with EtOAc. EtOAc was removed *in vacuo* and the product was isolated as a colourless oil by column chromatography (hexane/EtOAc 1:1).

Yield: 0.03 g, 0.11 mmol, 72%.

Characterisation of this compound is previously documented. (Section 6.2.18).

6.3   Chapter 4 Synthesis

6.3.1   Synthesis   of   1-(9-(3-((tert-butyldimethylsilyl)oxy)-4-methoxyphenyl)-7-hydroxy-2,3,4-trimethoxy-5H-benzo[7]annulen-6-yl)ethanone *(4.20)*.

(2.07) (0.07 g, 0.144 mmol) was dissolved in dry THF (1 mL) under a blanket of N_2 and stirred at -78 °C. To this solution was added dropwise a 0.25 M solution of LDA (1.16 mL, 0.29 mmol). The mixture was stirred for 10 min affording a dark red solution. Pyruvonitrile (0.011 g, 0.144 mmol) was dissolved in THF (0.5 mL) and added dropwise to the red solution over 2 min. After stirring for 1 h at -78 °C, the reaction was quenched using 0.5 M aq. HCl (20 mL) and washed with Et_2O (3×15 mL). The combined organic extracts were washed with H_2O (2×20 mL) and dried using $MgSO_4$. After concentration *in vacuo*, the product was purified using column chromatography (hexane/EtOAc 8:1) to yield the product as a red viscous oil.

Yield: 0.06 g, 0.113 mmol, 79%.

^{1}H NMR (CDCl$_3$, 400 MHz) δ_H ppm: 0.18 (s, 6H, 2×CH$_3$), 1.01 (s, 9H, tBu), 1.28 (br s, 2H, CH$_2$), 2.51 (s, 3H, OCH$_3$), 3.63 (s, 3H, OCH$_3$), 3.88 (s, 3H, OCH$_3$), 3.92 (s, 3H, OCH$_3$), 4.02 (s, 3H, OCH$_3$), 6.38 (s, 1H), 6.62 (s, 1H), 6.88 (d, J=8.46Hz, 1H, ArH), 6.94 (d, J=4.46Hz, 1H, ArH), 7.01 (dd, J=8.36Hz, 4.8Hz, 1H, ArH), 15.62 (s, 1H, C=C-OH).

^{13}C NMR (CDCl$_3$, 100.71 MHz) δ_c ppm: -4.4 (CH$_3$), 1.2 (CH$_3$), 18.6 (Q), 23.6 (CH$_2$), 25.8 (CH$_3$), 55.4 (CH$_3$), 56.0 (CH$_3$), 60.9 (CH$_3$), 61.4 (CH$_3$), 109.3 (CH), 110.7 (Q), 111.5 (CH), 121.9 (CH), 123.0 (CH), 123.4 (CH), 127.7 (Q), 132.1 (Q), 135.0 (Q), 143.7 (Q), 144.7 (Q), 148.7 (Q), 150.9 (Q), 151.6 (Q), 151.7 (Q), 174.83 (C=C-OH), 197.4 (C=O).

MS (+ ESI): Calculated Mass 526.2387. Found 525.2319 (M-H)$^-$.

V_{max} (DCM)/cm^{-1}: 3400 (-OH), 3055, 2931, 1711, 1510, 1266, 1119, 740.

6.3.2 Synthesis of 1-(7-hydroxy-9-(3-hydroxy-4-methoxyphenyl)-2,3,4-trimethoxy-5H-benzo[7]annulen-6-yl)ethanone *(4.18).*

To a stirred solution of *(4.20)* (0.04 g, 0.075 mmol) in THF (1 mL) was added a 1 M TBAF (0.04 mL, 0.075 mmol) in THF. The mixture was stirred for 10 min. TLC (hexane/EtOAc 1:1) showed complete consumption of starting materials. The solvents were removed *in vacuo* and the remaining residue was placed directly on a column. The product was isolated as a yellow-red solid using a mobile phase system of hexane/EtOAc (2:1).

Yield: 0.028 g, 0.067 mmol, 90%.

^{1}H NMR (CDCl$_3$, 400 MHz) δ_H ppm: 1.29 (br s, 2H, CH$_2$) 2.52 (s, 3H, OCH$_3$), 3.66 (s, 3H, OCH$_3$), 3.89-3.91 (m, 2H, CH$_2$), 3.94 (s, 3H, OCH$_3$), 3.96 (s, 3H, OCH$_3$), 4.01 (s, 3H, OCH$_3$), 5.69 (s, 1H, ArOH), 6.41 (s, 1H), 6.65 (s, 1H), 6.89 (d, J=8.32Hz, 1H, ArH), 6.98-7.02 (m, 2H, 2xArH), 15.57 (s, 1H, C=C-OH).

^{13}C NMR (CDCl$_3$, 100.71 MHz) δ_c ppm: 23.6 (CH$_2$), 25.6 (CH$_3$), 56.0 (CH$_3$), 56.1 (CH$_3$), 60.9 (CH$_3$), 61.4 (CH$_3$), 109.4 (CH), 110.3 (CH), 110.7 (Q), 115.6 (CH), 121.2 (CH), 123.7 (CH), 127.8 (Q), 132.0 (Q), 135.7 (Q), 145.4 (Q), 147.2 (Q), 148.7 (Q), 150.9 (Q), 151.6 (Q), 174.7 (C=C-OH), 197.5 (C=O).

MS (+ ESI): Calculated Mass 412.1522. Found 411.1495 (M-H)$^-$.

Melting point: 75-78 ^{o}C.

V$_{max}$ (DCM)/cm^{-1}: 3430 (OH stretch), 2938, 2851, 1736 (C=O stretch), 1582, 1554, 1509, 1492, 1289, 1117, 1029, 963, 703.

6.4 Chapter 5 Synthesis

6.4.1 Synthesis of (Z)-8,9-dihydro-5-(3-hydroxy-4-methoxyphenyl)-1,2,3-trimethoxybenzo [7]annulen-7-one *(2.01)*.

To a stirred solution of *(2.07)* (0.20 g, 0.41 mmol) in THF (1 mL) under N_2 at 0 °C was added a 1 M solution TBAF (0.041 mL, 0.41 mmol) in THF. The mixture was stirred for 10 min. After TLC (hexane/EtOAc 1:1) had shown complete consumption of starting materials, the solvents were removed *in vacuo* and the remaining residue was placed directly on a column. The product was isolated as a yellow solid using a mobile phase system of hexane/EtOAc (2:1).

Yield: 0.11 g, 0.29 mmol, 73%.

^{1}H NMR (CDCl$_3$, 400MHz) δ_H ppm: 2.72 (2H, t, J=7Hz, C$\underline{H}_2$), 3.16 (2H, t, J=6Hz C$\underline{H}_2$), 3.65 (3H, s, C$\underline{H}_3$), 3.90 (3H, s, C$\underline{H}_3$), 3.91 (3H, s, C$\underline{H}_3$), 3.93 (3H, s, C$\underline{H}_3$), 5.63 (1H, s, br, ArO$\underline{H}$), 6.39 (1H, s, C=C$\underline{H}$), 6.39 (1H, s, Ar$\underline{H}$), 6.87 (1H, d, J=8.3Hz Ar$\underline{H}$), 6.92 (2H, m, 2×Ar$\underline{H}$).

^{13}C NMR (CDCl$_3$, 100.71 MHz) δ_c ppm: 20.1 ($\underline{C}H_2$), 27.5 ($\underline{C}H_3$), 55.9 (O$\underline{Me}$), 55.9 ($\underline{C}H_3$), 60.8 ($\underline{C}H_3$), 61.3 ($\underline{C}H_3$), 110.0 ($\underline{C}H_3$), 111.8 ($\underline{C}H$), 115.3 ($\underline{C}H$), 121.0 ($\underline{C}H$), 128.0 ($\underline{C}H$), 129.0 (Q), 132.3 (Q), 135.9 (Q), 143.1 (Q), 145.1 (Q), 147.2 (Q), 149.8 (Q), 151.0 (Q), 151.5 (Q), 204.0 ($\underline{C}$=O).

MS (+ ESI): Calculated Mass 370.1416. Found 369.1561 (M-H)⁻.

V$_{max}$ (DCM)/cm^{-1}: 2099, 1643, 1509, 1493.

Melting point: 149-152 °C.

6.4.2 Synthesis of *(5.09)*

Under an atmosphere of N_2, a solution of *(2.01)* (0.0232 g, 0.062 mmol) was dissolved in dry DCM (2 mL). To this solution was added artesunate (0.0240 g, 0.062 mmol) in DCM (1 mL), followed by EDCI (0.0144 g, 0.075 mmol) in DCM (1 mL) and finally by a solution of DMAP

(0.031 g, 0.250 mmol) in DCM (1 mL). The mixture was stirred under these conditions for 12 h. Extraction between 5% aq. Na₂CO₃ (20 mL) and Et₂O (3 x 20 mL) afforded the product. The combined organic layers were washed with H_2O (20 mL) and dried using MgSO₄ and concentrated in vacuo to yield the product in crude form. Following column chromatography (Hexane/EtOAc 3:1), the desired compound was isolated as a colourless solid.

Yield: 0.027 g, 0.036 mmol, 59.3%.

^{1}H NMR (CDCl₃, 400MHz) δ$_H$ ppm: 0.84 (d, J=7 Hz, 3H, C$\underline{H}_3$), 0.97 (d, J=6 Hz, 3H, C$\underline{H}_3$), 1.02-1.13 (m, 2H, 2×ring C$\underline{H}_2$), 1.27-1.37 (m, 3H, 2×C$\underline{H}$, 1×ring C$\underline{H}_2$), 1.43 (s, 3H, C$\underline{H}_3$), 1.46-1.56 (m, 1H, ring C$\underline{H}_2$), 1.59-1.67 (m, 1H, ring C$\underline{H}$), 1.70-1.79 (m, 2H, 1×ring C$\underline{H}$, 1×ring C$\underline{H}_2$), 1.86-1.92 (m, 1H, ring C$\underline{H}_2$), 2.00-2.08 (m, 1H, ring C$\underline{H}_2$), 2.38 (td, J$_1$=14.1 Hz, J$_2$=4 Hz, 1H, ring C$\underline{H}_2$), 2.53-2.60 (m, 1H, 2H, ring C$\underline{H}_2$), 2.72 (dd, J$_1$=7 Hz, J$_2$=4.5Hz, 2H, C$\underline{H}_2$), 2.85 (q, J=7 Hz, 2H, C$\underline{H}_2$), 2.90-3.02 (m, 2H, C$\underline{H}_2$), 3.14 (t, J=6 Hz, 2H, ring C$\underline{H}_2$), 3.63 (s, 3H, OC$\underline{H}_3$), 3.88 (s, 3H, OC$\underline{H}_3$), 3.90 (s, 3H, OC$\underline{H}_3$), 3.95 (s, 3H, OC$\underline{H}_3$), 5.45 (s, 1H, O-C$\underline{H}$-C), 5.82 (d, J=10 Hz, 1H, O-C$\underline{H}$-O), 6.37 (s, 1H), 6.39 (s, 1H), 6.98 (d, J=8.5 Hz, 1H), 7.01 (d, J=2 Hz, 1H), 7.29 (dd, J = 8.4 Hz, J = 2 Hz, 1H).

^{13}C NMR (CDCl₃, 100.71 MHz) δ$_c$ ppm: 11.6 (C$\underline{H}_3$), 19.7 (C$\underline{H}_2$), 19.8 (C$\underline{H}_3$), 21.5 (C$\underline{H}_2$), 24.1 (C$\underline{H}_2$), 25.5 (C$\underline{H}_3$), 28.1 (C$\underline{H}_2$), 28.7 (C$\underline{H}_2$), 29.2 (C$\underline{H}_2$), 31.3 (CH), 33.6 (C$\underline{H}_2$), 35.7 (C$\underline{H}_2$), 36.8 (CH), 44.7 (CH), 45.2 (C$\underline{H}_2$), 51.1 (C$\underline{H}$), 55.5 (2×C$\underline{H}_3$), 60.5 (C$\underline{H}_3$), 61.0 (C$\underline{H}_3$), 79.7 (Q), 91.1 (CH), 91.8 (C$\underline{H}$), 104.0 (Q), 111.2 (C$\underline{H}$), 111.5 (C$\underline{H}$), 123.6 (C$\underline{H}$), 127.1 (C$\underline{H}$), 127.9 (C$\underline{H}$), 128.7 (Q), 131.6 (Q), 134.6 (Q), 138.7 (Q), 142.8 (Q), 149.5 (Q), 150.2 (Q), 150.7 (Q), 151.3 (Q), 169.8 (C=O), 170.4 (C=O), 203.6 (Q, C=O).

MS (+ ESI): Calculated Mass 734.3302. Found 759.3032 (M+Na)$^+$.

Melting point: 117-124 °C.

V$_{max}$ (DCM)/cm^{-1}: 3418, 2925, 1756, 1657, 1453, 1362, 1116, 764.

6.4.3 Synthesis of *(5.10)*.

Under an atmosphere of N_2, a solution of *(2.07)* (0.09 g, 0.18 mmol) was dissolved in dry DCM (2 mL). To this solution was added artesunate (0.072 g, 0.18 mmol) in DCM (1 mL) followed by EDC (0.0426 g, 0.222 mmol) in DCM (1 mL) and finally by a solution of DMAP (0.090 g, 0.74 mmol) in DCM (1 mL). The mixture was stirred under these conditions for 48 h. Extraction between H_2O (20 mL) and Et_2O (3x20 mL) afforded the product. The combined organic layers were dried using $MgSO_4$ and concentrated in vacuo to yield the product in crude form. Following column chromatography (hexane/EtOAc 3:1), the desired compound was isolated as a colourless solid.

Yield: 0.07 g, 0.082 mmol, 46%.

^{1}H NMR (CDCl$_3$, 400MHz) δ_H ppm: 0.14 (d, J=5Hz, 6H, C$\underline{H}_3$), 0.86 (d, J=6 Hz, 3H, C$\underline{H}_3$), 0.97 (d, J=6 Hz, 3H, C$\underline{H}_3$), 0.98 (s, 9H, ^{t}Bu), 1.32-1.37 (m, 4H), 1.44 (s, 3H, C$\underline{H}$3), 1.45-1.5 (m, 3H), 1.60-1.67 (m, 2H), 1.70-1.84 (m, 2H), 1.86-1.94 (m, 1H), 2.00-2.22 (m, 3H), 2.33-2.44 (m, 2H), 2.50-2.63 (m, 2H), 2.65-2.81 (m, 2H), 3.01-3.10 (m, 1H), 3.63 (s, 3H, OC$\underline{H}_3$), 3.82 (s, 3H, OC$\underline{H}_3$), 3.91 (s, 3H, OC$\underline{H}_3$), 3.92 (s, 3H, OC$\underline{H}_3$), 5.13-5.23 (m, 1H, C$\underline{H}$OH), 5.46 (s, 1H, OC$\underline{H}$C), 5.83 (d, J= 9.5 Hz, 1H, OC$\underline{H}$O), 6.12 (d, J= 5Hz, 1H, C=C$\underline{H}$) 6.35 (s, 1H, Ar$\underline{H}$), 6.76 (d, J=2.1 Hz, 1H, Ar$\underline{H}$), 6.81 (d, J=6.7Hz, 1H, Ar$\underline{H}$), 6.88 (d, J=6.7Hz, 2.1Hz, 1H, Ar$\underline{H}$).

^{13}C NMR (CDCl$_3$, 100.71 MHz) δ_c ppm: -5.0 ($\underline{C}H_3$ (TBDMS)), 11.6 ($\underline{C}H_3$), 18.0 (Q(TBDMS)), 19.8 ($\underline{C}H_3$), 21.0 ($\underline{C}H_2$), 21.5 ($\underline{C}H_2$), 24.1 ($\underline{C}H_2$), 25.3 ($\underline{C}H_3$, ^{t}Bu), 25.5 ($\underline{C}H_3$), 28.6 ($\underline{C}H_2$), 28.8 ($\underline{C}H_2$), 29.2 ($\underline{C}H_2$), 31.3 ($\underline{C}H$), 33.6 ($\underline{C}H_2$), 35.7 ($\underline{C}H_2$), 36.8 ($\underline{C}H$), 39.6 ($\underline{C}H_2$), 44.8 ($\underline{C}H$), 51.0 ($\underline{C}H$), 55.0 ($\underline{C}H_3$), 55.5 ($\underline{C}H_3$), 60.4 ($\underline{C}H_3$), 61.2 ($\underline{C}H_3$), 70.7 (Q), 72.0 ($\underline{C}H$), 91.0 ($\underline{C}H$), 91.7 ($\underline{C}H$), 104.0 (Q), 108.5 ($\underline{C}H$), 111.1 ($\underline{C}H$), 120.3 ($\underline{C}H$), 121.1 ($\underline{C}H$), 126.0 ($\underline{C}H$), 126.9 (Q), 133.4 (Q), 134.5 (Q), 139.2 (Q), 141.1 (Q), 144.1 (Q), 150.2 (Q), 150.3 (Q), 150.7 (Q), 170.7 ($\underline{C}$=O), 170.9 ($\underline{C}$=O).

MS (+ ESI): Calculated Mass 852.4324. Found 875.4000 (M+Na)$^+$.

Melting point: 126-129 $^{\circ}$C.

V_{max} (DCM)/cm^{-1}: 3517, 2929, 1737, 1509, 1263, 1115, 1036, 839.

6.4.4   Deprotection to yield (5.11).

To a stirred solution of *(5.10)* (0.05 g, 0.058 mmol) in dry THF (2 mL) under an atmosphere of N_2 at 0 $^{\circ}$C was added 1 M TBAF in THF (0.10 mL, 0.10 mmol). After stirring for 10 min, the product was extracted using Et_2O (3×20 mL) and H_2O (20 mL). The combined organic extracts were dried using $MgSO_4$ and concentrated *in vacuo*. The resultant residue was purified using flash column chromatography (hexane/EtOAc 1:1), yielding *(5.11)* as a colourless solid.

Yield: 0.04 g, 0.052 mmol, 92%.

^{1}H NMR (CDCl$_3$, 400MHz) δ_H ppm: 0.82 (d, J=7.20 Hz, 3H, C$\underline{H}_3$), 0.94 (d, J=6 Hz, 3H, C$\underline{H}_3$), 0.98-1.05 (m, 1H, ring C$\underline{H}_2$), 1.21-1.37 (m, 4H, 2×ring C$\underline{H}$, 2×ring C$\underline{H}_2$), 1.40 (s, 3H, C$\underline{H}_3$), 1.42-1.52 (m, 1H, ring C$\underline{H}_2$), 1.55-1.63 (m, 1H, ring C$\underline{H}$), 1.65-1.78 (m, 2H, 2×ring C$\underline{H}_2$), 1.82-1.91 (m, 1H, ring C$\underline{H}_2$), 1.96-2.05 (m, 1H, ring C$\underline{H}_2$), 2.07-2.14 (m, 1H, ring C$\underline{H}$), 2.28-2.40 (m, 2H, 2×ring C$\underline{H}_2$), 2.45-2.73 (m, 7H, 2×C$\underline{H}_2$, ring C$\underline{H}$, 3×ring C$\underline{H}_2$), 3.01-3.10 (m, 1H, C$\underline{H}_2$), 3.65 (s, 3H, C$\underline{H}_3$), 3.87 (s, 3H, C$\underline{H}_3$), 3.88 (s, 3H, C$\underline{H}_3$), 3.89 (s, 3H, C$\underline{H}_3$), 5.13 (ddd, J= 10.4 Hz, 7.7Hz, 5.0Hz, 1H, C$\underline{H}$OC), 5.40 (br s, 1H, -O$\underline{H}$), 5.41 (s, 1H, OC$\underline{H}$C), 5.76 (d, J=9.8 Hz, 1H, OC$\underline{H}$O), 6.10 (d, J= 5 Hz, 1H, C=C$\underline{H}$), 6.32 (s, 1H, Ar$\underline{H}$), 6.76 (s, 2H, 2×Ar$\underline{H}$), 6.86 (s, 1H, Ar$\underline{H}$).

^{13}C NMR (CDCl$_3$, 100.71 MHz) δ_c ppm: 12.1 ($\underline{C}$H$_3$), 20.2 ($\underline{C}$H$_3$), 21.5 ($\underline{C}$H$_2$), 22.0 ($\underline{C}$H$_2$), 24.6 ($\underline{C}$H$_2$), 26.0 ($\underline{C}$H$_3$), 29.1 ($\underline{C}$H$_2$), 29.2 ($\underline{C}$H$_2$), 31.8 ($\underline{C}$H), 34.1 ($\underline{C}$H$_2$), 36.2 ($\underline{C}$H$_2$), 37.3 ($\underline{C}$H), 40.0 ($\underline{C}$H$_2$), 45.2 ($\underline{C}$H), 51.6 ($\underline{C}$H), 56.0 ($\underline{C}$H$_3$), 56.1 ($\underline{C}$H$_3$), 60.9 ($\underline{C}$H$_3$), 61.6 ($\underline{C}$H$_3$), 72.5 ($\underline{C}$H), 80.2 (Q), 91.5 ($\underline{C}$H), 92.2 ($\underline{C}$H), 104.5 (Q), 109.0 ($\underline{C}$H), 110.3 ($\underline{C}$H), 114.3 ($\underline{C}$H), 120.0 ($\underline{C}$H), 127.0 ($\underline{C}$H), 127.4 (Q), 134.5 (Q), 134.8 (Q), 139.6 (Q), 141.7 (Q), 145.3 (Q), 146.3 (Q), 150.8 (Q), 151.3 (Q), 171.2 ($\underline{C}$=O), 171.4 ($\underline{C}$=O).

HRMS (+ ESI): Calculated Mass 736.3459 Found 735.3376 (M-H)$^-$.

Melting Point: 109-114 $^{\circ}$C.

V$_{max}$ (DCM)/cm^{-1}: 3429, 2857, 1737, 1509, 1406, 1264, 1115, 1036, 839, 737.

6.4.5 Synthesis of 9-(3-hydroxy-4-methoxyphenyl)-2,3,4-trimethoxy-6,7-dihydro-5H-benzo[7]annulen-7-ol *(5.12)*.

To a stirred solution of *(2.07)* (0.30 g, 0.62 mmol) in THF (1 mL) under N_2 at 0 °C was added a 1 M solution TBAF (0.62 mL, 0.62 mmol) in THF. The mixture was stirred for 10 min. After TLC (hexane/EtOAc 1:1) had shown complete consumption of starting materials, the solvents were removed *in vacuo* and the remaining residue was placed directly on a column. The product was isolated as a yellow oil using a mobile phase system of hexane/EtOAc (2:1).

Yield: 0.20 g, 0.53 mmol, 86%.

^{1}H NMR (CDCl$_3$, 400MHz) δ_H ppm: 2.06-2.14 (1H, m, C$\underline{H}_2$), 2.29-2.37 (1H, m, C$\underline{H}_2$), 2.26-2.55 (1H, m, C$\underline{H}_2$), 2.63 (1H, br s, O$\underline{H}$), 2.99-3.04 (1H, m, C$\underline{H}_2$), 3.66 (3H, s, C$\underline{H}_3$), 3.88 (3H, s, C$\underline{H}_3$), 3.89 (3H, s, C$\underline{H}_3$), 3.91 (3H, s, C$\underline{H}_3$), 4.10-4.18 (1H, m, C$\underline{H}$OH), 6.02 (1H, s br, O$\underline{H}$), 6.28 (1H, d, J = 5 Hz, C=C$\underline{H}$), 6.36 (1H, s , Ar$\underline{H}$), 6.78 (2H, s, 2×Ar$\underline{H}$), 6.89 (1H, s, Ar$\underline{H}$).

^{13}C NMR (CDCl$_3$, 100.71 MHz) δ_c ppm: 21.1 ($\underline{C}H_2$), 43.3 ($\underline{C}H_2$), 56.0 (2×O$\underline{Me}$), 60.9 (O$\underline{Me}$), 61.6 (O$\underline{Me}$), 69.7 ($\underline{C}$HOH), 108.8 ($\underline{C}$H), 110.4 ($\underline{C}$H), 114.4 (C=$\underline{C}$H) 119.8 ($\underline{C}$H), 128.0 (Q), 131.8 ($\underline{C}$H), 134.6 (Q), 135.3 (Q), 138.5 (Q), 141.4 (Q), 145.4 (Q), 146.4 (Q), 150.7 (Q), 151.1 (Q).

MS (+ ESI): Calculated Mass 371.1573. Found 371.1484 (M-H)$^-$.

V$_{max}$ (DCM)/cm^{-1}: 3411, 2935, 2838, 1717, 1580.

6.4.6 Synthesis of *(5.14)*.

To a stirred solution of *(5.13)* (0.10 g, 0.27 mmol) in dry DCM (2 mL) under a blanket of N_2 was added sequentially artesunate (0.19 g, 0.54 mmol) in DCM (1 mL), EDCI (0.042 g, 0.27 mmol) in DCM (1 mL) and DMAP (0.12 g, 1 mmol) in DCM (1 mL). The mixture was stirred for 72 h before the reaction was quenched in H_2O (20 mL) and washed with Et_2O (3×20 mL). The combined organic extracts were dried over MgSO$_4$ and filtered before concentration in vacuo isolated the product in crude from. The product was obtained as a colourless solid using

Flash Column Chromatography collecting each homogeneous fraction using hexane/EtOAc 1:1 as mobile phase.

^{1}H NMR (CDCl$_3$, 400MHz) δ$_H$ ppm: 0.81 (s, J= 7.20 Hz, 3H, CH$_3$), 0.94 (d, J=6.2 Hz, 3H, CH$_3$), 1.27-1.36 (m, 3H), 1.41 (s, 3H, CH$_3$), 1.43-1.51 (m, 2H), 1.57-1.62 (m, 1H), 1.66-1.78 (m, 3H), 1.83-1.91 (m, 2H), 1.97-2.02 (m, 1H), 2.05-2.14 (m, 1H), 2.27-2.37 (m, 2H), 2.43-2.60 (m, 3H), 2.80-2.85 (m, 2H), 2.87-3.04 (m, 3H), 3.67 (s, 3H, CH$_3$), 3.81 (s, 3H, CH$_3$), 3.87 (s, 3H, CH$_3$), 3.89 (s, 3H, CH$_3$), 4.14-4.17 (m, 1H, CHOH), 5.42 (s, 1H, OCHC), 5.79 (d, J=9.90 Hz, 1H, OCHO), 6.27 (d, J=5.1 Hz, C=CH), 6.34 (s, 1H, ArH), 6.88 (d, J=8.6 Hz, ArH), 6.99 (d, J=2.1 Hz, 1H, ArH), 7.13 (d, J=8.6 Hz, 2.1 Hz, 1H, ArH).

^{13}C NMR (CDCl$_3$, 100.71 MHz) δ$_c$ ppm: 12.0 (CH$_3$), 20.2 (CH$_3$), 21.8 (CH$_2$), 22.0 (CH$_2$), 24.6 (CH$_2$), 25.9 (CH$_3$), 28.7 (CH$_2$), 29.3 (CH$_2$), 31.8 (CH), 34.1 (CH$_2$), 36.2 (CH$_2$), 37.2 (CH), 43.4 (CH$_2$), 45.2 (CH), 51.5 (CH), 55.9 (CH$_3$), 56.0 (CH$_3$), 60.8 (CH$_3$), 61.5 (CH$_3$), 69.8 (CH), 80.1 (Q), 91.5 (CH), 92.2 (CH), 104.5 (Q), 108.6 (CH), 112.0 (CH), 122.4 (CH), 126.3 (CH), 128.1 (Q), 132.1 (CH), 134.7 (Q), 137.8 (Q), 139.4 (Q), 141.5 (Q), 145.3 (Q), 149.0 (Q), 150.5 (Q), 151.2 (Q), 170.3 (C=O), 170.8 (C=O).

MS (+ ESI): Calculated Mass 736.3459. Found 737.3547 (M+H)$^+$.

V$_{max}$ (DCM)/cm^{-1}: 3499, 2928, 1757, 1510, 1150, 1017.

Melting point: 121-126 °C.

Biological Experimental

7.1 Introduction

The biological activity of the synthesised compounds was assessed using the APN inhibition assay, the MTT cell proliferation assay and the cell migration assay as described in their corresponding chapters. Prior to this evaluation, all residual solvents were removed upon placement of the compounds *in vacuo* for several days. Stock solutions of compounds were obtained by weighing quantities using a microbalance and reconstituting in DMSO. Sequential dilution of these stock solutions afforded solutions of appropriate concentration for assay.

7.2 Aminopeptidase N UV Spectrophotometric Assay

The APN inhibition activity of the test compounds was determined using a UV spectrophotometric assay as detailed in Chapter 2.[135b] The enzymatic hydrolysis of L-Leucine-*p*-nitroanilide APN in the presence of the test compounds was measured by spectrophotometry. By comparing the blank absorbance with the test absorbance the observed percentage inhibition was calculated.

7.2.1 Materials

Bestatin, aminopeptidase N, L-Leucine-*p*-nitroanilide, Leucine aminopeptidase (microsomal from porcine kidney, Type VI-S, lyophilized powder, 15-25 units/mg protein), and 4-(2-Hydroxyethyl)piperazine-1-ethanesulfonic acid (HEPES) were purchased from Sigma-Aldrich®. Greiner 96-well cell culture U-bottom microplates were purchased from Cruinn, Ireland.

7.2.2 Equipment

Fluostar Optima 96 well plate reader equipped with a thermostat function

7.2.3 Buffers and Solutions

HEPES buffer consisting of 50 mM HEPES dry powder and 154 mM NaCl was prepared with deionised water. The pH of the resultant solution was adjusted to 7.4 by the dropwise addition of 2.5 M aq. NaOH aqueous solution. The buffer was then stored at 4 °C.

The substrate solution containing 2 mM L-Leucine-p-nitroanilide was prepared using HEPES buffer.

The enzyme solution containing 95 mU leucine aminopeptidase was prepared using HEPES buffer.

7.2.4 Assay protocol

The 2 mM enzyme substrate (L-Leucine-p-nitroanilide) solution (50 μL) and HEPES buffer solution (40 μL) were pipetted into each well of a 96 well plate. The test compound solution (50 μL), control containing DMSO (0.1%) in HEPES buffer (50 μL) or 200 μM bestatin solution in HEPES (50 μL) were then added to their assigned wells. Upon commencement of the enzymatic hydrolysis upon addition of 95 mU enzyme solution (10 μL) to each well, each test well of the 96 well plate contained a final volume of 200 μL. The plate was incubated at 37 °C for 2 h. The absorbance at 405 nm was then determined using the Fluostar Optima microplate reader. The 200 μM bestatin solution in HEPES acted as negative control while the solutions containing DMSO (0.1%) in HEPES were used as positive controls. A blank containing HEPES buffer (150 μL) and substrate (50 μL) only also acted as a negative control. Each concentration of compound was assayed in triplicate. Furthermore, all assays were carried out on three separate occasions. APN inhibitory activity was determined by comparison to blank controls.

7.2.5 Plate reader settings

Measurement type	Kinetic, 1 cycle of 20 readings
Absorbance wavelength	405 nm
Temperature	37 °C
Shaking	Once before first measurement, 15 seconds, double orbital

7.2.6 Interpretation of data

Percentage inhibition was calculated according to the following formula:

Percentage Inhibition (%) = [(blank absorbance-test absorbance)/Blank absorbance] x 100

The results were analysed using GraphPad Prism software. Dose-response curves were obtained by plotting the percentage APN inhibition (%) against log (compound concentration). Non-linear regression was used to analyse the data. The best fit IC_{50} values ± SEM were then calculated using GraphPad Prism.

7.3 MTT Cell proliferation assay

The MTT assay was used to assess the antiproliferative activity of the novel compounds synthesised. This assay, initially described by Mosmann et al,[212] is quantitative colorimetric assay which detects viable, but not dead cells by generating a signal proportional to the degree of cellular function . In the presence of viable cells, the yellow tetrazole MTT is reduced by an active mitochondrial reductase enzyme system, to afford purple formazan crystals. These crystals are then dissolved in DMSO to give a coloured solution whose absorbance is detected using the microplate reader.

7.3.1 Materials

Dimethyl sulfoxide (DMSO), thiazolyl blue tetrazolium bromide (MTT), foetal bovine serum (FBS), streptomycin/penicillin solution and 0.25% trypsin/EDTA solution were all purchased from Sigma-Aldrich®, Ireland. Phosphate buffered saline (PBS) tablets were purchased from Invitrogen, Ireland. Greiner CELLSTAR® 75 cm^2 cell culture flasks and Greiner 96-well PS cell culture U-bottom microplates were purchased from Cruinn, Ireland.

7.3.2 Equipment

Fluostar Optima 96 well plate reader equipped with a thermostat function

NuAire class II biological safety cabinet

Olympus CKX41 inverted microscope (Mason Technology, Ireland)

7.3.3 Test compounds

All DMSO stock solutions were diluted in cell culture medium affording a final DMSO concentration of $\leq 0.1\%$. Control solutions consisted of 0.1 % DMSO in cell culture medium.

7.3.4 Cell line

The PC-3 human prostate adenocarcinoma cell line was purchased from LGC Standards, UK. The cells were cultured in F12K medium supplemented with 10% FBS and 10 mL/L penicillin/streptomycin solution. Cell culltures were kept at 37 °C in a humidified atmosphere, containing 5% CO_2 at all times.

7.3.5 Cell maintenance and sub-culture

Cell culture experiments were performed in a NuAire class II biological safety cabinet, following aseptic techniques at all times to prevent contamination. The cells were cultured in 75 cm^2 cell culture flasks using 15 mL of complete medium. The cell culture medium was typically replaced every 2 days. Cells were monitored using an Olympus CKX41 inverted microscope (Mason Technology, Ireland). Cells were sub-cultured into fresh flasks once they had reached 70-80% confluence. The protocol followed for sub-culture was as follows:

The old medium was removed from the cell culture flask. The cell monolayer was gently rinsed with PBS solution (10 mL). Trypsin/EDTA solution (3 mL) was added and the cells were incubated at 37 °C until 90% of the cells acquired a rounded morphology. The flask was tapped to encourage detachment of the cells and complete medium (5 mL) was added. The contents of the flask was then transferred to a sterile centrifuge tube. The flask was rinsed with a further aliquot of medium (5 mL) and this was also added to the centrifuge tube. The cell suspension was centrifuged at 1000 rpm at 25 °C for 5 min. The supernatant was removed and fresh medium (2-3 mL) was added to the tube to re-suspend the cell pellet. New flasks containing fresh medium (15 mL) at 37 °C were prepared in parallel. The cell suspension was then sub-cultured into these new flasks at 1:4 or 1:6 seeding densities and returned to the incubator. After 24 h, the cells were examined under the microscope and the medium was replaced with fresh, pre-equilibrated medium.

7.3.6   Cell count

A haemocytometer was used to estimate the cells density in cell suspensions used in the MTT cell proliferation assay. Once cells reached 70-80% confluence, same procedure as above was followed. After the centrifugation step, the cell pellet was re-suspended in 10 mL of cell medium, upon removal of the supernatant. The haemocytometer was cleaned thoroughly with 70% ethanol solution and the cover slip was affixed using gentle pressure and circular motions. The haemocytometer was filled by carefully pipetting the appropriate volume of suspension (10 μL) onto the haemocytometer, adjacent to the cover slip filling the haemocytometer by capillary action. The haemocytometer was then viewed under the microscope using the x4 objective lens to maintain focus on the grid lines. The number of cells in the 16 corner squares was counted using a hand tally counter. Cells were only included in the count if they were within the square or positioned on the left or top boundary lines. This process was repeated for the haemocytometer's 5 sets of corner squares (including the middle set of 16 squares). The average count was obtained by dividing the total cell count for the 5 sets of squares by 5. The haemocytometer is designed so that the number of cells in on set of 16 corner squares is equivalent to the number of cells x 10^4/ml. Therefore, to calculate the number of cells/ml, the average count of cells was multiplied by 10 (depending on the total volume of cell suspension) and then by 10^4.

7.3.7   Assay protocol

PC-3 cells were seeded into a 96-well plate at a density of 2000 cells per well using an appropriate volume of cell suspension. The volume of liquid in each well was then adjusted to 180 μL. The plate was incubated for 24 h at 37 °C. Compound test solutions or control solutions of either CA-4 or 0.1% DMSO blank (20 μL) were then added to each well and the plate was incubated for 72 h at 37 °C. After incubation, the cell medium was removed and 0.5 mg/mL MTT solution in complete medium (200 μL) was added. The plate was then incubated for a further 4 h. The supernatant was then removed from the plate and the purple formazan crystals

dissolved in DMSO (180 μL). Absorbance values for the resulting solutions were obtained using the Fluostar Optima 96 well plate reader. Each compound concentration was tested in quadruplicate and each experiment was performed three independent times.

7.3.8   Plate reader settings

Measurement type	Kinetic, 1 cycle of 20 readings
Absorbance wavelength	485 nm
Temperature	Ambient
Shaking	Once before first measurement, 10 seconds, double orbital

7.3.9   Interpretation of data

The percentage growth inhibition was calculated according to the following formula:

Percentage growth Inhibition (%) = [(control absorbance-test absorbance)/control absorbance] x 100

Statistical analysis of the data was carried out using GraphPad Prism, version 5. The normalised percentage inhibition was plotted against the log(compound concentration) and analysed by non-linear regression. The best fit IC_{50} values ± SEM were then calculated by Prism.

7.4   Cell Migration Assay

The extent of cell migration upon treatment of compounds was measured using the scratch assay as detailed in chapter 2.[213]

7.4.1 Materials

Bestatin, Dimethyl sulfoxide (DMSO), foetal bovine serum (FBS), streptomycin/penicillin solution and 0.25% trypsin/EDTA solution were all purchased from Sigma-Aldrich®, Ireland. Phosphate buffered saline (PBS) tablets were purchased from Invitrogen, Ireland. Greiner CELLSTAR® 75 cm^2 cell culture flasks and Greiner 12-well PS cell culture plates, sterile with lid were purchased from Cruinn, Ireland.

7.4.2 Equipment

NuAire class II biological safety cabinet.

Olympus CKX41 inverted microscope (Mason Technology, Ireland).

Olympus Cell^A software

Tscratch software.

7.4.3 Test compounds

All DMSO stock solutions were diluted in cell culture medium to afford a final DMSO concentration of $\leq 0.1\%$. Control solutions consisted of 0.1 % DMSO in cell culture medium.

7.4.4 Cell line

The PC-3 human prostate adenocarcinoma cell line was purchased from LGC Standards, UK. The cells were cultured in F12K medium supplemented with 10% FBS and 10 mL/L penicillin/streptomycin solution. Cell culltures were kept at 37 °C in a humidified atmosphere containing maintaining 5% CO_2 levels at all times.

7.4.5   Cell maintenance and sub-culture

PC-3 human prostate cells were maintained in a Nuaire class II biological safety cabinet following the same procedure as outlined in Section 7.3.5 above.

7.4.6   Cell migration assay protocol

Once cells had reached 70-80% confluence and isolated in pellet form following the procedure as detailed in Section 7.3.5, they were resuspended in F-12K medium (3 mL). To a 75 cm^2 cell culture flask was added F-12K medium (30 mL) and incubated for 30 min at 37 $^{\circ}$C in the Nuaire class II biological safety cabinet. The cell suspension (1 mL) was added to the 75 cm^2 cell culture flask and incubated for 5 mins. To each well of a 12 well plate was added the resulting cell culture suspension (1.3 mL). The cells were incubated for 24 h, before replacement of the medium. Once the cells had reached 70-80% confluence, a scratch was made in the centre of each well with a sterile plastic 200 μL pipette tip. Cells were incubated with a 0.1% DMSO blank solution, increasing amounts of test compound as detailed in the corresponding chapters, *(2.01)*, CA-4 and bestatin. Images of the wounds were acquired using the Olympus CKX41 inverted microscope at 4× magnification and its associated Cell^A software at 0 h, 24 h, 36 h and 48 h. The wound areas at these time points were measured using Tscratch software and compared to the 0 h area to determine the migration distance. Each compound was tested in triplicate and each experiment was performed three individual times.

7.4.7   Interpretation of data

The cell migration distance was calculated by subtracting the wound width at each time point from the width at 0 h. Wound width at 0 h was calculated by measuring its distance in pixels. Each pixel is calibrated to represent 0.8625 nm. Pictures acquired were in 2080×1044 resolution. Converting pixel distance to wound width (nm) was achieved using the formula:

$$\text{Wound width} = 0.8625 \times 2080 \times \text{pixel distance.}$$

Statistical analysis of the data was carried out using GraphPad Prism, version 5. The cell migration distances were analysed using a group table, showing the average cell migration distance ± SEM.

Bibliography

1. Jemal, A.; Siegel, R.; Ward, E.; Murray, T.; Xu, J.; Thun, M. J., Cancer Statistics, 2007. *CA: A Cancer Journal for Clinicians* **2007,** *57* (1), 43-66.

2. Bray, F.; Moller, B., Predicting the future burden of cancer. *Nature Reviews Cancer* **2006,** *6* (1), 63-74.

3. NCRI *Cancer in 2011: Annual Report of the National Cancer Registry*; National Cancer Registry of Ireland: Ireland, 2011.

4. http://www.cancer.ie/about-us/media-centre/cancer-statistics (accessed 13 November 2012).

5. (a) Weinberg, R. A., *The biology of cancer*. Garland Science New York: 2007; Vol. 1; (b) Hanahan, D.; Weinberg, R. A., The Hallmarks of Cancer. *Cell* **2000,** *100* (1), 57-70.

6. Sainsbury, R.; Johnston, C.; Haward, B., Effect on survival of delays in referral of patients with breast-cancer symptoms: a retrospective analysis. *Lancet* **1999,** *353* (9159), 1132-1135.

7. Donnelly, S.; Walsh, D., The symptoms of advanced cancer. *Seminars in oncology* **1995,** *22* (2 Suppl 3), 67-72.

8. http://www.behindlifestyle.com/wp-content/uploads//2012/04/cancer-incidence.jpeg (accessed January 2 2013).

9. Anand, P.; Kunnumakara, A.; Sundaram, C.; Harikumar, K.; Tharakan, S.; Lai, O.; Sung, B.; Aggarwal, B., Cancer is a Preventable Disease that Requires Major Lifestyle Changes. *Pharm Res* **2008,** *25* (9), 2097-2116.

10. Hamilton, A. S.; Mack, T. M., Puberty and Genetic Susceptibility to Breast Cancer in a Case–Control Study in Twins. *New England Journal of Medicine* **2003,** *348* (23), 2313-2322.

11. Irigaray, P.; Newby, J. A.; Clapp, R.; Hardell, L.; Howard, V.; Montagnier, L.; Epstein, S.; Belpomme, D., Lifestyle-related factors and environmental agents causing cancer: An overview. *Biomedicine & Pharmacotherapy* **2007,** *61* (10), 640-658.

12. Tuyns, A. J., Epidemiology of Alcohol and Cancer. *Cancer Research* **1979,** *39* (7 Part 2), 2840-2843.

13. (a) Chao,A.; Thun M. J.; Connell, C. J.; Jacobs, E. J; Flanders, W. D.; Rodriguez, C.; Calle, E.E.; Meat consumption and risk of colorectal cancer. *JAMA: The Journal of the American Medical Association* **2005,** *293* (2), 172-182; (b) Hogg, N., Red meat and colon cancer: Heme proteins and nitrite in the gut. A commentary on "Diet-induced endogenous formation of nitroso compounds in the GI tract". *Free Radical Biology and Medicine* **2007,** *43* (7), 1037-1039.

14. Calle, E. E.; Rodriguez, C.; Walker-Thurmond, K.; Thun, M. J., Overweight, Obesity, and Mortality from Cancer in a Prospectively Studied Cohort of U.S. Adults. *New England Journal of Medicine* **2003,** *348* (17), 1625-1638.

15. Blumberg, B. S.; Larouzé, B.; London, W. T.; Werner, B.; Hesser, J. E.; Millman, I.; Saimot, G.; Payet, M., The relation of infection with the hepatitis B agent to primary hepatic carcinoma. *American Journal of Pathology* **1975,** *81* (3), 669-682.

16. Song, S.; Pitot, H. C.; Lambert, P. F., The Human Papillomavirus Type 16 E6 Gene Alone Is Sufficient To Induce Carcinomas in Transgenic Animals. *Journal of Virology* **1999,** *73* (7), 5887-5893.

17. Belpomme, D.; Irigaray, P.; Hardell, L.; Clapp, R.; Montagnier, L.; Epstein, S.; Sasco, A. J., The multitude and diversity of environmental carcinogens. *Environmental Research* **2007,** *105* (3), 414-429.

18. Harikumar, K. B.; Aggarwal, B. B., Resveratrol: A multitargeted agent for age-associated chronic diseases. *Cell Cycle* **2008,** *7* (8), 1020-1035.

19. Nishino, H.; Murakoshi, M.; Ii, T.; Takemura, M.; Kuchide, M.; Kanazawa, M.; Yang Mou, X.; Wada, S.; Masuda, M.; Ohsaka, Y.; Yogosawa, S.; Satomi, Y.; Jinno, K., Carotenoids in Cancer Chemoprevention. *Cancer Metastasis Rev* **2002,** *21* (3-4), 257-264.

20. (a) Anand, P.; Sundaram, C.; Jhurani, S.; Kunnumakkara, A. B.; Aggarwal, B. B., Curcumin and cancer: An "old-age" disease with an "age-old" solution. *Cancer letters* **2008,** *267* (1), 133-164; (b) Surh, Y.-J., Anti-tumor promoting potential of selected spice ingredients with antioxidative and anti-inflammatory activities: a short review. *Food and Chemical Toxicology* **2002,** *40* (8), 1091-1097.

21. Hajdu, S. I., A Note From History: Landmarks in History of Cancer, Part 1. *Cancer* **2011,** *117* (5), 1097-1102.

22. Glimelius, B.; Grönberg, H.; Järhult, J.; Wallgren, A.; Cavallin-ståhl, E., A Systematic Overview of Radiation Therapy Effects in Rectal Cancer. *Acta Oncologica* **2003,** *42* (5-6), 476-492.

23. Zhao, D.; Jin, X.; Li, F.; Liang, J.; Lin, Y., Integrin αvβ3 Imaging of Radioactive Iodine–Refractory Thyroid Cancer Using 99mTc-3PRGD2. *Journal of Nuclear Medicine* **2012,** *53* (12), 1872-1877.

24. Sofou, S., Radionuclide carriers for targeting of cancer. *International Journal of Nanomedicine* **2008,** *3* (2), 181-199.

25. Tahir, S. K.; Kovar, P.; Rosenberg, S. H.; Ng, S. C., Rapid Colchicine Competition-Binding Scintillation Proximity Assay Using Biotin-Labeled Tubulin. *Biotechniques* **2000,** *29* (1), 156-60.

26. Hurley, L. H., DNA and its associated processes as targets for cancer therapy. *Nature Reviews Cancer* **2002,** *2* (3), 188-200.

27. Gascoigne, K. E.; Taylor, S. S., How do anti-mitotic drugs kill cancer cells? *Journal of Cell Science* **2009,** *122* (15), 2579-2585.

28. Peters, G. J.; van der Wilt, C. L.; van Moorsel, C. J. A.; Kroep, J. R.; Bergman, A. M.; Ackland, S. P., Basis for effective combination cancer chemotherapy with antimetabolites. *Pharmacology & Therapeutics* **2000,** *87* (2–3), 227-253.

29. Kim, R.; Emi, M.; Tanabe, K., Cancer immunosuppression and autoimmune disease: beyond immunosuppressive networks for tumour immunity. *Immunology* **2006,** *119* (2), 254-264.

30. Gill, P.; Grothey, A.; Loprinzi, C., Nausea and Vomiting in the Cancer Patient. In *Oncology*, Chang, A.; Hayes, D.; Pass, H.; Stone, R.; Ganz, P.; Kinsella, T.; Schiller, J.; Strecher, V., Eds. Springer New York: 2006; pp 1482-1496.

31. Meirow, D.; Schenker, J. G., Infertility: Cancer and male infertility. *Human Reproduction* **1995,** *10* (8), 2017-2022.

32. Tannock, I. F.; Ahles, T. A.; Ganz, P. A.; van Dam, F. S., Cognitive Impairment Associated With Chemotherapy for Cancer: Report of a Workshop. *Journal of Clinical Oncology* **2004,** *22* (11), 2233-2239.

33. Mechetner, E.; Kyshtoobayeva, A.; Zonis, S.; Kim, H.; Stroup, R.; Garcia, R.; Parker, R. J.; Fruehauf, J. P., Levels of multidrug resistance (MDR1) P-glycoprotein expression by human breast cancer correlate with in vitro resistance to taxol and doxorubicin. *Clinical Cancer Research* **1998,** *4* (2), 389-398.

34. (a) Yin, S.; Zeng, C.; Hari, M.; Cabral, F., Random Mutagenesis of β-Tubulin Defines a Set of Dispersed Mutations That Confer Paclitaxel Resistance. *Pharm Res* **2012,** *29* (11), 2994-3006; (b) Kavallaris, M., Microtubules and resistance to tubulin-binding agents. *Nature Reviews Cancer* **2010,** *10* (3), 194-204.

35. Vogelstein, B.; Kinzler, K. W., Cancer genes and the pathways they control. *Nature Medicine* **2004,** *10* (8), 789-799.

36. Czernilofsky, A. P.; Levinson, A. D.; Varmus, H. E.; Bishop, J. M.; Tischer, E.; Goodman, H. M., Nucleotide sequence of an avian sarcoma virus oncogene (src) and proposed amino acid sequence for gene product. *Nature* **1980,** *287* (5779), 198-203.

37. Bos, J. L., ras Oncogenes in Human Cancer: A Review. *Cancer Research* **1989,** *49* (17), 4682-4689.

38. Rabbitts, T. H.; Hamlyn, P. H.; Baer, R., Altered nucleotide sequences of a translocated c-myc gene in Burkitt lymphoma. *Nature* **1983,** *306* (5945), 760-765.

39. Baker, S. J.; Fearon, E. R.; Nigro, J. M.; Hamilton, S. R.; Preisinger, A. C.; Jessup, J. M.; vanTuinen, P.; Ledbetter, D. H.; Barker, D. F.; Nakamura, Y.; White, R.; Vogelstein, B., Chromosome 17 deletions and p53 gene mutations in colorectal carcinomas. *Science* **1989,** *244* (4901), 217-221.

40. Lohmann, D. R., RB1 gene mutations in retinoblastoma. *Human Mutation* **1999,** *14* (4), 283-288.

41. Friedenson, B., The BRCA1/2 pathway prevents hematologic cancers in addition to breast and ovarian cancers. *BMC Cancer* **2007,** *7*, 152-162.

42. Hanahan, D.; Weinberg, Robert A., Hallmarks of Cancer: The Next Generation. *Cell* **2011,** *144* (5), 646-674.

43. Lieu, C.; Heymach, J.; Overman, M.; Tran, H.; Kopetz, S., Beyond VEGF: Inhibition of the Fibroblast Growth Factor Pathway and Antiangiogenesis. *Clinical Cancer Research* **2011,** *17* (19), 6130-6139.

44. Morphy, R.; Rankovic, Z., Designed Multiple Ligands. An Emerging Drug Discovery Paradigm. *Journal of Medicinal Chemistry* **2005,** *48* (21), 6523-6543.

45. Carmeliet, P.; Jain, R. K., Angiogenesis in cancer and other diseases. *Nature* **2000,** *407* (6801), 249-257.

46. Bossi, P.; Viale, G.; Lee, A. K. C.; Alfano, R.; Coggi, G.; Bosari, S., Angiogenesis in Colorectal Tumors: Microvessel Quantitation in Adenomas and Carcinomas with Clinicopathological Correlations. *Cancer Research* **1995,** *55* (21), 5049-5053.

47. Ferrara, N., Role of vascular endothelial growth factor in regulation of physiological angiogenesis. *American Journal of Physiology - Cell Physiology* **2001,** *280* (6), C1358-C1366.

48. Hanahan, D.; Folkman, J., Patterns and Emerging Mechanisms of the Angiogenic Switch during Tumorigenesis. *Cell* **1996,** *86* (3), 353-364.

49. Khurana, R.; Simons, M.; Martin, J. F.; Zachary, I. C., Role of Angiogenesis in Cardiovascular Disease: A Critical Appraisal. *Circulation* **2005,** *112* (12), 1813-1824.

50. Noël, A.; Jost, M.; Lambert, V.; Lecomte, J.; Rakic, J.-M., Anti-angiogenic therapy of exudative age-related macular degeneration: current progress and emerging concepts. *Trends in molecular medicine* **2007,** *13* (8), 345-352.

51. Heidenreich, R.; Röcken, M.; Ghoreschi, K., Angiogenesis drives psoriasis pathogenesis. *International Journal of Experimental Pathology* **2009,** *90* (3), 232-248.

52. Prager, G. W.; Poettler, M., Angiogenesis in cancer: Basic mechanisms and therapeutic advances. *Hamostaseologie* **2012,** *32* (2), 105-114.

53. Ferrara, N., The role of vascular endothelial growth factor in pathological angiogenesis. *Breast Cancer Res Tr* **1995,** *36* (2), 127-137.

54. Folkman, J., Tumor Angiogenesis: Therapeutic Implications. *New England Journal of Medicine* **1971,** *285* (21), 1182-1186.

55. Hayden, E. C., Cutting off cancer's supply lines. *Nature* **2009,** *458*, 686-687.

56. http://www.omicsonline.org/ArchiveJBB/2009/August/03/images/JBB1.52Figure1.html (accessed Jan 3 2013).

57. Bergers, G.; Benjamin, L. E., Tumorigenesis and the angiogenic switch. *Nature reviews. Cancer* **2003,** *3* (6), 401-10.

58. Hur, E.; Kim, H.-H.; Choi, S. M.; Kim, J. H.; Yim, S.; Kwon, H. J.; Choi, Y.; Kim, D. K.; Lee, M.-O.; Park, H., Reduction of Hypoxia-Induced Transcription through the Repression of Hypoxia-Inducible Factor-1α/Aryl Hydrocarbon Receptor Nuclear Translocator DNA Binding by the 90-kDa Heat-Shock Protein Inhibitor Radicicol. *Molecular Pharmacology* **2002,** *62* (5), 975-982.

59.   Gerhardt, H.; Golding, M.; Fruttiger, M.; Ruhrberg, C.; Lundkvist, A.; Abramsson, A.; Jeltsch, M.; Mitchell, C.; Alitalo, K.; Shima, D.; Betsholtz, C., VEGF guides angiogenic sprouting utilizing endothelial tip cell filopodia. *J Cell Biol* **2003**, *161* (6), 1163-77.

60.   Potente, M.; Gerhardt, H.; Carmeliet, P., Basic and Therapeutic Aspects of Angiogenesis. *Cell* **2011**, *146* (6), 873-887.

61.   Hall, A. P., Review of the Pericyte during Angiogenesis and its Role in Cancer and Diabetic Retinopathy. *Toxicologic Pathology* **2006**, *34* (6), 763-775.

62.   Jain, R. K., Normalisation of tumour vasculature: an emerging concept in antiangiogenic therapy. *Science* **2005**, *307* (5706), 58-62.

63.   (a) Wu, J.; Ding, D.; Ren, G.; Xu, X.; Yin, X.; Hu, Y., Sustained delivery of endostatin improves the efficacy of therapy in Lewis lung cancer model. *Journal of Controlled Release* **2009**, *134* (2), 91-97; (b) He-Lan Wang, T. N., Mei Li, Ze-Jun Lu, Xi Yan, Qian Peng, Na Lei, ; Hui Zhang, a. F. L., Effect of endostatin on preventing postoperative progression of distant metastasis in a murine lung cancer model. *Tumori* **2011**, *97* (6), 787-793.

64.   Markovic, S. N.; Suman, V. J.; Rao, R. A.; Ingle, J. N.; Kaur, J. S.; Erickson, L. A.; Pitot, H. C.; Croghan, G. A.; McWilliams, R. R.; Merchan, J.; Kottschade, L. A.; Nevala, W. K.; Uhl, C. B.; Allred, J.; Creagan, E. T., A Phase II Study of ABT-510 (Thrombospondin-1 Analog) for the Treatment of Metastatic Melanoma. *American Journal of Clinical Oncology* **2007**, *30* (3), 303-309 10.1097/01.coc.0000256104.80089.35.

65.   Twombly, R., First Clinical Trials of Endostatin Yield Lukewarm Results. *Journal of the National Cancer Institute* **2002**, *94* (20), 1520-1521.

66.   Neufeld, G.; Cohen, T.; Gengrinovitch, S.; Poltorak, Z., Vascular endothelial growth factor (VEGF) and its receptors. *The FASEB Journal* **1999**, *13* (1), 9-22.

67.   Kerbel, R. S., Tumor Angiogenesis. *New England Journal of Medicine* **2008**, *358* (19), 2039-2049.

68.   Skobe, M.; Hawighorst, T.; Jackson, D. G.; Prevo, R.; Janes, L.; Velasco, P.; Riccardi, L.; Alitalo, K.; Claffey, K.; Detmar, M., Induction of tumor lymphangiogenesis by VEGF-C promotes breast cancer metastasis. *Nat Med* **2001,** *7* (2), 192-8.

69.   Vacca, A.; Ria, R.; Ribatti, D.; Semeraro, F.; Djonov, V.; Di Raimondo, F.; Dammacco, F., A paracrine loop in the vascular endothelial growth factor pathway triggers tumor angiogenesis and growth in multiple myeloma. *Haematologica* **2003,** *88* (2), 176-85.

70.   Kirwan, C.; Byrne, G.; Kumar, S.; McDowell, G., Platelet release of Vascular Endothelial Growth Factor (VEGF) in patients undergoing chemotherapy for breast cancer. *Journal of Angiogenesis Research* **2009,** *1* (1), 7.

71.   Cohen, M. H.; Gootenberg, J.; Keegan, P.; Pazdur, R., FDA Drug Approval Summary: Bevacizumab (Avastin®) Plus Carboplatin and Paclitaxel as First-Line Treatment of Advanced/Metastatic Recurrent Nonsquamous Non-Small Cell Lung Cancer. *The Oncologist* **2007,** *12* (6), 713-718.

72.   (a) FDA FDA approves new treatment for rare form of thyroid cancer. http://www.fda.gov/NewsEvents/Newsroom/PressAnnouncements/ucm250168.htm; (b) Langmuir, P. B.; Yver, A., Vandetanib for the Treatment of Thyroid Cancer. *Clin Pharmacol Ther* **2012,** *91* (1), 71-80.

73.   (a) Sleijfer, S.; Ray-Coquard, I.; Papai, Z.; Le Cesne, A.; Scurr, M.; Schöffski, P.; Collin, F.; Pandite, L.; Marreaud, S.; De Brauwer, A.; van Glabbeke, M.; Verweij, J.; Blay, J.-Y., Pazopanib, a Multikinase Angiogenesis Inhibitor, in Patients With Relapsed or Refractory Advanced Soft Tissue Sarcoma: A Phase II Study From the European Organisation for Research and Treatment of Cancer–Soft Tissue and Bone Sarcoma Group (EORTC Study 62043). *Journal of Clinical Oncology* **2009,** *27* (19), 3126-3132; (b) FDA FDA approves Votrient for advanced soft tissue sarcoma. http://www.fda.gov/NewsEvents/Newsroom/PressAnnouncements/ucm302065.htm.

74.   Authority, F. D. FDA Commissioner announces Avastin decision. http://www.fda.gov/NewsEvents/Newsroom/PressAnnouncements/ucm280536.htm.

75. (a) Emmanouilides, C.; Sfakiotaki, G.; Androulakis, N.; Kalbakis, K.; Christophylakis, C.; Kalykaki, A.; Vamvakas, L.; Kotsakis, A.; Agelaki, S.; Diamandidou, E.; Touroutoglou, N.; Chatzidakis, A.; Georgoulias, V.; Mavroudis, D.; Souglakos, J., Front-line Bevacizumab in combination with Oxaliplatin, Leucovorin and 5-Fluorouracil (FOLFOX) in patients with metastatic colorectal cancer: a multicenter phase II study. *BMC Cancer* **2007,** *7* (1), 91; (b) USA, G. http://www.avastin.com/ (accessed December 12 2012).

76. Van Cutsem, E.; Lambrechts, D.; Prenen, H.; Jain, R. K.; Carmeliet, P., Lessons From the Adjuvant Bevacizumab Trial on Colon Cancer: What Next? *Journal of Clinical Oncology* **2011,** *29* (1), 1-4.

77. Ratner, M., Genentech discloses safety concerns over Avastin. *Nature Biotech* **2004,** *22* (10), 1198.

78. Bardelli, A.; Janne, P. A., The road to resistance: EGFR mutation and cetuximab. *Nat Med* **2012,** *18* (2), 199-200.

79. Christensen, J., A preclinical review of sunitinib, a multitargeted receptor tyrosine kinase inhibitor with anti-angiogenic and antitumour activities. *Annals of Oncology* **2007,** *18* (suppl 10), x3-x10.

80. Shuman Moss, L. A.; Jensen-Taubman, S.; Stetler-Stevenson, W. G., Matrix Metalloproteinases: Changing Roles in Tumor Progression and Metastasis. *The American Journal of Pathology* **2012,** *181* (6), 1895-1899.

81. (a) Gomis-Rüth, F.; Gohlke, U.; Betz, M.; Knäuper, V.; Murphy, G.; Lopez-Otin, C.; Bode, W., The helping hand of collagenase-3 (MMP-13): 2.7 Å crystal structure of its C-terminal haemopexin-like domain. *J. Mol. Biol* **1996,** *264*, 556-566; (b) Fernandez-Catalan, C.; Bode, W.; Huber, R.; Turk, D.; Calvete, J. J.; Lichte, A.; Tschesche, H.; Maskos, K., Crystal structure of the complex formed by the membrane type 1-matrix metalloproteinase with the tissue inhibitor of metalloproteinases-2, the soluble progelatinase A receptor. *The EMBO journal* **1998,** *17* (17), 5238-5248.

82.   Iyer, S.; Visse, R.; Nagase, H.; Acharya, K. R., Crystal Structure of an Active Form of Human MMP-1. *Journal of Molecular Biology* **2006,** *362* (1), 78-88.

83.   Yong, V. W.; Zabad, R. K.; Agrawal, S.; Goncalves DaSilva, A.; Metz, L. M., Elevation of matrix metalloproteinases (MMPs) in multiple sclerosis and impact of immunomodulators. *Journal of the neurological sciences* **2007,** *259* (1), 79-84.

84.   Aranapakam, V.; Davis, J. M.; Grosu, G. T.; Baker; Ellingboe, J.; Zask, A.; Levin, J. I.; Sandanayaka, V. P.; Du, M.; Skotnicki, J. S.; DiJoseph, J. F.; Sung, A.; Sharr, M. A.; Killar, L. M.; Walter, T.; Jin, G.; Cowling, R.; Tillett, J.; Zhao, W.; McDevitt, J.; Xu, Z. B., Synthesis and Structure−Activity Relationship of N-Substituted 4-Arylsulfonylpiperidine-4-hydroxamic Acids as Novel, Orally Active Matrix Metalloproteinase Inhibitors for the Treatment of Osteoarthritis. *Journal of Medicinal Chemistry* **2003,** *46* (12), 2376-2396.

85.   Warnaar, N.; Hofker, S. H.; Maathuis, M. H. J.; Niesing, J.; Bruggink, A. H.; Dijkstra, G.; Ploeg, R. J.; Schuurs, T. A., Matrix metalloproteinases as profibrotic factors in terminal ileum in Crohn's disease. *Inflammatory Bowel Diseases* **2006,** *12* (9), 863-869 10.1097/01.mib.0000231568.43065.ed.

86.   (a) Zucker, S.; Vacirca, J., Role of matrix metalloproteinases (MMPs) in colorectal cancer. *Cancer Metastasis Rev* **2004,** *23* (1-2), 101-117; (b) Klein, G.; Vellenga, E.; Fraaije, M. W.; Kamps, W. A.; de Bont, E. S. J. M., The possible role of matrix metalloproteinase (MMP)-2 and MMP-9 in cancer, e.g. acute leukemia. *Critical Reviews in Oncology/Hematology* **2004,** *50* (2), 87-100.

87.   Adachi, Y.; Yamamoto, H.; Itoh, F.; Hinoda, Y.; Okada, Y.; Imai, K., Contribution of matrilysin (MMP-7) to the metastatic pathway of human colorectal cancers. *Gut* **1999,** *45* (2), 252-258.

88.   Chen, J.-S.; Huang, X.-h.; Wang, Q.; Huang, J.-Q.; Zhang, L.-j.; Chen, X.-L.; Lei, J.; Cheng, Z.-X., Sonic hedgehog signaling pathway induces cell migration and invasion through focal adhesion kinase/AKT signaling-mediated activation of matrix

metalloproteinase (MMP)-2 and MMP-9 in liver cancer. *Carcinogenesis* **2013,** *34* (1), 10-19.

89.   Buhmeida, A.; Bendardaf, R.; Hilska, M.; Collan, Y.; Laato, M.; Syrjänen, S.; Syrjänen, K.; Pyrhönen, S., Prognostic Significance of Matrix Metalloproteinase-9 (MMP-9) in Stage II Colorectal Carcinoma. *J Gastrointest Canc* **2009,** *40* (3-4), 91-97.

90.   Matsuyama, Y.; Takao, S.; Aikou, T., Comparison of matrix metalloproteinase expression between primary tumors with or without liver metastasis in pancreatic and colorectal carcinomas. *Journal of Surgical Oncology* **2002,** *80* (2), 105-110.

91.   Hilska, M.; Roberts, P. J.; Collan, Y. U.; Laine, V. J. O.; Kössi, J.; Hirsimäki, P.; Rahkonen, O.; Laato, M., Prognostic significance of matrix metalloproteinases-1, -2, -7 and -13 and tissue inhibitors of metalloproteinases-1, -2, -3 and -4 in colorectal cancer. *International Journal of Cancer* **2007,** *121* (4), 714-723.

92.   Ranogajec, I.; Jakić-Razumović, J.; Puzović, V.; Gabrilovac, J., Prognostic value of matrix metalloproteinase-2 (MMP-2), matrix metalloproteinase-9 (MMP-9) and aminopeptidase N/CD13 in breast cancer patients. *Med Oncol* **2012,** *29* (2), 561-569.

93.   Koskensalo, S.; Hagstrom, J.; Linder, N.; Lundin, M.; Sorsa, T.; Louhimo, J.; Haglund, C., Lack of MMP-9 expression is a marker for poor prognosis in Dukes' B colorectal cancer. *BMC Clinical Pathology* **2012,** *12* (1), 24.

94.   Zeng, Z. S.; Huang, Y.; Cohen, A. M.; Guillem, J. G., Prediction of colorectal cancer relapse and survival via tissue RNA levels of matrix metalloproteinase-9. *Journal of Clinical Oncology* **1996,** *14* (12), 3133-40.

95.   Leung, D.; Abbenante, G.; Fairlie, D. P., Protease inhibitors: current status and future prospects. *J Med Chem* **2000,** *43* (3), 305-41.

96.   Yadav, R. K.; Gupta, S. P.; Sharma, P. K.; Patil, V. M., Recent Advances in Studies on Hydroxamates as Matrix Metalloprotease Inhibitors: A Review. *Current Medicinal Chemistry* **2011,** *18*, 1704-1722.

97. (a) Montgomery, A. M. P.; Mueller, B. M.; Reisfeld, R. A.; Taylor, S. M.; DeClerck, Y. A., Effect of Tissue Inhibitor of the Matrix Metalloproteinases-2 Expression on the Growth and Spontaneous Metastasis of a Human Melanoma Cell Line. *Cancer Research* **1994,** *54* (20), 5467-5473; (b) Koop, S.; Khokha, R.; Schmidt, E. E.; MacDonald, I. C.; Morris, V. L.; Chambers, A. F.; Groom, A. C., Overexpression of Metalloproteinase Inhibitor in B16F10 Cells Does Not Affect Extravasation but Reduces Tumor Growth. *Cancer Research* **1994,** *54* (17), 4791-4797.

98. (a) Jayasankar, V.; Woo, Y. J.; Bish, L. T.; Pirolli, T. J.; Berry, M. F.; Burdick, J.; Bhalla, R. C.; Sharma, R. V.; Gardner, T. J.; Sweeney, H. L., Inhibition of Matrix Metalloproteinase Activity by TIMP-1 Gene Transfer Effectively Treats Ischemic Cardiomyopathy. *Circulation* **2004,** *110* (11 suppl 1), II-180-II-186; (b) Schultz, R. M.; Silberman, S.; Persky, B.; Bajkowski, A. S.; Carmichael, D. F., Inhibition by Human Recombinant Tissue Inhibitor of Metalloproteinases of Human Amnion Invasion and Lung Colonization by Murine B16-F10 Melanoma Cells. *Cancer Research* **1988,** *48* (19), 5539-5545.

99. Pavlaki, M.; Zucker, S., Matrix metalloproteinase inhibitors (MMPIs): The beginning of phase I or the termination of phase III clinical trials. *Cancer Metastasis Rev* **2003,** *22* (2-3), 177-203.

100. Coussens, L. M.; Fingleton, B.; Matrisian, L. M., Matrix Metalloproteinase Inhibitors and Cancer—Trials and Tribulations. *Science* **2002,** *295* (5564), 2387-2392.

101. Look, A. T.; Ashmun, R. A.; Shapiro, L. H.; Peiper, S. C., Human myeloid plasma membrane glycoprotein CD13 (gp150) is identical to aminopeptidase N. *The Journal of Clinical Investigation* **1989,** *83* (4), 1299-1307.

102. (a) Bhagwat, S. V.; Lahdenranta, J.; Giordano, R.; Arap, W.; Pasqualini, R.; Shapiro, L. H., CD13/APN is activated by angiogenic signals and is essential for capillary tube formation. *Blood* **2001,** *97* (3), 652-659; (b) Tokuhara, T.; Miyake, M.; Taki, T.; Yagita,

M., Suppression of metastasis by anti aminopeptidase N antibody. *AACR Meeting Abstracts* **2004,** *2004* (1), 424-a-.

103.   van Hensbergen, Y.; Broxterman, H. J.; Hanemaaijer, R.; Jorna, A. S.; van Lent, N. A.; Verheul, H. M. W.; Pinedo, H. M.; Hoekman, K., Soluble Aminopeptidase N/CD13 in Malignant and Nonmalignant Effusions and Intratumoral Fluid. *Clinical Cancer Research* **2002,** *8* (12), 3747-3754.

104.   (a) Reguera, J.; Santiago, C.; Mudgal, G.; Ordoño, D.; Enjuanes, L.; Casasnovas, J. M., Structural Bases of Coronavirus Attachment to Host Aminopeptidase N and Its Inhibition by Neutralizing Antibodies. *PLoS Pathogens* **2012,** *8* (8), e1002859; (b) Wong, A. H. M.; Zhou, D.; Rini, J. M., The X-ray Crystal Structure of Human Aminopeptidase N Reveals a Novel Dimer and the Basis for Peptide Processing. *Journal of Biological Chemistry* **2012,** *287* (44), 36804-36813.

105.   Favaloro, E. J.; Browning, T.; Nandurkar, H.; Sartor, M.; Bradstock, K. F.; Koutts, J., Aminopeptidase-N (CD13; gp 150): Contrasting patterns of enzymatic activity in blood from patients with myeloid or lymphoid leukemia. *Leukemia Research* **1995,** *19* (9), 659-666.

106.   Mayas, M. D.; Ramirez-Exposito, M. J.; Carrera, M. P.; COBO, M.; Martinez-Martos, J. M., Renin-angiotensin System-regulating Aminopeptidases in Tumor Growth of Rat C6 Gliomas Implanted at the Subcutaneous Region. *Anticancer Research* **2012,** *32* (9), 3675-3682.

107.   Larsen, S. L.; Pedersen, L. O.; Buus, S.; Stryhn, A., T cell responses affected by aminopeptidase N (CD13)-mediated trimming of major histocompatibility complex class II-bound peptides. *The Journal of Experimental Medicine* **1996,** *184* (1), 183-189.

108.   Peer, W. A., The role of multifunctional M1 metallopeptidases in cell cycle progression. *Annals of Botany* **2011,** *107* (7), 1171-1181.

109.   Patel, J. M.; Martens, J. R.; Li, Y. D.; Gelband, C. H.; Raizada, M. K.; Block, E. R., Angiotensin IV receptor-mediated activation of lung endothelial NOS is associated with

vasorelaxation. *American Journal of Physiology - Lung Cellular and Molecular Physiology* **1998**, *275* (6), L1061-L1068.

110.   Xu, Y.; Wellner, D.; Scheinberg, D. A., Substance P and Bradykinin Are Natural Inhibitors of CD13/Aminopeptidase N. *Biochemical and Biophysical Research Communications* **1995**, *208* (2), 664-674.

111.   Kontoyiannis, D. P.; Pasqualini, R.; Arap, W., Aminopeptidase N inhibitors and SARS. *The Lancet* **2003**, *361* (9368), 1558.

112.   Santos, A. N.; Langner, J.; Herrmann, M.; Riemann, D., Aminopeptidase N/CD13 Is Directly Linked to Signal Transduction Pathways in Monocytes. *Cellular Immunology* **2000**, *201* (1), 22-32.

113.   Menrad, A.; Speicher, D.; Wacker, J.; Herlyn, M., Biochemical and Functional Characterization of Aminopeptidase N Expressed by Human Melanoma Cells. *Cancer Research* **1993**, *53* (6), 1450-1455.

114.   (a) Kehlen, A.; Lendeckel, U.; Dralle, H.; Langner, J.; Hoang-Vu, C., Biological Significance of Aminopeptidase N/CD13 in Thyroid Carcinomas. *Cancer Research* **2003**, *63* (23), 8500-8506; (b) Hashida, H.; Takabayashi, A.; Kanai, M.; Adachi, M.; Kondo, K.; Kohno, N.; Yamaoka, Y.; Miyake, M., Aminopeptidase N is involved in cell motility and angiogenesis: Its clinical significance in human colon cancer. *Gastroenterology* **2002**, *122* (2), 376-386; (c) Bauvois, B.; Dauzonne, D., Aminopeptidase-N/CD13 (EC 3.4.11.2) inhibitors: Chemistry, biological evaluations, and therapeutic prospects. *Medicinal Research Reviews* **2006**, *26* (1), 88-130; (d) Bogenrieder, T.; Finstad, C. L.; Freeman, R. H.; Papandreou, C. N.; Scher, H. I.; Albino, A. P.; Reuter, V. E.; Nanus, D. M., Expression and localization of aminopeptidase A, aminopeptidase N, and dipeptidyl peptidase IV in benign and malignant human prostate tissue. *The Prostate* **1997**, *33* (4), 225-232.

115.   (a) Murakami, H.; Yokoyama, A.; Kondo, K.; Nakanishi, S.; Kohno, N.; Miyake, M., Circulating Aminopeptidase N/CD13 Is an Independent Prognostic Factor in Patients

with Non–Small Cell Lung Cancer. *Clinical Cancer Research* **2005,** *11* (24), 8674-8679; (b) Tokuhara, T.; Hattori, N.; Ishida, H.; Hirai, T.; Higashiyama, M.; Kodama, K.; Miyake, M., Clinical Significance of Aminopeptidase N in Non–Small Cell Lung Cancer. *Clinical Cancer Research* **2006,** *12* (13), 3971-3978.

116.   Rangel, R.; Sun, Y.; Guzman-Rojas, L.; Ozawa, M. G.; Sun, J.; Giordano, R. J.; Van Pelt, C. S.; Tinkey, P. T.; Behringer, R. R.; Sidman, R. L.; Arap, W.; Pasqualini, R., Impaired angiogenesis in aminopeptidase N-null mice. *Proceedings of the National Academy of Sciences* **2007,** *104* (11), 4588-4593.

117.   Aoyagi, T.; Yoshida, S.; Nakamura, Y.; Shigihara, Y.; Hamada, M.; Takeuchi, T., Probestin, a new inhibitor of Aminopeptidase M, produced by streptomyces azureus MH663-2F6 I. Taxonomy, production, isolation, physico-chemical properties and biological activities. *The Journal of Antibiotics* **1990,** *43* (2), 143-148.

118.   Rich, D. H.; Moon, B. J.; Harbeson, S., Inhibition of aminopeptidases by amastatin and bestatin derivatives. Effect of inhibitor structure on slow-binding processes. *Journal of Medicinal Chemistry* **1984,** *27* (4), 417-422.

119.   Inoue, T.; Kanzaki, H.; Imai, K.; Narukawa, S.; Higuchi, T.; Katsuragawa, H.; Maeda, M.; Mori, T., Bestatin, a potent aminopeptidase-N inhibitor, inhibits in vitro decidualization of human endometrial stromal cells. *Journal of Clinical Endocrinology & Metabolism* **1994,** *79* (1), 171-5.

120.   Lee, J.; Shim, J. S.; Jung, S.-A.; Lee, S.-T.; Kwon, H. J., N-Hydroxy-2-(naphthalene-2-ylsulfanyl)-acetamide, a novel hydroxamic acid-based inhibitor of aminopeptidase N and its anti-angiogenic activity. *Bioorganic & Medicinal Chemistry Letters* **2005,** *15* (1), 181-183.

121.   Chen, L.; Mou, J.; Xu, Y.; Fang, H.; Xu, W., Design, synthesis and activity study of aminopeptidase N targeted 3-amino-2-hydroxy-4-phenyl-butanoic acid derivatives. *Drug Discovery & Therapeutics* **2011,** *5* (2), 61-65.

122.   Yoneda, J.; Saiki, I.; Fujii, H.; Abe, F.; Kojima, Y.; Azuma, I., Inhibition of tumor invasion and extracellular matrix degradation by ubenimex (bestatin). *Clin Exp Metast* **1992,** *10* (1), 49-59.

123.   Krige, D.; Needham, L. A.; Bawden, L. J.; Flores, N.; Farmer, H.; Miles, L. E. C.; Stone, E.; Callaghan, J.; Chandler, S.; Clark, V. L.; Kirwin-Jones, P.; Legris, V.; Owen, J.; Patel, T.; Wood, S.; Box, G.; Laber, D.; Odedra, R.; Wright, A.; Wood, L. M.; Eccles, S. A.; Bone, E. A.; Ayscough, A.; Drummond, A. H., CHR-2797: An Antiproliferative Aminopeptidase Inhibitor that Leads to Amino Acid Deprivation in Human Leukemic Cells. *Cancer Research* **2008,** *68* (16), 6669-6679.

124.   Mishima, Y.; Terui, Y.; Sugimura, N.; Matsumoto-Mishima, Y.; Rokudai, A.; Kuniyoshi, R.; Hatake, K., Continuous treatment of bestatin induces anti-angiogenic property in endothelial cells. *Cancer Science* **2007,** *98* (3), 364-372.

125.   Ueda, M.; Ueki, M.; Fujii, H.; Yoshizawa, K.; Nakajima, M., Inhibitory effects of ubenimex (bestatin) on the invasion of uterine cervical carcinoma cells and their production and activation of gelatinase A. *J Med* **1997,** *28* (3-4), 175-90.

126.   Ezawa, K.; Minato, K.; Dobashi, K., Induction of apoptosis by ubenimex (Bestatin®) in human non-small-cell lung cancer cell lines. *Biomedicine & Pharmacotherapy* **1996,** *50* (6–7), 283-289.

127.   Sakuraya, M.; Tamura, J.; Itoh, K.; Kubota, K.; Naruse, T., Aminopeptidase Inhibitor Ubenimex Inhibits the Growth of Leukaemic Cell Lines and Myeloma Cells through Its Cytotoxicity. *Journal of International Medical Research* **2000,** *28* (5), 214-221.

128.   Aozuka, Y.; Koizumi, K.; Saitoh, Y.; Ueda, Y.; Sakurai, H.; Saiki, I., Anti-tumor angiogenesis effect of aminopeptidase inhibitor bestatin against B16-BL6 melanoma cells orthotopically implanted into syngeneic mice. *Cancer Letters* **2004,** *216* (1), 35-42.

129. Ota, K.; Ogawa, N., Randomized controlled study of chemoimmunotherapy with bestatin of acute nonlymphocytic leukemia in adults. *Biomedicine & Pharmacotherapy* **1990,** *44* (2), 93-101.

130. Ichinose, Y.; Genka, K.; Koike, T.; Kato, H.; Watanabe, Y.; Mori, T.; Iioka, S.; Sakuma, A.; Ohta, M.; Group, F. t. N. L. C. S., Randomized Double-Blind Placebo-Controlled Trial of Bestatin in Patients With Resected Stage I Squamous-Cell Lung Carcinoma. *Journal of the National Cancer Institute* **2003,** *95* (8), 605-610.

131. Tsukamoto, H.; Shibata, K.; Kajiyama, H.; Terauchi, M.; Nawa, A.; Kikkawa, F., Aminopeptidase N (APN)/CD13 inhibitor, Ubenimex, enhances radiation sensitivity in human cervical cancer. *BMC Cancer* **2008,** *8* (1), 74.

132. Chung, M.-C.; Lee, H.-J.; Chun, H.-K.; Lee, C.-H.; Kim, S.-I.; Kho, Y.-H., Bestatin Analogue from Streptomyces neyagawaensis SL-387. *Bioscience, Biotechnology, and Biochemistry* **1996,** *60* (5), 898-900.

133. Gao, J.-J.; Xue, X.; Gao, Z.-H.; Cui, S.-X.; Cheng, Y.-N.; Xu, W.-F.; Tang, W.; Qu, X.-J., LYP, a bestatin dimethylaminoethyl ester, inhibited cancer angiogenesis both in vitro and in vivo. *Microvascular Research* **2011,** *82* (2), 122-130.

134. Xu, Y.; Lai, L. T.; Gabrilove, J. L.; Scheinberg, D. A., Antitumor activity of actinonin in vitro and in vivo. *Clinical cancer research : an official journal of the American Association for Cancer Research* **1998,** *4* (1), 171-6.

135. (a) Shim, J. S.; Kim, J. H.; Cho, H. Y.; Yum, Y. N.; Kim, S. H.; Park, H.-J.; Shim, B. S.; Choi, S. H.; Kwon, H. J., Irreversible Inhibition of CD13/Aminopeptidase N by the Antiangiogenic Agent Curcumin. *Chemistry & Biology* **2003,** *10* (8), 695-704; (b) Melzig, M. F.; Bormann, H., Betulinic Acid Inhibits Aminopeptidase N Activity. *Planta Med* **1998,** *64* (07), 655-657.

136. Albrecht, S.; Defoin, A.; Salomon, E.; Tarnus, C.; Wetterholm, A.; Haeggström, J. Z., Synthesis and structure activity relationships of novel non-peptidic metallo-

aminopeptidase inhibitors. *Bioorganic & Medicinal Chemistry* **2006**, *14* (21), 7241-7257.

137.   Babine, R. E.; Bender, S. L., Molecular Recognition of Protein–Ligand Complexes: Applications to Drug Design. *Chemical Reviews* **1997**, *97* (5), 1359-1472.

138.   Krzeski, P.; Buckland-Wright, C.; Balint, G.; Cline, G.; Stoner, K.; Lyon, R.; Beary, J.; Aronstein, W.; Spector, T., Development of musculoskeletal toxicity without clear benefit after administration of PG-116800, a matrix metalloproteinase inhibitor, to patients with knee osteoarthritis: a randomized, 12-month, double-blind, placebo-controlled study. *Arthritis Research & Therapy* **2007**, *9* (5), R109.

139.   Wojtowicz-Praga, S.; Torri, J.; Johnson, M.; Steen, V.; Marshall, J.; Ness, E.; Dickson, R.; Sale, M.; Rasmussen, H. S.; Chiodo, T. A.; Hawkins, M. J., Phase I trial of Marimastat, a novel matrix metalloproteinase inhibitor, administered orally to patients with advanced lung cancer. *Journal of Clinical Oncology* **1998**, *16* (6), 2150-6.

140.   (a) Bramhall, S. R.; Schulz, J.; Nemunaitis, J.; Brown, P. D.; Baillet, M.; Buckels, J. A. C., A double-blind placebo-controlled, randomised study comparing gemcitabine and marimastat with gemcitabine and placebo as first line therapy in patients with advanced pancreatic cancer. *British Journal of Cancer* **2002**, *87* (2), 161-167; (b) Bramhall, S. R.; Hallissey, M. T.; Whiting, J.; Scholefield, J.; Tierney, G.; Stuart, R. C.; Hawkins, R. E.; McCulloch, P.; Maughan, T.; Brown, P. D.; Baillet, M.; Fielding, J. W. L., Marimastat as maintenance therapy for patients with advanced gastric cancer: a randomised trial. *British Journal of Cancer* **2002**, *86* (12), 1864-1870.

141.   Krüger, A.; Soeltl, R.; Sopov, I.; Kopitz, C.; Arlt, M.; Magdolen, V.; Harbeck, N.; Gänsbacher, B.; Schmitt, M., Hydroxamate-Type Matrix Metalloproteinase Inhibitor Batimastat Promotes Liver Metastasis. *Cancer Research* **2001**, *61* (4), 1272-1275.

142.   Hande, K. R.; Collier, M.; Paradiso, L.; Stuart-Smith, J.; Dixon, M.; Clendeninn, N.; Yeun, G.; Alberti, D.; Binger, K.; Wilding, G., Phase I and Pharmacokinetic Study of

Prinomastat, a Matrix Metalloprotease Inhibitor. *Clinical Cancer Research* **2004,** *10* (3), 909-915.

143.   (a) Duvic, M.; Vu, J., Vorinostat: a new oral histone deacetylase inhibitor approved for cutaneous T-cell lymphoma. *Expert Opinion on Investigational Drugs* **2007,** *16* (7), 1111-1120; (b) Richon, V. M., Cancer biology: mechanism of antitumour action of vorinostat (suberoylanilide hydroxamic acid), a novel histone deacetylase inhibitor. *Br J Cancer* **2006,** *95* (S1), S2-S6.

144.   Yeo, W.; Chung, H. C.; Chan, S. L.; Wang, L. Z.; Lim, R.; Picus, J.; Boyer, M.; Mo, F. K. F.; Koh, J.; Rha, S. Y.; Hui, E. P.; Jeung, H. C.; Roh, J. K.; Yu, S. C. H.; To, K. F.; Tao, Q.; Ma, B. B.; Chan, A. W. H.; Tong, J. H. M.; Erlichman, C.; Chan, A. T. C.; Goh , B. C., Epigenetic Therapy Using Belinostat for Patients With Unresectable Hepatocellular Carcinoma: A Multicenter Phase I/II Study With Biomarker and Pharmacokinetic Analysis of Tumors From Patients in the Mayo Phase II Consortium and the Cancer Therapeutics Research Group. *Journal of Clinical Oncology* **2012,** *30* (27), 3361-3367.

145.   Prince, H.; Prince, M., *Panobinostat (LBH589): a novel pan-deacetylase inhibitor with activity in T cell lymphoma.* 2009; Vol. 3.

146.   Singh, J.; Conzentino, P.; Cundy, K.; Gainor, J. A.; Gilliam, C. L.; Gordon, T. D.; Johnson, J. A.; Morgan, B. A.; Schneider, E. D.; Wahl, R. C.; Whipple, D. A., Relationship between structure and bioavailability in a series of hydroxamate based metalloprotease inhibitors. *Bioorganic & Medicinal Chemistry Letters* **1995,** *5* (4), 337-342.

147.   (a) Peng, S. X.; Strojnowski, M. J.; Hu, J. K.; Smith, B. J.; Eichhold, T. H.; Wehmeyer, K. R.; Pikul, S.; Almstead, N. G., Gas chromatographic–mass spectrometric analysis of hydroxylamine for monitoring the metabolic hydrolysis of metalloprotease inhibitors in rat and human liver microsomes. *Journal of Chromatography B: Biomedical Sciences and Applications* **1999,** *724* (1), 181-187; (b) Summers, J. B.; Gunn, B. P.; Mazdiyasni,

H.; Goetze, A. M.; Young, P. R.; Bouska, J. B.; Dyer, R. D.; Brooks, D. W.; Carter, G. W., In vivo characterization of hydroxamic acid inhibitors of 5-lipoxygenase. *Journal of Medicinal Chemistry* **1987**, *30* (11), 2121-2126; (c) Evelo, C. T. A.; Spooren, A. A. M. G.; Bisschops, R. A. G.; Baars, L. G. M.; Neis, J. M., Two Mechanisms for Toxic Effects of Hydroxylamines in Human Erythrocytes: Involvement of Free Radicals and Risk of Potentiation. *Blood Cells, Molecules, and Diseases* **1998**, *24* (3), 280-295.

148.   Hajduk, P. J.; Shuker, S. B.; Nettesheim, D. G.; Craig, R.; Augeri, D. J.; Betebenner, D.; Albert, D. H.; Guo, Y.; Meadows, R. P.; Xu, L.; Michaelides, M.; Davidsen, S. K.; Fesik, S. W., NMR-Based Modification of Matrix Metalloproteinase Inhibitors with Improved Bioavailability. *Journal of Medicinal Chemistry* **2002**, *45* (26), 5628-5639.

149.   Michaelides, M. R.; Dellaria, J. F.; Gong, J.; Holms, J. H.; Bouska, J. J.; Stacey, J.; Wada, C. K.; Heyman, H. R.; Curtin, M. L.; Guo, Y.; Goodfellow, C. L.; Elmore, I. B.; Albert, D. H.; Magoc, T. J.; Marcotte, P. A.; Morgan, D. W.; Davidsen, S. K., Biaryl Ether Retrohydroxamates as Potent, Long-lived, Orally Bioavailable MMP Inhibitors. *Bioorganic & Medicinal Chemistry Letters* **2001**, *11* (12), 1553-1556.

150.   Flipo, M.; Beghyn, T.; Charton, J.; Leroux, V. A.; Deprez, B. P.; Deprez-Poulain, R. F., A library of novel hydroxamic acids targeting the metallo-protease family: Design, parallel synthesis and screening. *Bioorganic & Medicinal Chemistry* **2007**, *15* (1), 63-76.

151.   Su, L.; Jia, Y.; Zhang, L.; Xu, Y.; Fang, H.; Xu, W., Design, synthesis and biological evaluation of novel amino acid ureido derivatives as aminopeptidase N/CD13 inhibitors. *Bioorganic & Medicinal Chemistry* **2012**, *20* (12), 3807-3815.

152.   (a) Li, Q.; Fang, H.; Wang, X.; Xu, W., Novel cyclic-imide peptidomimetics as aminopeptidase N inhibitors. Structure-based design, chemistry and activity evaluation. II. *European Journal of Medicinal Chemistry* **2010**, *45* (4), 1618-1626; (b) Li, Q.; Fang, H.; Xu, W., Novel 3-galloylamido-N'-substituted-2,6-piperidinedione-N-acetamide peptidomimetics as metalloproteinase inhibitors. *Bioorganic & Medicinal Chemistry*

Letters **2007,** *17* (10), 2935-2938; (c) Li, Q.; Fang, H.; Wang, X.; Hu, L.; Xu, W., Novel cyclic-imide peptidomimetics as aminopeptidase N inhibitors. Design, chemistry and activity evaluation. Part I. *European Journal of Medicinal Chemistry* **2009,** *44* (12), 4819-4825.

153.   Wang, X.; Jing, F.; Zhu, H.; Fang, H.; Zhang, J.; Xu, W., Activity screening and structure–activity relationship of the hit compounds targeting APN/CD13. *Fundamental & Clinical Pharmacology* **2011,** *25* (2), 217-228.

154.   (a) Grzywa, R.; Oleksyszyn, J.; Salvesen, G. S.; Drąg, M., Identification of very potent inhibitor of human aminopeptidase N (CD13). *Bioorganic & Medicinal Chemistry Letters* **2010,** *20* (8), 2497-2499; (b) Drag, M.; Grzywa, R.; Oleksyszyn, J., Novel hydroxamic acid-related phosphinates: Inhibition of neutral aminopeptidase N (APN). *Bioorganic & Medicinal Chemistry Letters* **2007,** *17* (6), 1516-1519.

155.   Pasqualini, R.; Koivunen, E.; Kain, R.; Lahdenranta, J.; Sakamoto, M.; Stryhn, A.; Ashmun, R. A.; Shapiro, L. H.; Arap, W.; Ruoslahti, E., Aminopeptidase N Is a Receptor for Tumor-homing Peptides and a Target for Inhibiting Angiogenesis. *Cancer Research* **2000,** *60* (3), 722-727.

156.   Wickström, M.; Larsson, R.; Nygren, P.; Gullbo, J., Aminopeptidase N (CD13) as a target for cancer chemotherapy. *Cancer Science* **2011,** *102* (3), 501-508.

157.   Gregorc, V.; Zucali, P. A.; Santoro, A.; Ceresoli, G. L.; Citterio, G.; De Pas, T. M.; Zilembo, N.; De Vincenzo, F.; Simonelli, M.; Rossoni, G.; Spreafico, A.; Grazia Viganò, M.; Fontana, F.; De Braud, F. G.; Bajetta, E.; Caligaris-Cappio, F.; Bruzzi, P.; Lambiase, A.; Bordignon, C., Phase II Study of Asparagine-Glycine-Arginine–Human Tumor Necrosis Factor α, a Selective Vascular Targeting Agent, in Previously Treated Patients With Malignant Pleural Mesothelioma. *Journal of Clinical Oncology* **2010,** *28* (15), 2604-2611.

158.   Gregorc, V.; Santoro, A.; Bennicelli, E.; Punt, C. J. A.; Citterio, G.; Timmer-Bonte, J. N. H.; Caligaris Cappio, F.; Lambiase, A.; Bordignon, C.; van Herpen, C. M. L., Phase

Ib study of NGR-hTNF, a selective vascular targeting agent, administered at low doses in combination with doxorubicin to patients with advanced solid tumours. *British Journal of Cancer* **2009**, *101* (2), 219-224.

159.   Curnis, F.; Sacchi, A.; Corti, A., Improving chemotherapeutic drug penetration in tumors by vascular targeting and barrier alteration. *The Journal of Clinical Investigation* **2002**, *110* (4), 475-482.

160.   Thorpe, P. E.; Chaplin, D. J.; Blakey, D. C., The First International Conference on Vascular Targeting: Meeting Overview. *Cancer Research* **2003**, *63* (5), 1144-1147.

161.   Jain, R. K., Normalization of Tumor Vasculature: An Emerging Concept in Antiangiogenic Therapy. *Science* **2005**, *307* (5706), 58-62.

162.   Brooks, A. C.; Kanthou, C.; Cook, I. H.; Tozer, G. M.; Barber, P. R.; Vojnovic, B.; Nash, G. B.; Parkins, C. S., The vascular targeting agent combretastatin A-4-phosphate induces neutrophil recruitment to endothelial cells in vitro. *Anticancer Res* **2003**, *23* (4), 3199-3206.

163.   Farace, F.; Massard, C.; Borghi, E.; Bidart, J.-M.; Soria, J.-C., Vascular disrupting therapy-induced mobilization of circulating endothelial progenitor cells. *Annals of Oncology* **2007**, *18* (8), 1421-1422.

164.   Veenendaal, L. M.; Jin, H.; Ran, S.; Cheung, L.; Navone, N.; Marks, J. W.; Waltenberger, J.; Thorpe, P.; Rosenblum, M. G., In vitro and in vivo studies of a VEGF121/rGelonin chimeric fusion toxin targeting the neovasculature of solid tumors. *Proceedings of the National Academy of Sciences* **2002**, *99* (12), 7866-7871.

165.   DeRose, P.; Thorpe, P. E.; Gerber, D. E., Development of bavituximab, a vascular targeting agent with immune-modulating properties, for lung cancer treatment. *Immunotherapy* **2011**, *3* (8), 933-944.

166.   Stack, G.; Walsh, J., Optimising the Delivery of Tubulin Targeting Agents through Antibody Conjugation. *Pharm Res* **2012**, *29* (11), 2972-2984.

167. Gasparini, G.; Brooks, P. C.; Biganzoli, E.; Vermeulen, P. B.; Bonoldi, E.; Dirix, L. Y.; Ranieri, G.; Miceli, R.; Cheresh, D. A., Vascular integrin alpha(v)beta3: a new prognostic indicator in breast cancer. *Clinical Cancer Research* **1998,** *4* (11), 2625-2634.

168. Arap, W.; Pasqualini, R.; Ruoslahti, E., Cancer treatment by targeted drug delivery to tumor vasculature in a mouse model. *Science* **1998,** *279* (5349), 377-380.

169. Temming, K.; Lacombe, M.; Schaapveld, R. Q. J.; Orfi, L.; Kéri, G.; Poelstra, K.; Molema, G.; Kok, R. J., Rational Design of RGD–Albumin Conjugates for Targeted Delivery of the VEGF-R Kinase Inhibitor PTK787 to Angiogenic Endothelium. *ChemMedChem* **2006,** *1* (11), 1200-1203.

170. Winter, P. M.; Neubauer, A. M.; Caruthers, S. D.; Harris, T. D.; Robertson, J. D.; Williams, T. A.; Schmieder, A. H.; Hu, G.; Allen, J. S.; Lacy, E. K.; Zhang, H.; Wickline, S. A.; Lanza, G. M., Endothelial $\alpha v \beta 3$ Integrin–Targeted Fumagillin Nanoparticles Inhibit Angiogenesis in Atherosclerosis. *Arteriosclerosis, Thrombosis, and Vascular Biology* **2006,** *26* (9), 2103-2109.

171. Buchanan, C. M.; Shih, J. H.; Astin, J. W.; Rewcastle, G. W.; Flanagan, J. U.; Crosier, P. S.; Shepherd, P. R., DMXAA (Vadimezan, ASA404) is a multi-kinase inhibitor targeting VEGFR2 in particular *Clinical Science* **2012,** *122* (19), 449-457.

172. Seshadri, M.; Spernyak, J.; Maier, P.; Cheney, R. T.; Mazurrchuk, R.; Bellnier, D. A., Visualizing the acute effects of vascular-targeted therapy in vivo using intravital microscopy and magnetic resonance imaging: correlation with endothelial apoptosis, cytokine induction and treatment outcome. *Neoplasia* **2007,** *9* (2), 128-135.

173. McKeage, M. J.; Von Pawel, J.; Reck, M.; Jameson, M. B.; Rosenthal, M. A.; Sullivan, R.; Gibbs, D.; Mainwaring, P. N.; Serke, M.; Lafitte, J.-J.; Chouaid, C.; Freitag, L.; Quoix, E., Randomised phase II study of ASA404 combined with carboplatin and paclitaxel in previously untreated advanced non-small cell lung cancer. *British Journal of Cancer* **2008,** *99* (12), 2006-2012.

174. (a) Lara, P. N.; Douillard, J.-Y.; Nakagawa, K.; von Pawel, J.; McKeage, M. J.; Albert, I.; Losonczy, G.; Reck, M.; Heo, D.-S.; Fan, X.; Fandi, A.; Scagliotti, G., Randomized Phase III Placebo-Controlled Trial of Carboplatin and Paclitaxel With or Without the Vascular Disrupting Agent Vadimezan (ASA404) in Advanced Non–Small-Cell Lung Cancer. *Journal of Clinical Oncology* **2011,** *29* (22), 2965-2971; (b) LoRusso, P. M.; Boerner, S. A.; Hunsberger, S., Clinical Development of Vascular Disrupting Agents: What Lessons Can We Learn From ASA404? *Journal of Clinical Oncology* **2011,** *29* (22), 2952-2955.

175. Eng, H.; Lund, K.; Campenot, R. B., Synthesis of β-Tubulin, Actin, and Other Proteins in Axons of Sympathetic Neurons in Compartmented Cultures. *The Journal of Neuroscience* **1999,** *19* (1), 1-9.

176. Verhey, K. J.; Gaertig, J., The Tubulin Code. *Cell Cycle* **2007,** *6* (17), 2152-2160.

177. Jordan, M. A.; Wilson, L., Microtubules as a target for anticancer drugs. *Nature Reviews Cancer* **2004,** *4* (4), 253-265.

178. Dumontet, C.; Jordan, M. A., Microtubule-binding agents: a dynamic field of cancer therapeutics. *Nature Reviews Drug Discovery* **2010,** *9* (10), 790-803.

179. Conde, C.; Caceres, A., Microtubule assembly, organization and dynamics in axons and dendrites. *Nature Reviews Neuroscience* **2009,** *10* (5), 319-332.

180. Fisher, R. I.; Gaynor, E. R.; Dahlberg, S.; Oken, M. M.; Grogan, T. M.; Mize, E. M.; Glick, J. H.; Coltman, C. A.; Miller, T. P., Comparison of a Standard Regimen (CHOP) with Three Intensive Chemotherapy Regimens for Advanced Non-Hodgkin's Lymphoma. *New England Journal of Medicine* **1993,** *328* (14), 1002-1006.

181. Nguyen, T. L.; Xu, X.; Gussio, R.; Ghosh, A. K.; Hamel, E., The Assembly-Inducing Laulimalide/Peloruside A Binding Site on Tubulin: Molecular Modeling and Biochemical Studies with [3H]Peloruside A. *Journal of Chemical Information and Modeling* **2010,** *50* (11), 2019-2028.

182.   ter Haar, E.; Kowalski, R. J.; Hamel, E.; Lin, C. M.; Longley, R. E.; Gunasekera, S. P.; Rosenkranz, H. S.; Day, B. W., Discodermolide, A Cytotoxic Marine Agent That Stabilizes Microtubules More Potently Than Taxol†,‡. *Biochemistry* **1996,** *35* (1), 243-250.

183.   Honore, S.; Kamath, K.; Braguer, D.; Horwitz, S. B.; Wilson, L.; Briand, C.; Jordan, M. A., Synergistic Suppression of Microtubule Dynamics by Discodermolide and Paclitaxel in Non-Small Cell Lung Carcinoma Cells. *Cancer Research* **2004,** *64* (14), 4957-4964.

184.   Wilson, L.; Meza, I., The mechanism of action of colchicine: colchicine binding properties of the sea urchin sperm tail outer doublet tubulin. *The Journal of Cell Biology* **1973,** *58* (3), 709-719.

185.   Dorléans, A.; Gigant, B.; Ravelli, R. B. G.; Mailliet, P.; Mikol, V.; Knossow, M., Variations in the colchicine-binding domain provide insight into the structural switch of tubulin. *Proceedings of the National Academy of Sciences* **2009,** *106* (33), 13775-13779.

186.   Hill, S. A.; Lonergan, S. J.; Denekamp, J.; Chaplin, D. J., Vinca alkaloids: Anti-vascular effects in a murine tumour. *European Journal of Cancer* **1993,** *29* (9), 1320-1324.

187.   (a) Dark, G. G.; Hill, S. A.; Prise, V. E.; Tozer, G. M.; Pettit, G. R.; Chaplin, D. J., Combretastatin A-4, an Agent That Displays Potent and Selective Toxicity toward Tumor Vasculature. *Cancer Research* **1997,** *57* (10), 1829-1834; (b) Messaoudi, S.; Tréguier, B.; Hamze, A.; Provot, O.; Peyrat, J.-F. o.; De Losada, J. R.; Liu, J.-M.; Bignon, J. r. m.; Wdzieczak-Bakala, J.; Thoret, S.; Dubois, J. l.; Brion, J.-D.; Alami, M. d., Isocombretastatins A versus Combretastatins A: The Forgotten isoCA-4 Isomer as a Highly Promising Cytotoxic and Antitubulin Agent. *Journal of Medicinal Chemistry* **2009,** *52* (14), 4538-4542.

188. (a) McGown, A.; Fox, B., Structural and biochemical comparison of the anti-mitotic agents colchicine, combretastatin A4 and amphethinile. *Anticancer Drug Design* **1989**, *3* (4), 249-254; (b) Tozer, G. M.; Kanthou, C.; Baguley, B. C., Disrupting tumour blood vessels. *Nature Reviews Cancer* **2005**, *5* (6), 423-435; (c) Lin, C. M.; Ho, H. H.; Pettit, G. R.; Hamel, E., Antimitotic natural products combretastatin A-4 and combretastatin A-2: studies on the mechanism of their inhibition of the binding of colchicine to tubulin. *Biochemistry* **1989**, *28* (17), 6984-6991.

189. Tozer, G. M.; Kanthou, C.; Parkins, C. S.; Hill, S. A., The biology of the combretastatins as tumour vascular targeting agents. *International Journal of Experimental Pathology* **2002**, *83* (1), 21-38.

190. Kanthou, C.; Tozer, G. M., The tumor vascular targeting agent combretastatin A–4-phosphate induces reorganization of the actin cytoskeleton and early membrane blebbing in human endothelial cells. *Blood* **2002**, *99* (6), 2060-2069.

191. Salmon, H. W.; Siemann, D. W., Effect of the Second-Generation Vascular Disrupting Agent OXi4503 on Tumor Vascularity. *Clinical Cancer Research* **2006**, *12* (13), 4090-4094.

192. Ley, C. D.; Horsman, M. R.; Kristjansen, P. E., Early Effects of Combretastatin-A4 Disodium Phosphate on Tumor Perfusion and Interstitial Fluid Pressure. *Neoplasia* **2007**, *9* (2), 108-112.

193. Holwell, S.; Cooper, P.; Grosios, K.; Lippert, J.; Pettit GR; Shnyder, S.; Bibby, M., Combretastatin A-1 phosphate a novel tubulin-binding agent with in vivo anti vascular effects in experimental tumours. *Anticancer Research* **2002**, *22* (2A), 707-711.

194. Pettit, G. R.; Temple, C., Jr.; Narayanan, V. L.; Varma, R.; Simpson, M. J.; Boyd, M. R.; Rener, G. A.; Bansal, N., Antineoplastic agents 322. synthesis of combretastatin A-4 prodrugs. *Anti-cancer drug design* **1995**, *10* (4), 299-309.

195. Griggs, J.; Metcalfe, J. C.; Hesketh, R., Targeting tumour vasculature: the development of combretastatin A4. *The Lancet Oncology* **2001**, *2* (2), 82-87.

196.   Rustin, G. J. S.; Galbraith, S. M.; Anderson, H.; Stratford, M.; Folkes, L. K.; Sena, L.; Gumbrell, L.; Price, P. M., Phase I Clinical Trial of Weekly Combretastatin A4 Phosphate: Clinical and Pharmacokinetic Results. *Journal of Clinical Oncology* **2003,** *21* (15), 2815-2822.

197.   Rustin, G. J.; Shreeves, G.; Nathan, P. D.; Gaya, A.; Ganesan, T. S.; Wang, D.; Boxall, J.; Poupard, L.; Chaplin, D. J.; Stratford, M. R. L.; Balkissoon, J.; Zweifel, M., A Phase Ib trial of CA4P (combretastatin A-4 phosphate), carboplatin, and paclitaxel in patients with advanced cancer. *British Journal of Cancer* **2010,** *102* (9), 1355-1360.

198.   Zweifel, M.; Jayson, G. C.; Reed, N. S.; Osborne, R.; Hassan, B.; Ledermann, J.; Shreeves, G.; Poupard, L.; Lu, S.-P.; Balkissoon, J.; Chaplin, D. J.; Rustin, G. J. S., Phase II trial of combretastatin A4 phosphate, carboplatin, and paclitaxel in patients with platinum-resistant ovarian cancer. *Annals of Oncology* **2011,** *22* (9), 2036-2041.

199.   (a) Delmonte, A.; Sessa, C., AVE8062: a new combretastatin derivative vascular disrupting agent. *Expert Opinion on Investigational Drugs* **2009,** *18* (10), 1541-1548; (b) Hori, K.; Saito, S.; Kubota, K., A novel combretastatin A-4 derivative, AC7700, strongly stanches tumour blood flow and inhibits growth of tumours developing in various tissues and organs. *British Journal of Cancer* **2002,** *86* (10), 1604-614.

200.   Ombrabulin (AVE8062). https://www.sanofioncology.com/pipeline/ombrabulin.aspx (accessed Jan 7 2013).

201.   Pettit, G. R.; Toki, B.; Herald, D. L.; Verdier-Pinard, P.; Boyd, M. R.; Hamel, E.; Pettit, R. K., Antineoplastic Agents. 379. Synthesis of Phenstatin Phosphate1a,†. *Journal of Medicinal Chemistry* **1998,** *41* (10), 1688-1695.

202.   Lu, Y.; Chen, J.; Xiao, M.; Li, W.; Miller, D., An Overview of Tubulin Inhibitors That Interact with the Colchicine Binding Site. *Pharm Res* **2012,** *29* (11), 2943-2971.

203.   Ghatak, A.; Dorsey, J. M.; Garner, C. M.; Pinney, K. G., Synthesis of methoxy and hydroxy containing tetralones: versatile intermediates for the preparation of biologically relevant molecules. *Tetrahedron Letters* **2003,** *44* (21), 4145-4148.

204. Flynn, B. L.; Hamel, E.; Jung, M. K., One-Pot Synthesis of Benzo[b]furan and Indole Inhibitors of Tubulin Polymerization. *Journal of Medicinal Chemistry* **2002,** *45* (12), 2670-2673.

205. Wang, L.; Woods, K. W.; Li, Q.; Barr, K. J.; McCroskey, R. W.; Hannick, S. M.; Gherke, L.; Credo, R. B.; Hui, Y.-H.; Marsh, K.; Warner, R.; Lee, J. Y.; Zielinski-Mozng, N.; Frost, D.; Rosenberg, S. H.; Sham, H. L., Potent, Orally Active Heterocycle-Based Combretastatin A-4 Analogues: Synthesis, Structure–Activity Relationship, Pharmacokinetics, and In Vivo Antitumor Activity Evaluation. *Journal of Medicinal Chemistry* **2002,** *45* (8), 1697-1711.

206. Nelson, A. R.; Fingleton, B.; Rothenberg, M. L.; Matrisian, L. M., Matrix Metalloproteinases: Biologic Activity and Clinical Implications. *Journal of Clinical Oncology* **2000,** *18* (5), 1135.

207. Grams, F.; Crimmin, M.; Hinnes, L.; Huxley, P.; Pieper, M.; Tschesche, H.; Bode, W., Structure determination and analysis of human neutrophil collagenase complexed with a hydroxamate inhibitor. *Biochemistry* **1995,** *34* (43), 14012-14020.

208. Botos, I.; Scapozza, L.; Zhang, D.; Liotta, L. A.; Meyer, E. F., Batimastat, a potent matrix mealloproteinase inhibitor, exhibits an unexpected mode of binding. *Proceedings of the National Academy of Sciences* **1996,** *93* (7), 2749-2754.

209. (a) Shah, R. The Design & Synthesis of Novel Inhibitors of Tubulin Polymerisation Ph. D, Trinity College Dublin, Ireland, 2002; (b) Hudson, G. Design, synthesis and evaluation of novel tumour antiogenic/vasculator targeting agents Ph.D Thesis, Trinity College Dublin, Ireland, 2006.

210. Shelanski, M. L.; Gaskin, F.; Cantor, C. R., Microtubule Assembly in the Absence of Added Nucleotides. *Proceedings of the National Academy of Sciences* **1973,** *70* (3), 765-768.

211. Bai, R.; Covell, D. G.; Pei, X.-F.; Ewell, J. B.; Nguyen, N. Y.; Brossi, A.; Hamel, E., Mapping the Binding Site of Colchicinoids on β-Tubulin: 2-chloroacetyl-2-

demethylthiocolchicine covalently reacts predominantly with cysteine 239 and secondarily with cysteine 354. *Journal of Biological Chemistry* **2000,** *275* (51), 40443-40452.

212.   Mosmann, T., Rapid colorimetric assay for cellular growth and survival: Application to proliferation and cytotoxicity assays. *Journal of Immunological Methods* **1983,** *65* (1–2), 55-63.

213.   Todaro, G. J.; Lazar, G. K.; Green, H., The initiation of cell division in a contact-inhibited mammalian cell line. *Journal of Cellular and Comparative Physiology* **1965,** *66* (3), 325.

214.   Stack, G. D. Ph. D, Trinity College Dublin, Ireland, 2013.

215.   Xu, Y.; McLaughlin, M.; Chen, C.-y.; Reamer, R. A.; Dormer, P. G.; Davies, I. W., A General Method for the Synthesis of 3,5-Diarylcyclopentenones via Friedel–Crafts Acylation of Vinyl Chlorides. *The Journal of Organic Chemistry* **2009,** *74* (14), 5100-5103.

216.   Parham, W. E.; Piccirilli, R. M., Selective halogen-lithium exchange in 2,5-dibromobenzenes and 2,5-dibromopyridine. *The Journal of Organic Chemistry* **1977,** *42* (2), 257-260.

217.   Caddick, S.; Cheung, S.; Doyle, V. E.; Frost, L. M.; Soscia, M. G.; Delisser, V. M.; Williams, M. R. V.; Etheridge, Z. C.; Khan, S.; Hitchcock, P. B.; Pairaudeau, G.; Vile, S., Stereoselective synthesis of polyfunctionalised hydroxylated cyclopentanes from dihydroxylated 2-cyclopentenone derivatives. *Tetrahedron* **2001,** *57* (29), 6295-6303.

218.   O'Byrne, P. Ph.D, Trinity College Dublin, Ireland, 2010.

219.   Grubbs, E. J.; Milligan, R. J.; Goodrow, M. H., Phenylation of oxime anions with diphenyliodonium bromide. *The Journal of Organic Chemistry* **1971,** *36* (13), 1780-1785.

220.   Gilon, C.; Knobler, Y.; Sheradsky, T., Synthesis of ω-aminooxy acids by oxygen-alkyl fission of lactones : An improved synthesis of dl-canaline. *Tetrahedron* **1967,** *23* (11), 4441-4447.

221.   Lachman, A., Benzophenone Oxime. *Organic Syntheses* **1943,** *Collective Volume 2*, 70-76.

222.   Coogan, A., Trinity College Dublin: Ireland, 2013.

223.   Jung, Y. J.; Lee, J. S.; Kim, Y. M., Colon-specific prodrugs of 5-aminosalicylic acid: Synthesis and in vitro/in vivo properties of acidic amino acid derivatives of 5-aminosalicylic acid. *Journal of Pharmaceutical Sciences* **2001,** *90* (11), 1767-1775.

224.   Paradis, R.; Pagé, M., New active paclitaxel amino acids derivatives with improved water solubility. *Anticancer Research* **1998,** *18* (4A), 2711-2716.

225.   Miyaura, N.; Yamada, K.; Suzuki, A., A new stereospecific cross-coupling by the palladium-catalyzed reaction of 1-alkenylboranes with 1-alkenyl or 1-alkynyl halides. *Tetrahedron Letters* **1979,** *20* (36), 3437-3440.

226.   Kondolff, I.; Doucet, H.; Santelli, M., Tetraphosphine/palladium catalysed Suzuki cross-coupling reactions of aryl halides with alkylboronic acids. *Tetrahedron* **2004,** *60* (17), 3813-3818.

227.   (a) Kirchhoff, J. H.; Netherton, M. R.; Hills, I. D.; Fu, G. C., Boronic Acids: New Coupling Partners in Room-Temperature Suzuki Reactions of Alkyl Bromides. Crystallographic Characterization of an Oxidative-Addition Adduct Generated under Remarkably Mild Conditions. *Journal of the American Chemical Society* **2002,** *124* (46), 13662-13663; (b) Lu, Z.; Wilsily, A.; Fu, G. C., Stereoconvergent Amine-Directed Alkyl–Alkyl Suzuki Reactions of Unactivated Secondary Alkyl Chlorides. *Journal of the American Chemical Society* **2011,** *133* (21), 8154-8157.

228.   Barder, T. E.; Walker, S. D.; Martinelli, J. R.; Buchwald, S. L., Catalysts for Suzuki−Miyaura Coupling Processes: Scope and Studies of the Effect of Ligand Structure. *Journal of the American Chemical Society* **2005,** *127* (13), 4685-4696.

229. Nguyen, H. N.; Huang, X.; Buchwald, S. L., The First General Palladium Catalyst for the Suzuki–Miyaura and Carbonyl Enolate Coupling of Aryl Arenesulfonates. *Journal of the American Chemical Society* **2003,** *125* (39), 11818-11819.

230. Marshall, J. A.; Johns, B. A., Total Synthesis of (+)-Discodermolide. *The Journal of Organic Chemistry* **1998,** *63* (22), 7885-7892.

231. Meng, D.; Bertinato, P.; Balog, A.; Su, D.-S.; Kamenecka, T.; Sorensen, E. J.; Danishefsky, S. J., Total Syntheses of Epothilones A and B. *Journal of the American Chemical Society* **1997,** *119* (42), 10073-10092.

232. Occhiato, E. G.; Trabocchi, A.; Guarna, A., Suzuki Reaction of Vinyl Triflates from Six- and Seven-Membered N-Alkoxycarbonyl Lactams with Boronic Acids and Esters. *The Journal of Organic Chemistry* **2001,** *66* (7), 2459-2465.

233. Ishiyama, T.; Murata, M.; Miyaura, N., Palladium(0)-Catalyzed Cross-Coupling Reaction of Alkoxydiboron with Haloarenes: A Direct Procedure for Arylboronic Esters. *The Journal of Organic Chemistry* **1995,** *60* (23), 7508-7510.

234. Hayashi, T.; Konishi, M.; Kobori, Y.; Kumada, M.; Higuchi, T.; Hirotsu, K., Dichloro[1,1'-bis(diphenylphosphino)ferrocene]palladium(II): an effective catalyst for cross-coupling of secondary and primary alkyl Grignard and alkylzinc reagents with organic halides. *Journal of the American Chemical Society* **1984,** *106* (1), 158-163.

235. Breen, E. C. Ph.D, Trinity College Dublin, Ireland, 2012.

236. Frérot, E.; Coste, J.; Pantaloni, A.; Dufour, M.-N.; Jouin, P., PyBOP® and PyBroP: Two reagents for the difficult coupling of the α,α-dialkyl amino acid, Aib. *Tetrahedron* **1991,** *47* (2), 259-270.

237. (a) Wang, H.; Wang, F.; Tao, X.; Cheng, H., Ammonia-containing dimethyl sulfoxide: An improved solvent for the dissolution of formazan crystals in the 3-(4,5-dimethylthiazol-2-yl)-2,5-diphenyl tetrazolium bromide (MTT) assay. *Analytical Biochemistry* **2012,** *421* (1), 324-326; (b) Twentyman, P. R.; Luscombe, M., A study of

some variables in a tetrazolium dye (MTT) based assay for cell growth and chemosensitivity. *British Journal of Cancer* **1987,** *56,* 279-285.

238.   Berridge, M. V.; Herst, P. M.; Tan, A. S., Tetrazolium dyes as tools in cell biology: New insights into their cellular reduction. In *Biotechnology Annual Review*, El-Gewely, M. R., Ed. Elsevier: 2005; Vol. Volume 11, pp 127-152.

239.   Sargent, J., The Use of the MTT Assay to Study Drug Resistance in Fresh Tumour Samples. In *Chemosensitivity Testing in Oncology*, Reinhold, U.; Tilgen, W., Eds. Springer Berlin Heidelberg: 2003; Vol. 161, pp 13-25.

240.   Romijn, J. C.; Verkoelen, C. F.; Schroeder, F. H., Application of the MTT assay to human prostate cancer cell lines in vitro: Establishment of test conditions and assessment of hormone-stimulated growth and drug induced cytostatic and cytotoxic effects. *The Prostate* **1988,** *12* (1), 99-110.

241.   Boyden, S., The chemotactic effect of mixtures of antibody and antigen on polymorphonuclear leucocytes. *The Journal of Experimental Medicine* **1962,** *115* (3), 453-466.

242.   (a) Liang, C.-C.; Park, A. Y.; Guan, J.-L., In vitro scratch assay: a convenient and inexpensive method for analysis of cell migration in vitro. *Nature Protocols* **2007,** *2* (2), 329-333; (b) Cory, G., Scratch-Wound Assay. In *Cell Migration*, Wells, C. M.; Parsons, M., Eds. Humana Press: 2011; Vol. 769, pp 25-30; (c) O'Brien, K.; Rani, S.; Corcoran, C.; Wallace, R.; Hughes, L.; Friel, A. M.; McDonnell, S.; Crown, J.; Radomski, M. W.; O'Driscoll, L., Exosomes from triple-negative breast cancer cells can transfer phenotypic traits representing their cells of origin to secondary cells. *European Journal of Cancer* (0).

243.   Geback, T.; Schulz, M. M. P.; Koumoutsakos, P.; Detmar, M., TScratch: a novel and simple software tool for automated analysis of monolayer wound healing assays. *BioTechniques* **2009,** *46* (4), 265-274.

244.   (a) Roudnicky, F.; Poyet, C.; Wild, P.; Krampitz, S.; Negrini, F.; Huggenberger, R.; Rogler, A.; Stöhr, R.; Hartmann, A.; Provenzano, M.; Otto, V. I.; Detmar, M., Endocan Is Upregulated on Tumor Vessels in Invasive Bladder Cancer Where It Mediates VEGF-A–Induced Angiogenesis. *Cancer Research* **2013,** *73* (3), 1097-1106; (b) Ramirez, N. E.; Zhang, Z.; Madamanchi, A.; Boyd, K. L.; x; Rear, L. D.; Nashabi, A.; Li, Z.; Dupont, W. D.; Zijlstra, A.; Zutter, M. M., The α2β1 integrin is a metastasis suppressor in mouse models and human cancer. *The Journal of Clinical Investigation* **2011,** *121* (1), 226-237.

245.   Ikawa, M.; Stahmann, M. A.; Link, K. P., Studies on 4-Hydroxycoumarins. V. The Condensation of α,β-Unsaturated Ketones with 4-Hydroxycoumarin1. *Journal of the American Chemical Society* **1944,** *66* (6), 902-906.

246.   Rowan, S. J.; Sanders, J. K. M., Macrocycles Derived from Cinchona Alkaloids: A Thermodynamic vs Kinetic Study. *The Journal of Organic Chemistry* **1998,** *63* (5), 1536-1546.

247.   Corey, E. J.; Schmidt, G., Useful procedures for the oxidation of alcohols involving pyridinium dichromate in approtic media. *Tetrahedron Letters* **1979,** *20* (5), 399-402.

248.   Rappoport, Z.; Marek, I., *The Chemistry of Organomagnesium Compounds*. John Wiley & Sons: 2008; p 920.

249.   Weiberth, F. J.; Hall, S. S., Copper(I)-activated addition of Grignard reagents to nitriles. Synthesis of ketimines, ketones, and amines. *The Journal of Organic Chemistry* **1987,** *52* (17), 3901-3904.

250.   Donadel, O. J.; Martín, T.; Martín, V. S.; Villar, J.; Padrón, J. M., The tert-butyl dimethyl silyl group as an enhancer of drug cytotoxicity against human tumor cells. *Bioorganic & Medicinal Chemistry Letters* **2005,** *15* (15), 3536-3539.

251.   McHugh, A. Masters, Trinity College Dublin, Ireland, 2007.

252.   (a) Wittig, G.; Schöllkopf, U., Über Triphenyl-phosphin-methylene als olefinbildende Reagenzien (I. Mitteil. *Chemische Berichte* **1954,** *87* (9), 1318-1330; (b) Wittig, G.;

Haag, W., Über Triphenyl-phosphinmethylene als olefinbildende Reagenzien (II. Mitteil.1)). *Chemische Berichte* **1955,** *88* (11), 1654-1666.

253.   Maercker, A., The Wittig Reaction. In *Organic Reactions*, John Wiley & Sons, Inc.: 2004.

254.   Vedejs, E.; Meier, G. P.; Snoble, K. A. J., Low-temperature characterization of the intermediates in the Wittig reaction. *Journal of the American Chemical Society* **1981,** *103* (10), 2823-2831.

255.   Wadsworth, W. S.; Emmons, W. D., The Utility of Phosphonate Carbanions in Olefin Synthesis. *Journal of the American Chemical Society* **1961,** *83* (7), 1733-1738.

256.   Reitz, A. B.; Nortey, S. O.; Jordan, A. D.; Mutter, M. S.; Maryanoff, B. E., Dramatic concentration dependence of stereochemistry in the Wittig reaction. Examination of the lithium salt effect. *The Journal of Organic Chemistry* **1986,** *51* (17), 3302-3308.

257.   Maryanoff, B. E.; Reitz, A. B.; Duhl-Emswiler, B. A., Stereochemistry of the Wittig reaction. Effect of nucleophilic groups in the phosphonium ylide. *Journal of the American Chemical Society* **1985,** *107* (1), 217-226.

258.   Krohn, K.; Loock, U.; Paavilainen, K.; Hausen, B. M.; Schmalle, H.; Kiesele, H., Synthesis and electrochemistry of annoquinone-A, cypripedin methyl ether, denbinobin and related 1,4-phenanthrenequinones. *ARKIVOK* **2001,** *2001* ((i)), 88-130.

259.   Shih-Yuan Lee, A.; Lin, L.-S., Synthesis of allyl ketone via Lewis acid promoted Barbier-type reaction. *Tetrahedron Letters* **2000,** *41* (45), 8803-8806.

260.   Walsh, J. J.; Coughlan, D.; Heneghan, N.; Gaynor, C.; Bell, A., A novel artemisinin-quinine hybrid with potent antimalarial activity. *Bioorganic & Medicinal Chemistry Letters* **2007,** *17*, 3599-3602.

261.   Wuts, P. G. M.; Greene, T., W., *Greene's Protective Groups in Organic Synthesis, 4th Edition*. Wiley: 2006; Vol. 4th, p 1110.

262.   Cornforth, R. H.; Cornforth, J. W.; Popják, G., Preparation of R- and S-mevalonolactones. *Tetrahedron* **1962,** *18* (12), 1351-1354.

263.   Chidambaram, N.; Bhat, S.; Chandrasekaran, S., A highly selective methodology for the direct conversion of acetals to esters. *The Journal of Organic Chemistry* **1992,** *57* (18), 5013-5015.

264.   Ladenheim, H.; Bender, M. L., Acylium Ion Formation in the Reactions of Carboxylic Acid Derivatives. I. Application of the HR Acidity Function to the Diazotization of Benzamide in Sulfuric Acid1. *Journal of the American Chemical Society* **1960,** *82* (8), 1895-1900.

265.   Clayden, J.; Greeves, N.; Warren, S.; Wothers, P., *Organic Chemistry*. Oxford University Press: Oxford, 2001; Vol. 1, p 1512.

266.   Casadei, M. A.; Galli, C.; Mandolini, L., Ring-closure reactions. 22. Kinetics of cyclization of diethyl (.omega.-bromoalkyl)malonates in the range of 4- to 21-membered rings. Role of ring strain. *Journal of the American Chemical Society* **1984,** *106* (4), 1051-1056.

267.   Baldwin, J. E., Rules for ring closure. *Journal of the Chemical Society, Chemical Communications* **1976,** *0* (18), 734-736.

268.   McCormack, E. Design, synthesis and in vitro evaluation of novel anti-cancer compounds Ph. D, Trinity College Dublin, Ireland, 2002.

269.   Zhang, T. Ph.D, Trinity College Dubli, Ireland, 2010.

270.   Hardy, J. P.; Kerrin, S. L.; Manatt, S. L., 1-Butanol-hydrogen chloride. Allegedly anhydrous esterification reagent. *The Journal of Organic Chemistry* **1973,** *38* (24), 4196-4200.

271.   Jockel, H.; Schmidt, R., Kinetics of the direct borane reduction of pinacolone in THF. *Journal of the Chemical Society, Perkin Transactions 2* **1997,** *0* (12), 2719-2724.

272.   Renz, M.; Meunier, B., 100 Years of Baeyer–Villiger Oxidations. *Eur. J. Org. Chem.* **1999,** *1999* (4), 737-750.

273.   Mohan, R. S.; Whalen, D. L., Acid-catalyzed hydrolysis of cis- and trans-anethole oxides: discrete carbocation intermediates and syn/anti hydration ratios. *The Journal of Organic Chemistry* **1993,** *58* (10), 2663-2669.

274.   Centko, R. S.; Mohan, R. S., The Discovery-Oriented Approach to Organic Chemistry. 4. Epoxidation of p-Methoxy-trans-β[beta]-methylstyrene: An Exercise in NMR and IR Spectroscopy for Sophomore Organic Laboratories. *Journal of Chemical Education* **2001,** *78* (1), 77.

275.   Araki, K.; Suenaga, K.; Sengoku, T.; Uemura, D., Total synthesis of attenols A and B. *Tetrahedron* **2002,** *58* (10), 1983-1995.

276.   (a) Burghardt, T. E., Developments in the deprotection of thioacetals. *Journal of Sulfur Chemistry* **2005,** *26* (4-5), 411-427; (b) Corey, E. J.; Erickson, B. W., Oxidative hydrolysis of 1,3-dithiane derivatives to carbonyl compounds using N-halosuccinimide reagents. *The Journal of Organic Chemistry* **1971,** *36* (23), 3553-3560.

277.   Langille, N. F.; Dakin, L. A.; Panek, J. S., A Mild, Chemoselective Protocol for the Removal of Thioketals and Thioacetals Mediated by Dess–Martin Periodinane. *Organic Letters* **2003,** *5* (4), 575-578.

278.   Ganguly, N. C.; Mondal, P., Mild, Efficient, and Greener Dethioacetalization Protocol Using 30% Hydrogen Peroxide in Catalytic Combination with Ammonium Iodide. *Synthetic Communications* **2011,** *41* (16), 2374-2384.

279.   Negi, P. S.; Jayaprakasha, G. K.; Jagan Mohan Rao, L.; Sakariah, K. K., Antibacterial Activity of Turmeric Oil: A Byproduct from Curcumin Manufacture. *Journal of Agricultural and Food Chemistry* **1999,** *47* (10), 4297-4300.

280.   Lin, J. K.; Lin-Shiau, S. Y., Mechanisms of cancer chemoprevention by curcumin. *Proceedings of the National Science Council, Republic of China. Part B, Life sciences* **2001,** *25* (2), 59-66.

281.   Fu, Y.; Zheng, S.; Lin, J.; Ryerse, J.; Chen, A., Curcumin Protects the Rat Liver from CCl4-Caused Injury and Fibrogenesis by Attenuating Oxidative Stress and Suppressing Inflammation. *Molecular Pharmacology* **2008,** *73* (2), 399-409.

282.   Hong, J.; Bose, M.; Ju, J.; Ryu, J.-H.; Chen, X.; Sang, S.; Lee, M.-J.; Yang, C. S., Modulation of arachidonic acid metabolism by curcumin and related β-diketone derivatives: effects on cytosolic phospholipase A2, cyclooxygenases and 5-lipoxygenase. *Carcinogenesis* **2004,** *25* (9), 1671-1679.

283.   Arbiser, J. L.; Klauber, N.; Rohan, R.; van Leeuwen, R.; Huang, M. T.; Fisher, C.; Flynn, E.; Byers, H. R., Curcumin is an in vivo inhibitor of angiogenesis. *Molecular Medicine* **1998,** *4* (6), 376-383.

284.   Deeb, D.; Jiang, H.; Gao, X.; Hafner, M. S.; Wong, H.; Divine, G.; Chapman, R. A.; Dulchavsky, S. A.; Gautam, S. C., Curcumin sensitizes prostate cancer cells to tumor necrosis factor–related apoptosis-inducing ligand/Apo2L by inhibiting nuclear factor-κB through suppression of IκBα phosphorylation. *Molecular Cancer Therapeutics* **2004,** *3* (7), 803-812.

285.   Singh, S.; Aggarwal, B. B., Activation of Transcription Factor NF-κB Is Suppressed by Curcumin (Diferuloylmethane). *Journal of Biological Chemistry* **1995,** *270* (42), 24995-25000.

286.   Thomas, S. L.; Zhong, D.; Zhou, W.; Malik, S.; Liotta, D.; Snyder, J. P.; Hamel, E.; Giannakakou, P., EF24, a novel curcumin analog, disrupts the microtubule cytoskeleton and inhibits HIF-1. *Cell Cycle* **2008,** *7* (15), 2409-2417.

287.   Hahm, E.-R.; Gho, Y. S.; Park, S.; Park, C.; Kim, K.-W.; Yang, C.-H., Synthetic curcumin analogs inhibit activator protein-1 transcription and tumor-induced angiogenesis. *Biochemical and Biophysical Research Communications* **2004,** *321* (2), 337-344.

288.   Chakraborti, S.; Das, L.; Kapoor, N.; Das, A.; Dwivedi, V.; Poddar, A.; Chakraborti, G.; Janik, M.; Basu, G.; Panda, D.; Chakrabarti, P.; Surolia, A.; Bhattacharyya, B.,

Curcumin Recognizes a Unique Binding Site of Tubulin. *Journal of Medicinal Chemistry* **2011,** *54* (18), 6183-6196.

289.   Barzegar, A.; Moosavi-Movahedi, A. A., Intracellular ROS Protection Efficiency and Free Radical-Scavenging Activity of Curcumin. *PLoS ONE* **2011,** *6* (10), e26012.

290.   Baum, L.; Ng, A., Curcumin interaction with copper and iron suggests one possible mechanism of action in Alzheimer's disease animal models. *Journal of Alzheimer's Disease* **2004,** *6* (4), 367-377.

291.   Jung, Y.; Xu, W.; Kim, H.; Ha, N.; Neckers, L., Curcumin-induced degradation of ErbB2: A role for the E3 ubiquitin ligase CHIP and the Michael reaction acceptor activity of curcumin. *Biochimica et Biophysica Acta (BBA) - Molecular Cell Research* **2007,** *1773* (3), 383-390.

292.   (a) Bora-Tatar, G.; Dayangaç-Erden, D.; Demir, A. S.; Dalkara, S.; Yelekçi, K.; Erdem-Yurter, H., Molecular modifications on carboxylic acid derivatives as potent histone deacetylase inhibitors: Activity and docking studies. *Bioorganic & Medicinal Chemistry* **2009,** *17* (14), 5219-5228; (b) Majhi, A.; Rahman, G. M.; Panchal, S.; Das, J., Binding of curcumin and its long chain derivatives to the activator binding domain of novel protein kinase C. *Bioorganic & Medicinal Chemistry* **2010,** *18* (4), 1591-1598.

293.   Cheng AL; Hsu CH; Lin JK; Hsu MM; Ho YF; Shen TS; Ko JY; Lin JT; Lin BR; Ming-Shiang W; Yu HS; Jee SH; Chen GS; Chen TM; Chen CA; Lai MK; Pu YS; Pan MH; Wang YJ; Tsai CC; CY., H., Phase I clinical trial of curcumin, a chemopreventive agent, in patients with high-risk or pre-malignant lesions. *Anticancer Research* **2001,** *21* (4B), 2895-2900.

294.   Rajasekaran, S. A., Therapeutic potential of curcumin in gastrointestinal diseases. *World journal of Gastrointestinal Pathophysiology* **2011,** *2* (1), 1-14.

295.   Anand, P.; Kunnumakara, A. B.; Newman, R. A.; Aggarwal, B. B., Bioavailability of Curcumin: Problems and Promises. *Molecular Pharmaceutics* **2007,** *4* (6), 807-818.

296. Garcea, G.; Jones, D. J. L.; Singh, R.; Dennison, A. R.; Farmer, P. B.; Sharma, R. A.; Steward, W. P.; Gescher, A. J.; Berry, D. P., Detection of curcumin and its metabolites in hepatic tissue and portal blood of patients following oral administration. *British Journal of Cancer* **2004,** *90* (5), 1011-1015.

297. Shoba, G.; Joy, D.; Joseph, T.; Majeed, M.; Rajendran, R.; Srinivas, P. S. S. R., Influence of Piperine on the Pharmacokinetics of Curcumin in Animals and Human Volunteers. *Planta Medica* **1998,** *64* (4), 353-356.

298. Bhardwaj, R. K.; Glaeser, H.; Becquemont, L.; Klotz, U.; Gupta, S. K.; Fromm, M. F., Piperine, a Major Constituent of Black Pepper, Inhibits Human P-glycoprotein and CYP3A4. *Journal of Pharmacology and Experimental Therapeutics* **2002,** *302* (2), 645-650.

299. Anand, K.; Sarkar, A.; Kumar, A.; Ambasta, R. K.; Kumar, P., Combinatorial Antitumor Effect of Naringenin and Curcumin Elicit Angioinhibitory Activities In Vivo. *Nutrition and Cancer* **2012,** *64* (5), 714-724.

300. Bhawana; Basniwal, R. K.; Buttar, H. S.; Jain, V. K.; Jain, N., Curcumin Nanoparticles: Preparation, Characterization, and Antimicrobial Study. *Journal of Agricultural and Food Chemistry* **2011,** *59* (5), 2056-2061.

301. Gou, M.; Men, K.; Shi, H.; Xiang, M.; Zhang, J.; Song, J.; Long, J.; Wan, Y.; Luo, F.; Zhao, X.; Qian, Z., Curcumin-loaded biodegradable polymeric micelles for colon cancer therapy in vitro and in vivo. *Nanoscale* **2011,** *3* (4), 1558-1567.

302. Kitture, R.; Ghosh, S.; Kulkarni, P.; Liu, X. L.; Maity, D.; Patil, S. I.; Jun, D.; Dushing, Y.; Laware, S. L.; Chopade, B. A.; Kale, S. N., Fe_3O_4-citrate-curcumin: Promising conjugates for superoxide scavenging, tumor suppression and cancer hyperthermia. *Journal of Applied Physics* **2012,** *111*, 064702.

303. Shaikh, J.; Ankola, D. D.; Beniwal, V.; Singh, D.; Kumar, M. N. V. R., Nanoparticle encapsulation improves oral bioavailability of curcumin by at least 9-fold when

compared to curcumin administered with piperine as absorption enhancer. *European Journal of Pharmaceutical Sciences* **2009,** *37* (3–4), 223-230.

304.   Ganta, S.; Amiji, M., Coadministration of Paclitaxel and Curcumin in Nanoemulsion Formulations To Overcome Multidrug Resistance in Tumor Cells. *Molecular Pharmaceutics* **2009,** *6* (3), 928-939.

305.   Sup Shim, J.; Hoon Kim, D.; Jung, H. J.; Hee Kim, J.; Lim, D.; Lee, S.-K.; Kim, K.-W.; Ahn, J. W.; Yoo, J.-S.; Rho, J.-R.; Shin, J.; Jeong Kwon, H., Hydrazinocurcumin, a novel synthetic curcumin derivative, Is a potent inhibitor of endothelial cell proliferation. *Bioorganic & Medicinal Chemistry* **2002,** *10* (8), 2439-2444.

306.   (a) Xiaofei Wang, Y. Z., Xiwen Zhang, Wenxia Tian, Wenli Feng, Tingmei Chen, The curcumin analogue hydrazinocurcumin exhibits potent suppressive activity on carcinogenicity of breast cancer cells via STAT3 inhibition. *International Journal of Oncology* **2011,** *40* (4), 1189-1195; (b) Rathore, R.; Jain, J. P.; Srivastava, A.; Jachak, S. M.; Kumar, N., Simultaneous determination of hydrazinocurcumin and phenol red in samples from rat intestinal permeability studies: HPLC method development and validation. *Journal of Pharmaceutical and Biomedical Analysis* **2008,** *46* (2), 374-380.

307.   Kim, J. H.; Shim, J. S.; Lee, S.-K.; Kim, K.-W.; Rha, S. Y.; Chung, H. C.; Kwon, H. J., Microarray-based Analysis of Anti-angiogenic Activity of Demethoxycurcumin on Human Umbilical Vein Endothelial Cells: Crucial Involvement of the Down-regulation of Matrix Metalloproteinase. *Cancer Science* **2002,** *93* (12), 1378-1385.

308.   Gupta, K. K.; Bharne, S. S.; Rathinasamy, K.; Naik, N. R.; Panda, D., Dietary antioxidant curcumin inhibits microtubule assembly through tubulin binding. *FEBS Journal* **2006,** *273* (23), 5320-5332.

309.   Chen, C.; Liu, Y.; Chen, Y.; Xu, J., C086, a novel analog of curcumin, induces growth inhibition and down-regulation of NFκB in colon cancer cells and xenograft tumors. *Cancer Biology & Therapy* **2011,** *12* (9), 797-807.

310. Robinson, T. P.; Ehlers, T.; Hubbard, I. V. R. B.; Bai, X.; Arbiser, J. L.; Goldsmith, D. J.; Bowen, J. P., Design, synthesis, and biological evaluation of angiogenesis inhibitors: aromatic enone and dienone analogues of curcumin. *Bioorganic & Medicinal Chemistry Letters* **2003,** *13* (1), 115-117.

311. Ohori, H.; Yamakoshi, H.; Tomizawa, M.; Shibuya, M.; Kakudo, Y.; Takahashi, A.; Takahashi, S.; Kato, S.; Suzuki, T.; Ishioka, C.; Iwabuchi, Y.; Shibata, H., Synthesis and biological analysis of new curcumin analogues bearing an enhanced potential for the medicinal treatment of cancer. *Molecular Cancer Therapeutics* **2006,** *5* (10), 2563-2571.

312. Zhu, S.; Moore, T. W.; Lin, X.; Morii, N.; Mancini, A.; Howard, R. B.; Culver, D.; Arrendale, R. F.; Reddy, P.; Evers, T. J.; Zhang, H.; Sica, G.; Chen, Z. G.; Sun, A.; Fu, H.; Khuri, F. R.; Shin, D. M.; Snyder, J. P.; Shoji, M., Synthetic curcumin analog EF31 inhibits the growth of head and neck squamous cell carcinoma xenografts. *Integrative Biology* **2012,** *4* (6), 633-640.

313. Shaabani, A.; Mirzaei, P.; Naderi, S.; Lee, D. G., Green oxidations. The use of potassium permanganate supported on manganese dioxide. *Tetrahedron* **2004,** *60* (50), 11415-11420.

314. Dahnke, K. R.; Paquette, L. A., Inverse electron-demand Diels-Alder cycloaddition of a ketene dithioacetal. Copper hydride-promoted reduction of a conjugated enone. 9-dithiolanobicyclo[3.2.2]non-6-en-2-2n-one from tropone. *Organic Syntheses* **1993,** *71* (1), 181.

315. (a) Claisen, L.; Claparède, A., Condensationen von Ketonen mit Aldehyden. *Berichte der deutschen chemischen Gesellschaft* **1881,** *14* (2), 2460-2468; (b) Hauser, C. R.; Hudson, B. E., The Acetoacetic Ester Condensation and Certain Related Reactions. In *Organic Reactions*, John Wiley & Sons, Inc.: 2004.

316. (a) Arya, P.; Qin, H., Advances in Asymmetric Enolate Methodology. *Tetrahedron* **2000,** *56*, 917-947; (b) Tiong, E. A.; Rivalti, D.; Williams, B. M.; Gleason, J. L., A

Concise Total Synthesis of (R)-Puraquinonic Acid. *Angewandte Chemie International Edition* **2013,** *52* (12), 3442-3445.

317. Hayashi, Y.; Samanta, S.; Itoh, T.; Ishikawa, H., Asymmetric, Catalytic, and Direct Self-Aldol Reaction of Acetaldehyde Catalyzed by Diarylprolinol. *Organic Letters* **2008,** *10* (24), 5581-5583.

318. Mukaiyama, T. The Directed Aldol Reaction, *Organic Reactions*, **2004**, John Wiley & Sons, Inc.

319. del Mar Real, M.; Pérez Sestelo, J.; Sarandeses, L. A., Inner–outer ring 1,3-bis(trimethylsilyloxy)-1,3-dienes as useful intermediates in the synthesis of helicenes. *Tetrahedron Letters* **2002,** *43* (50), 9111-9114.

320. Zhang, J.; Yang, N.; Yang, L., Observation of 1,3-Diketones Formation in the Reaction of Bulky Acyl Chlorides with Methyllithium. *Molecules* **2012,** *17* (6), 6415-6423.

321. Williams, R. V.; Edwards, W. D.; Zhang, P.; Berg, D. J.; Mitchell, R. H., Experimental Verification of the Homoaromaticity of 1,3,5-Cycloheptatriene and Evaluation of the Aromaticity of Tropone and the Tropylium Cation by Use of the Dimethyldihydropyrene Probe. *Journal of the American Chemical Society* **2012,** *134* (40), 16742-16752.

322. Klayman, D. L.; Lin, A. J.; Acton, N.; Scovill, J. P.; Hoch, J. M.; Milhous, W. K.; Theoharides, A. D.; Dobek, A. S., Isolation of Artemisinin (Qinghaosu) from Artemisia annua Growing in the United States. *Journal of Natural Products* **1984,** *47* (4), 715-717.

323. Liu, R.; Dong, H.-F.; Jiang, M.-S., Artemisinin: the gifts from traditional Chinese medicine not only for malaria control but also for schistosomiasis control. *Parasitol Res* **2012,** *110* (5), 2071-2074.

324. Li, G.-Q.; Guo, X.-B.; Fu, L.-C.; Jian, H.-X.; Wang, X.-H., Clinical trials of artemisinin and its derivatives in the treatment of malaria in China. *Transactions of the Royal Society of Tropical Medicine and Hygiene* **1994,** *88, Supplement 1* (0), 5-6.

325.   (a) Dondorp, A. M.; Nosten, F.; Yi, P.; Das, D.; Phyo, A. P.; Tarning, J.; Lwin, K. M.; Ariey, F.; Hanpithakpong, W.; Lee, S. J.; Ringwald, P.; Silamut, K.; Imwong, M.; Chotivanich, K.; Lim, P.; Herdman, T.; An, S. S.; Yeung, S.; Singhasivanon, P.; Day, N. P. J.; Lindegardh, N.; Socheat, D.; White, N. J., Artemisinin Resistance in Plasmodium falciparum Malaria. *New England Journal of Medicine* **2009,** *361* (5), 455-467; (b) Noedl, H.; Se, Y.; Schaecher, K.; Smith, B. L.; Socheat, D.; Fukuda, M. M., Evidence of Artemisinin-Resistant Malaria in Western Cambodia. *New England Journal of Medicine* **2008,** *359* (24), 2619-2620.

326.   Rehwagen, C., WHO ultimatum on artemisinin monotherapy is showing results. *BMJ* **2006,** *332* (7551), 1176.

327.   O'Neill, P. M.; Barton, V. E.; Ward, S. A. M., 15, 1705-1721., The Molecular Mechanism of Action of Artemisinin—The Debate Continues. *Molecules* **2010,** *15* (3), 1705-1721.

328.   Olliaro, P. L.; Haynes, R. K.; Meunier, B.; Yuthavong, Y., Possible modes of action of the artemisinin-type compounds. *Trends in parasitology* **2001,** *17* (3), 122-126.

329.   Schmid, G.; Hofheinz, W., Total synthesis of qinghaosu. *Journal of the American Chemical Society* **1983,** *105* (3), 624-625.

330.   Paddon, C. J.; Westfall, P. J.; Pitera, D. J.; Benjamin, K.; Fisher, K.; McPhee, D.; Leavell, M. D.; Tai, A.; Main, A.; Eng, D.; Polichuk, D. R.; Teoh, K. H.; Reed, D. W.; Treynor, T.; Lenihan, J.; Fleck, M.; Bajad, S.; Dang, G.; Diola, D.; Dorin, G.; Ellens, K. W.; Fickes, S.; Galazzo, J.; Gaucher, S. P.; Geistlinger, T.; Henry, R.; Hepp, M.; Horning, T.; Iqbal, T.; Jiang, H.; Kizer, L.; Lieu, B.; Melis, D.; Moss, N.; Regentin, R.; Secrest, S.; Tsuruta, H.; Vazquez, R.; Westblade, L. F.; Xu, L.; Yu, M.; Zhang, Y.; Zhao, L.; Lievense, J.; Covello, P. S.; Keasling, J. D.; Reiling, K. K.; Renninger, N. S.; Newman, J. D., High-level semi-synthestic production of the potent antimalarial artemisinin. *Nature* **2013,** *Advance online publication.*

331. Westfall, P. J.; Pitera, D. J.; Lenihan, J. R.; Eng, D.; Woolard, F. X.; Regentin, R.; Horning, T.; Tsuruta, H.; Melis, D. J.; Owens, A.; Fickes, S.; Diola, D.; Benjamin, K. R.; Keasling, J. D.; Leavell, M. D.; McPhee, D. J.; Renninger, N. S.; Newman, J. D.; Paddon, C. J., Production of amorphadiene in yeast, and its conversion to dihydroartemisinic acid, precursor to the antimalarial agent artemisinin. *Proceedings of the National Academy of Sciences* **2012**.

332. Haynes, Richard K.; Chan, H.-W.; Cheung, M.-K.; Lam, W.-L.; Soo, M.-K.; Tsang, H.-W.; Voerste, A.; Williams, Ian D., C-10 Ester and Ether Derivatives of Dihydroartemisinin − 10-α Artesunate, Preparation of Authentic 10-β Artesunate, and of Other Ester and Ether Derivatives Bearing Potential Aromatic Intercalating Groups at C-10. *Eur. J. Org. Chem.* **2002**, *2002* (1), 113-132.

333. Singh, N. P.; Lai, H. C., Artemisinin Induces Apoptosis in Human Cancer Cells. *Anticancer Research* **2004**, *24* (4), 2277-2280.

334. Efferth, T.; Giaisi, M.; Merling, A.; Krammer, P. H.; Li-Weber, M., Artesunate Induces ROS-Mediated Apoptosis in Doxorubicin-Resistant T Leukemia Cells. *PLoS ONE* **2007**, *2* (8), e693.

335. Wang, S.-J.; Gao, Y.; Chen, H.; Kong, R.; Jiang, H.-C.; Pan, S.-H.; Xue, D.-B.; Bai, X.-W.; Sun, B., Dihydroartemisinin inactivates NF-κB and potentiates the anti-tumor effect of gemcitabine on pancreatic cancer both in vitro and in vivo. *Cancer Letters* **2010**, *293* (1), 99-108.

336. Chen, H.-H.; Zhou, H.-J.; Wang, W.-Q.; Wu, G.-D., Antimalarial dihydroartemisinin also inhibits angiogenesis. *Cancer Chemother Pharmacol* **2004**, *53* (5), 423-432.

337. Mao, Z.-g.; Zhou, J.; Wang, H.; He, D.-s.; Xiao, W.-w.; Liao, G.-z.; Qiu, L.-b.; Zhu, Y.-h.; Wang, H.-j., Artesunate inhibits cell proliferation and decreases growth hormone synthesis and secretion in GH3 cells. *Mol Biol Rep* **2012**, *39* (5), 6227-6234.

338. Reungpatthanaphong, P.; Mankhetkorn, S., Modulation of Multidrug Resistance by Artemisinin, Artesunate and Dihydroartemisinin in K562/adr and GLC4/adr Resistant Cell Lines. *Biological and Pharmaceutical Bulletin* **2002,** *25* (12), 1555-1561.

339. Chaijaroenkul, W.; Viyanant, V.; Mahavorasirikul, W.; Na-Bangchang, K., Cytotoxic activity of artemisinin derivatives against cholangiocarcinoma (CL-6) and hepatocarcinoma (Hep-G2) cell lines. *Asian Pacific Journal of Cancer Prevention* **2011,** *12* (1), 55-59.

340. Willoughby, J. A.; Sundar, S. N.; Cheung, M.; Tin, A. S.; Modiano, J.; Firestone, G. L., Artemisinin Blocks Prostate Cancer Growth and Cell Cycle Progression by Disrupting Sp1 Interactions with the Cyclin-dependent Kinase-4 (CDK4) Promoter and Inhibiting CDK4 Gene Expression. *Journal of Biological Chemistry* **2009,** *284* (4), 2203-2213.

341. (a) Le, N. T. V.; Richardson, D. R., The role of iron in cell cycle progression and the proliferation of neoplastic cells. *Biochimica et Biophysica Acta (BBA) - Reviews on Cancer* **2002,** *1603* (1), 31-46; (b) Head, J. F.; Wang, F.; Elliott, R. L., Antineoplastic drugs that interfere with iron metabolism in cancer cells. *Advances in Enzyme Regulation* **1997,** *37* (0), 147-169.

342. Crespo-Ortiz, M. P.; Wei, M. Q., Antitumor Activity of Artemisinin and Its Derivatives: From a Well-Known Antimalarial Agent to a Potential Anticancer Drug. *Journal of Biomedicine and Biotechnology* **2012,** *2012*.

343. Hamacher-Brady, A.; Stein, H. A.; Turschner, S.; Toegel, I.; Mora, R.; Jennewein, N.; Efferth, T.; Eils, R.; Brady, N. R., Artesunate Activates Mitochondrial Apoptosis in Breast Cancer Cells via Iron-catalyzed Lysosomal Reactive Oxygen Species Production. *Journal of Biological Chemistry* **2011,** *286* (8), 6587-6601.

344. Lai, H.; Sasaki, T.; Singh, N. P., Targeted treatment of cancer with artemisinin and artemisinin-tagged iron-carrying compounds. *Expert Opinion on Therapeutic Targets* **2005,** *9* (5), 995-1007.

345. Rasheed, S. A. K.; Efferth, T.; Asangani, I. A.; Allgayer, H., First evidence that the antimalarial drug artesunate inhibits invasion and in vivo metastasis in lung cancer by targeting essential extracellular proteases. *International Journal of Cancer* **2010,** *127* (6), 1475-1485.

346. Singh, N. P.; Panwar, V. K., Case Report of a Pituitary Macroadenoma Treated With Artemether. *Integrative Cancer Therapies* **2006,** *5* (4), 391-394.

347. Singh, N. P.; Verma, K. B., Case report of a laryngeal squamous cell carcinoma treated with artesunate. *Archive of Oncology* **2002,** *10* (4), 279-280.

348. Buommino, E.; Baroni, A.; Canozo, N.; Petrazzuolo, M.; Nicoletti, R.; Vozza, A.; Tufano, M., Artemisinin reduces human melanoma cell migration by down-regulating αVβ3 integrin and reducing metalloproteinase 2 production. *Invest New Drugs* **2009,** *27* (5), 412-418.

349. Wang, J.; Guo, Y.; Zhang, B. C.; Chen, Z. T.; Gao, J. F., Induction of apoptosis and inhibition of cell migration and tube-like formation by dihydroartemisinin in murine lymphatic endothelial cells. *Pharmacology* **2007,** *80* (4), 207-18.

350. Opsenica, I.; Opsenica, D.; Smith, K. S.; Milhous, W. K.; Šolaja, B. A., Chemical Stability of the Peroxide Bond Enables Diversified Synthesis of Potent Tetraoxane Antimalarials(1). *Journal of Medicinal Chemistry* **2008,** *51* (7), 2261-2266.

351. Kim, S. J.; Kim, M. S.; Lee, J. W.; Lee, C. H.; Yoo, H.; Shin, S. H.; Park, M. J.; Lee, S. H., Dihydroartemisinin enhances radiosensitivity of human glioma cells in vitro. *J Cancer Res Clin Oncol* **2006,** *132* (2), 129-135.

352. Horwedel, C.; Tsogoeva, S. B.; Wei, S.; Efferth, T., Cytotoxicity of Artesunic Acid Homo- and Heterodimer Molecules toward Sensitive and Multidrug-Resistant CCRF-CEM Leukemia Cells. *Journal of Medicinal Chemistry* **2010,** *53* (13), 4842-4848.

353. Sheehan, J.; Cruickshank, P.; Boshart, G., Notes- A Convenient Synthesis of Water-Soluble Carbodiimides. *The Journal of Organic Chemistry* **1961,** *26* (7), 2525-2528.